LUND UNIVERSITY

Identification of the Steering Dynamics of the Sea Stratus

Källström, Claes G.

1978

Link to publication

Total number of authors:
1

IDENTIFICATION OF THE STEERING

DYNAMICS OF THE SEA STRATUS

Claes G. Källström

IDENTIFICATION OF THE STEERING DYNAMICS
OF THE SEA STRATUS

CLAES G. KÄLLSTRÖM

Department of Automatic Control
Lund Institute of Technology
November 1978

Identification of the steering dynamics of the Sea Stratus

Referat (sammandrag)

System identification techniques are applied to determine the steering dynamics of the tanker Sea Stratus from 4 full-scale experiments. The output error method, the maximum likelihood method and the prediction error method are applied using the identification program LISPID. A few maximum likelihood identifications using the program IDPAC are also performed. Different linear and nonlinear models are investigated. Good estimates of the hydrodynamic derivatives are obtained by applying LISPID to data from the 4 experiments. Notice that one experiment was performed in closed loop.

TABLE OF CONTENTS

1. INTRODUCTION

System identification techniques are applied to determine
the steering dynamics of the Sea Stratus from 4 full-scale
experiments. Parameters of different linear and nonlinear
models are estimated. The identification program LISPID
(Källström, Essebo and Åström, 1976; Källström, 1978a) is
used to analyse the experiments. The output error method,
the maximum likelihood method and the prediction error
method are applied. A few maximum likelihood identifications
using the program IDPAC (Wieslander, 1976) are also presented.

The Sea Stratus is an oil tanker of 356 000 tdw built for the
Salén Shipping Companies, Stockholm, by Kockums Shipyard,
Malmö. The experiments were performed in ballast condition.
System identification techniques have previously been applied
to data from experiments performed with the Sea Splendour,
the Sea Scout and the Sea Swift, which are oil tankers of
255 000 tdw (Åström and Källström, 1973, 1976; Åström, Käll-
ström, Norrbin and Byström, 1975; Källström, 1977a, 1977c;
1978b; Norrbin, Byström, Åström and Källström, 1977; Byström
and Källström, 1978).

2. EXPERIMENTS

The Sea Stratus is a single-screw turbine tanker of 356 000 tdw
with a half-spade rudder. The maximum power at 86 rpm is 40 000
shp and the trial speed at full draught is 15.5 knots. The
length between perpendiculars L is 350 m, the breadth is 60 m,
and the draught is 22.3 m when the ship is fully loaded. The
displacement at full draught is 389 100 m^3.

The 4 experiments were performed in 1976, off the west coast
of Angola and South West Africa (Namibia). They are described
in detail by Källström (1976). The tanker was ballasted and
it had a displacement ∇ of 195 387 m^3. The draught at bow was
10.9 m and at stern 12.9 m. The ship speed V was approximately

12.6 knots and the propeller rate of revolution was about 70 rpm.
A head wind of 9-14 m/s was blowing, but the waves were relatively
small. The 4 experiments E1, E2, E3 and E4 lasted for 89, 19, 90
and 26 min. Experiments E1 and E4 were performed in open loop
by approximately using a PRBS as rudder perturbations. Experi-
ment E2 was a $5^O/5^O$ zig-zag test. Experiment E3 was carried out
in closed loop, but extra rudder perturbations were added to
secure the identifiability. The rudder command δ was determined
from the P-controller

$$\delta = k(\psi_m - \psi_{ref}) + \delta_o \tag{2.1}$$

where ψ_m is the measured heading angle, ψ_{ref} is the requested
heading angle and δ_o is the added perturbation signal, approxi-
mately chosen as a PRBS. The gain k was assigned the value 2 and
ψ_{ref} the value 146 deg during experiment E3. Identification of
processes in closed loop is discussed in Gustavsson, Ljung and
Söderström (1977). A rudder limit of 15 deg was used during
experiment E3. Rudder servo position, rudder angle, fore sway
velocity, yaw rate, heading angle, forward speed, propeller rate
of revolution, and propeller effect were measured during all
experiments. The data were punched on paper tape. The onboard
process computer made it possible to record the data with a
precise, constant sampling rate. The sampling interval T_s was
chosen to 10 s in all experiments. The input-output data used
for the system identification are shown in Figs. 2.1 - 2.4. The
rudder angles are positive towards port. The number of recorded
samples of experiments E1, E2, E3 and E4 are 536, 113, 538 and
154. In general the rudder commands are used as input signal.
However, a few investigations using the rudder angles are
also performed. It is always pointed out explicitly in the
sequel when the rudder angles are used instead of the rudder
commands.

The standard measurement equipment onboard the Sea Stratus was
used for the experiments. The sway velocities were measured by
an Atlas doppler sonar equipment with a resolution of about 0.02
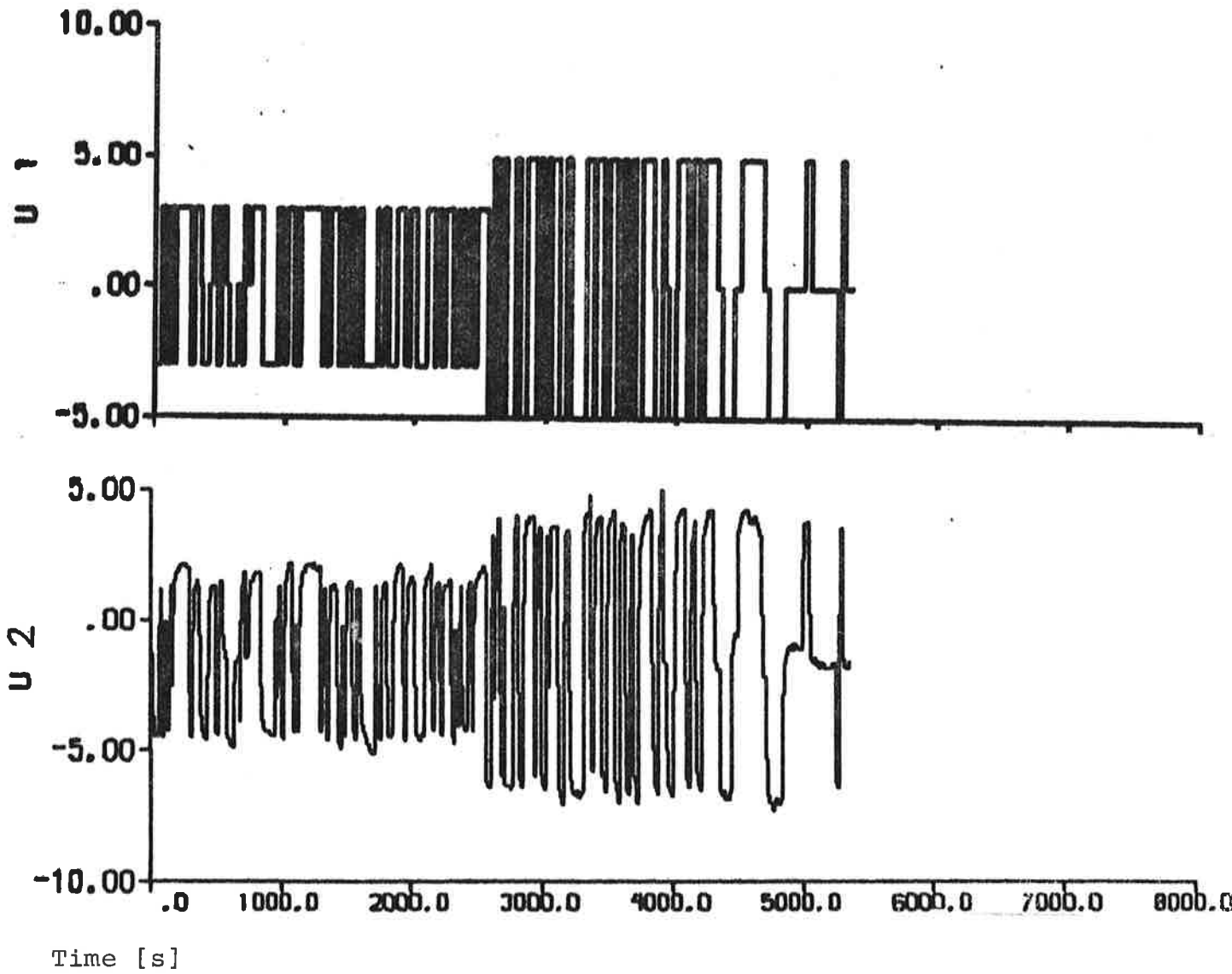
Fig. 2.1a - Input - output data obtained from experiment E1.
The inputs are the rudder command U1 [deg] and the
rudder angle U2 [deg], and the outputs are the fore
sway velocity Y1 [knots], the yaw rate Y2 [deg/s]
and the heading angle Y3 [deg].
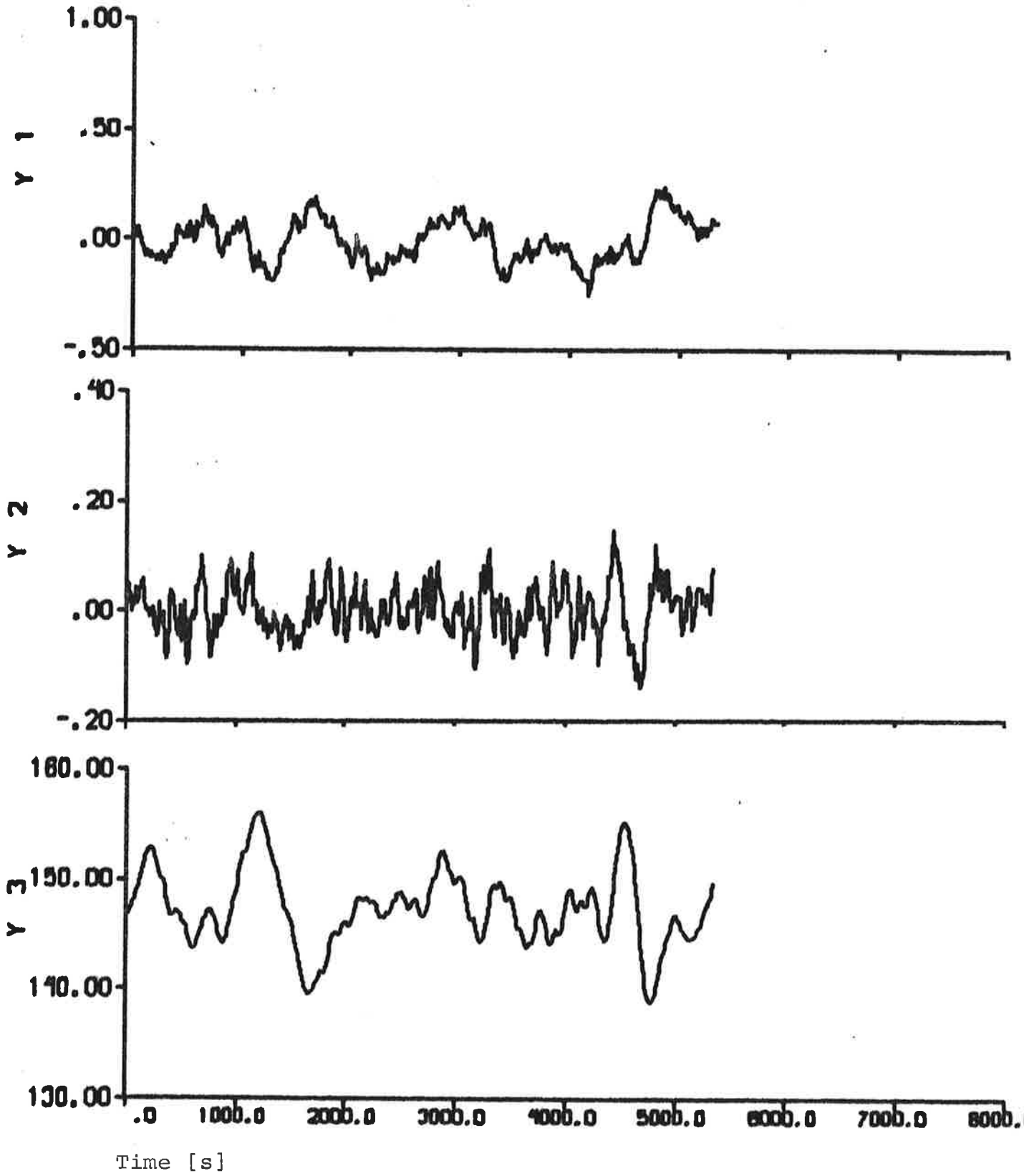
Fig. 2.1b
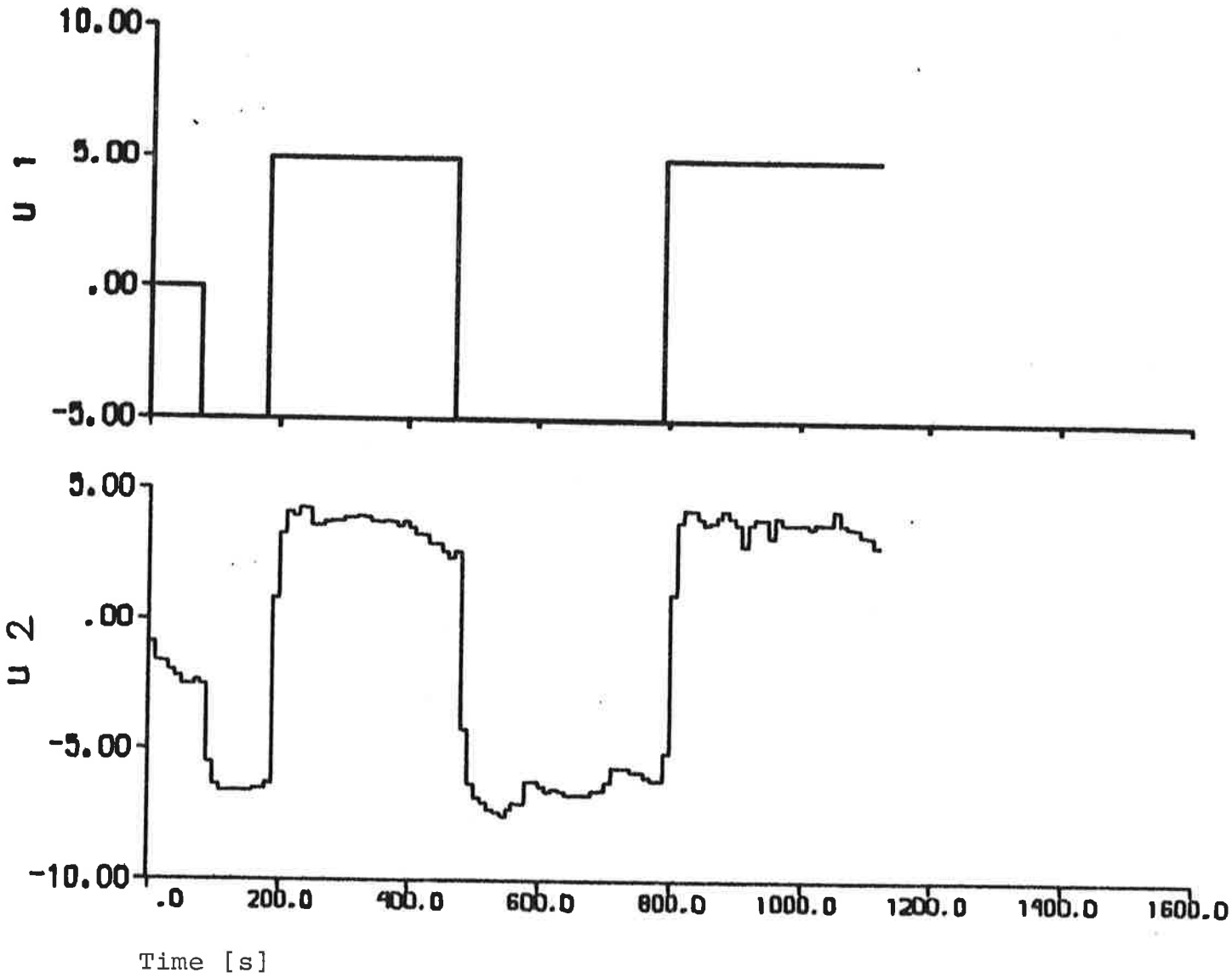
Fig. 2.2a - Input - output data obtained from experiment E2.
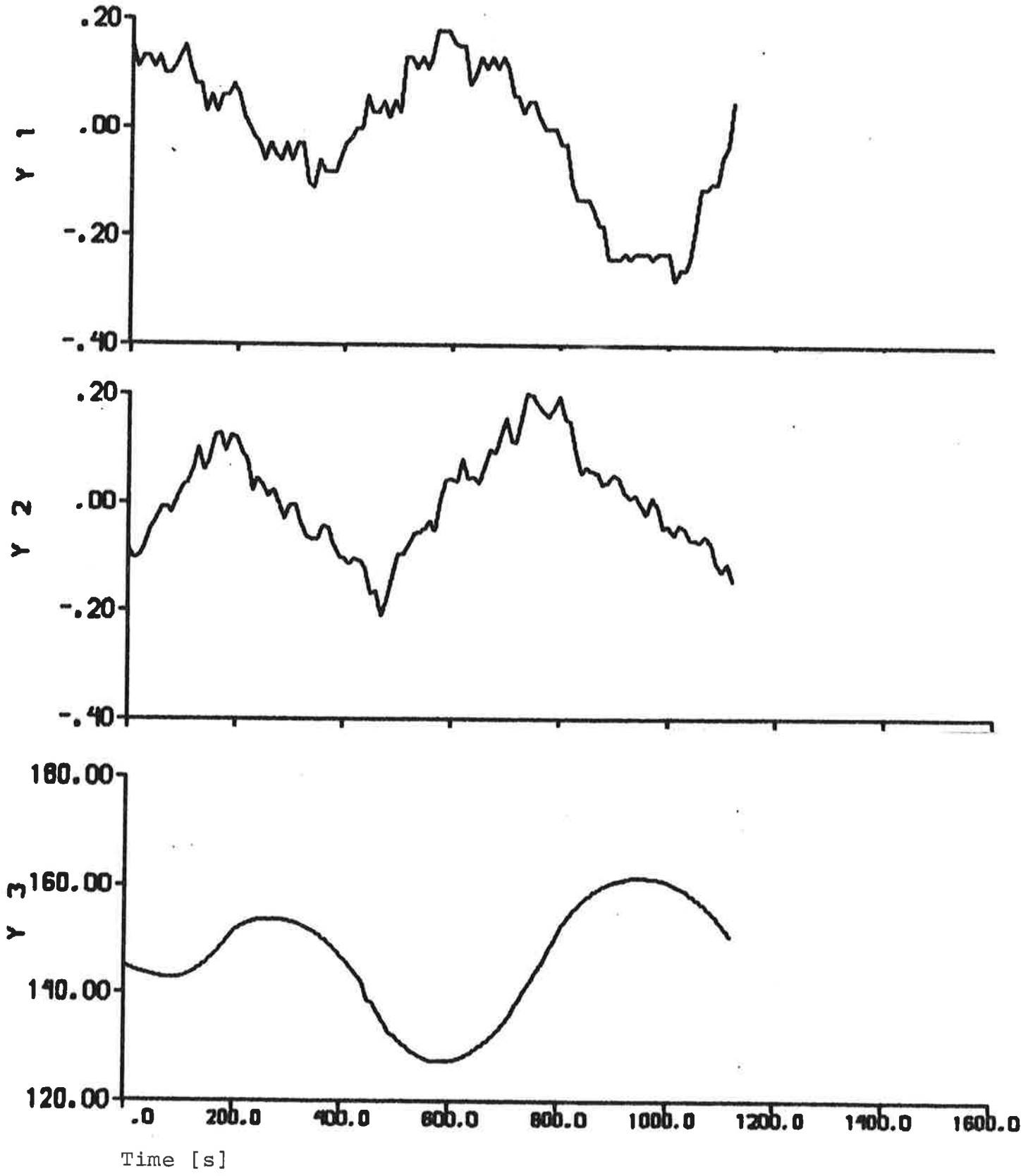
Fig. 2.2b
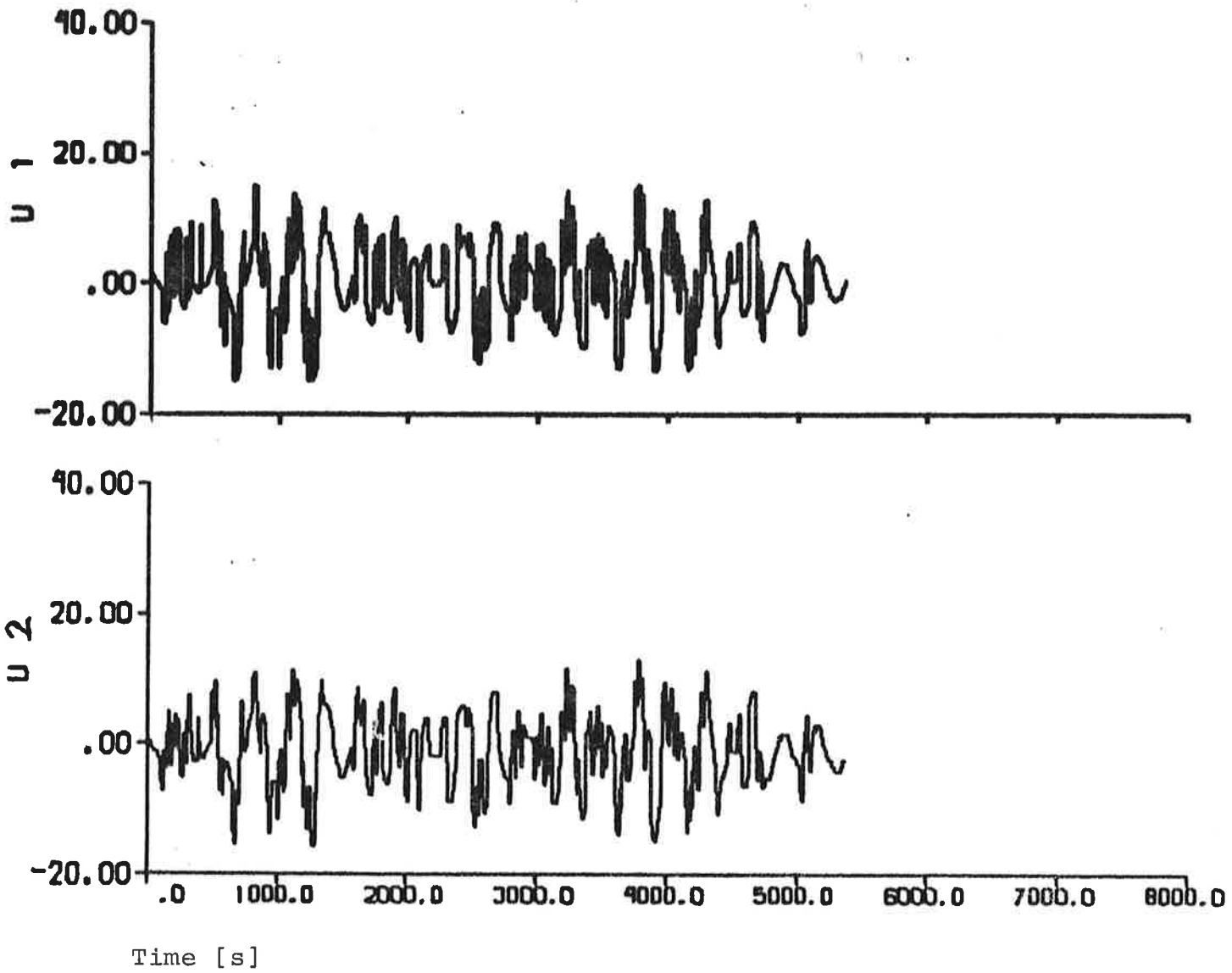
Fig. 2.3a - Input - output data obtained from
experiment E3.
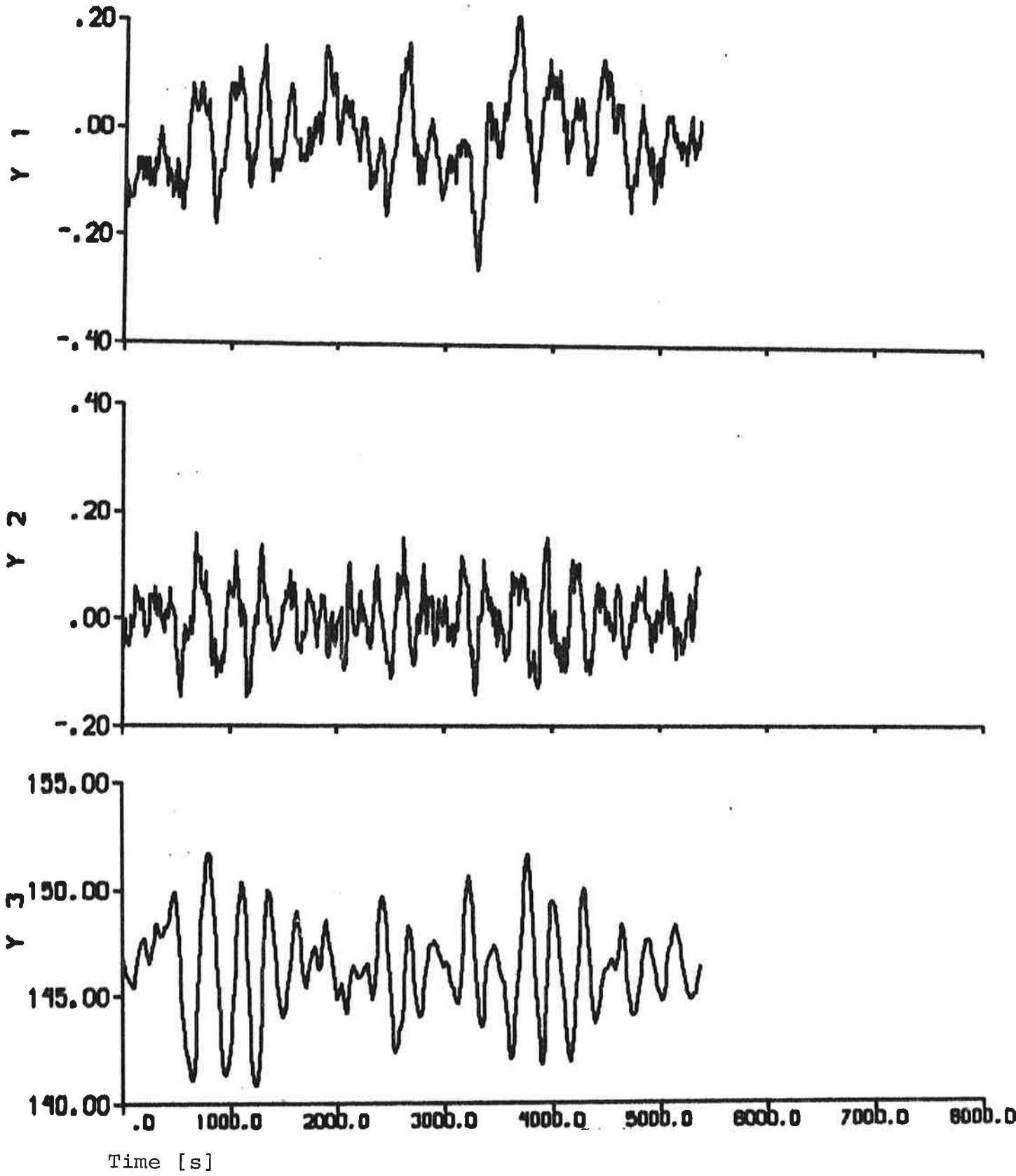
Fig. 2.3b
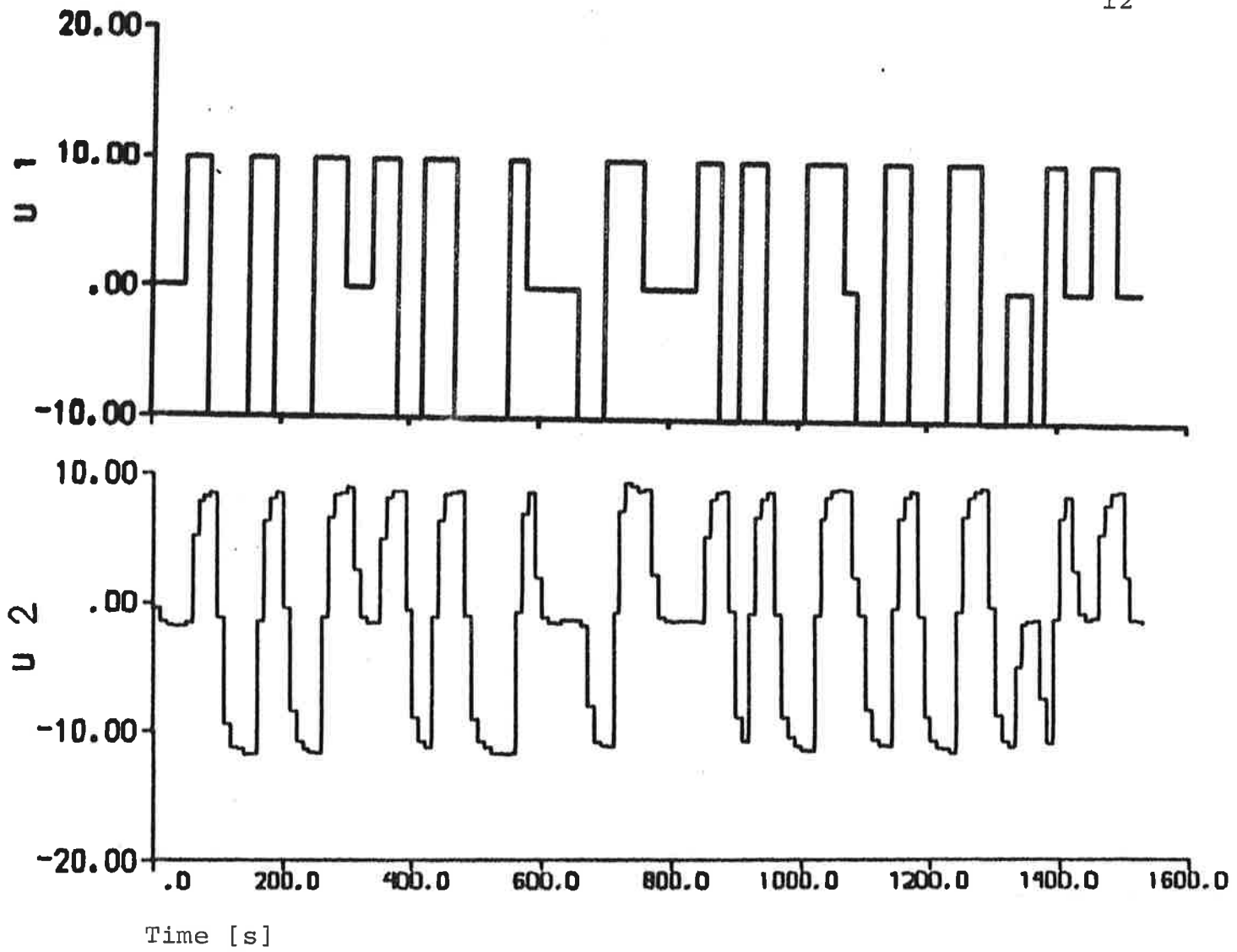
Fig. 2.4a - Input - output data obtained from
experiment E4.

Fig. 2.4b

knots. The distance L_1 from midship to the doppler log was 164.35 m. The yaw rates were measured by a rate gyro from AB ATEW, Flen, Sweden. The drift rate given by the manufacturer is 3 deg/h (0.0008 deg/s). However, the quality of the rate gyro signal varies with the sea conditions and the way the gyro is mounted, and an accuracy of about 0.005 deg/s seems to be realistic. The heading angles were measured by a Sperry gyro compass with an accuracy of about 0.1 deg. The heading signal was transformed by a synch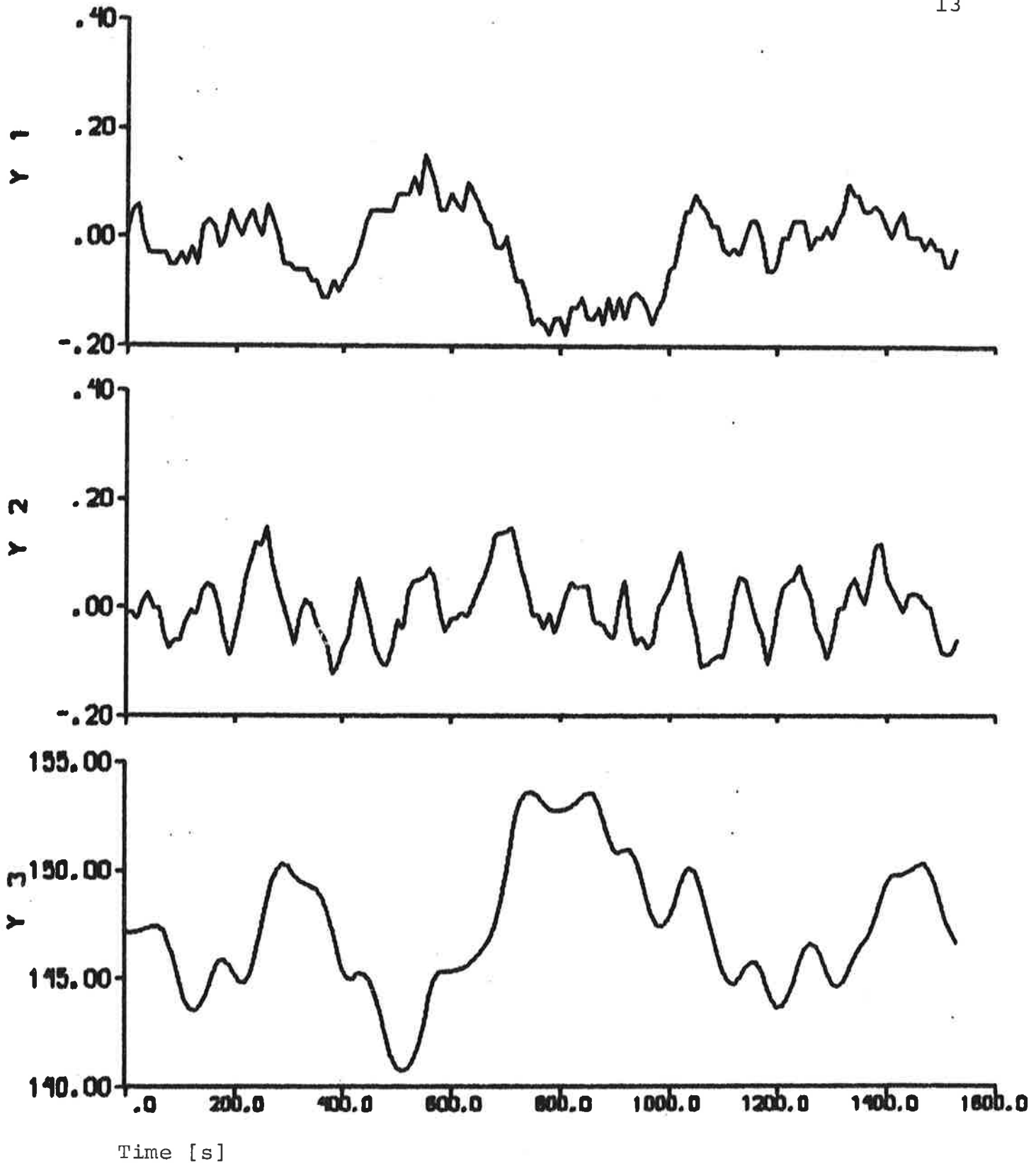ro-digital converter with an accuracy of about 0.02 deg. Notice that the doppler sonar and the rate gyro may have biases.

3. SHIP STEERING DYNAMICS

The identification results described in Sections 4 and 5 are based on the following model of the ship steering dynamics (Aström, Norrbin, Källström and Byström, 1974; Aström, Källström, Norrbin and Byström, 1975):

$$
\begin{bmatrix} \frac{L}{V^2}\theta_1 & \frac{L^2}{V^2}\theta_2 & 0 \\[6pt] \frac{L}{V^2}\theta_3 & \frac{L^2}{V^2}\theta_4 & 0 \\[6pt] 0 & 0 & 1 \end{bmatrix} \begin{bmatrix} dv \\[6pt] dr \\[6pt] d\psi \end{bmatrix} = \begin{bmatrix} \frac{1}{V}\theta_5 & \frac{L}{V}\theta_6 & \theta_9 \\[6pt] \frac{1}{V}\theta_7 & \frac{L}{V}\theta_8 & \theta_9 \cdot \theta_{10} \\[6pt] 0 & 1 & 0 \end{bmatrix} \begin{bmatrix} v(t) \\[6pt] r(t) \\[6pt] \psi(t) \end{bmatrix} \cdot dt +
$$

$$
+ \begin{bmatrix} \alpha_1 \cdot \theta_{11} & \theta_{13} \\[6pt] -\alpha_1 \cdot \theta_{11}\theta_{12} & \theta_{14} \\[6pt] 0 & 0 \end{bmatrix} \begin{bmatrix} \delta(t-T_D) \\[6pt] U \end{bmatrix} \cdot dt + \theta_{35} \cdot \begin{bmatrix} f_Y(v,r) \\[6pt] f_N(v,r) \\[6pt] 0 \end{bmatrix} \cdot dt + dw
$$

$$(3.1)$$

$$
\begin{bmatrix} v_1(t_k) \\[6pt] r_m(t_k) \\[6pt] \psi_m(t_k) \end{bmatrix} = \begin{bmatrix} \alpha_2 & L_1\alpha_2 & 0 \\[6pt] 0 & 1/\alpha_1 & 0 \\[6pt] 0 & 0 & 1/\alpha_1 \end{bmatrix} \begin{bmatrix} v(t_k) \\[6pt] r(t_k) \\[6pt] \psi(t_k) \end{bmatrix} +
$$

$$+ \begin{bmatrix} 0 & \theta_{15} \\ 0 & \theta_{17} \\ 0 & 0 \end{bmatrix} \cdot \begin{bmatrix} \delta(t_k - T_D) \\ U \end{bmatrix} + e(t_k) \quad k = 0,1,\ldots,N-1$$

The Wiener process w has the incremental covariance $R_1 dt$, where

$$R_1 = \begin{bmatrix} |\theta_{18}| & \sqrt{|\theta_{18}||\theta_{19}|}\sin\theta_{20} & 0 \\ \sqrt{|\theta_{18}||\theta_{19}|}\sin\theta_{20} & |\theta_{19}| & 0 \\ 0 & 0 & 0 \end{bmatrix}$$

The measurement errors $[e(t_k)]$ are assumed to be independent and gaussian with zero mean and covariance R_2, where

$$R_2 = \begin{bmatrix} |\theta_{21}| & 0 & 0 \\ 0 & |\theta_{23}| & 0 \\ 0 & 0 & |\theta_{24}| \end{bmatrix}$$

The initial state is given by

$$\begin{bmatrix} v(t_0) \\ r(t_0) \\ \psi(t_0) \end{bmatrix} = \begin{bmatrix} \theta_{25}/\alpha_2 \\ \alpha_1 \cdot \theta_{26} \\ \alpha_1 \cdot \theta_{27} \end{bmatrix}$$

and the time delay T_D is computed as

$$T_D = T_s - T_s |\sin\theta_{34}|$$

where T_s is the sampling interval.

The following variables are introduced in (3.1):

Inputs

δ - rudder command or rudder angle [deg]

U - artificial unit step input [-]

States

v - sway velocity at midship [m/s]

r - yaw rate [rad/s]

ψ - heading angle [rad]

Outputs

v_1 - fore sway velocity [knots]

r_m - yaw rate [deg/s]

ψ_m - heading angle [deg]

The model (3.1) is provided with the following fixed parameter values:

V - ship speed (6.5 m/s)

L - ship length (350 m)

L_1- distance from midship to fore doppler log (164.35 m)

α_1- conversion factor from degrees to radians (0.01745)

α_2- conversion factor from m/s to knots (1.944)

T_s- sampling interval (10s)

The parameters θ_1 - θ_{35} can be estimated in LISPID. Notice, however, that it is possible to estimate only a subset of the 35 parameters and to give the other parameters arbitrary fixed values. The parameters θ_{16}, θ_{22}, θ_{28} - θ_{33} have been omitted in the model (3.1), because they have no meaning for the analysis performed in this report. It is concluded from (3.1) that θ_1 - θ_4 are normalized acceleration hydrodynamic derivatives, θ_5 - θ_8, θ_{11} and $-\theta_{11}\theta_{12}$ are normalized linear hydrodynamic derivatives, θ_9 and θ_{10} are wind parameters, θ_{13} and θ_{14} are force and moment biases, and θ_{15} and θ_{17} are measurement biases. The time delay T_D can be regarded as an approximation of the effective time constant of the steering engine (Källström, 1977c), provided that the rudder command is used as input signal.

The only unknown parameter of the nonlinear contributions
in the model (3.1) is the effective cross-flow drag coefficient
θ_{35} = C. The value is expected to be of the order of 0.4 < C < 1.4.
The commonly used linear model of the steering dynamics is
obtained from (3.1) if θ_{35} = 0. The nonlinear functions f_y and
f_N have been derived in Norrbin (1976) by considering the cross-
flow drag. The nonlinear model (3.1) is in LISPID transformed
into a linear model by introducing f_y/m' and f_N/m' as additional
inputs, where m' = $2\nabla/L^3$ = 0.009114. The functions f_y and f_N
are dependent on the true sway velocity v and the true yaw rate r,
which are unknown. The estimates $\hat{x}_1$ and $\hat{x}_2$ of v and r obtained
through the filter

$$\hat{x}(t_{k+1}|t_k) = A\,\hat{x}\,(t_k|t_k) + Bu(t_k)$$

$$\hat{x}(t_k|t_k) = \hat{x}(t_k|t_{k-1}) + \bar{K}[y(t_k) - C\hat{x}(t_k|t_{k-1}) - Du(t_k)]$$

$$k = 0,\ldots,N-1$$

(3.2)

are instead used when the additional inputs are generated. The
input vector u, the state vector $\hat{x}$, and the output vector y
are the same as in the model (3.1). The filter (3.2) is obtained
from (3.1) by assuming θ_{35} = 0 and by sampling. The stationary
filter gain $\bar{K}$ is calculated by solving an appropriate, discrete
Riccati equation (Aström, 1970). Notice that $\bar{K}$ = 0 if there is
no process noise in (3.1), i.e. when w = 0. The problem of
estimating unknown parameters in the nonlinear model (3.1) with
$\theta_{35} \neq 0$ is thus transformed into the much easier problem of
estimating parameters in a linear model.

The unknown parameters are in LISPID estimated with the pre-
diction error method by minimizing the loss function

$$V = \frac{1}{N-p}\,\det\left[\sum_{k=p}^{N-1}\epsilon_p(t_k)\epsilon_p^T(t_k)\right]$$

(3.3)

where N is the number of samples. The p-step prediction errors ϵ_p are determined recursively from the innovations representation (see Källström, Essebo and Åström, 1976):

$$\epsilon_p(t_k) = y(t_k) - C \hat{x}(t_k|t_{k-p}) - Du(t_k)$$

$$\hat{x}(t_{i+1}|t_{k-p}) = A \hat{x}(t_i|t_{k-p}) + Bu(t_i), \quad i=k-p+1,\ldots, k-1$$

$$\hat{x}(t_{k-p+1}|t_{k-p}) = A \hat{x}(t_{k-p}|t_{k-p-1}) + Bu(t_{k-p}) + K\epsilon_o(t_{k-p}) \tag{3.4}$$

$$\epsilon_o(t_{k-p}) = y(t_{k-p}) - C \hat{x}(t_{k-p}|t_{k-p-1}) - Du(t_{k-p})$$

$$k = p,\ldots, N-1$$

Notice that $K = A\bar{K}$ and that the last two equations of (3.4) and (3.2) are equivalent if $\theta_{35} = 0$, i.e. if a linear model is used. The input vector u of (3.4) also contains the additional inputs when $\theta_{35} \neq 0$, i.e. when a nonlinear model is analysed.

The one-step prediction errors, i.e. the residuals, are minimized in the maximum likelihood method. This method is in LISPID obtained by assigning p=0 in (3.3) and (3.4), and by only using the last two equations of (3.4). The case p=1 has no meaning in LISPID. The output error method is easily obtained from the maximum likelihood method by assuming no process noise in (3.1), i.e. w=0. This implies that K=0 in (3.4). Different models obtained by the output error method and the maximum likelihood method can be compared by using Akaike's information criterion (Akaike, 1972):

$$AIC = -2 \log \hat{L} + 2 \nu \tag{3.5}$$

where $\hat{L}$ is the maximum of the likelihood function and ν is the number of estimated parameters. According to Akaike the quantity AIC should be minimum for the correct model structure. The following relation is obtained from (3.3) and (3.5):

$$AIC = (N-p) \log V + 2\nu + (1-n_y)(N-p) \log(N-p) + n_y(N-p)(1+\log 2\pi) \tag{3.6}$$

where n_y is the number of outputs from the model.

The program LISPID allows for both uniform and varying sampling. The data from the Sea Stratus experiments were, however, usually recorded with a constant sampling interval, so the nonuniform sampling facility will not be used.

It was concluded in Källström (1977a) that it is questionable if the wind parameters θ_9 and θ_{10} should be estimated, when the wind speed is less than 10 m/s. Since the wind speed was 9-14 m/s during the Sea Stratus experiments it is decided to estimate θ_9 and θ_{10} in some cases and to assume $\theta_9 = \theta_{10} = 0$ in other cases.

The transfer function relating the heading ψ to the rudder angle δ (in radians), when the wind parameters θ_9 and θ_{10}, the time delay T_D, and the parameter θ_{35} are zero, is obtained from (3.1):

$$G_{\psi\delta}(s) = \frac{K(1+sT_3)}{s(1+sT_1)(1+sT_2)} = \frac{K_1(s+1/T_3)}{s(s+1/T_1)(s+1/T_2)} \tag{3.7}$$

where $K_1 = \dfrac{KT_3}{T_1 T_2}$. The corresponding transfer function relating

the sway velocity v to the rudder angle δ (in radians) is

$$G_{v\delta}(s) = \frac{K_v(1+sT_{3v})}{(1+sT_1)(1+sT_2)} = \frac{K_{1v}(s+1/T_{3v})}{(s+1/T_1)(s+1/T_2)} \tag{3.8}$$

where $K_{1v} = \dfrac{K_v T_{3v}}{T_1 T_2}$. It is customary to normalize the gains and

time constants of (3.7) and (3.8) by use of the 'prime' system:

$$K' = K \cdot L/V \qquad T_1' = T_1 \cdot V/L$$

$$K_1' = K_1 \cdot L^2/V^2 \qquad T_2' = T_2 \cdot V/L \qquad (3.9)$$

$$K_v' = K_v/V \qquad T_3' = T_3 \cdot V/L$$

$$K_{1v}' = K_{1v} \cdot L/V^2 \qquad T_{3v}' = T_{3v} \cdot V/L$$

The identifiability aspects of the model (3.1) were discussed in Åström and Källström (1973, 1976). The linear hydrodynamic derivatives $\theta_5 - \theta_8$, θ_{11}, $- \theta_{11}\theta_{12}$, the wind parameters $\theta_9 - \theta_{10}$, the biases $\theta_{13} - \theta_{17}$, and the parameter θ_{35} can be determined if the acceleration hydrodynamic derivatives $0_1 - 0_4$ are known and if the parameter values are such that the model (3.1) is completely observable and completely controllable. It is necessary that measurements of the sway velocity are available together with measurements of the yaw rate or the heading angle. All parameters $\theta_{18} - \theta_{24}$ of the covariance matrices R_1 and R_2 can not be determined when the prediction error method or the maximum likelihood method is applied, since it is possible to multiply R_1 and R_2 by an arbitrary coefficient and still obtain the same filter gain K (cf. (3.4)). Therefore, the parameter θ_{24} is always fixed in the sequel.

The hydrodynamic derivatives of the linear model (3.1) have been estimated by SSPA for the Sea Stratus. The estimates are shown in Table 3.1. The acceleration derivatives $\theta_1 - \theta_4$ are always fixed in the sequel to the values given in Table 3.1.

The transfer function relating the heading to the rudder angle is determined in Section 6. The only measurement signal used is the heading. The following state space model is then used in LISPID (Åström, Norrbin, Källström and Byström, 1974; Åström Källström, Norrbin and Byström, 1975):

$$
\begin{bmatrix} dx_1 \\ dr \\ d\psi \end{bmatrix} = \begin{bmatrix} 0 & 0 & -\dfrac{v^3}{L^3}\varphi_3 \\ 1 & -\dfrac{v}{L}\varphi_1 & -\dfrac{v^2}{L^2}\varphi_2 \\ 0 & 1 & 0 \end{bmatrix} \begin{bmatrix} x_1(t) \\ r(t) \\ \psi(t) \end{bmatrix} dt \quad +
$$

$$
+ \begin{bmatrix} \alpha_1\dfrac{v^3}{L^3}\varphi_5 & \varphi_6 \\ \alpha_1\dfrac{v^2}{L^2}\varphi_4 & \varphi_7 \\ 0 & 0 \end{bmatrix} \begin{bmatrix} \delta(t-T_D) \\ U \end{bmatrix} dt + dw \qquad\qquad (3.10)
$$

$$
\psi_m(t_k) = \begin{bmatrix} 0 & 0 & 1/\alpha_1 \end{bmatrix} \begin{bmatrix} x_1(t_k) \\ r(t_k) \\ \psi(t_k) \end{bmatrix} + e(t_k) \quad k = 0,1,\ldots, N-1
$$

The Wiener process w has the incremental covariance $R_1\, dt$, where

$$
R_1 = \begin{bmatrix} |\varphi_9| & \sqrt{|\varphi_9|\,|\varphi_{10}|}\ \sin\varphi_{11} & 0 \\ \sqrt{|\varphi_9|\,|\varphi_{10}|}\ \sin\varphi_{11} & |\varphi_{10}| & 0 \\ 0 & 0 & 0 \end{bmatrix}
$$

The measurement errors $\{e(t_k)\}$ are assumed to be independent and gaussian with zero mean and covariance R_2, where $R_2 = |\varphi_{13}|$. The initial state is given by

$$
\begin{bmatrix} x_1(t_0) \\ r(t_0) \\ \psi(t_0) \end{bmatrix} = \begin{bmatrix} \varphi_{15} \\ \alpha_1\cdot\varphi_{16} \\ \alpha_1\cdot\varphi_{17} \end{bmatrix}
$$

$m' - Y_{\dot{v}}'$	(θ_1)	0.01621
$m'x_G' - Y_{\dot{r}}'$	(θ_2)	0
$m'x_G' - N_{\dot{v}}'$	(θ_3)	0
$I_z' - N_{\dot{r}}'$	(θ_4)	0.00094
Y_v'	(θ_5)	-0.00687
$Y_r' - m'$	(θ_6)	-0.00724
N_v'	(θ_7)	-0.00254
$N_r' - m'x_G'$	(θ_8)	-0.00161
Y_δ'	(θ_{11})	0.00201
N_δ'	$(-\theta_{11}\theta_{12})$	-0.00095

Table 3.1 - Hydrodynamic derivatives estimated by SSPA.
They are normalized by use of the 'prime' system with
mass unit $\rho L^3/2$. The corresponding values in the
'bis' system are obtained by dividing with m' =
0.009114. The origin of the co-ordinate system is
assumed to be at midship.

and the time delay T_D is computed as

$$T_D = T_s - T_s \ |sin \ \varphi_{24}|$$

where T_s is the sampling interval.

The notations are the same as in the model (3.1). The state $x_1 \ [1/s^2]$ is a linear combination of v, r and ψ. The parameters $\varphi_1 - \varphi_{24}$, or a subset of these parameters, can be estimated in LISPID. The parameters φ_8, φ_{12}, φ_{14}, $\varphi_{18} - \varphi_{23}$ have been omitted in the model (3.10), because they have no meaning for the analysis performed in this report. Notice that φ_3 is a wind parameter and that φ_6 and φ_7 are biases.

The transfer function relating the heading ψ to the rudder angle δ (in radians), when the time delay T_D is zero, is obtained from (3.10):

$$G_{\psi\delta}(s) = \frac{\dfrac{v^2}{L^2} \varphi_4 \ s + \dfrac{v^3}{L^3} \varphi_5}{s^3 + \dfrac{v}{L} \varphi_1 \ s^2 + \dfrac{v^2}{L^2} \varphi_2 \ s + \dfrac{v^3}{L^3} \varphi_3} \tag{3.11}$$

If the wind parameter φ_3 is zero, (3.11) becomes (cf.(3.7)):

$$G_{\psi\delta}(s) = \frac{\dfrac{v^2}{L^2} \varphi_4 \ s + \dfrac{v^3}{L^3} \varphi_5}{s[s^2 + \dfrac{v}{L} \varphi_1 \ s + \dfrac{v^2}{L^2} \varphi_2]} = \tag{3.12}$$

$$= \frac{K(1+s \ T_3)}{s(1+sT_1)(1+sT_2)} = \frac{K_1(s+1/T_3)}{s(s+1/T_1)(s+1/T_2)}$$

Notice that Nomoto's model is obtained when $\varphi_2 = \varphi_5 = 0$:

$$G_{\psi\delta}(s) = \frac{\frac{V^2}{L^2}\varphi_4}{s(s+\frac{V}{L}\varphi_1)} = \frac{K}{s(1+sT)} = \frac{K_1}{s(s+1/T)} \qquad (3.13)$$

where $K_1 = K/T$. The corresponding normalized parameters are defined by $K_1' = K_1 \cdot L^2/V^2$ and $T' = T \cdot V/L$ (cf. (3.9)).

The unknown parameters are in LISPID estimated by minimizing the loss function (3.3) and by using (3.4), where the recursion now is based on the model (3.10) instead of (3.1).

The identifiability aspects of the model (3.10) were discussed in Åström and Källström (1973, 1976). Tha parameters can be determined except in the case when there is a pole - zero cancellation. It is, however, necessary to fix one of the parameters of the covariance matrices R_1 and R_2, when the prediction error method or the maximum likelihood method is applied. Therefore, the parameter φ_{13} is always fixed in the sequel as well as the wind parameter φ_3.

The following transfer function parameters are obtained from SSPA:s model (Table 3.1):

$$\varphi_1 = 2.14$$
$$\varphi_2 = -0.48$$
$$\varphi_4 = -1.01 \qquad (3.14)$$
$$\varphi_5 = -0.76$$

The sampled version of the model (3.10) can be represented by the difference equation model

$$\psi_m(t) + a_1 \, \psi_m(t-1) + \ldots + a_n \, \psi_m(t-n) =$$

$$= b_1 \delta(t-1) + \ldots + b_n \delta(t-n) + \tag{3.15}$$

$$+ \lambda [e(t) + c_1 e(t-1) + \ldots + c_n e(t-n)]$$

where a constant, unit sampling interval is assumed and where $\{e(t)\}$ is a sequence of random variables which accounts for the combined effect of process disturbances and measurement errors. The maximum likelihood estimation of the parameters of (3.15) can be simplified significantly as described in Åström and Bohlin (1965). The interactive program IDPAC (Wieslander, 1976) performs this. The program minimizes the loss function

$$V = \frac{1}{N} \sum_0^{N-1} \varepsilon^2(t) \tag{3.16}$$

which is a special case of (3.3). Notice that (3.16) can be combined with (3.6).

If Nomoto's model (3.13) is combined with a time delay T_D describing the steering engine, then the following transfer function is obtained:

$$G_{\psi\delta}(s) = \frac{K}{s(1+sT)} e^{-sT_D} \tag{3.17}$$

The discrete time model (cf. (3.15))

$$\psi_m(t) + a_1 \, \psi_m(t-1) + a_2 \, \psi_m(t-2) =$$

$$\tag{3.18}$$

$$= b_1 \delta(t-1) + b_2 \delta(t-2) + b_3 \delta(t-3)$$

is obtained by sampling (3.17), where

$$a_1 = -(e^{-T_s/T} + 1)$$

$$a_2 = e^{-T_s/T}$$

$$b_1 = K[T\, e^{(T_D - T_s)/T} + T_s - T_D - T] \tag{3.19}$$

$$b_2 = -K[2T\, e^{(T_D - T_s)/T} + (T_s - T_D - T)\, e^{-T_s/T} - T_D - T]$$

$$b_3 = K[T\, e^{(T_D - T_s)/T} - (T_D + T)\, e^{-T_s/T}]$$

and where T_s is the sampling interval. Notice that $b_3 = 0$ when $T_D = 0$. If the parameters of the model (3.18) are known, then the parameters of (3.17) can be computed through

$$K = \frac{b_1 + b_2 + b_3}{T_s(1 - a_2)}$$

$$T = -\frac{T_s}{\log a_2} \tag{3.20}$$

$$T_D = T_s \left[\frac{1}{\log a_2} + \frac{1}{1 - a_2} + \frac{b_3 - b_1}{b_1 + b_2 + b_3} \right]$$

provided that the model (3.18) has been obtained by sampling (3.17). One necessary conditon is $1 + a_1 + a_2 = 0$, i.e. (3.18) contains a pure integrator.

4. IDENTIFICATION OF LINEAR MODELS

Results of fitting the linear version of the model (3.1) to data from the 4 experiments are presented in this section. The following fixed parameter values are then used:

$$\theta_1 = 0.01621$$
$$\theta_2 = 0$$
$$\theta_3 = 0$$
$$\theta_4 = 0.00094 \qquad\qquad (4.1)$$
$$\theta_{12} = 0.471$$
$$\theta_{24} = 0.01 \text{ deg}^2$$
$$\theta_{35} = 0$$

Notice that $\theta_{12} = -N_\delta'/Y_\delta'$ is fixed to the value obtained from SSPA:s model (Table 3.1). It was suggested in Källström (1977a and 1977b) to assign this relation a fixed value, since the relation is easy to determine from the hull geometry.

Estimated parameters from output error, ML and prediction error (p = 4 and 6) identifications are shown in Tables 4.1 - 4.4. The results of output error, ML and prediction error (p = 6) identifications are shown in Figs 4.1 - 4.20. The continuous lines are the measurements and the dashed lines are the outputs of the deterministic models. The dashed lines in the diagrams of the correlation functions are the ±2σ-limits.

The performance of SSPA:s model is shown in Figs. 4.1, 4.6, 4.11 and 4.16. The wind parameters, the biases, the initial state and the time delay are then fitted to the data from the 4 experiments by use of the output error method. It is concluded that improvements seem to be possible. Especially the sway velocity outputs differ much from the measurements. A possible explanation to this is that the sway velocity measurements are filtered rather much.

The results of output error identifications when the hydrodynamic derivatives also are estimated are shown in Figs. 4.2, 4.7, 4.12 and 4.17. The parameter estimates obtained from experiments E1, E2 and E4 are reasonable. Especially experiment E4 gave parameter estimates very close to SSPA:s values. A strange model was, however, obtained from experiment E3.

The models obtained by applying the ML method to data from the 4 experiments are strange in all cases. The reason is probably that a prediction interval of 10 s is too short compared to the inertia of the ship and with respect to the disturbance dynamics (Källström, 1977c, 1978b). Notice, however, that Akaike's information criterion AIC distinctly indicates that the process noise should be modelled. The prediction errors obtained from experiment E2 are almost white and uncorrelated to the rudder input (see Fig. 4.8c and d), while the other experiments gave less reasonable prediction errors. Notice that large values of the heading prediction error were obtained after 440 s of experiment E2 (Fig. 4.8b) and after 3380 s of experiment E3 (Fig. 4.13b). It is found from the original data record that one sampling event was missed in the first case and that two consecutive, incorrect sampling intervals of 19 s and 1 s were obtained in the second case instead of a sampling interval of 10 s. The failures were probably caused by a temporary overload of the computer.

The results are improved when the prediction error method is applied. The parameter estimates obtained with $p = 4$ and $p = 6$, i.e. a prediction interval of 40 s and 60 s, are shown in Tables 4.1 - 4.4. Notice that it was necessary to fix the parameter θ_{23} of the covariance matrix R_2 and the parameters $\theta_{25} - \theta_{27}$ of the initial state to obtain reasonable results. The wind parameters θ_9 and θ_{10} were also fixed, since it was possible to conclude from the output error and ML identifications that these parameters were not significant. The estimates obtained with $p = 6$ are usually somewhat improved compared to $p = 4$. Figures 4.4, 4.9, 4.14 and 4.19 show the results of prediction error identifications with $p = 6$. The corresponding filter gains K (cf. (3.4)) obtained from experiments E1 - E4 are:

$$K = \begin{pmatrix} 3.8 \ 10^{-1} & -2.0 \ 10^{-1} & -5.3 \ 10^{-2} \\ -3.6 \ 10^{-4} & 1.2 \ 10^{-3} & 3.2 \ 10^{-4} \\ -3.2 \ 10^{-3} & 4.6 \ 10^{-2} & 1.8 \ 10^{-2} \end{pmatrix} \quad (4.2)$$

$$K = \begin{pmatrix} 3.2 \ 10^{-2} & 6.8 \ 10^{-1} & 2.5 \ 10^{-2} \\ 6.6 \ 10^{-5} & 4.1 \ 10^{-3} & 1.6 \ 10^{-4} \\ 1.6 \ 10^{-3} & 8.1 \ 10^{-2} & 1.1 \ 10^{-2} \end{pmatrix} \quad (4.3)$$

$$K = \begin{pmatrix} 3.1 \ 10^{-2} & -1.8 \ 10^{-1} & -4.3 \ 10^{-2} \\ -1.7 \ 10^{-5} & 1.3 \ 10^{-3} & 3.0 \ 10^{-4} \\ -3.3 \ 10^{-4} & 4.7 \ 10^{-2} & 1.7 \ 10^{-2} \end{pmatrix} \quad (4.4)$$

$$K = \begin{pmatrix} 4.9 \ 10^{-5} & -4.4 \ 10^{-1} & -8.7 \ 10^{-2} \\ -3.3 \ 10^{-7} & 2.9 \ 10^{-3} & 5.8 \ 10^{-4} \\ -4.7 \ 10^{-6} & 5.7 \ 10^{-2} & 2.0 \ 10^{-2} \end{pmatrix} \quad (4.5)$$

A prediction interval of approximately 60 s is thus appropriate. It is, however, concluded from Tables 4.1 - 4.4 that the parameter estimates obtained with p = 6 differ rather much from SSPA:s values. The only exception is experiment E2. In this case the parameter estimates obtained with p = 6 were close to SSPA:s values. Figure 4.9 also indicates a good result.

The time delay T_D can be regarded as an approximation of the effective time constant of the steering engine. The value is known to be of the order of 5 s.

The results of using the rudder angle instead of the rudder command as input signal when the prediction error method (p = 6) is applied to the data are also shown in Tables 4.1 - 4.4. Figures 4.5, 4.10, 4.15 and 4.20 also illustrate the results. It is concluded that no significant improvements are obtained.

An unstable model of the Sea Stratus was determined by SSPA. However, all results of Tables 4.1 - 4.4, with one exception, indicate that a stable model is appropriate. The only unstable model was obtained when the output error method was applied to experiment E4.

	Output error (SSPA:s model)	Output error	M L	Prediction error p = 4	p = 6	p = 6 Rudder ang. is input
Figure	4.1	4.2	4.3	–	4.4	4.5
ν	10	15	20	14	14	14
V	2414	17	$9.6\cdot10^{-4}$	0.17	0.43	0.48
AIC	2020	–621	–5845	–	–	–
Y_v'	-0.00687^*	–0.01892	–0.01341	–0.00872	–0.04190	–0.02160
$Y_r'-m'$	-0.00724^*	–0.00488	–0.00419	–0.00180	–0.01757	–0.00882
N_v'	-0.00254^*	–0.00316	0.00068	–0.00023	0.00022	–0.00006
$N_r'-m'x_G'$	-0.00161^*	–0.00120	–0.00005	–0.00040	–0.00011	–0.00021
Y_δ'	0.00201^*	0.00130	0.00090	0.00130	0.00157	0.00141
N_δ'	-0.00095^*	–0.00061	–0.00043	–0.00061	–0.00074	–0.00066
θ_9	$-1.3\cdot10^{-5}$	$-2.1\cdot10^{-5}$	$1.5\cdot10^{-4}$	0^*	0^*	0^*
θ_{10}	0.102	0.027	–0.069	0^*	0^*	0^*
θ_{13}	$-1.9\cdot10^{-6}$	$8.4\cdot10^{-6}$	$1.4\cdot10^{-4}$	$2.5\cdot10^{-5}$	$8.3\cdot10^{-4}$	$2.8\cdot10^{-4}$
θ_{14}	$5.3\cdot10^{-8}$	$-1.8\cdot10^{-6}$	$2.2\cdot10^{-6}$	$3.8\cdot10^{-6}$	$-5.0\cdot10^{-7}$	$-1.2\cdot10^{-5}$
θ_{15} [knots]	0.04	0.02	–0.52	–0.05	–0.26	–0.15
θ_{17} [deg/s]	0.018	0.004	0.002	0.002	0.002	0.002
$R_1(1,1)$ [s]	–	–	$1.5\cdot10^{-1}$	$1.4\cdot10^{-2}$	$7.3\cdot10^{-3}$	$6.6\cdot10^{-3}$
$R_1(1,2)$ [s]	–	–	$-1.3\cdot10^{-4}$	$-1.1\cdot10^{-4}$	$-1.1\cdot10^{-4}$	$-8.5\cdot10^{-5}$
$R_1(2,2)$ [s]	–	–	$1.2\cdot10^{-7}$	$8.7\cdot10^{-7}$	$1.7\cdot10^{-6}$	$1.1\cdot10^{-6}$
$R_2(1,1)$ [knots]^2	–	–	$1.7\cdot10^{-4}$	$6.2\cdot10^{-3}$	$2.8\cdot10^{-8}$	$7.0\cdot10^{-8}$
$R_2(2,2)$ [deg/s]^2	–	–	$6.7\cdot10^{-2}$	10^{-4*}	10^{-4*}	10^{-4*}
θ_{25} [knots]	0.07	0.17	0.62	0^*	0^*	0^*
θ_{26} [deg/s]	0.003	0.006	–0.009	0^*	0^*	0^*
θ_{27} [deg]	147.29	150.38	146.88	146.89^*	146.89^*	146.89^*
T_D [s]	6.1	7.8	6.6	8.2	2.1	0.0
K'	1.59	–2.16	–1.47	–1.83	–3.63	–3.51
K_1'	–1.00	–0.65	–	–0.65	–0.79	–0.71
K_v'	–1.38	0.63	0.53	0.53	1.56	1.50
K_{1v}'	0.12	0.08	–	0.08	0.10	0.09
T_1'	–4.88	4.67	complex	3.25	4.47	5.07
T_2'	0.43	0.45	poles	1.53	0.40	0.73
T_3'	1.32	0.63	1.36	1.76	0.39	0.75
T_{3v}'	0.19	0.27	0.47	0.75	0.11	**0.22**

* = fixed value

Table 4.1 - Estimated parameters from identifications to data from experiment E1.

	Output error (SSPA:s model)	Output error	M L	Prediction error p = 4	p = 6	p = 6 Rudd. angl. is input
Figure	4.6	4.7	4.8	–	4.9	4.10
ν	10	15	20	14	14	14
V	3.95	$9.0 \cdot 10^{-3}$	$1.8 \cdot 10^{-4}$	$3.3 \cdot 10^{-3}$	$7.1 \cdot 10^{-3}$	$7.2 \cdot 10^{-3}$
AIC	70	–601	–1029	–	–	–
Y_v'	-0.00687^*	–0.01810	–0.02462	–0.03036	–0.02121	–0.02277
$Y_r'-m'$	-0.00724^*	–0.00889	–0.01144	–0.01412	–0.01010	–0.01112
N_v'	-0.00254^*	–0.00410	0.00153	–0.00009	–0.00258	–0.00152
$N_r'-m'x_G'$	-0.00161^*	–0.00222	0.00051	–0.00024	–0.00144	–0.00084
Y_δ'	0.00201^*	0.00245	0.00092	0.00141	0.00203	0.00165
N_δ'	-0.00095^*	–0.00115	–0.00043	–0.00066	–0.00096	–0.00077
θ_9	$7.2 \cdot 10^{-6}$	$-1.9 \cdot 10^{-6}$	$3.0 \cdot 10^{-4}$	0^*	0^*	0^*
θ_{10}	0.322	0.133	–0.006	0^*	0^*	0^*
θ_{13}	$-7.3 \cdot 10^{-6}$	$-7.3 \cdot 10^{-5}$	$-5.5 \cdot 10^{-4}$	$2.1 \cdot 10^{-4}$	$5.3 \cdot 10^{-5}$	$-4.0 \cdot 10^{-4}$
θ_{14}	$3.8 \cdot 10^{-6}$	$-5.2 \cdot 10^{-6}$	$-3.2 \cdot 10^{-6}$	$7.1 \cdot 10^{-6}$	$1.5 \cdot 10^{-5}$	$-4.3 \cdot 10^{-5}$
θ_{15} [knots]	0.03	0.05	–0.12	–0.10	–0.04	0.23
θ_{17} [deg/s]	–0.007	0.001	0.002	0.003	0.004	0.004
$R_1(1,1)$ [s]	–	–	$8.9 \cdot 10^{-7}$	$8.9 \cdot 10^{-3}$	$2.8 \cdot 10^{-6}$	$1.2 \cdot 10^{-6}$
$R_1(1,2)$ [s]	–	–	$-1.1 \cdot 10^{-7}$	$8.9 \cdot 10^{-5}$	$3.0 \cdot 10^{-7}$	$8.1 \cdot 10^{-8}$
$R_1(2,2)$ [s]	–	–	$1.3 \cdot 10^{-8}$	$9.0 \cdot 10^{-7}$	$3.2 \cdot 10^{-8}$	$5.5 \cdot 10^{-9}$
$R_2(1,1)$ [knots]^2	–	–	$2.6 \cdot 10^{-6}$	$1.7 \cdot 10^{-6}$	$5.1 \cdot 10^{-2}$	127.2
$R_2(2,2)$ [deg/s]^2	–	–	$2.2 \cdot 10^{-3}$	10^{-4*}	10^{-4*}	10^{-4*}
θ_{25} [knots]	0.01	–0.06	0.71	0^*	0^*	0^*
θ_{26} [deg/s]	–0.020	–0.027	–0.084	0^*	0^*	0^*
θ_{27} [deg]	140.75	143.28	144.80	144.67^*	144.67^*	144.67^*
T_D [s]	0.0	5.0	7.7	6.8	6.7	2.0
K'	1.59	–8.07	–1.88	–3.33	–5.74	–9.14
K_1'	–1.00	–1.23	–	–0.71	–1.01	–0.82
K_v'	–1.38	4.10	0.91	1.59	2.83	4.53
K_{1v}'	0.12	0.16	–	0.09	0.12	0.10
T_1'	–4.88	13.54	} complex	4.81	9.36	15.41
T_2'	0.43	0.29	poles	0.52	0.37	0.45
T_3'	1.32	0.60	0.76	0.53	0.61	0.62
T_{3v}'	0.19	0.15	0.19	0.14	0.15	0.15

* = fixed value

Table 4.2 – Estimated parameters from identifications to data from experiment E2.

	Output error (SSPA:s model)	Output error	M L	Prediction error p = 4	p = 6	p = 6 Rudd. angl. is input
Figure	4.11	4.12	4.13	–	4.14	4.15
ν	10	15	20	14	14	14
V	210369	5.75	$1.8 \cdot 10^{-3}$	0.34	0.21	0.22
AIC	4422	-1210	-5533	–	–	–
Y_v'	-0.00687^*	-0.01615	-0.00537	-0.00888	-0.26226	-0.27678
$Y_r'-m'$	-0.00724^*	0.00149	0.00123	0.00087	-0.10129	-0.10904
N_v'	-0.00254^*	-0.00272	-0.00067	-0.00054	0.00131	0.00075
$N_r'-m'x_G'$	-0.00161^*	-0.00096	-0.00075	-0.00078	0.00001	-0.00013
Y_δ'	0.00201^*	0.00061	0.00076	0.00101	0.00164	0.00166
N_δ'	-0.00095^*	-0.00029	-0.00036	-0.00048	-0.00077	-0.00078
θ_9	$-3.7 \cdot 10^{-5}$	$1.5 \cdot 10^{-4}$	$-1.2 \cdot 10^{-4}$	0^*	0^*	0^*
θ_{10}	0.090	0.265	0.065	0^*	0^*	0^*
θ_{13}	$2.3 \cdot 10^{-5}$	$1.8 \cdot 10^{-4}$	$1.2 \cdot 10^{-4}$	$5.5 \cdot 10^{-6}$	$-7.4 \cdot 10^{-4}$	$5.7 \cdot 10^{-3}$
θ_{14}	$-1.4 \cdot 10^{-6}$	$-4.2 \cdot 10^{-6}$	$-1.9 \cdot 10^{-6}$	$9.2 \cdot 10^{-7}$	$9.6 \cdot 10^{-6}$	$-3.0 \cdot 10^{-5}$
θ_{15} [knots]	0.08	-0.46	0.45	0.01	0.02	-0.27
θ_{17} [deg/s]	-0.005	0.002	0.002	0.001	0.002	0.001
$R_1(1,1)$ [s]	–	–	$1.8 \cdot 10^{-1}$	$1.3 \cdot 10^{-2}$	$3.5 \cdot 10^{-2}$	$1.9 \cdot 10^{-2}$
$R_1(1,2)$ [s]	–	–	$1.0 \cdot 10^{-4}$	$-1.2 \cdot 10^{-4}$	$-2.0 \cdot 10^{-4}$	$-6.2 \cdot 10^{-5}$
$R_1(2,2)$ [s]	–	–	$5.7 \cdot 10^{-8}$	$1.1 \cdot 10^{-6}$	$1.2 \cdot 10^{-6}$	$2.0 \cdot 10^{-7}$
$R_2(1,1)$ [knots]^2	–	–	1.2	$1.4 \cdot 10^{-2}$	$3.3 \cdot 10^{-5}$	$1.3 \cdot 10^{-3}$
$R_2(2,2)$ [deg/s]^2	–	–	$1.4 \cdot 10^{-2}$	10^{-4*}	10^{-4*}	10^{-4*}
θ_{25} [knots]	-0.01	0.46	-0.31	0^*	0^*	0^*
θ_{26} [deg/s]	0.000	-0.035	-0.042	0^*	0^*	0^*
θ_{27} [deg]	146.00	148.73	146.50	146.58^*	146.58^*	146.58^*
T_D [s]	3.0	10.0	7.8	10.0	6.0	0.6
K'	1.59	-0.32	-0.50	-0.65	-1.54	-1.82
K_1'	-1.00	–	-0.38	–	-0.84	-0.84
K_v'	-1.38	0.01	0.03	0.05	0.60	0.72
K_{1v}'	0.12	–	0.05	–	0.11	0.11
T_1'	-4.88	complex	1.84	complex	1.83	2.17
T_2'	0.43	poles	1.70	poles	0.06	0.06
T_3'	1.32	0.74	2.38	1.62	0.06	0.06
T_{3v}'	0.19	3.70	5.42	2.55	0.02	0.02

* = fixed value

Table 4.3 - Estimated parameters from identifications to data from experiment E3.

	Output error (SSPA:s model)	Output error	M L	Prediction error p = 4	p = 6	p = 6 Rudd. angl. is input
Figure	4.16	4.17	4.18	–	4.19	4.20
ν	10	15	20	14	14	14
V	0.38	0.16	$2.7 \cdot 10^{-4}$	$9.8 \cdot 10^{-3}$	$2.4 \cdot 10^{-2}$	$2,5 \cdot 10^{-2}$
AIC	-365	-487	-1454	–	–	–
$Y_v{}'$	-0.00687^*	-0.01047	-0.02387	-0.66046	-0.41722	-0.44198
$Y_r{}'-m'$	-0.00724^*	-0.00694	-0.00508	-0.27787	-0.17487	-0.18986
$N_v{}'$	-0.00254^*	-0.00249	0.00050	0.01806	-0.03403	-0.03288
$N_r{}'-m'x_G{}'$	-0.00161^*	-0.00128	-0.00043	0.00723	-0.01504	-0.01497
$Y_\delta{}'$	0.00201^*	0.00206	0.00046	0.00168	0.00272	0.00292
$N_\delta{}'$	-0.00095^*	-0.00097	-0.00022	-0.00079	-0.00128	-0.00138
θ_9	$-9.0 \cdot 10^{-6}$	$2.3 \cdot 10^{-5}$	$-2.6 \cdot 10^{-4}$	0^*	0^*	0^*
θ_{10}	-0.060	0.275	0.315	0^*	0^*	0^*
θ_{13}	$-5.6 \cdot 10^{-7}$	$-3.6 \cdot 10^{-5}$	$4.4 \cdot 10^{-3}$	$1.0 \cdot 10^{-3}$	$-1.9 \cdot 10^{-4}$	$-5.5 \cdot 10^{-5}$
θ_{14}	$4.3 \cdot 10^{-7}$	$-4.9 \cdot 10^{-7}$	$1.3 \cdot 10^{-4}$	$-2.2 \cdot 10^{-5}$	$-4.8 \cdot 10^{-6}$	$-3.3 \cdot 10^{-5}$
θ_{15} [knots]	0.01	-0.05	-2.00	-0.04	-0.01	-0.01
θ_{17} [deg/s]	-0.001	0.000	0.000	0.000	0.000	0.000
$R_1(1,1)$ [s]	–	–	2.2	$2.3 \cdot 10^{-3}$	$3.5 \cdot 10^{-4}$	$1.9 \cdot 10^{-3}$
$R_1(1,2)$ [s]	–	–	$-7.4 \cdot 10^{-4}$	$-7.1 \cdot 10^{-5}$	$3.5 \cdot 10^{-5}$	$1.3 \cdot 10^{-4}$
$R_1(2,2)$ [s]	–	–	$2.5 \cdot 10^{-7}$	$2.2 \cdot 10^{-6}$	$3.5 \cdot 10^{-6}$	$9.3 \cdot 10^{-6}$
$R_2(1,1)$ [knots]^2	–	–	$1.5 \cdot 10^{-4}$	2.7	27.7	11139.1
$R_2(2,2)$ [deg/s]^2	–	–	$9.6 \cdot 10^{-2}$	10^{-4*}	10^{-4*}	10^{-4*}
θ_{25} [knots]	-0.02	-0.17	2.05	0^*	0^*	0^*
θ_{26} [deg/s]	0.000	-0.072	-0.001	0^*	0^*	0^*
θ_{27} [deg]	146.83	148.75	147.10	147.13^*	147.13^*	147.13^*
T_D [s]	8.7	7.6	7.9	6.8	7.7	2.0
K'	1.59	3.97	-0.39	-2.03	-1.93	-1.88
$K_1{}'$	-1.00	-1.03	-0.23	-1.00	-1.49	-1.63
$K_v{}'$	-1.38	-2.43	0.10	0.86	0.82	0.81
$K_{1v}{}'$	0.12	0.13	0.03	0.14	0.21	0.23
$T_1{}'$	-4.88	-8.43	1.50	2.04	1.94	1.73
$T_2{}'$	0.43	0.47	0.79	0.03	0.02	0.02
$T_3{}'$	1.32	1.03	0.71	0.03	0.03	0.03
$T_{3v}{}'$	0.19	0.21	0.33	0.01	0.01	0.01

* = fixed value

Table 4.4 – Estimated parameters from identifications to data from experiment E4.
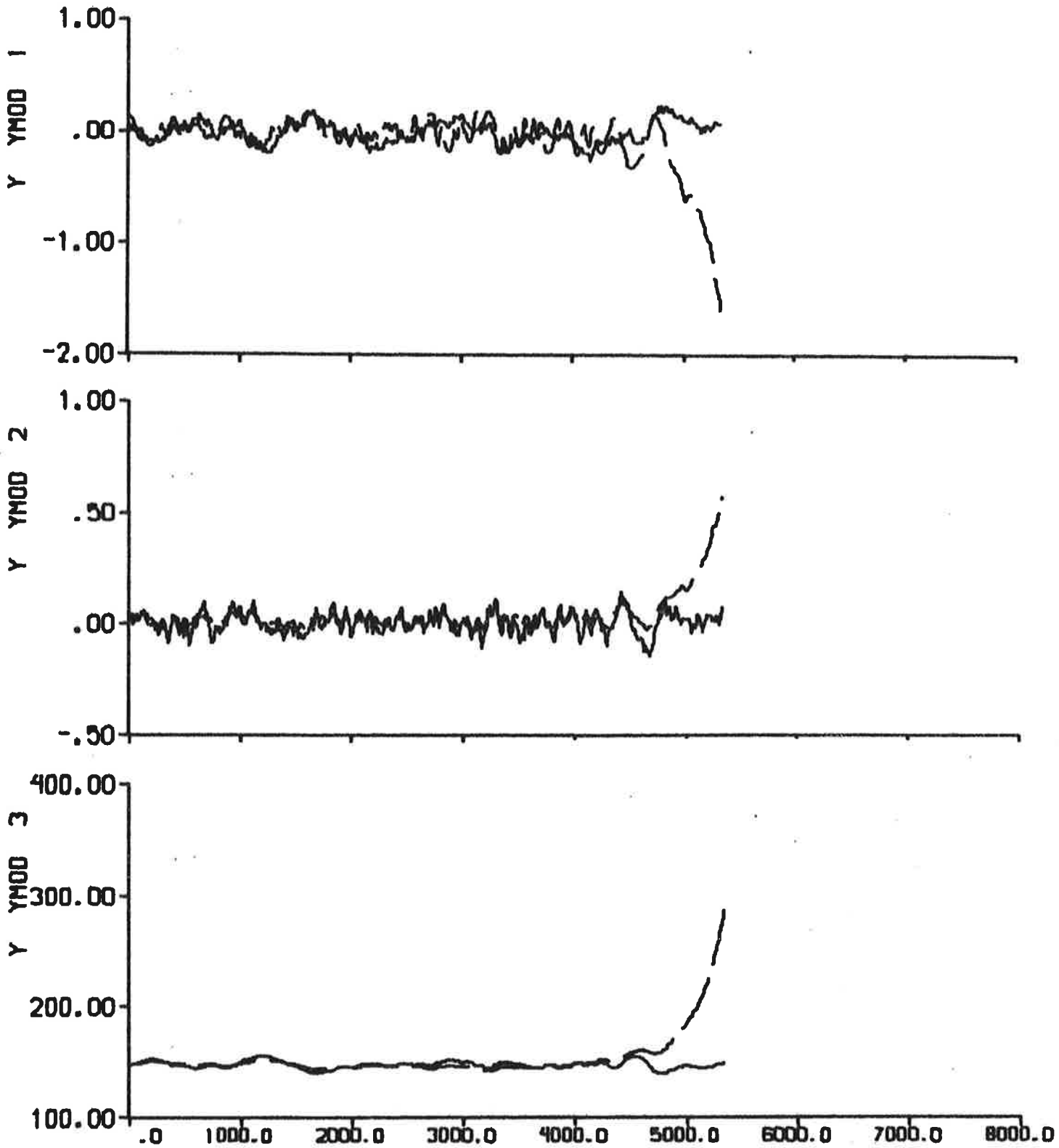
Fig. 4.1a - Result of output error identification to data
from experiment El, when the model is fixed
to SSPA:s model.
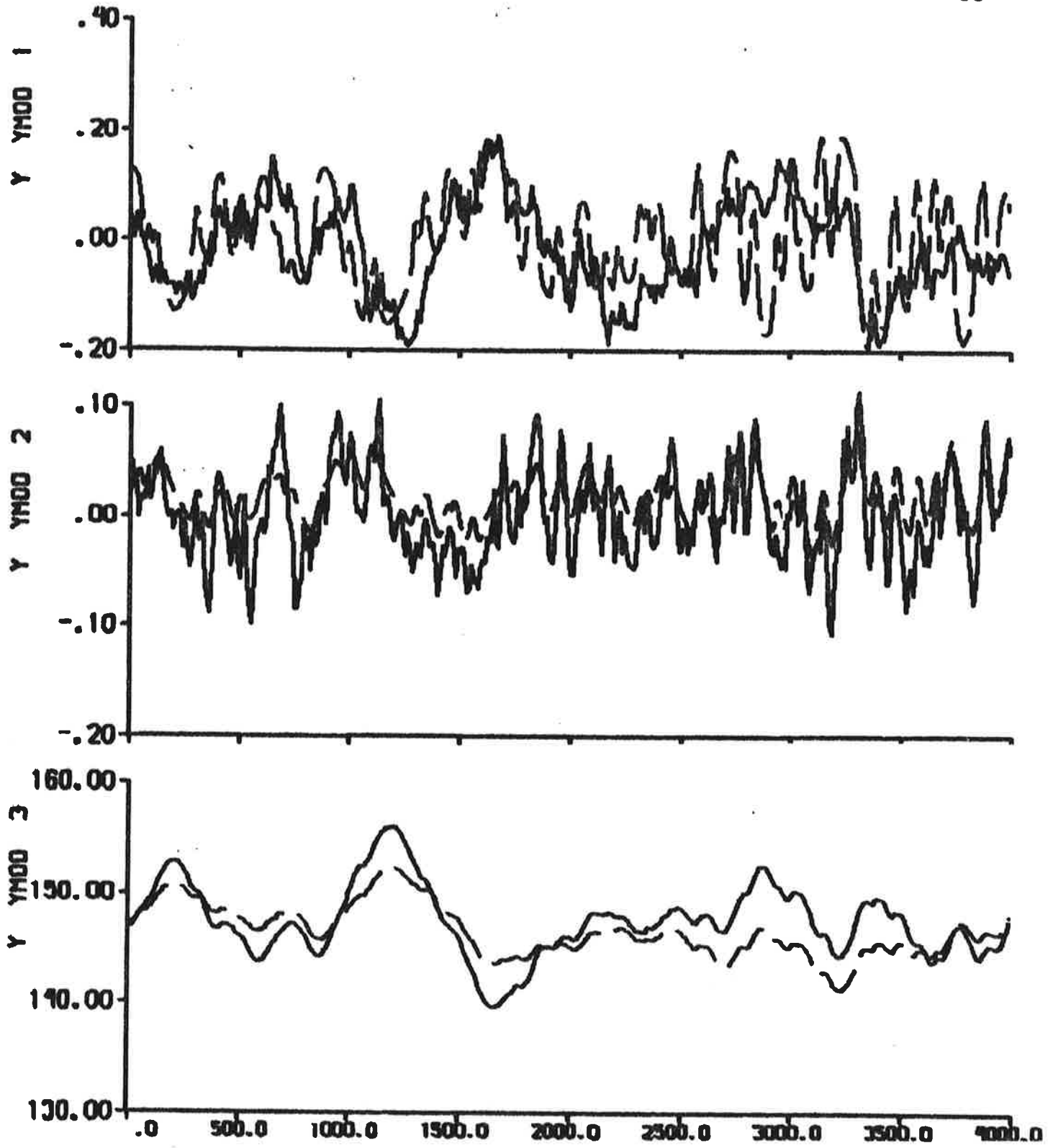
Fig. 4.1b - First part of Fig. 4.1a.
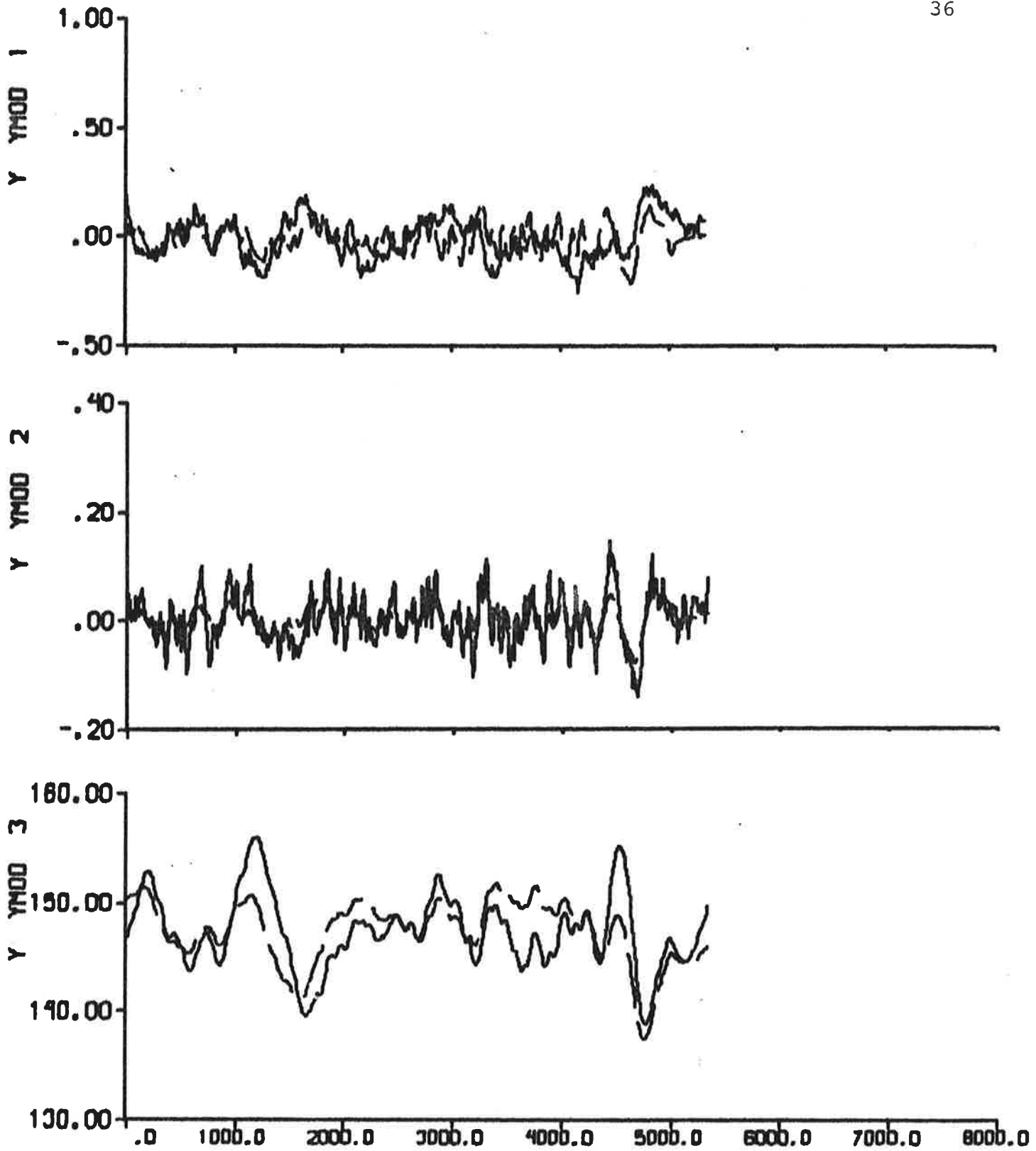
Fig. 4.2 - Result of output error identification to data from experiment El.
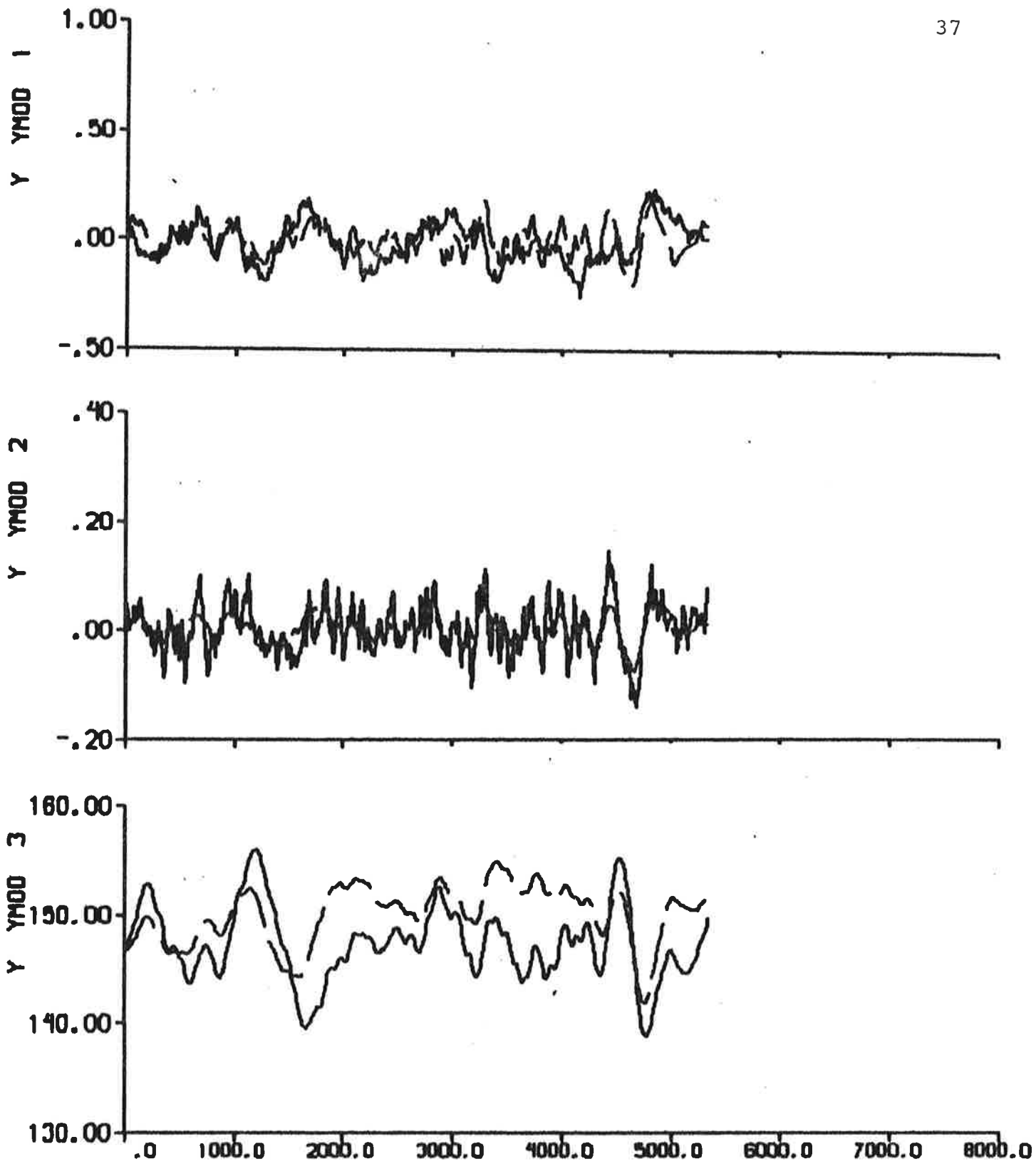
Fig. 4.3a – Result of ML identification to data
from experiment E1.
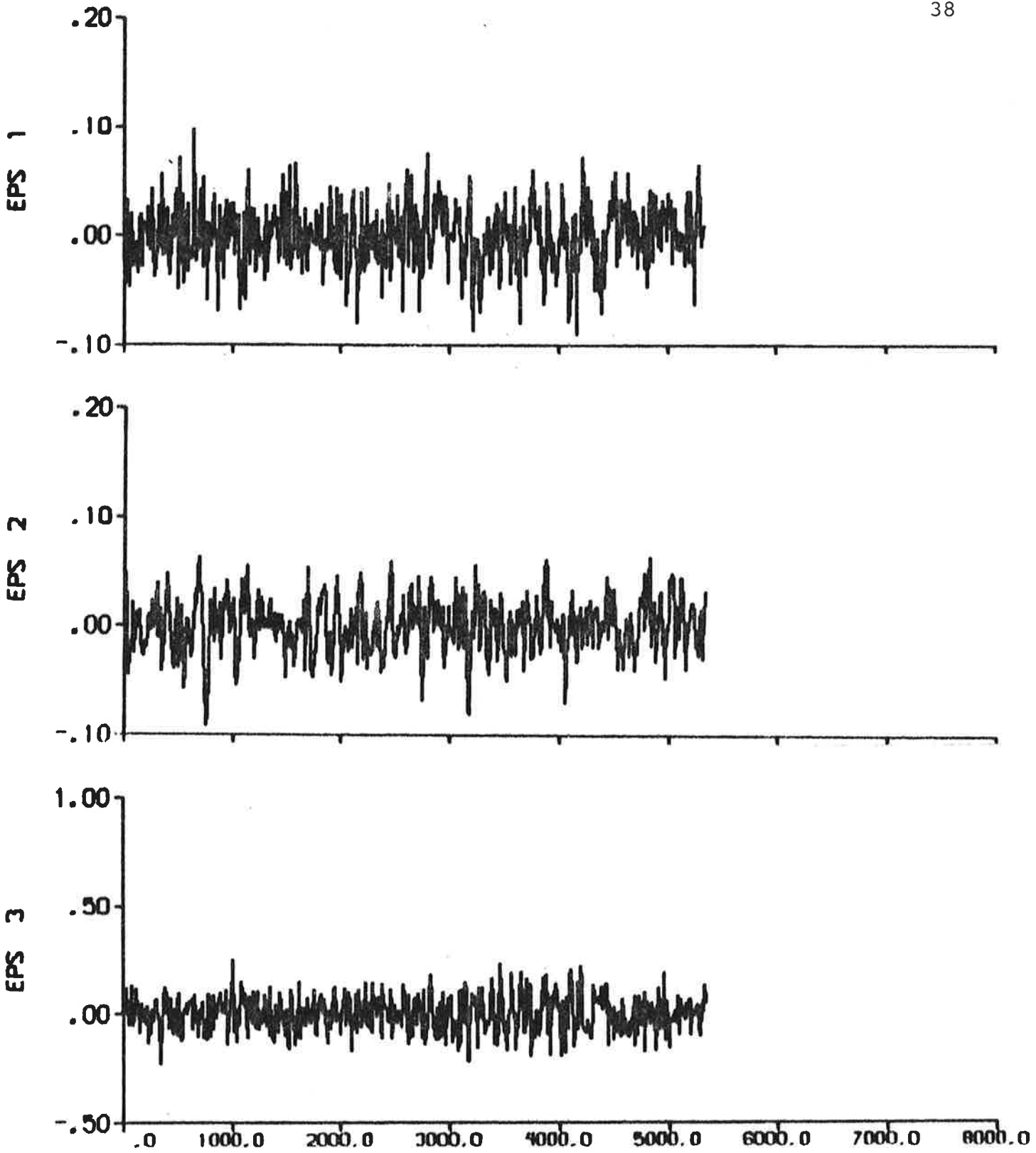
Fig. 4.3b - Prediction errors.
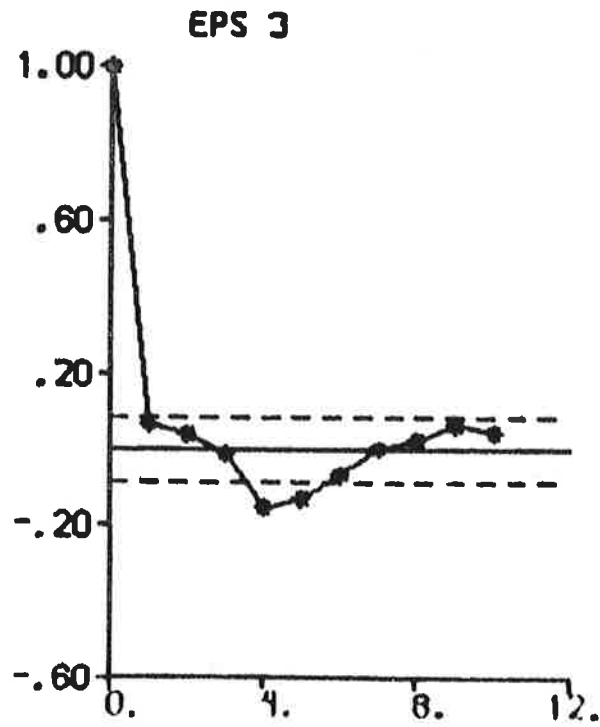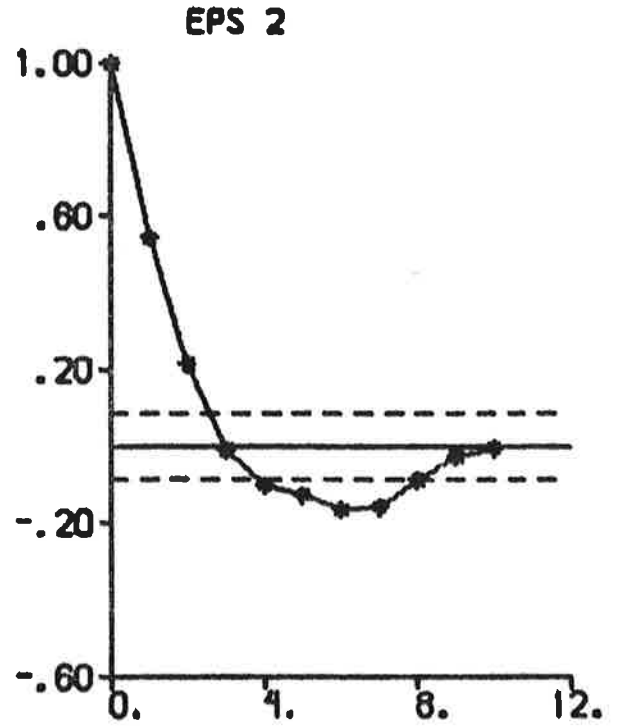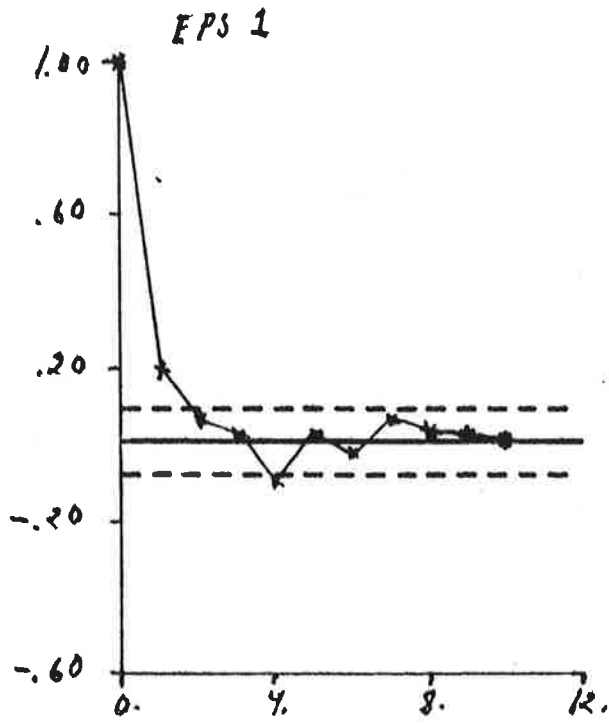
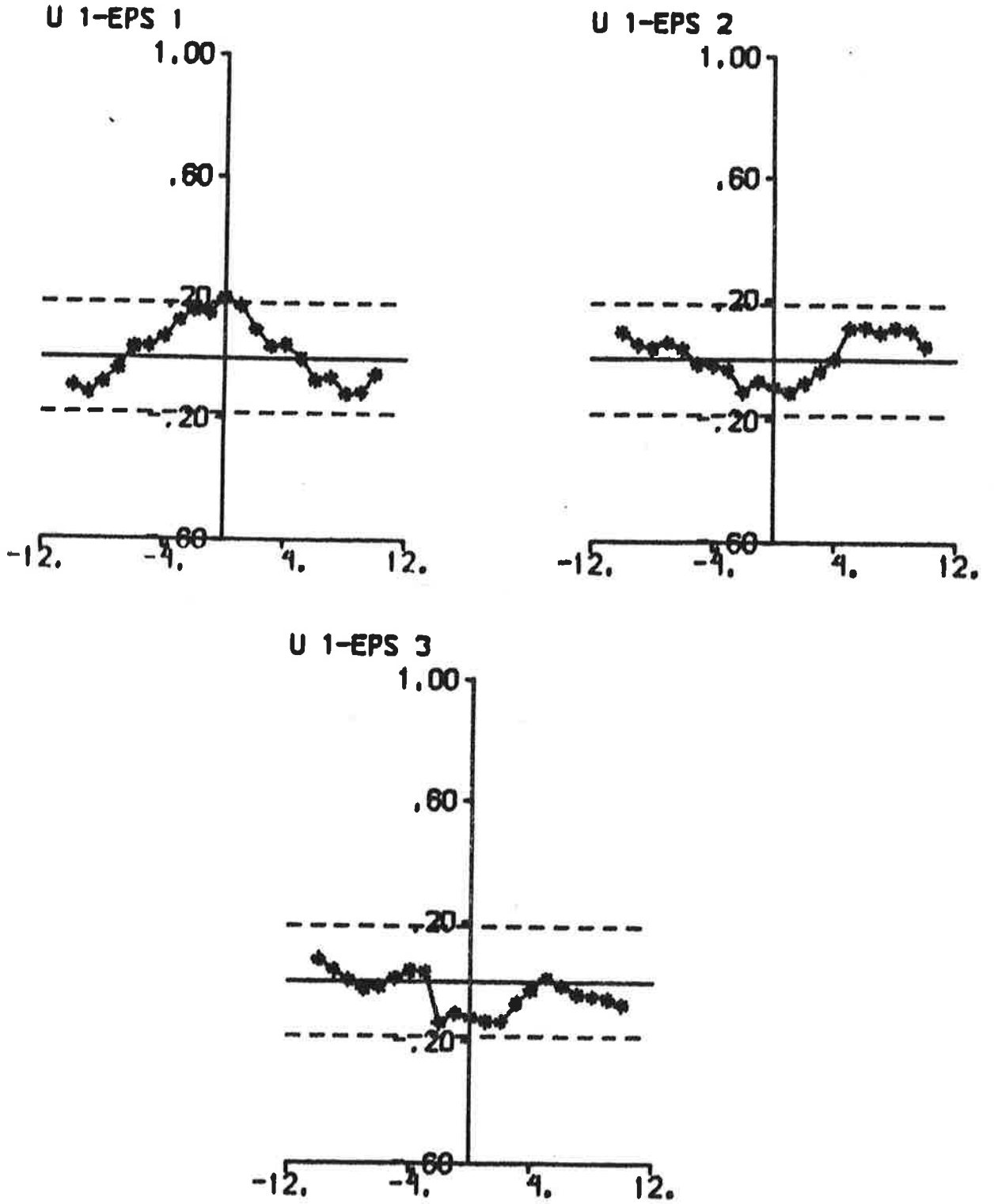Fig. 4.3c - Autocorrelation functions of
prediction errors.
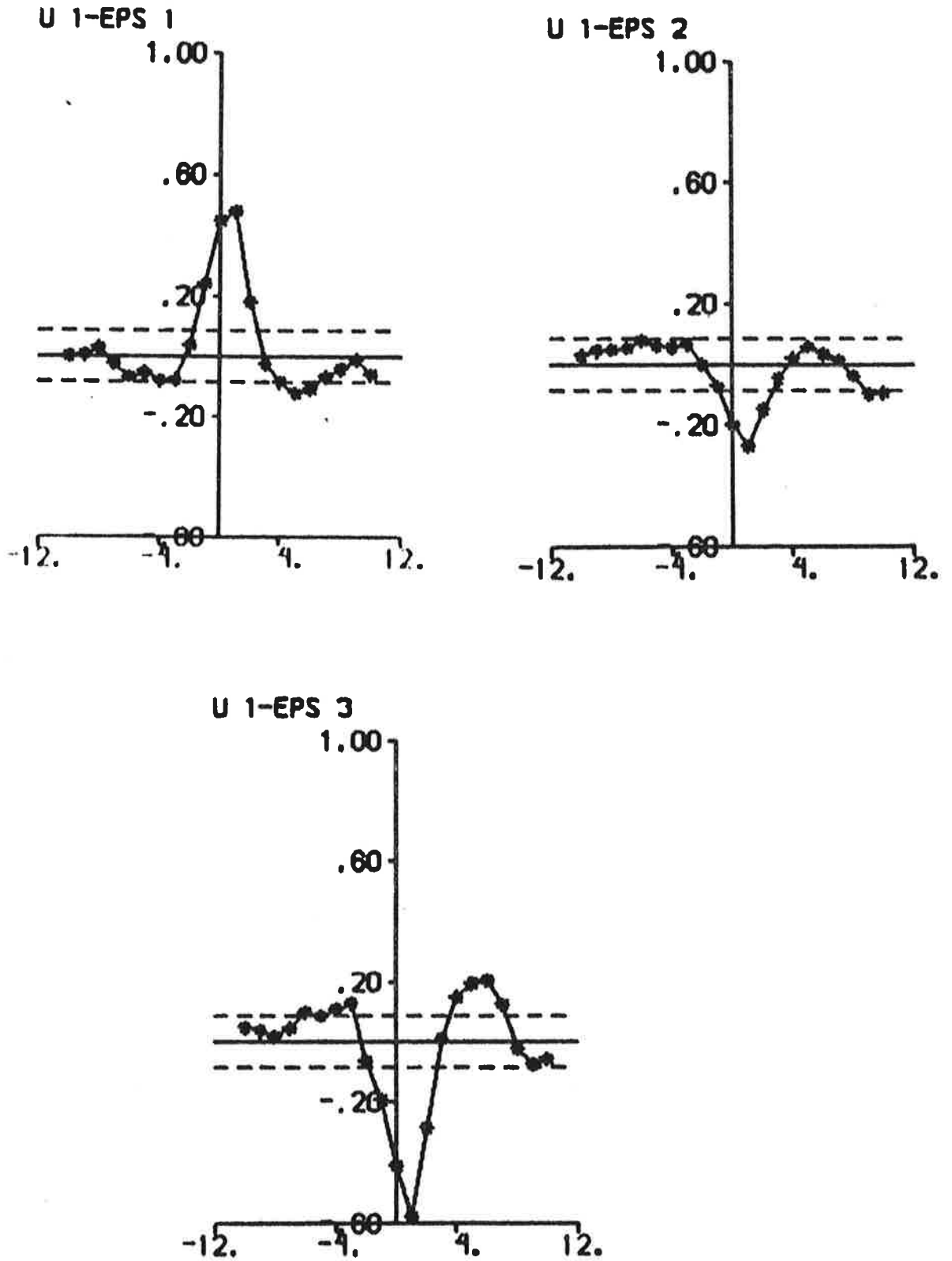
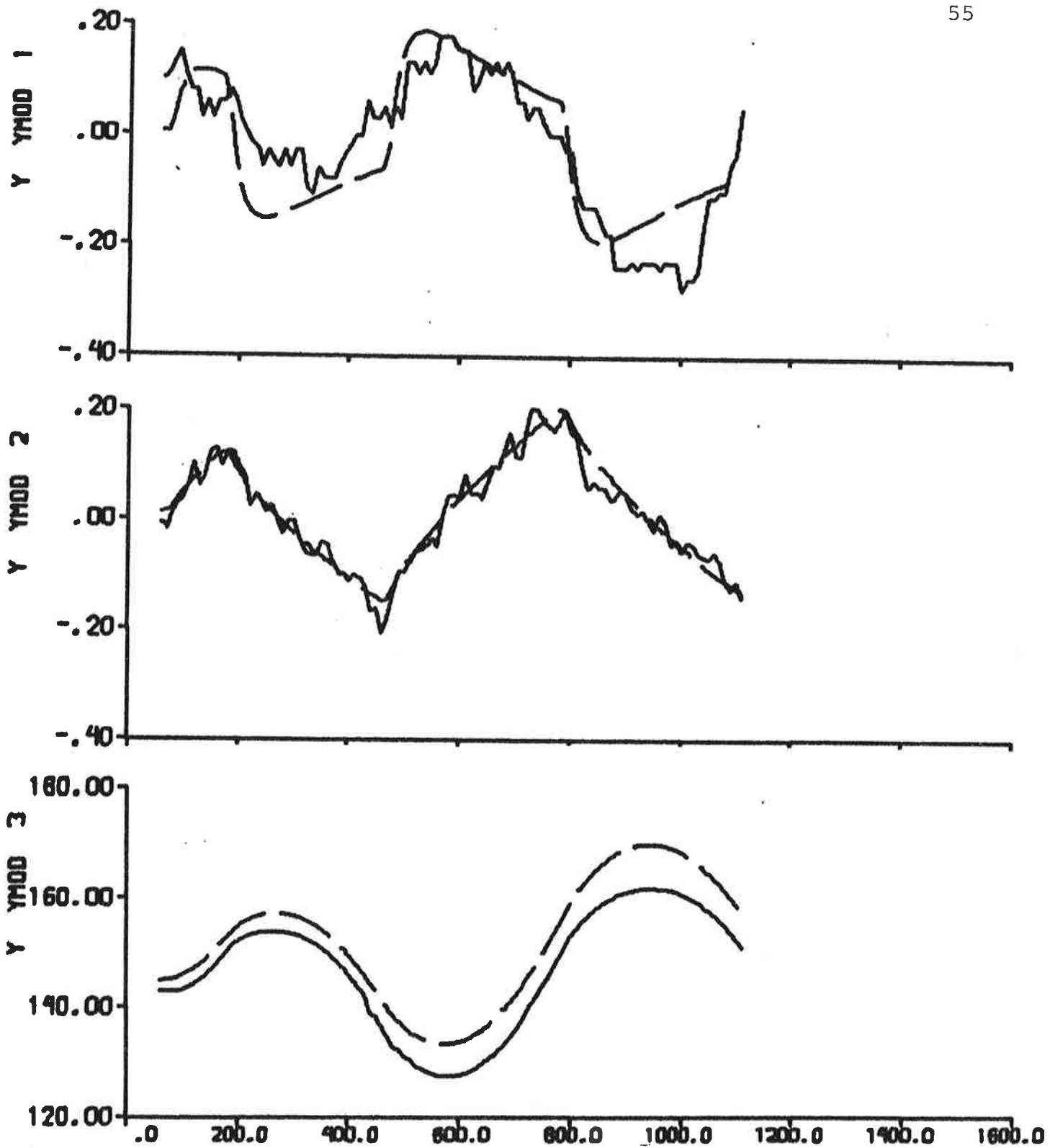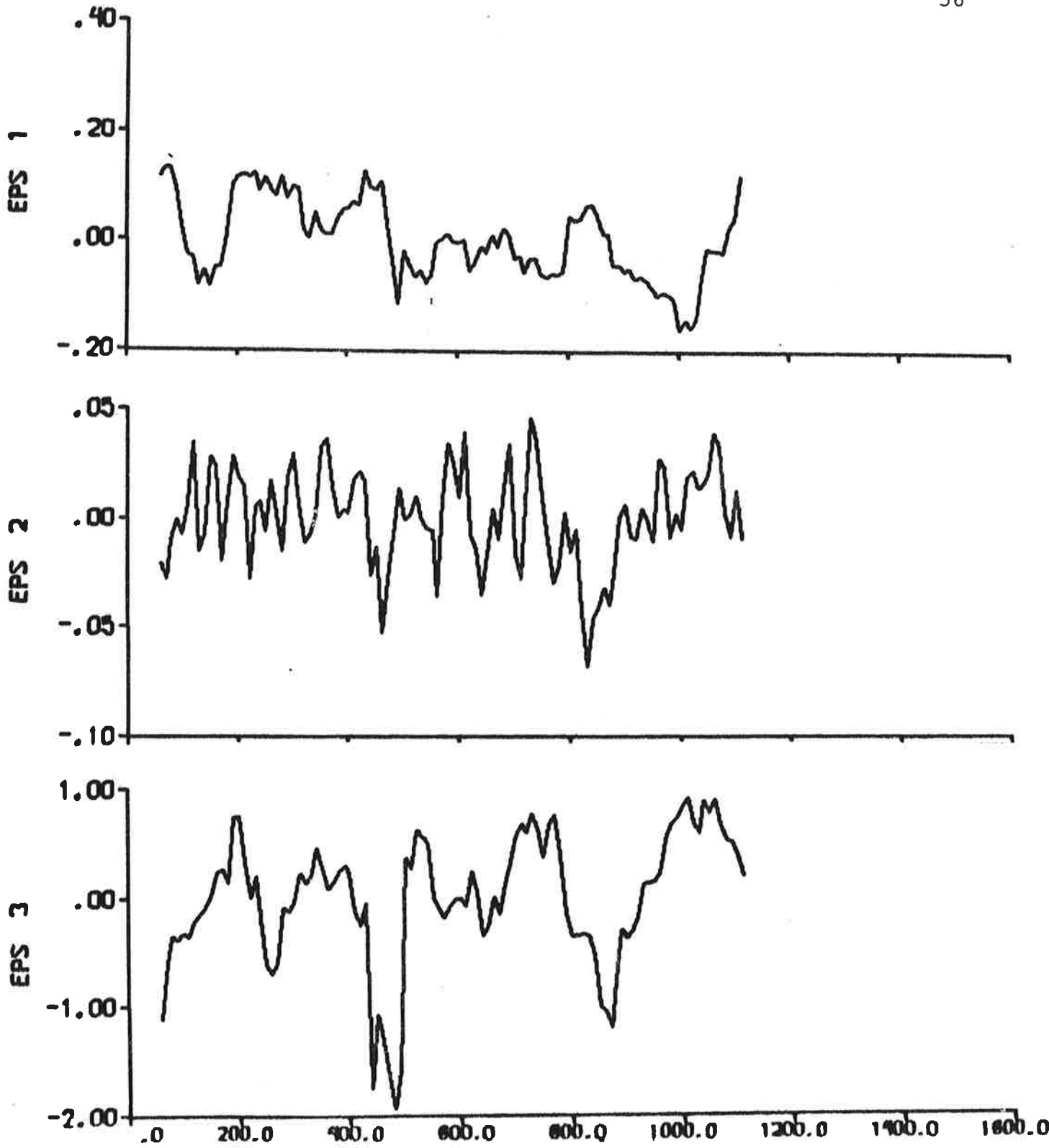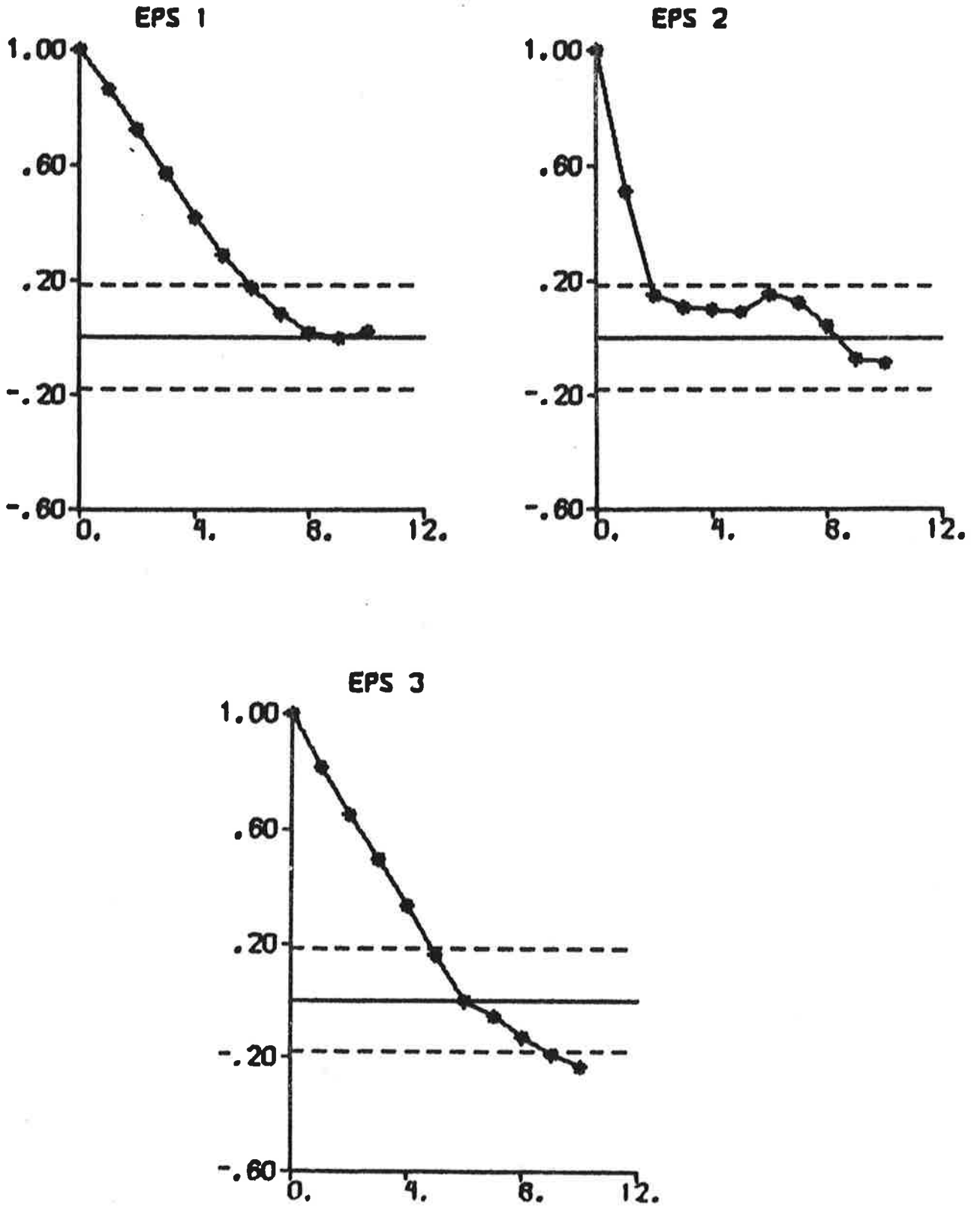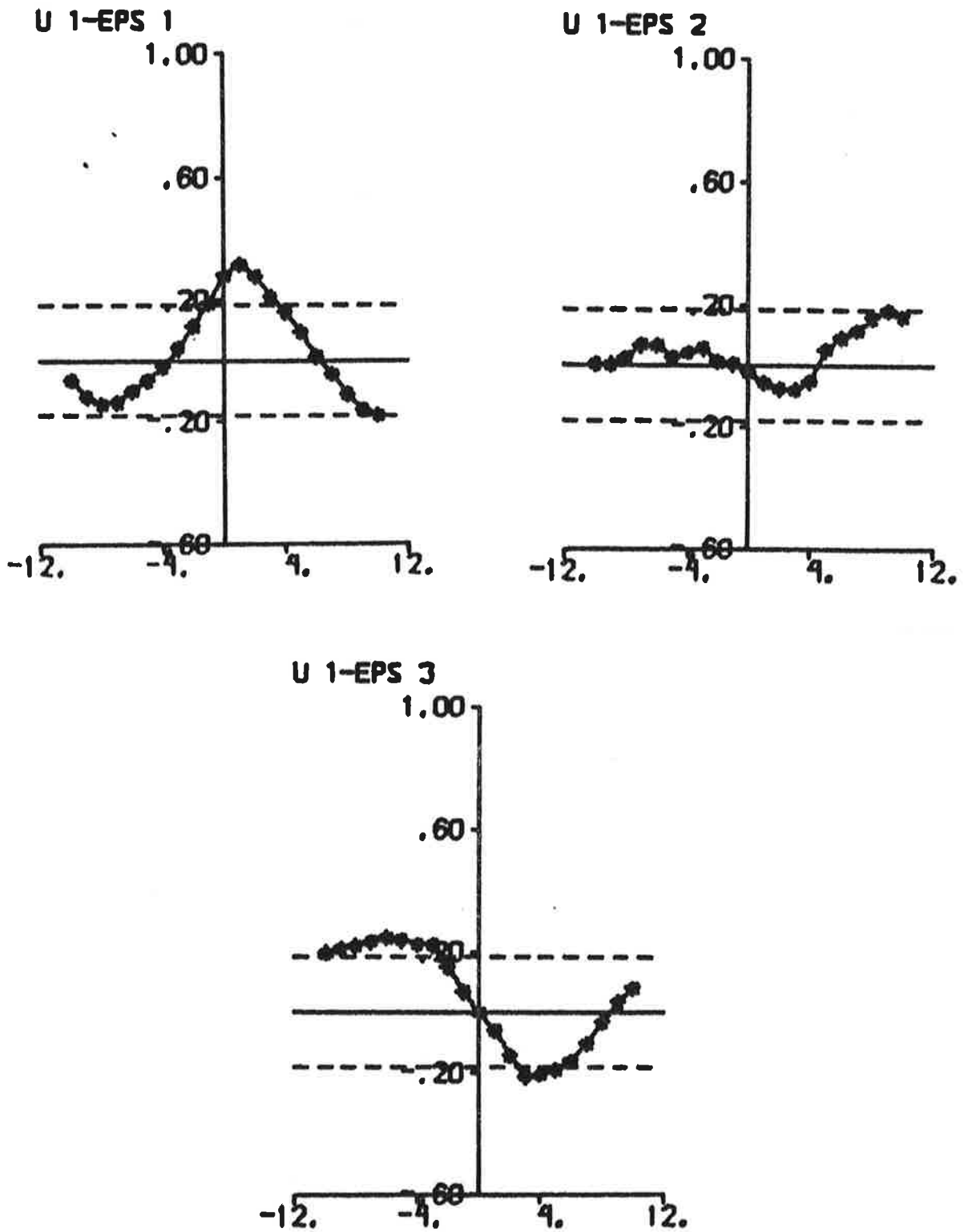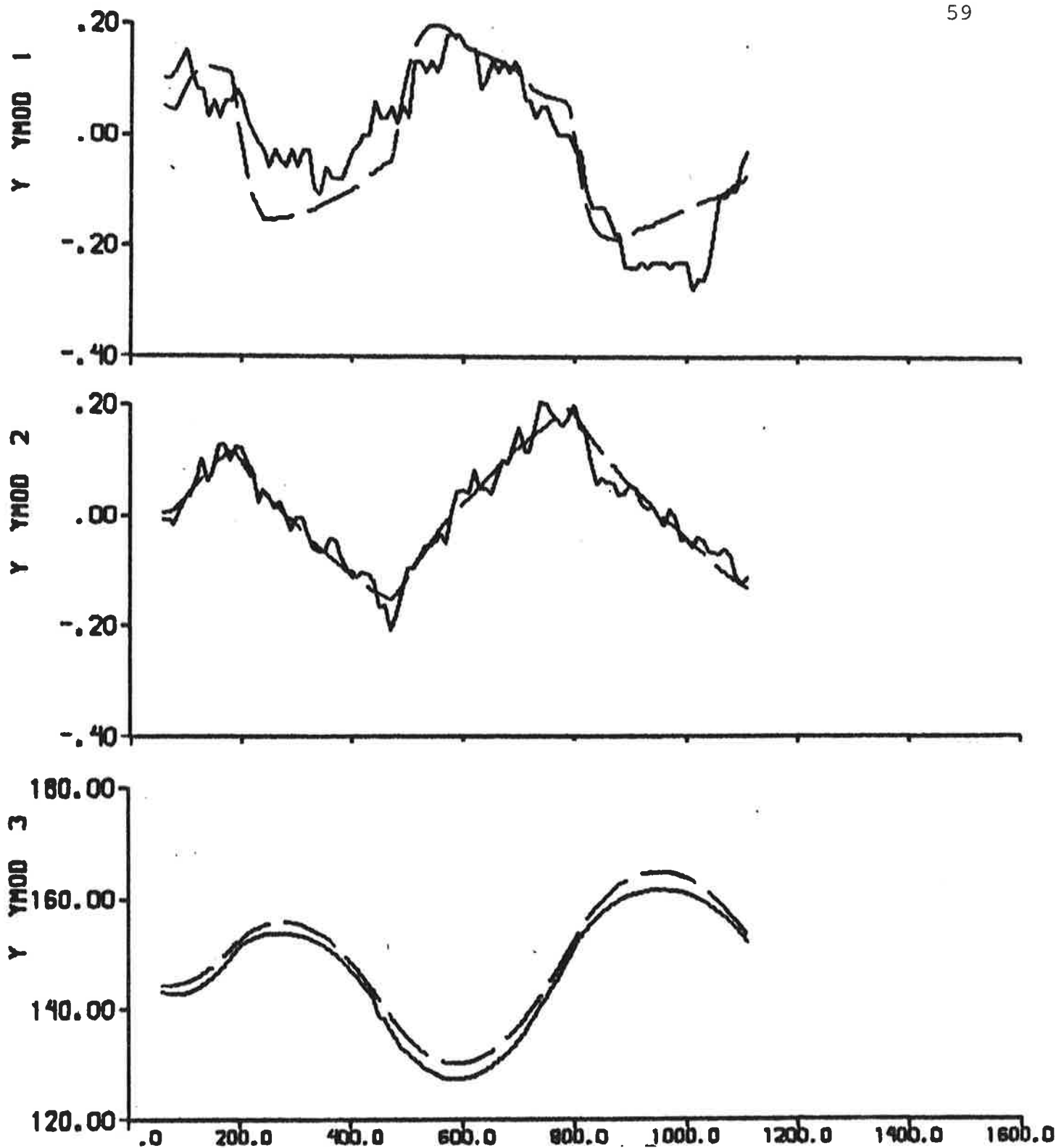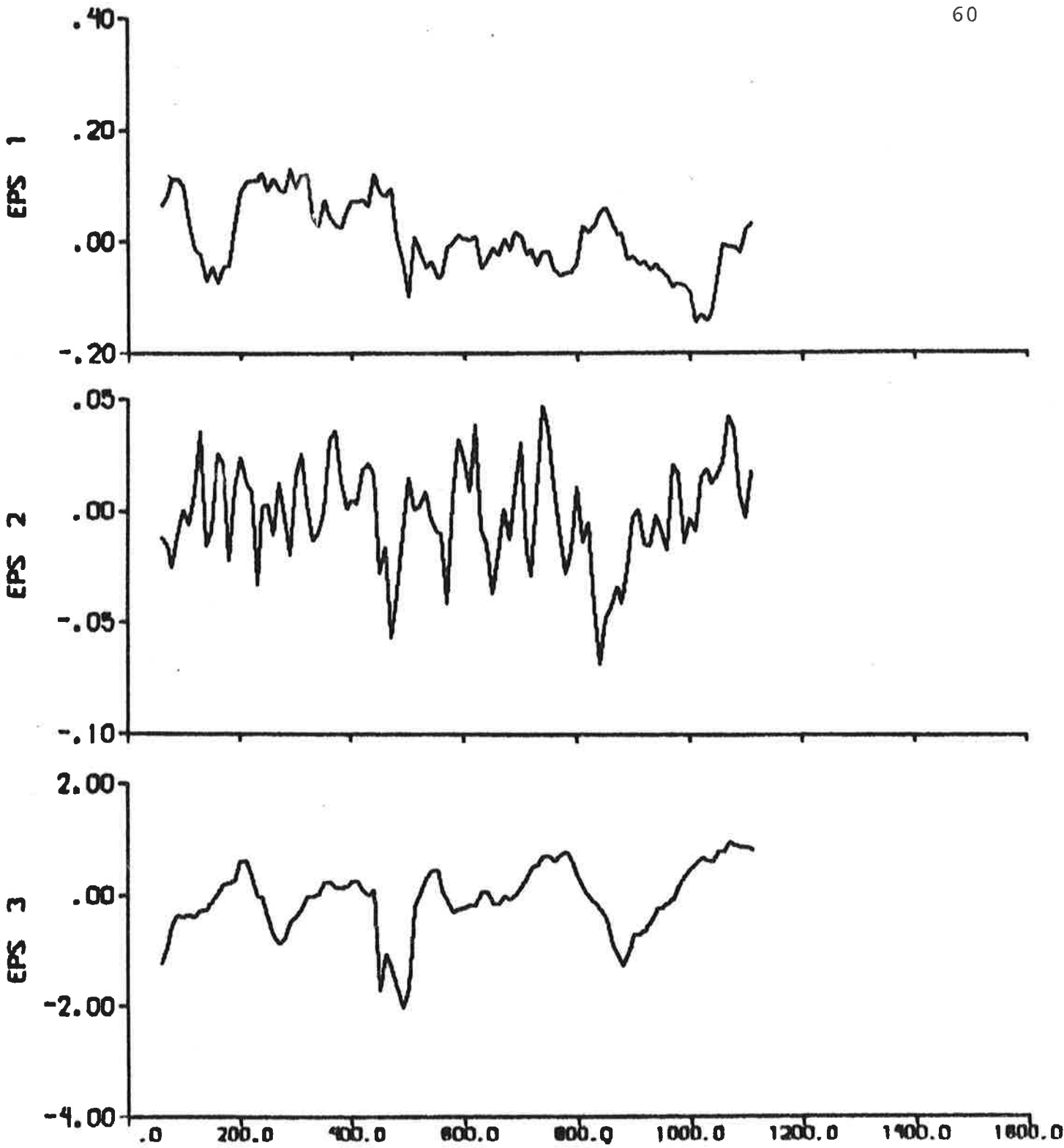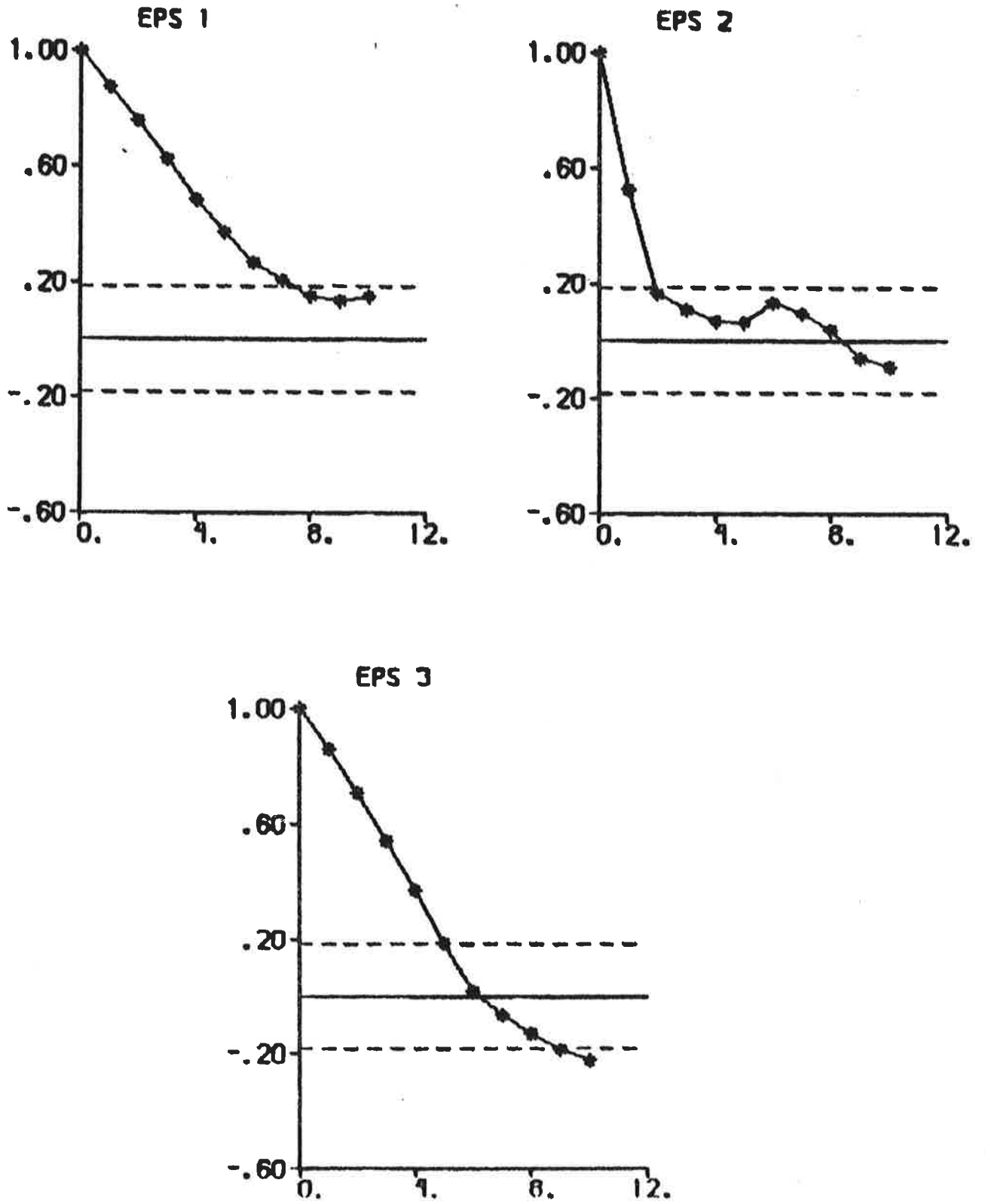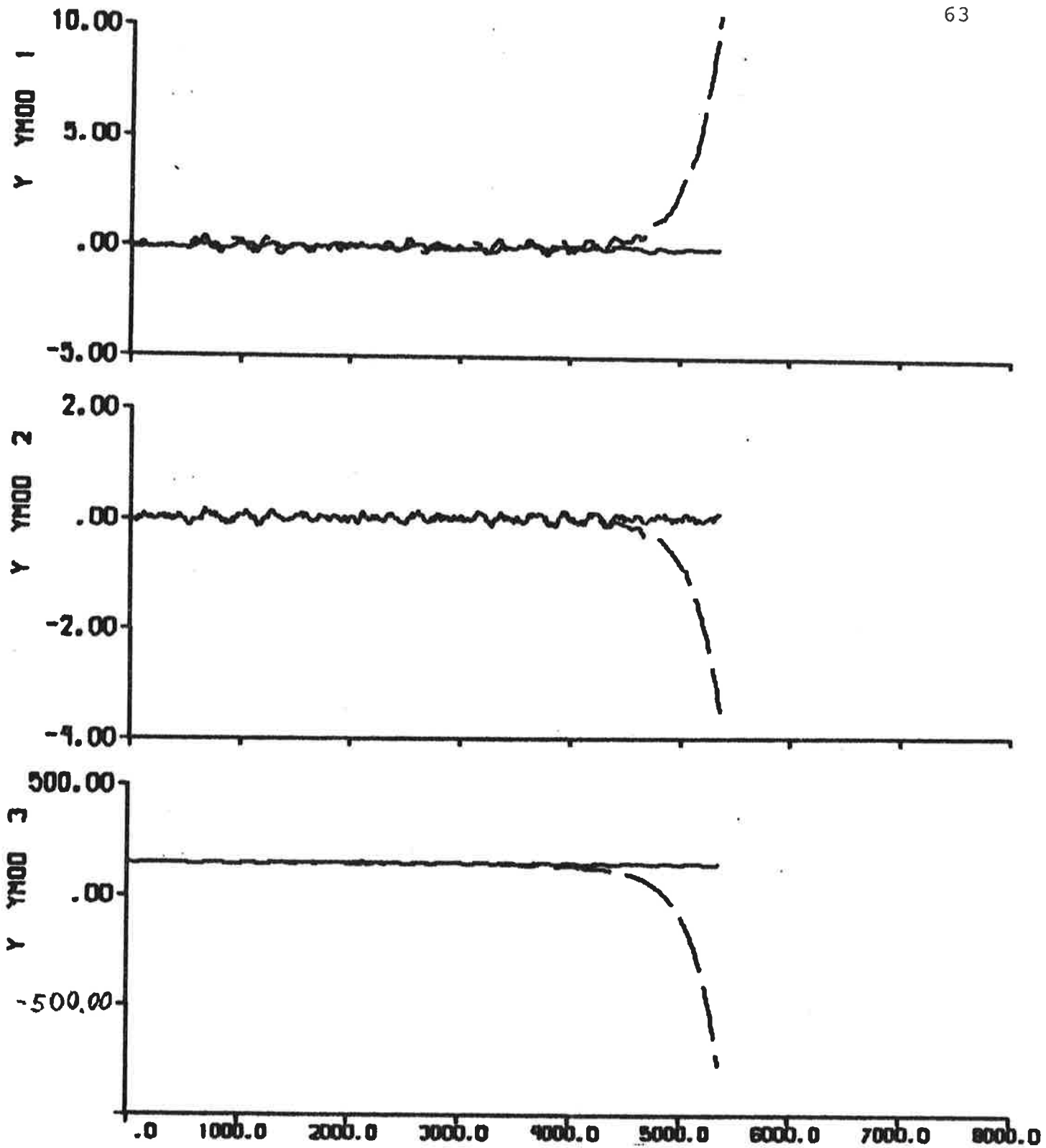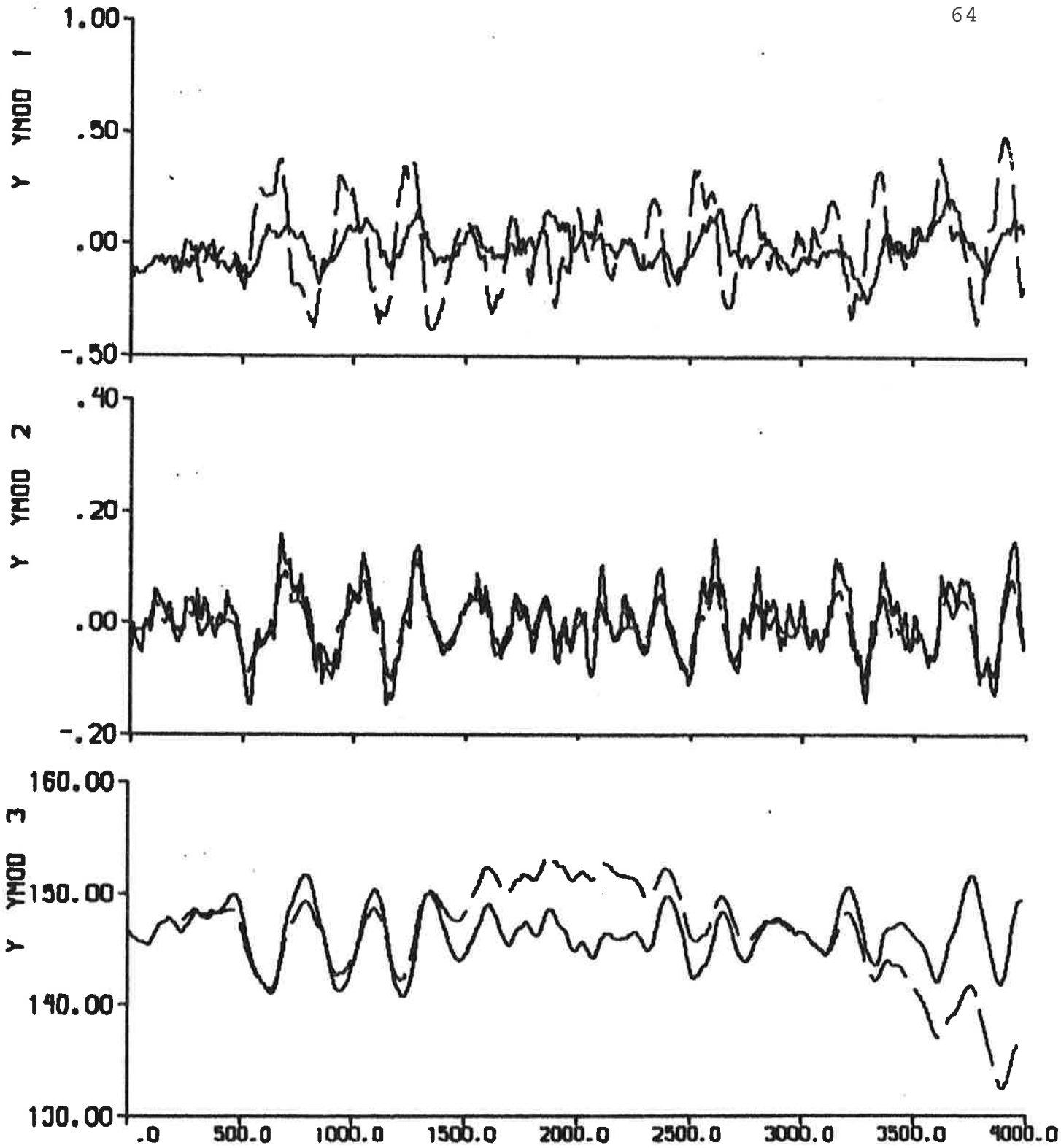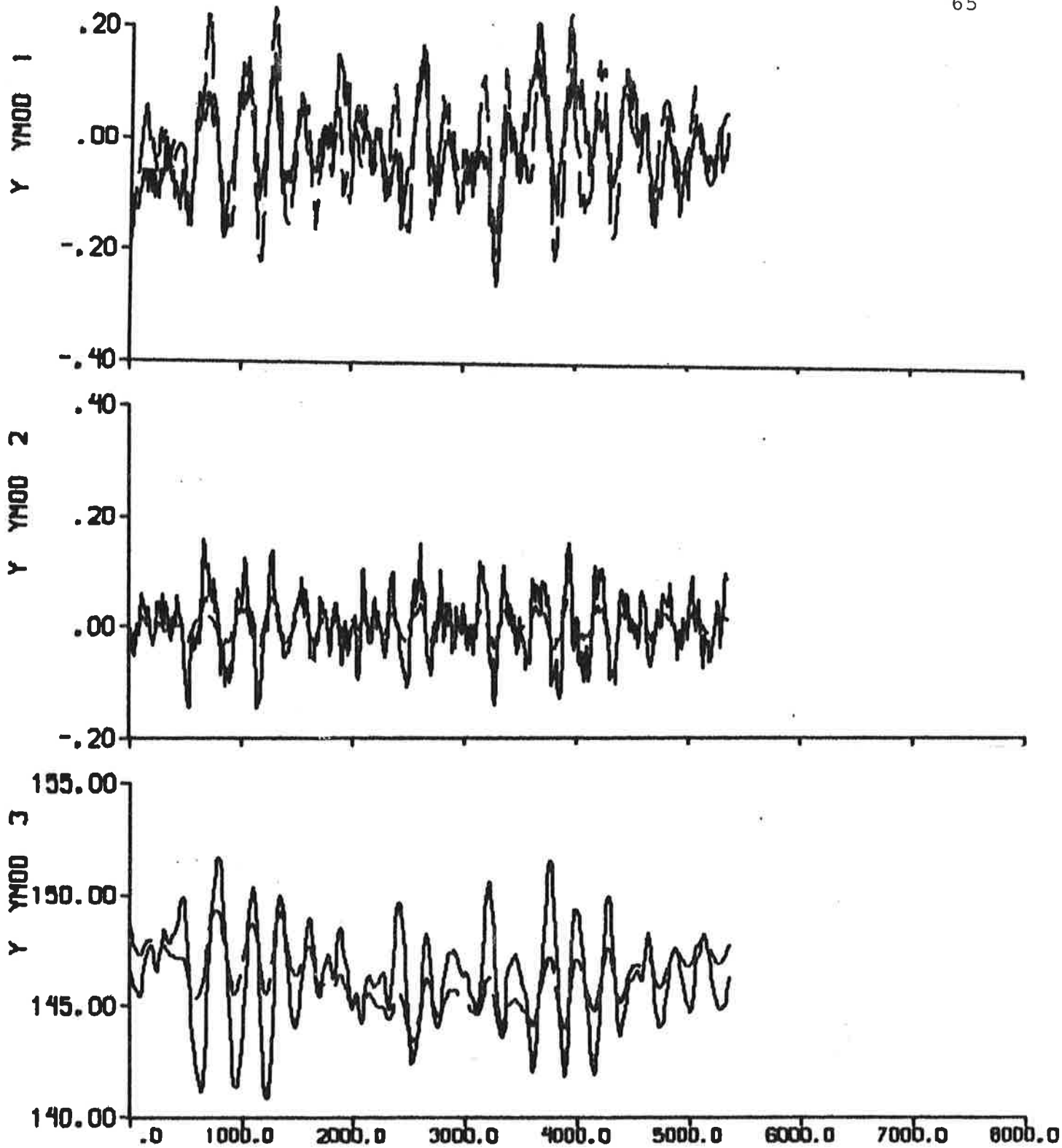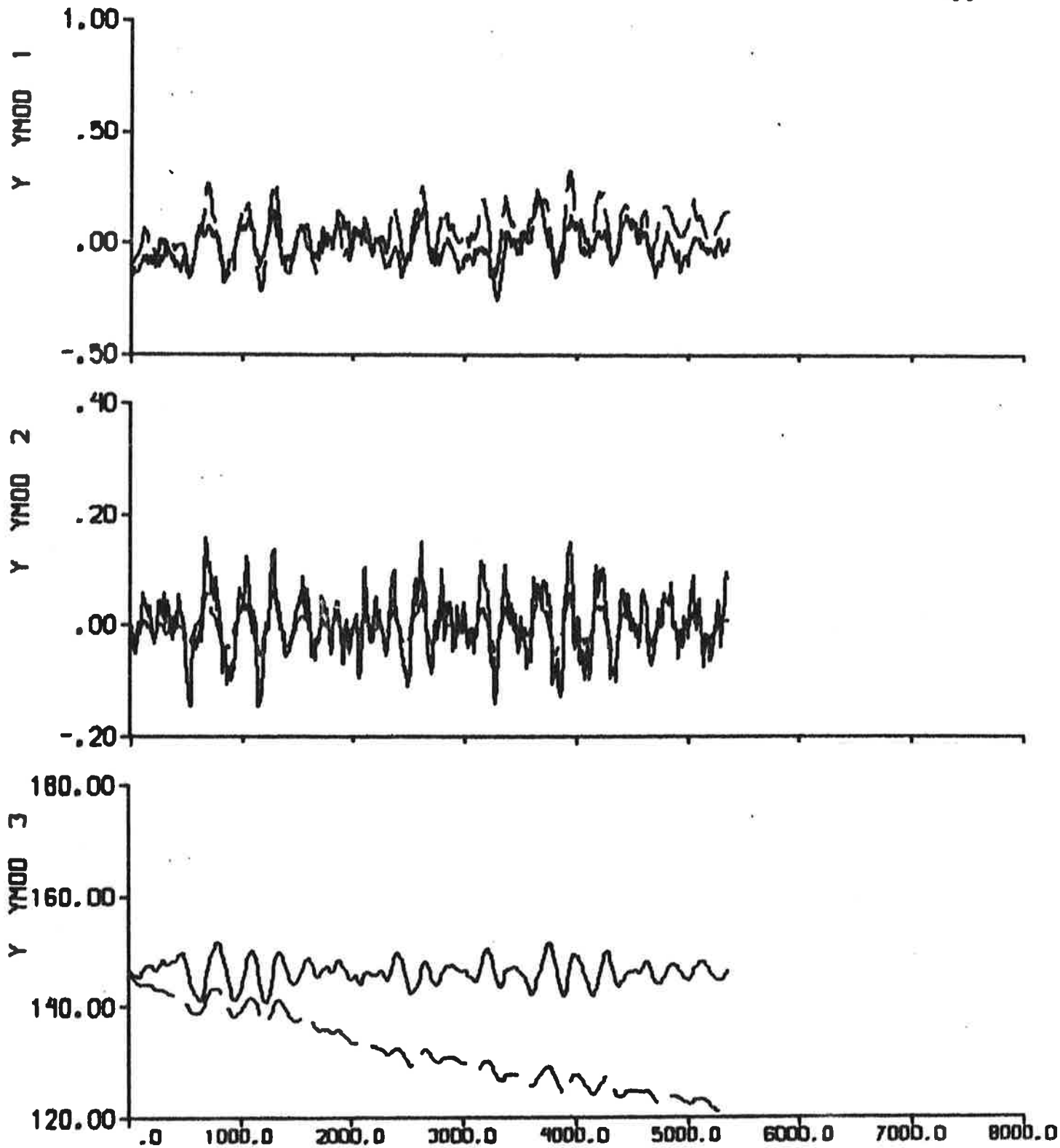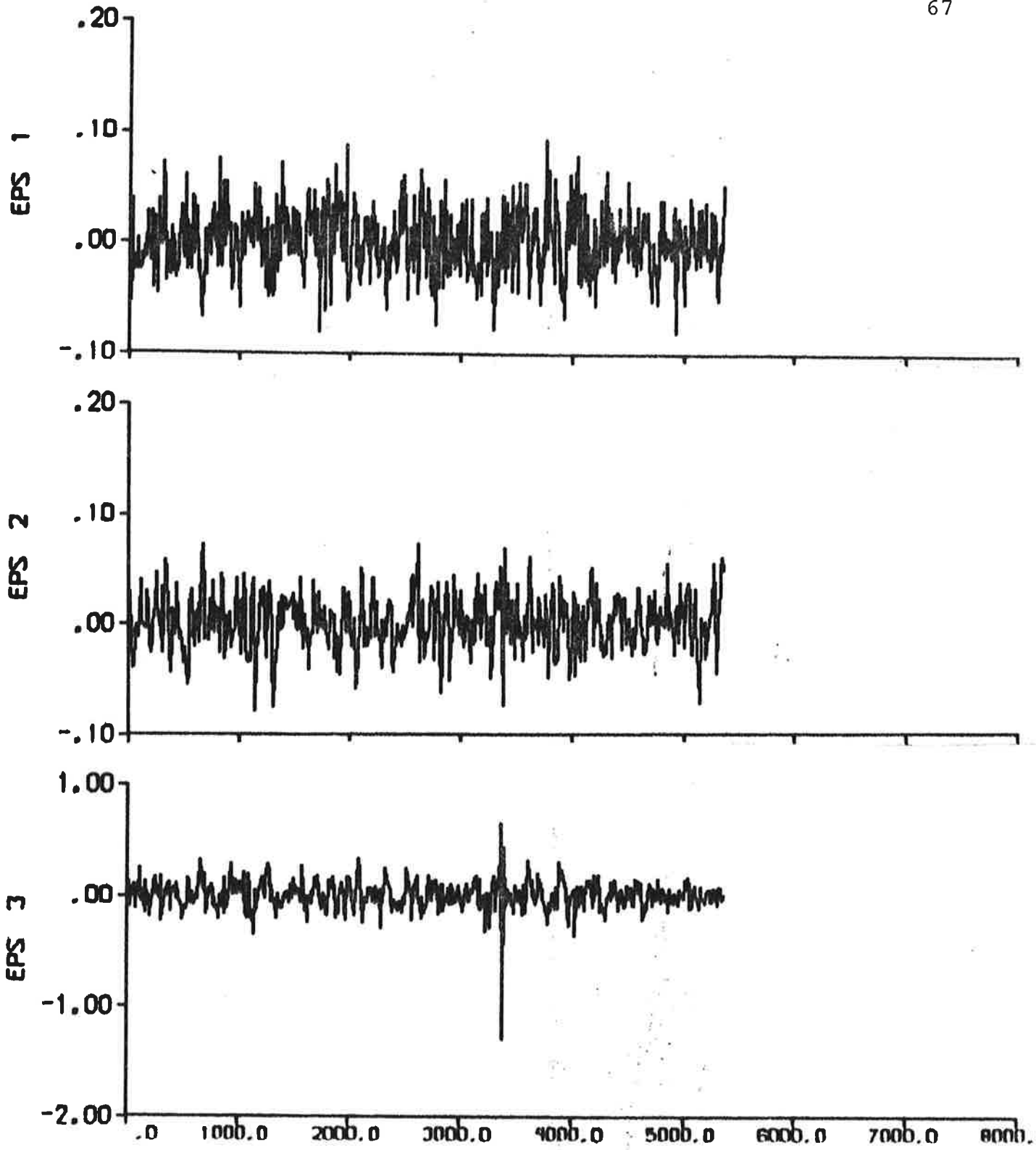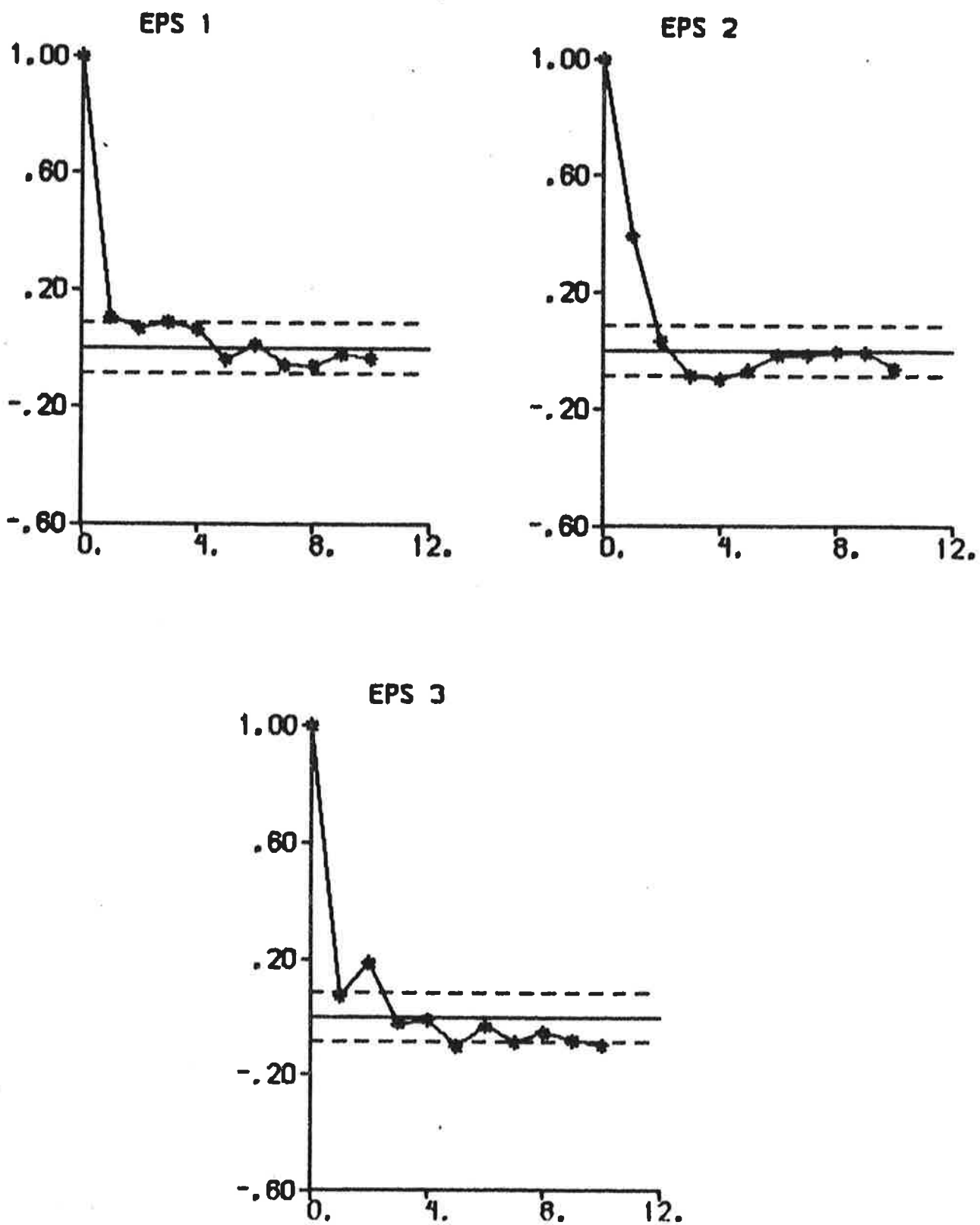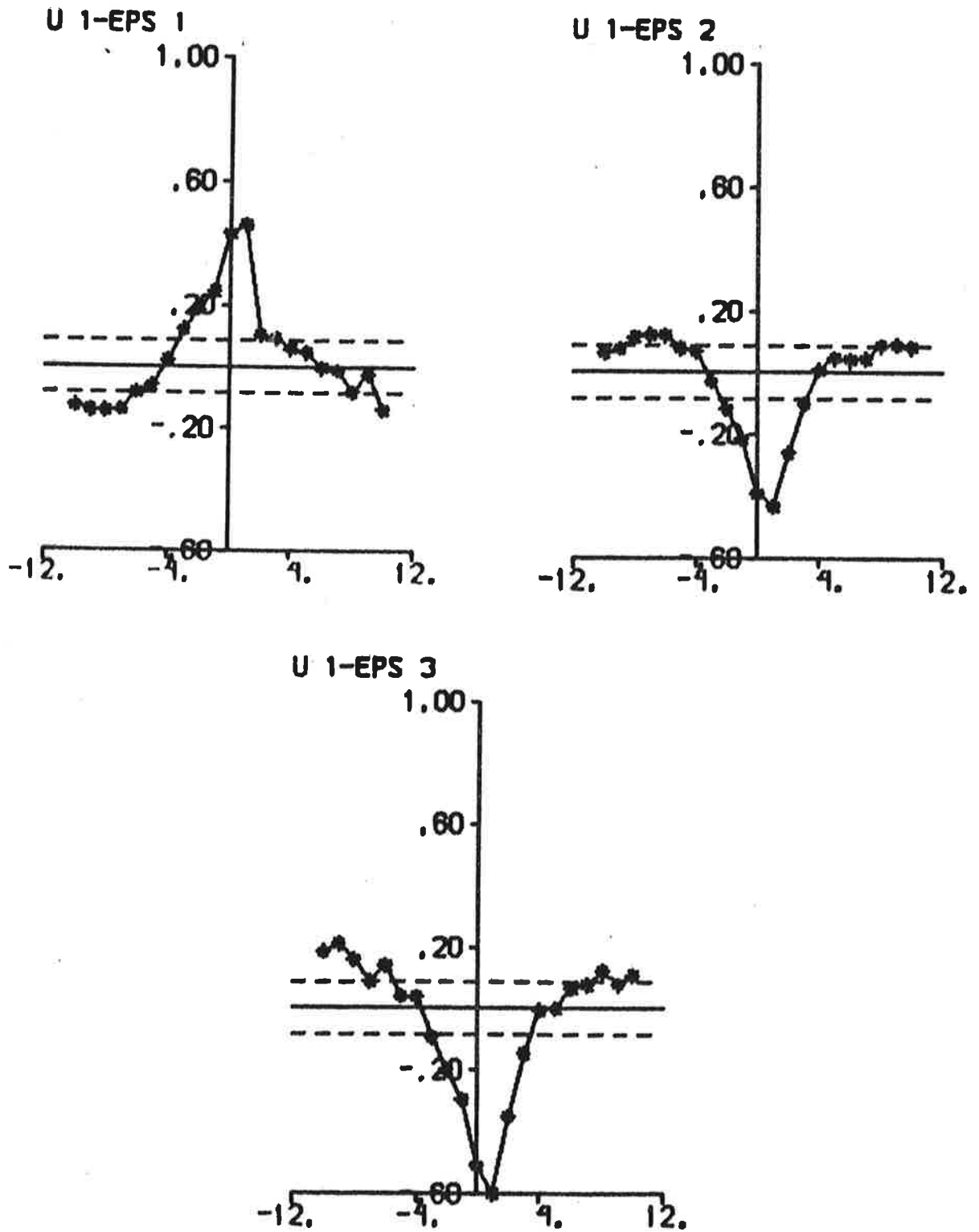Fig. 4.3d - Cross correlation functions between rudder
input and prediction errors.
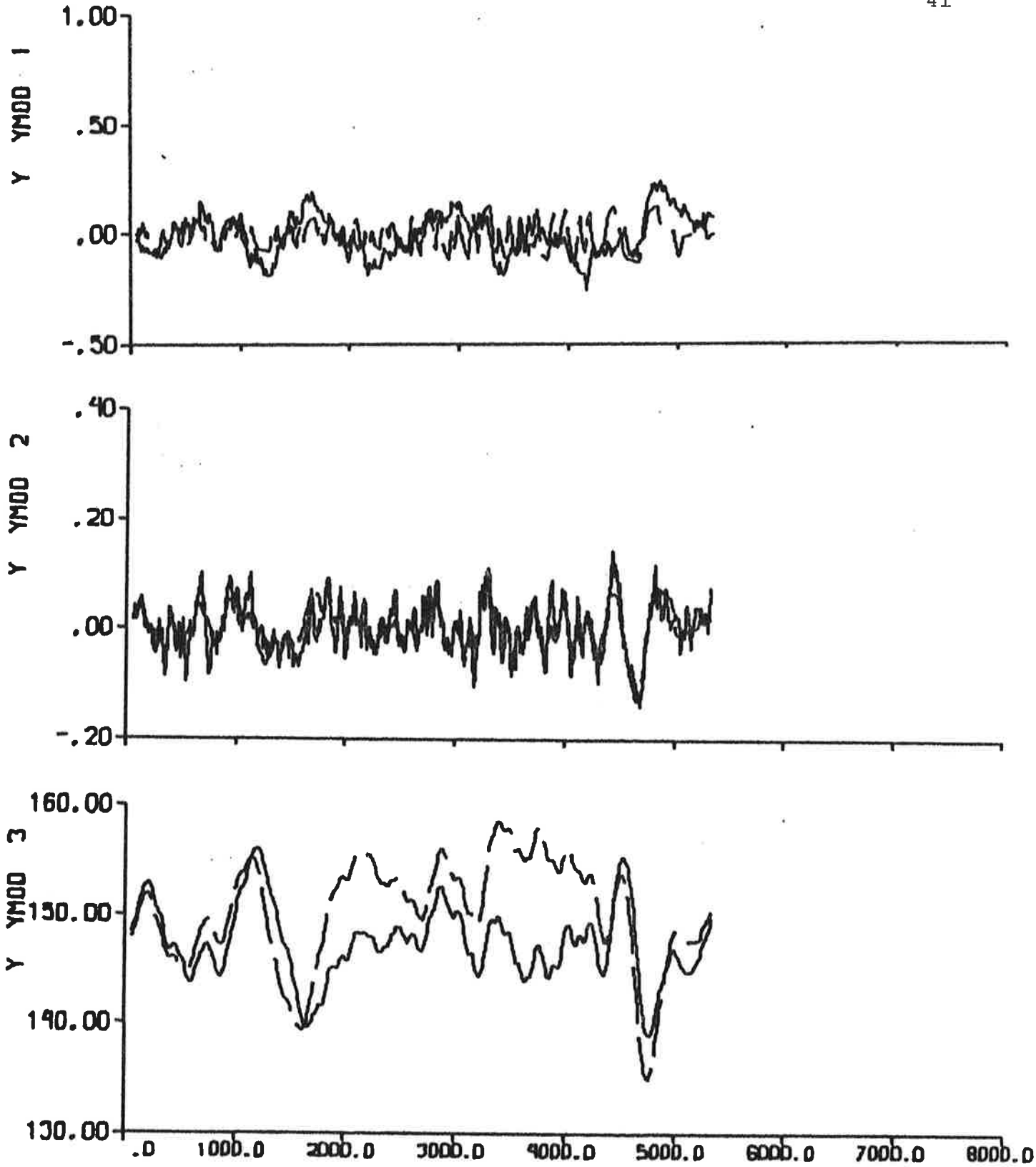
Fig. 4.4a – Result of prediction error identification (p = 6)
to data from experiment E1.
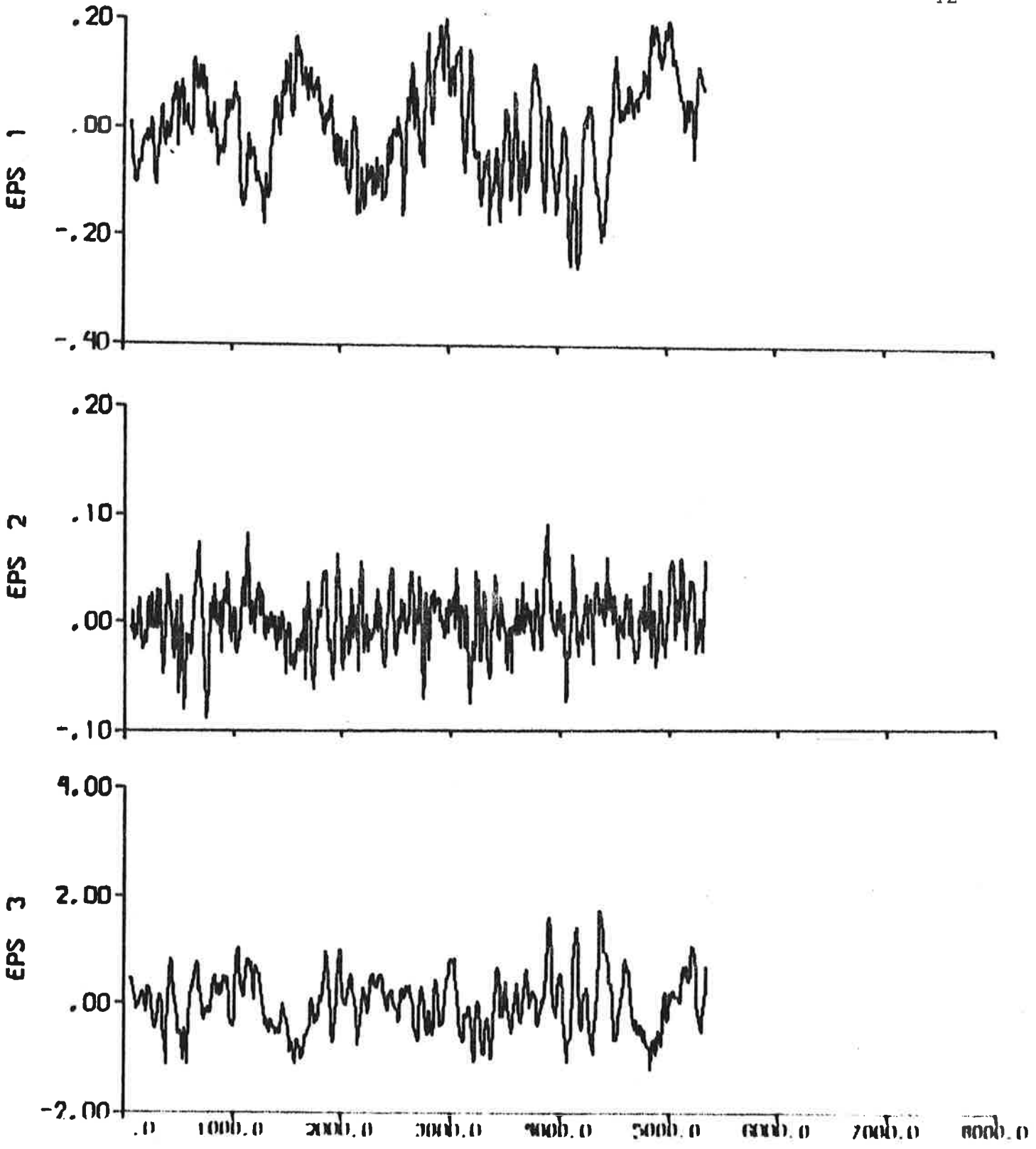
Fig. 4.4b - Prediction errors.
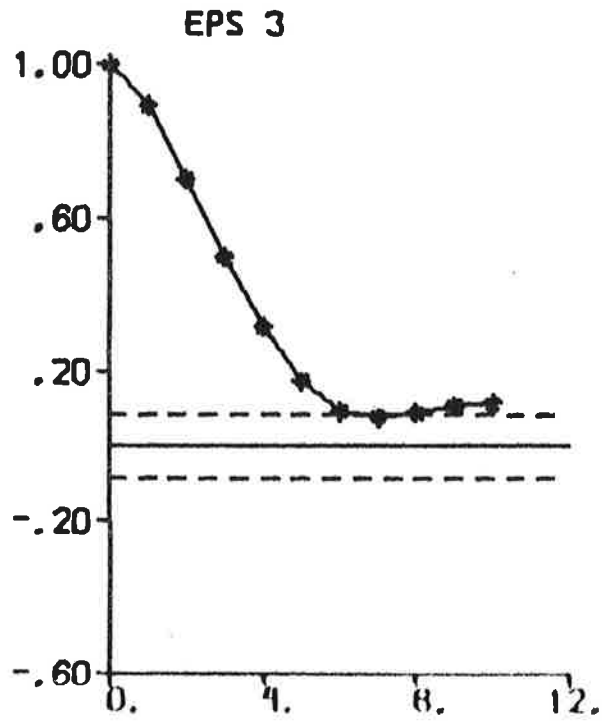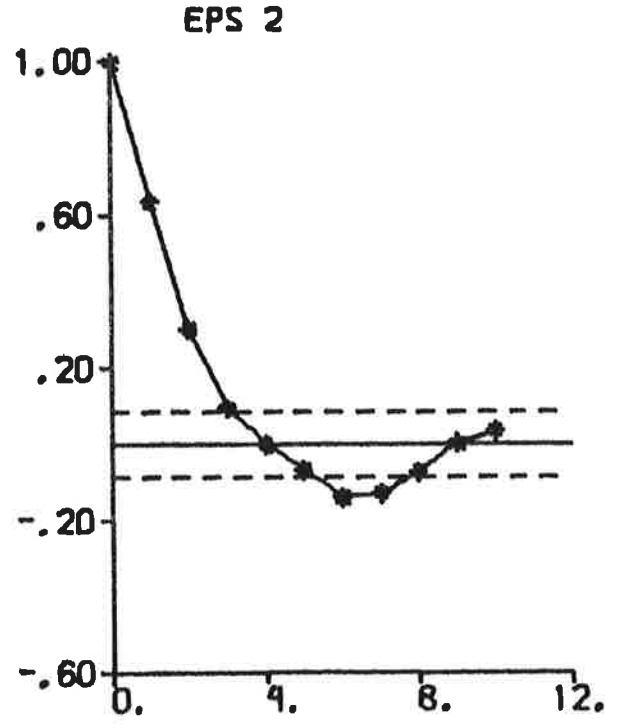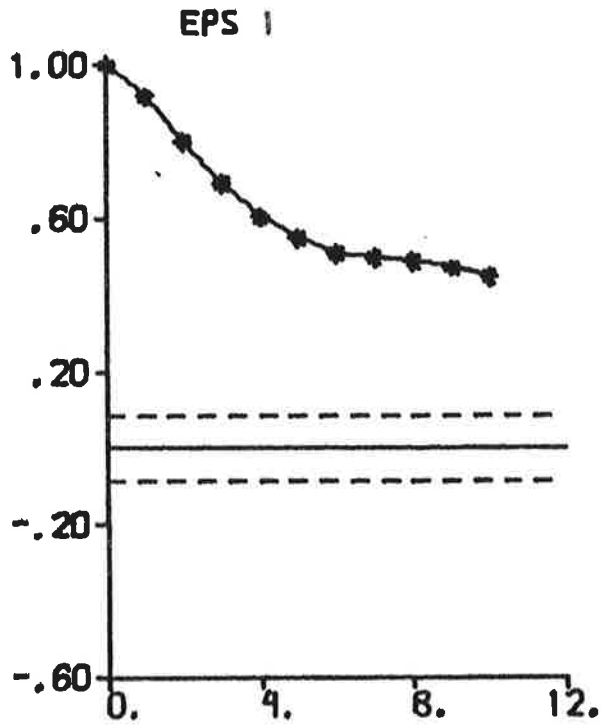
Fig. 4.4c - Autocorrelation functions of prediction errors.
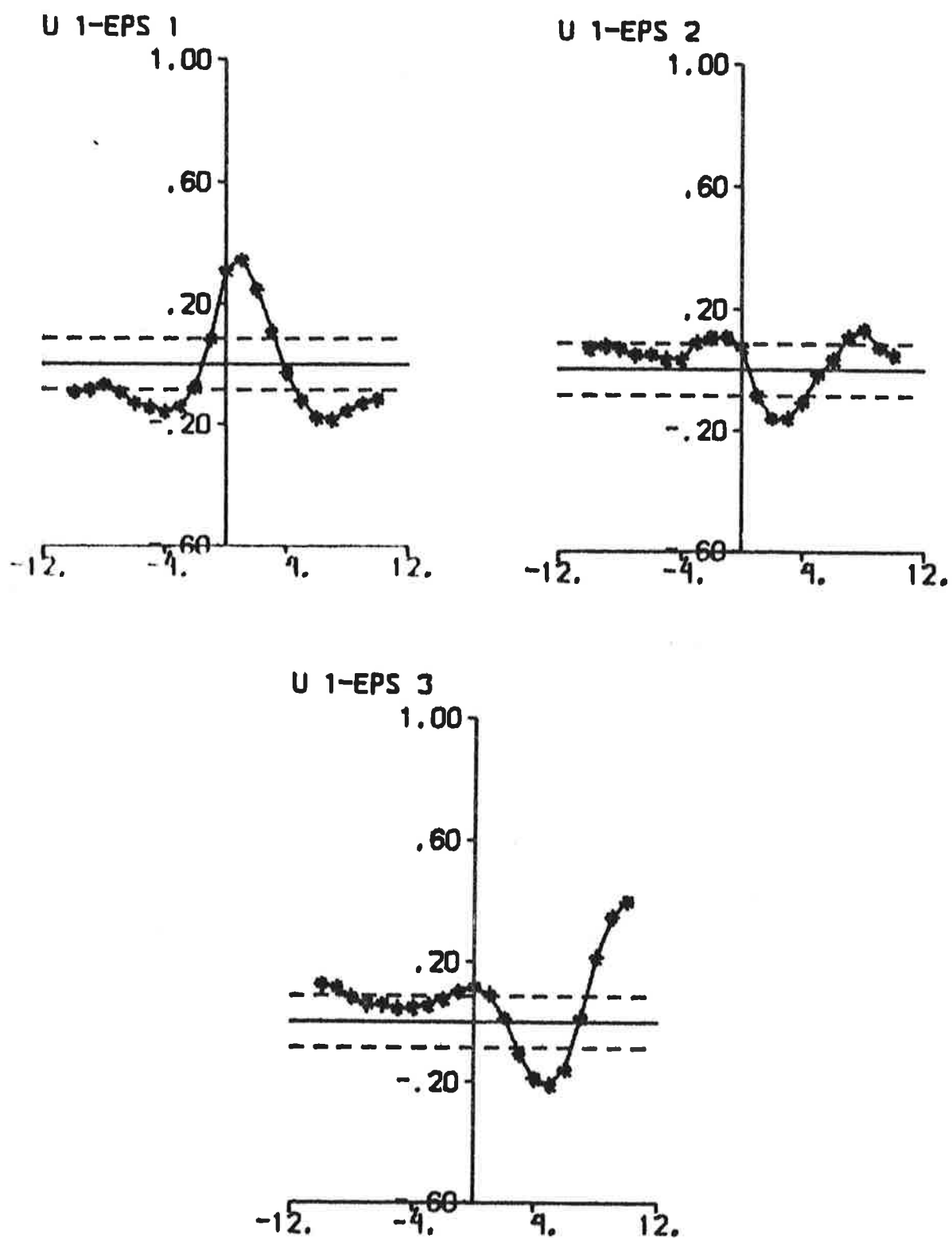
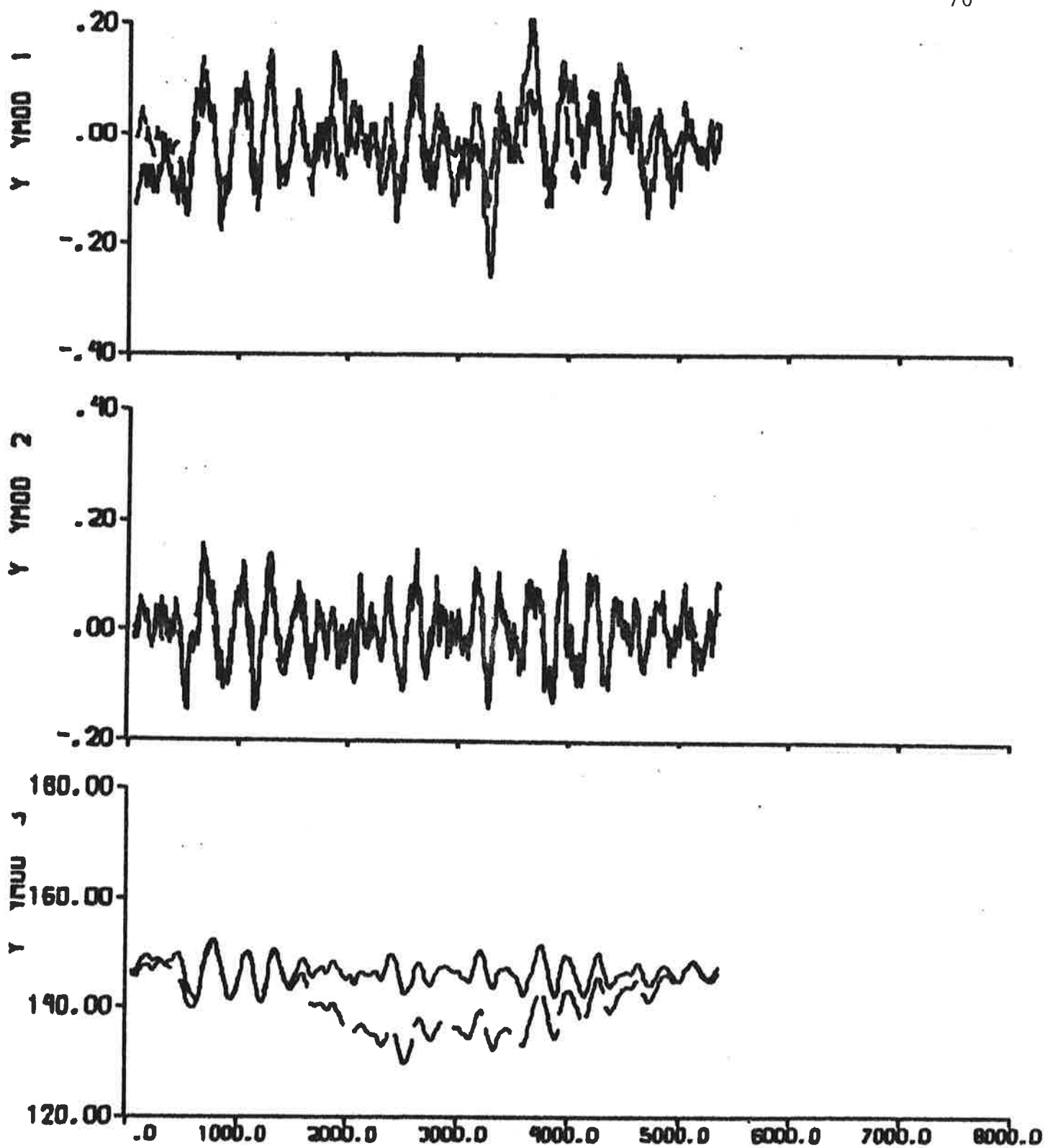Fig. 4.4d - Cross correlation functions between rudder
input and prediction errors.
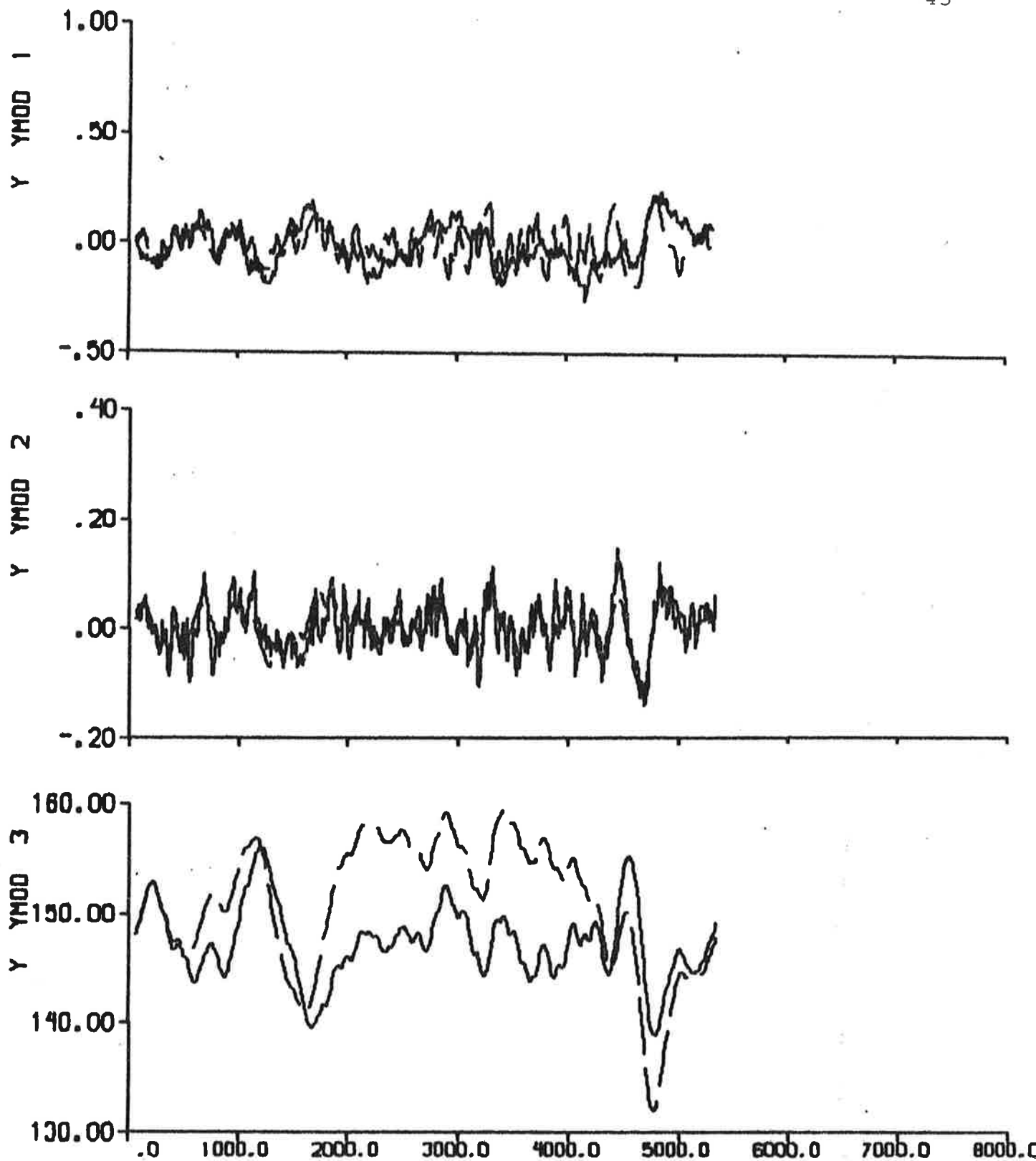
Fig. 4.5a - Result of prediction error identification (p = 6)
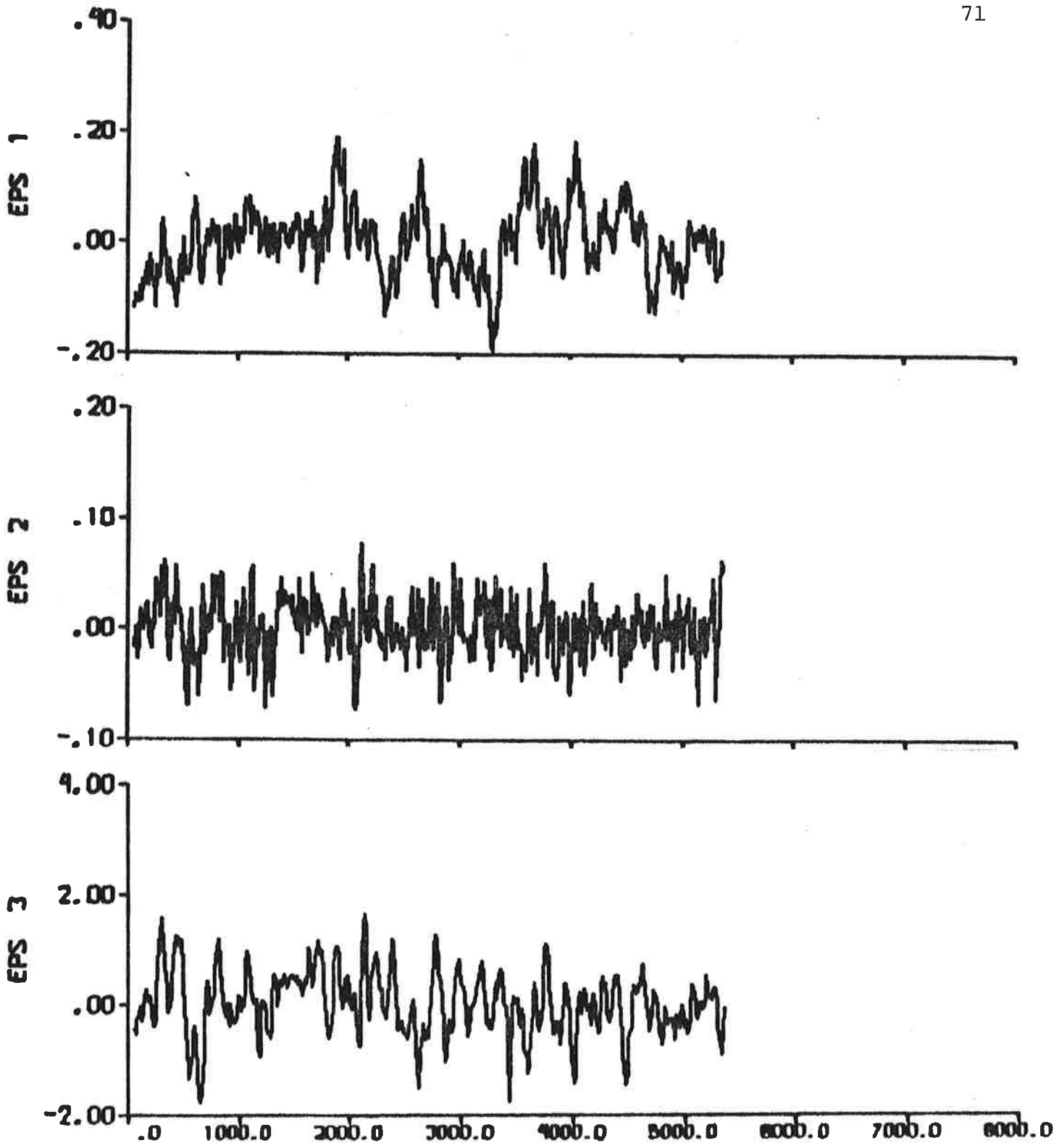   to data from experiment E1. The rudder angle is the
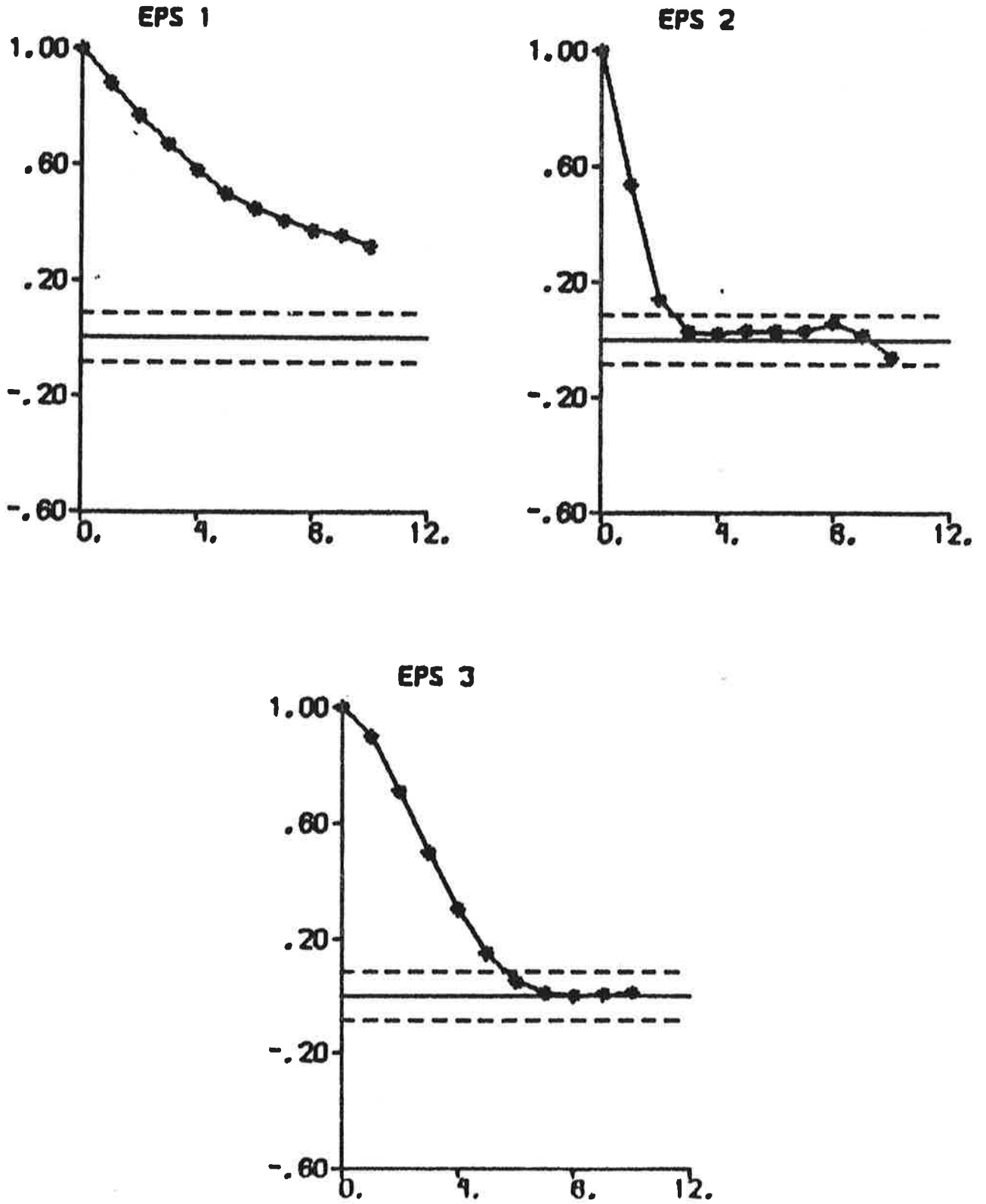   input signal.
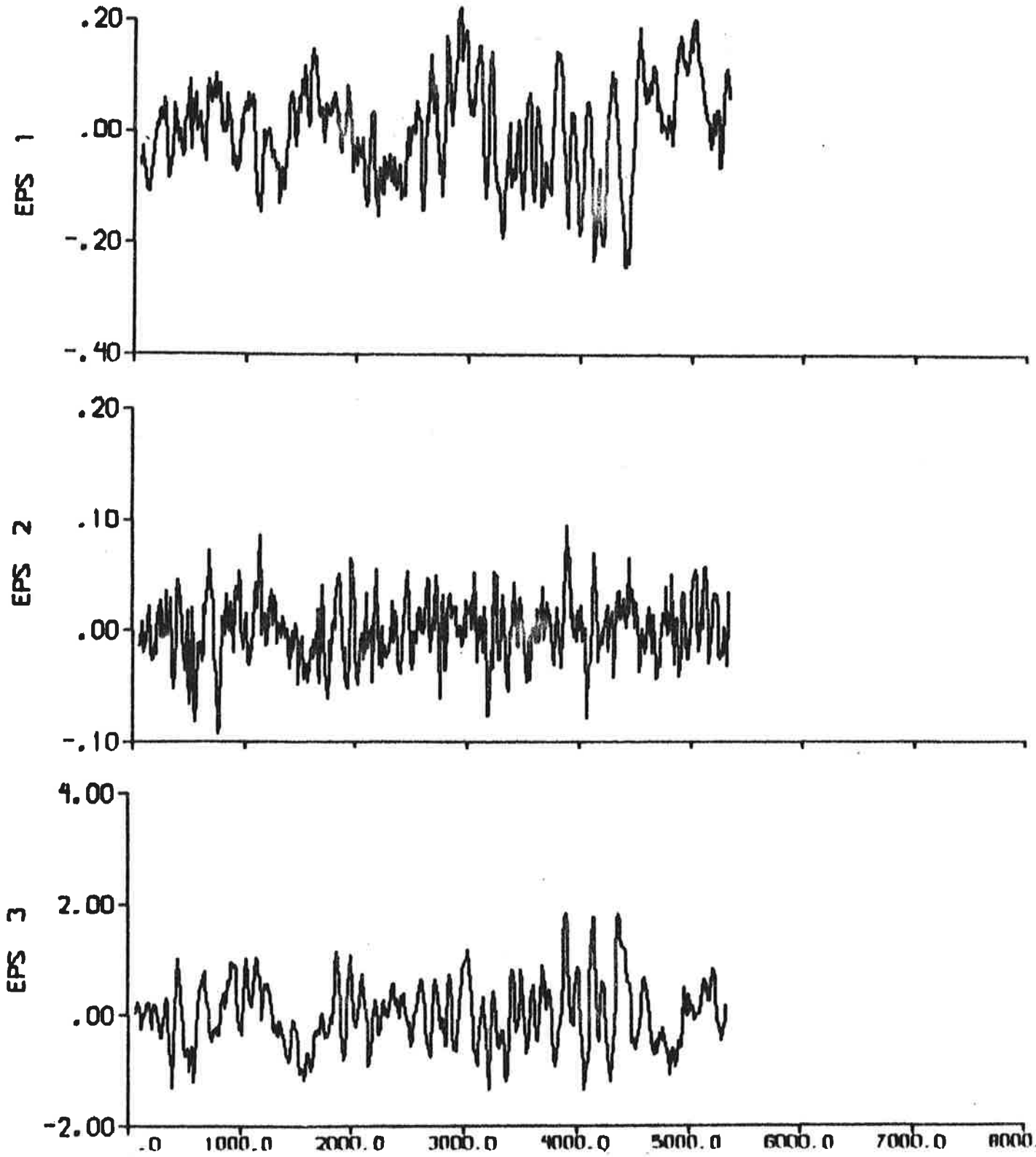
Fig. 4.5b - Prediction errors.
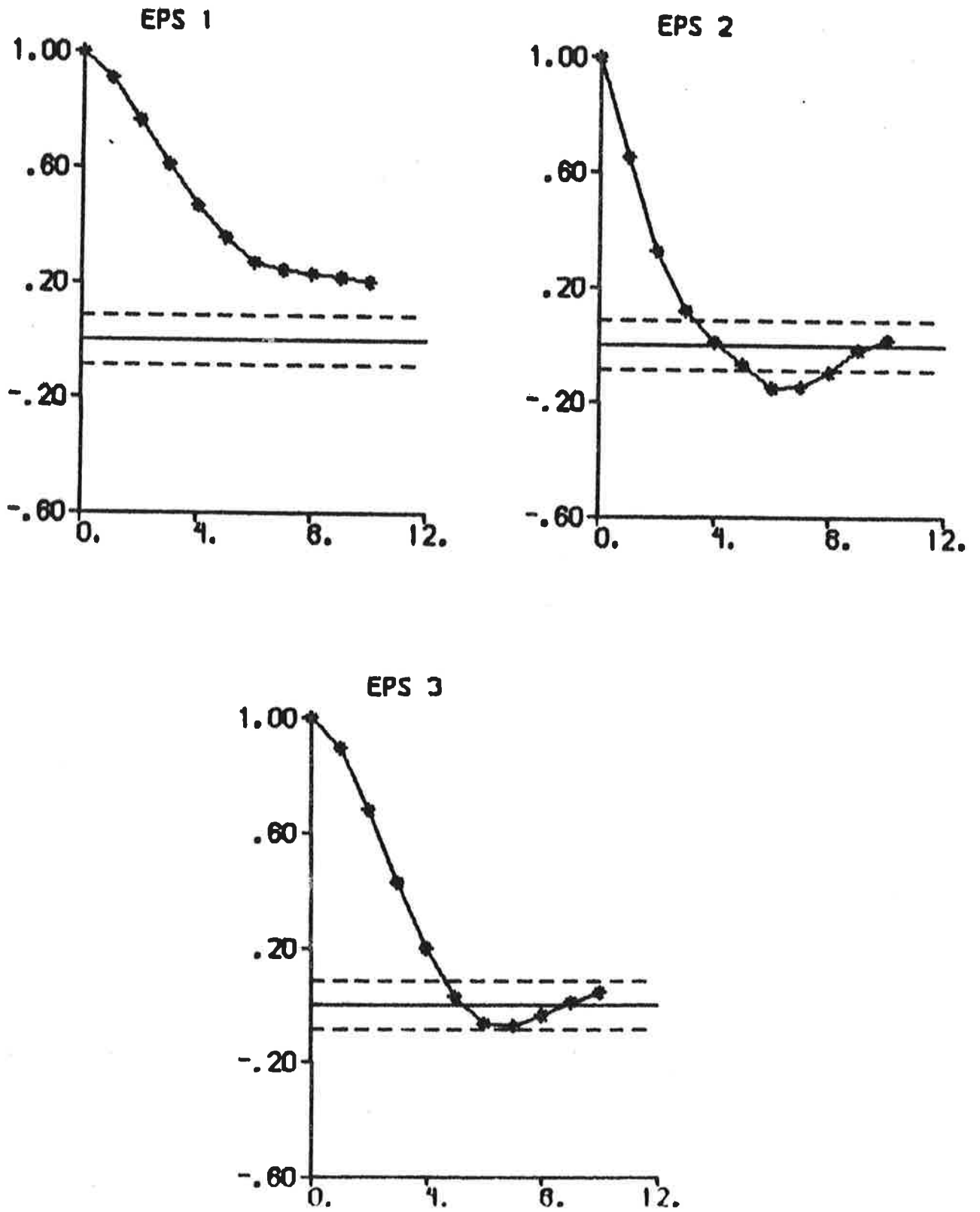
Fig. 4.5c - Autocorrelation functions of prediction errors.
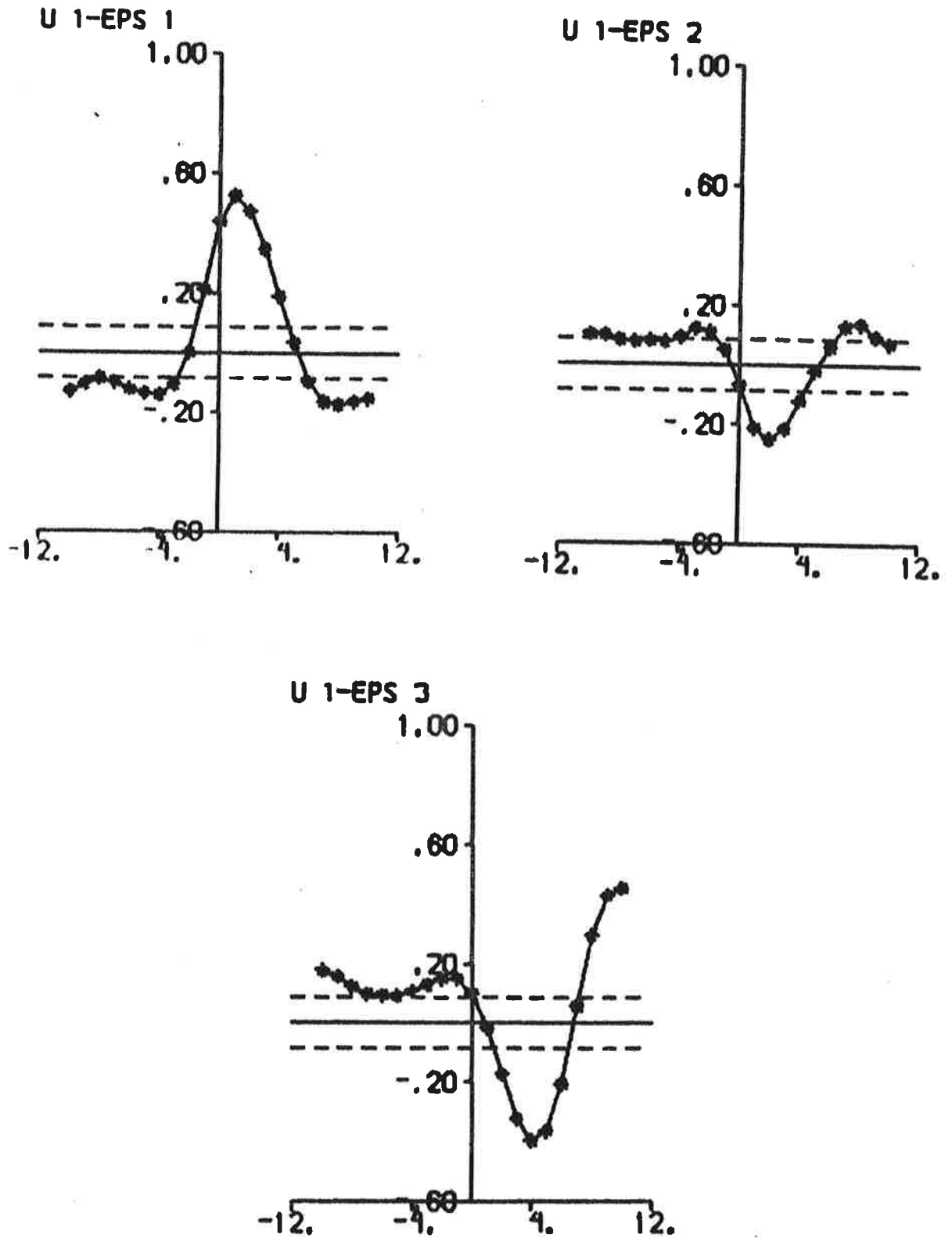
Fig. 4.5d - Cross correlation functions between rudder input and prediction errors.
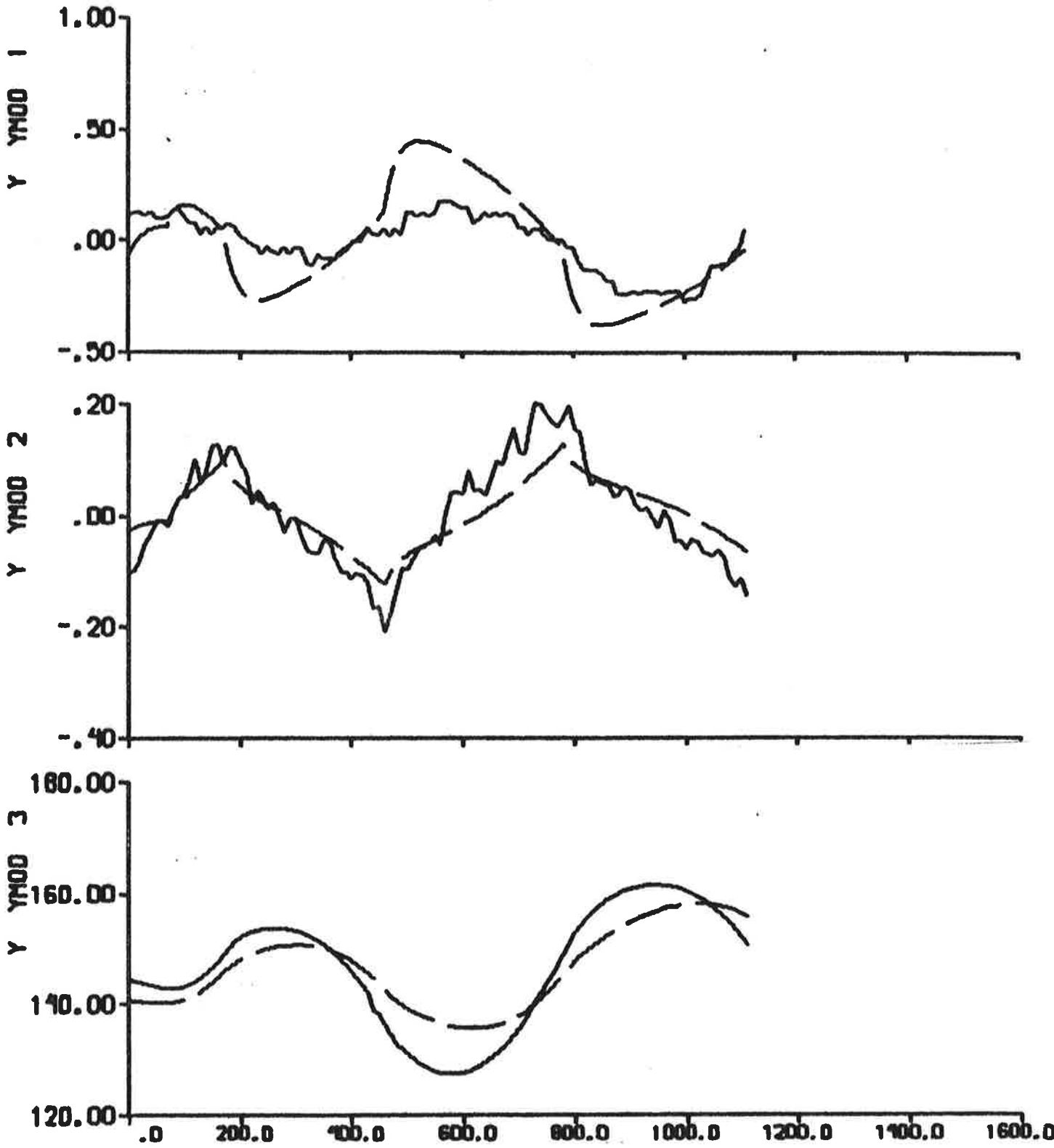
Fig. 4.6 - Result of output error identification to data from experiment E2, when the model is fixed to SSPA:s model.
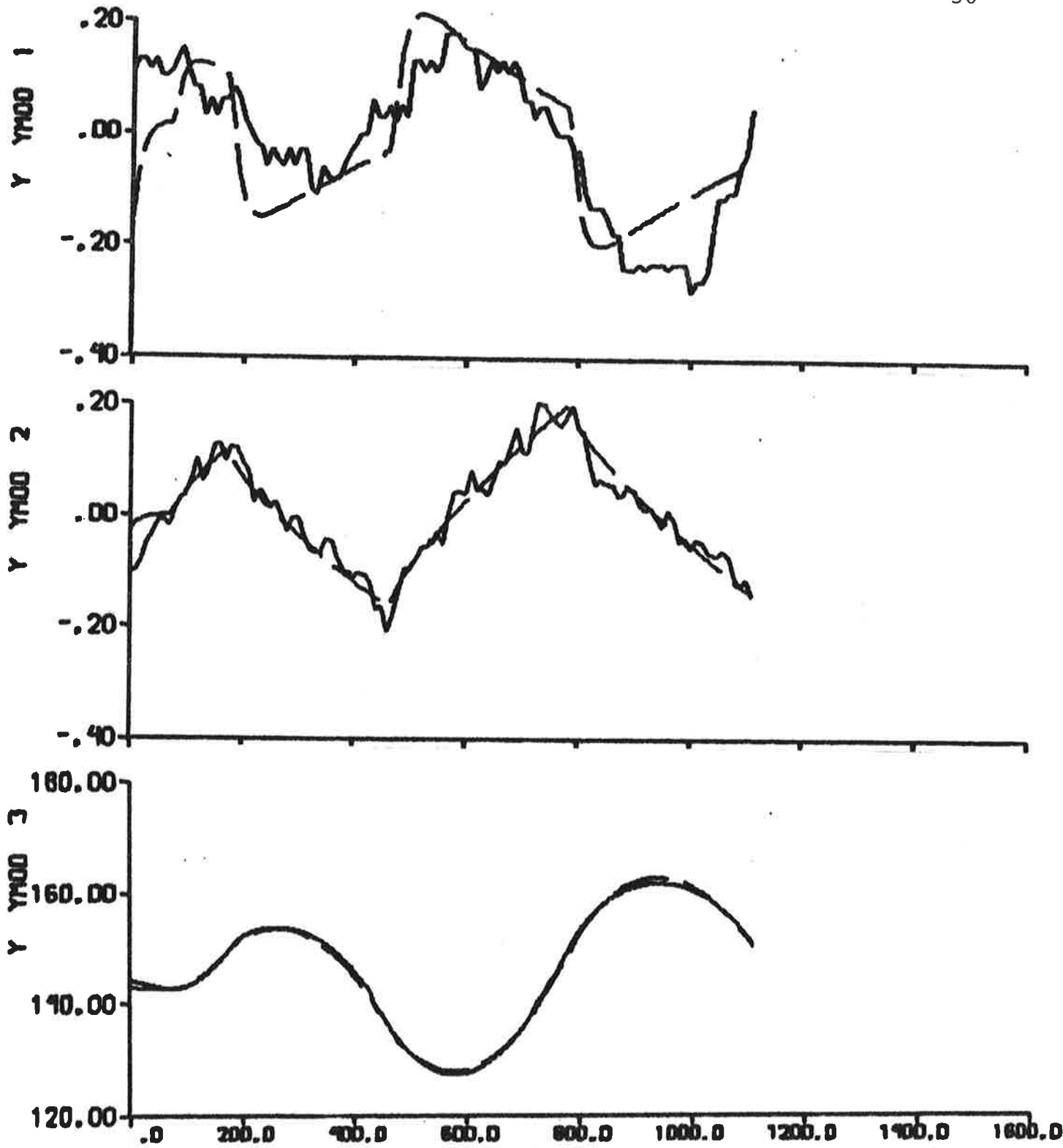
Fig. 4.7 - Result of output error identification
            to data from experiment E2.
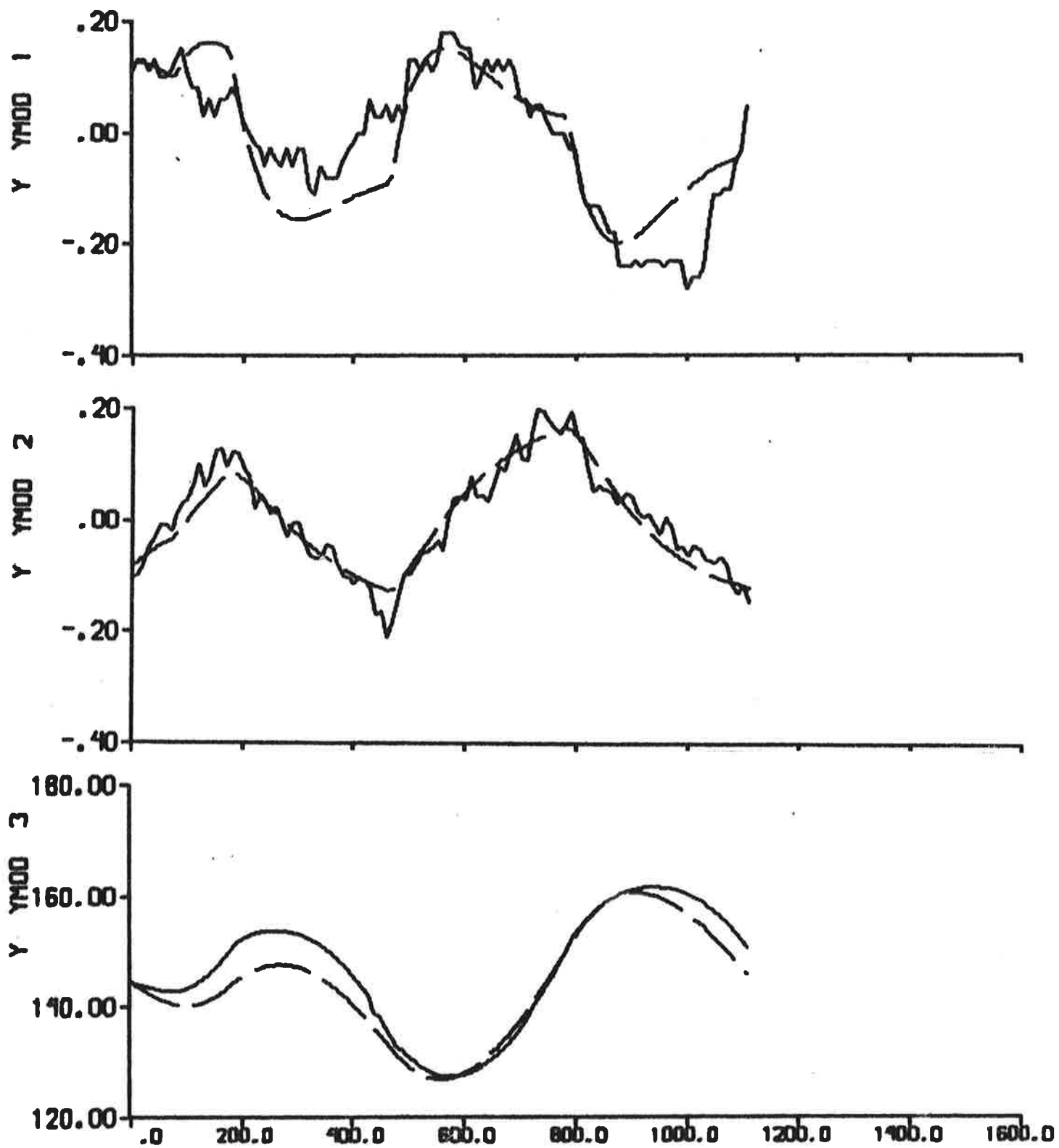
Fig. 4.8a - Result of ML identification to data from experiment E2.
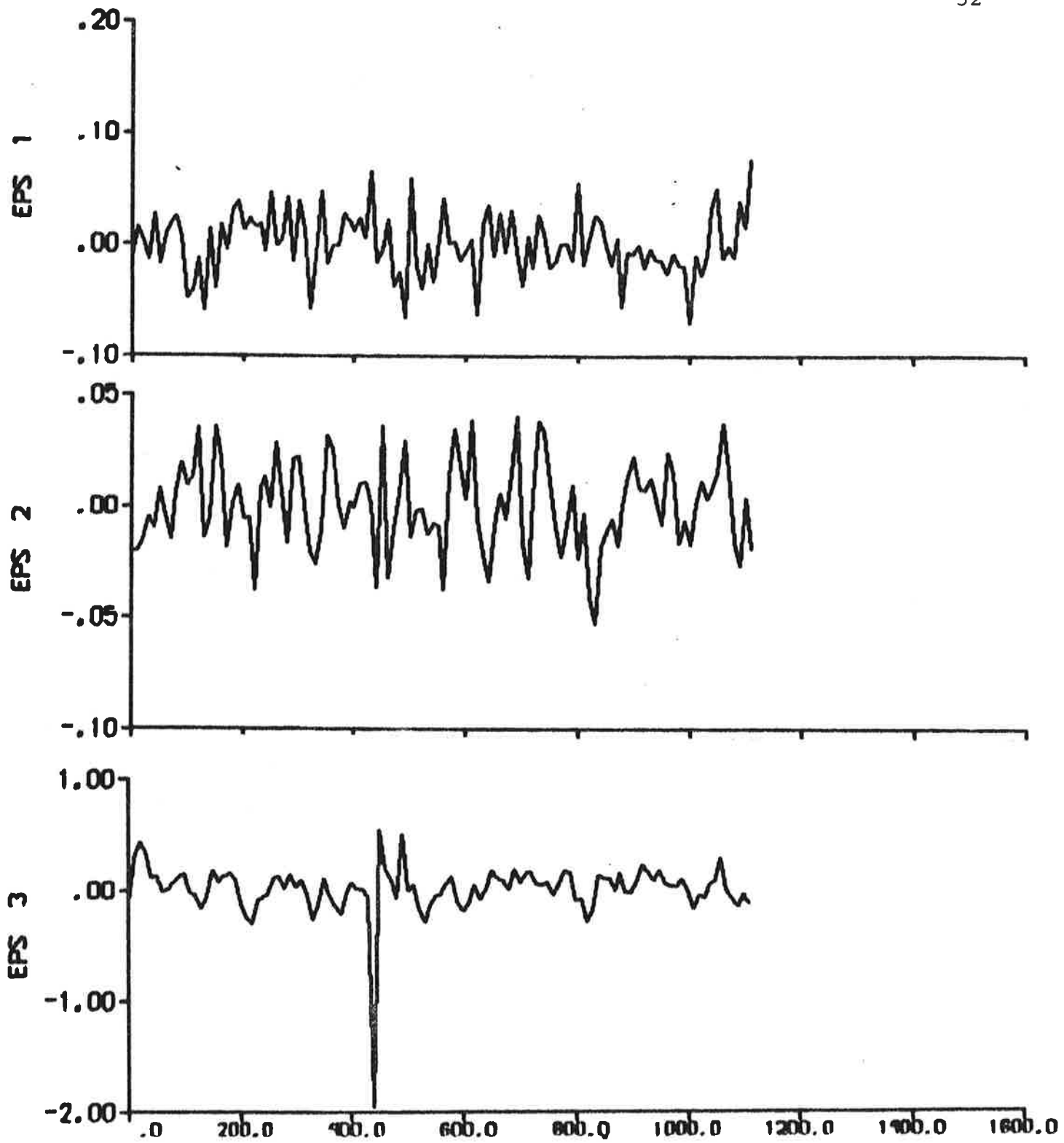
Fig. 4.8b - Prediction errors.
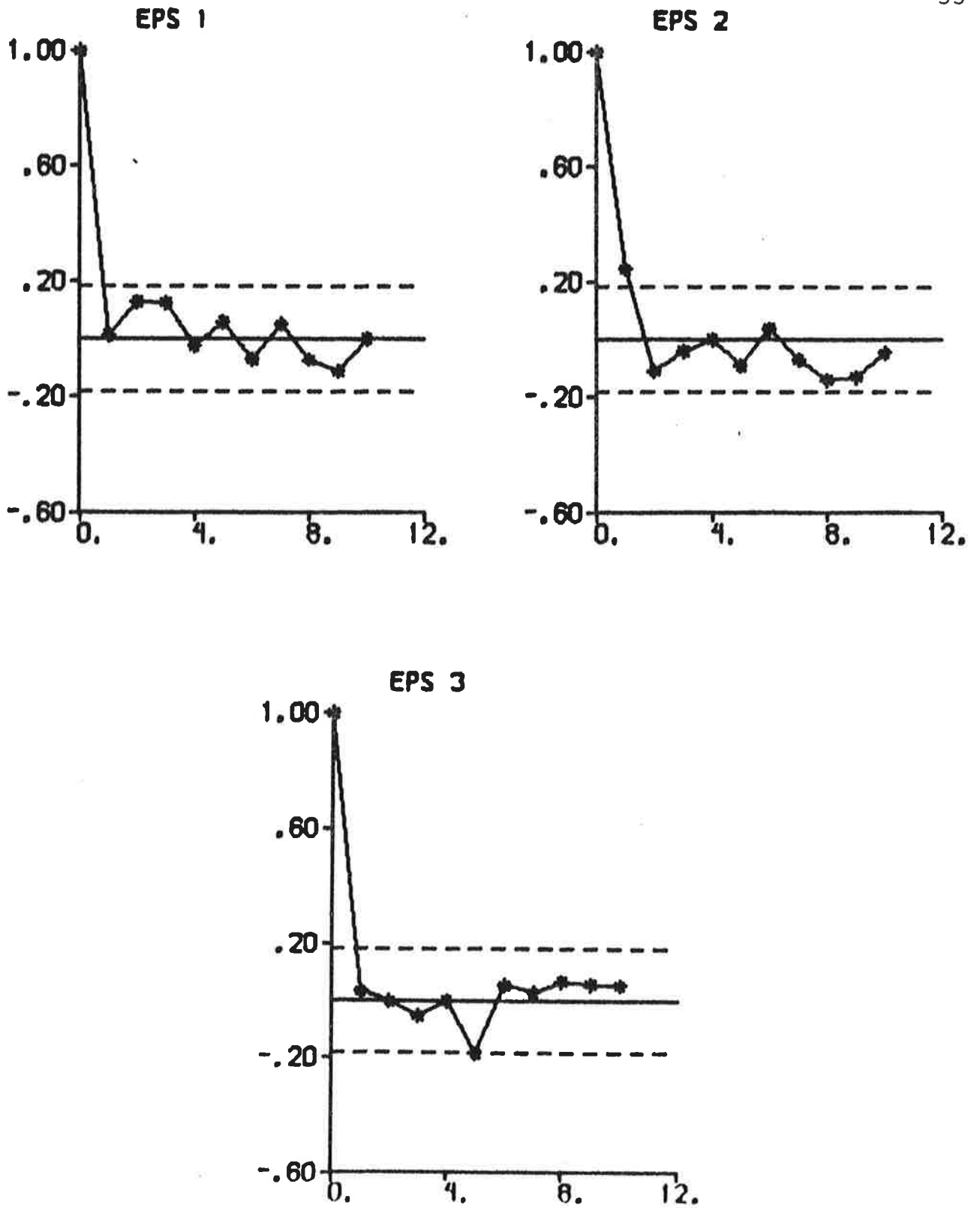
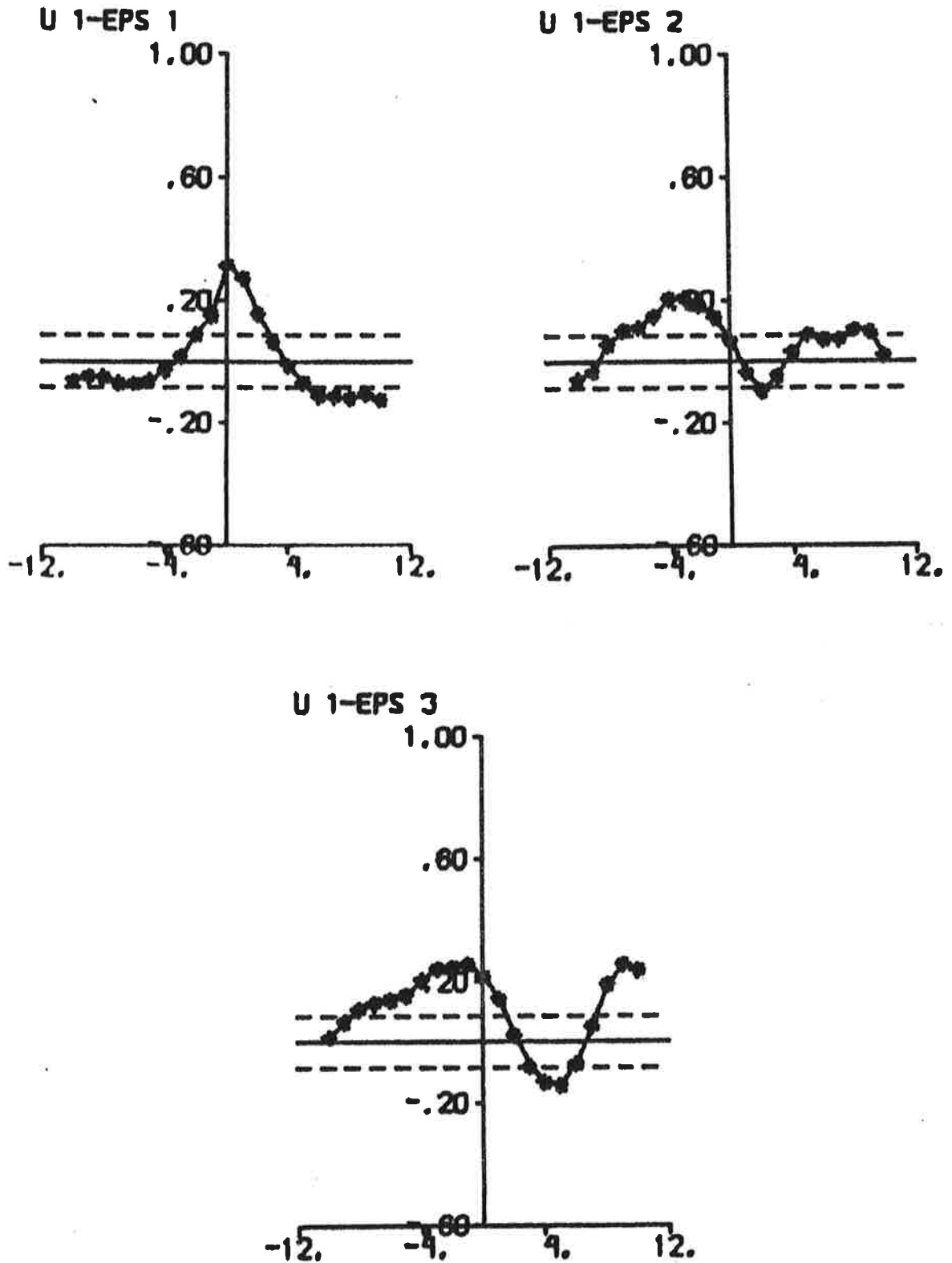Fig. 4.8c - Autocorrelation functions of prediction errors.

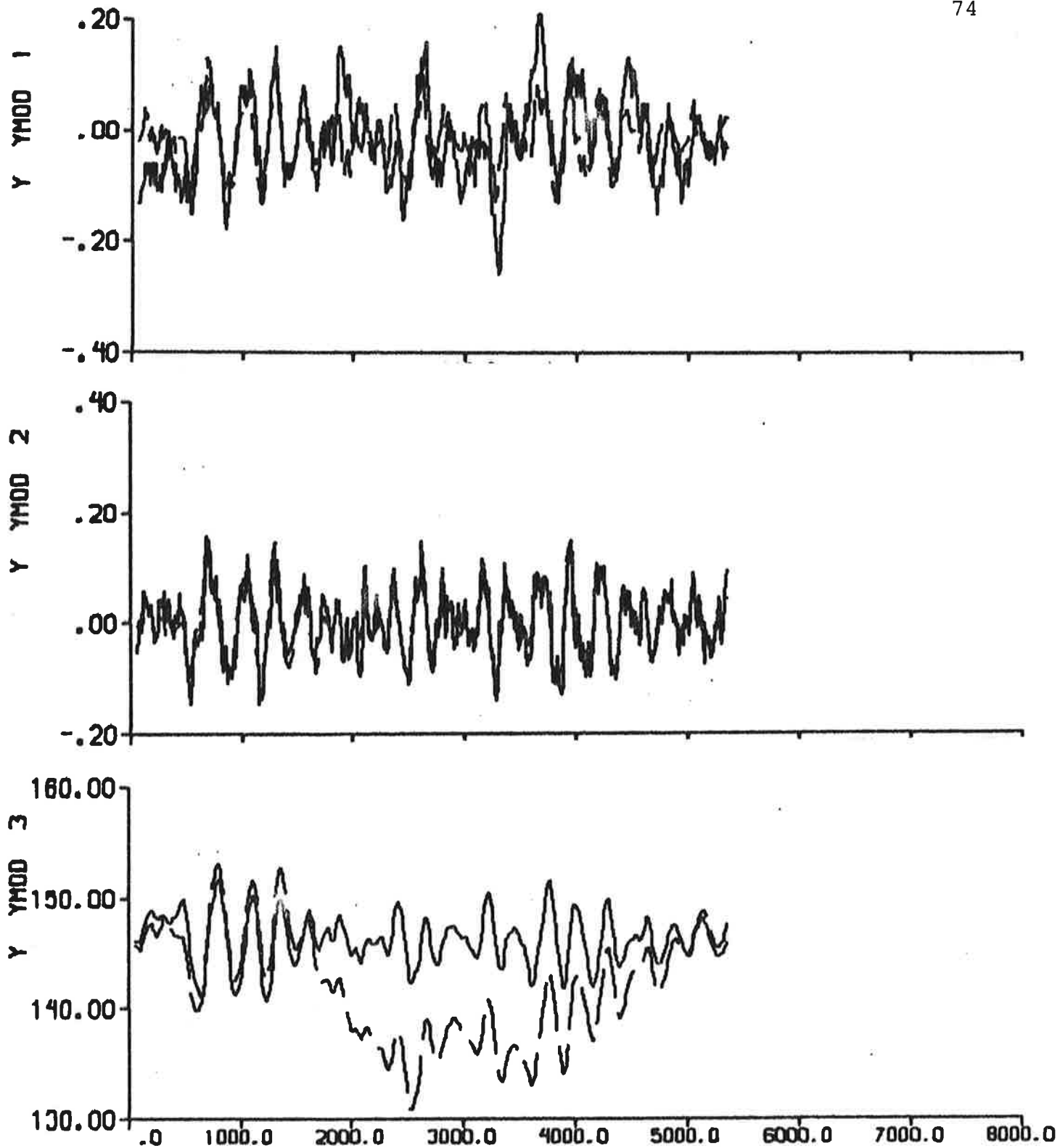Fig. 4.8d - Cross correlation functions between rudder input and prediction errors.

Fig. 4.9a - Result of prediction error identification (p = 6)
            to data from experiment E2.

Fig. 4.9b - Prediction errors.

Fig. 4.9c - Autocorrelation functions of prediction errors.

U 1-EPS 1

U 1-EPS 2

U 1-EPS 3

Fig. 4.9d - Cross correlation functions between rudder
input and prediction errors.

Fig. 4.10a - Result of prediction error identification (p = 6)
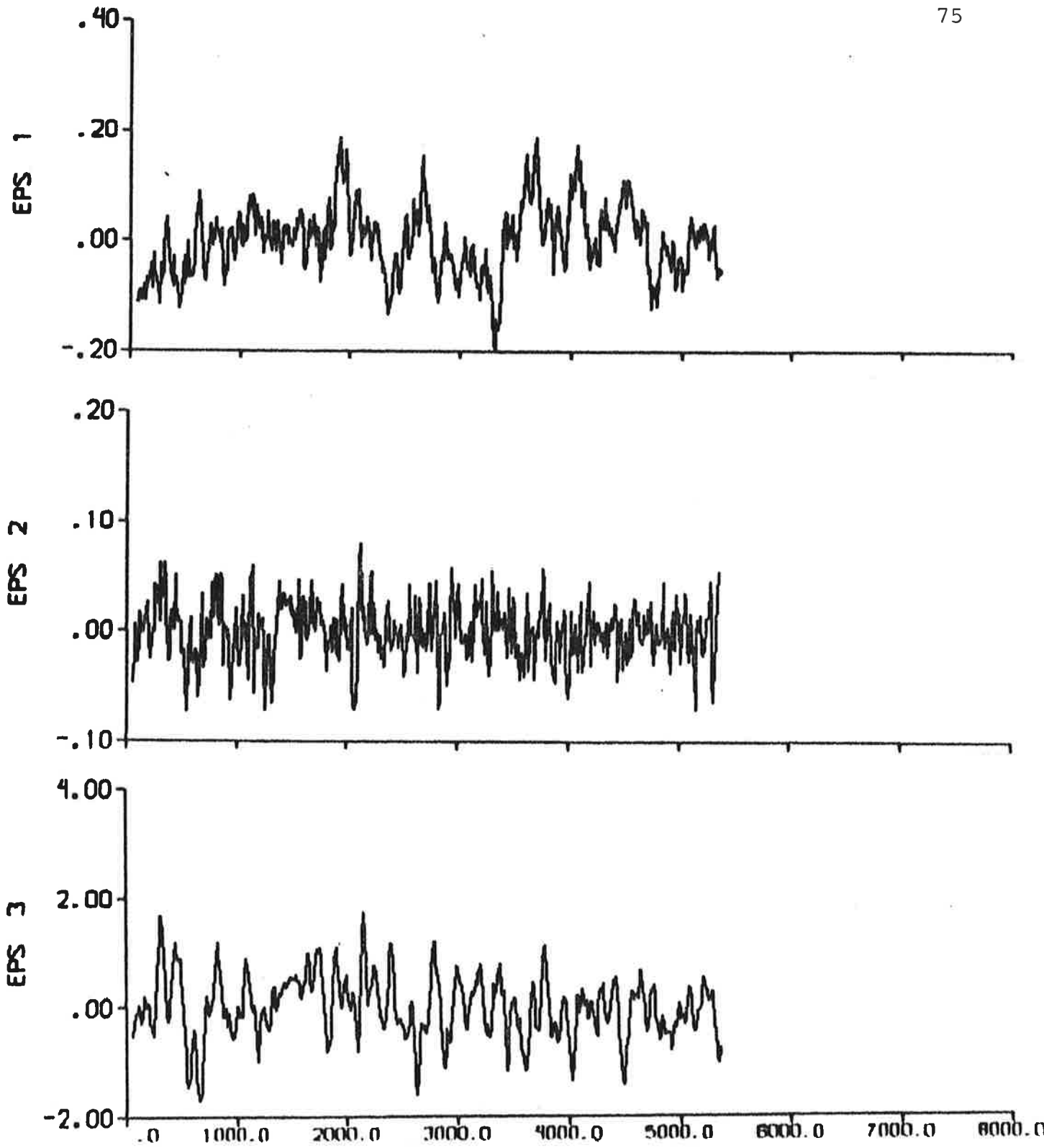to data from experiment E2. The rudder angle
is the input signal.
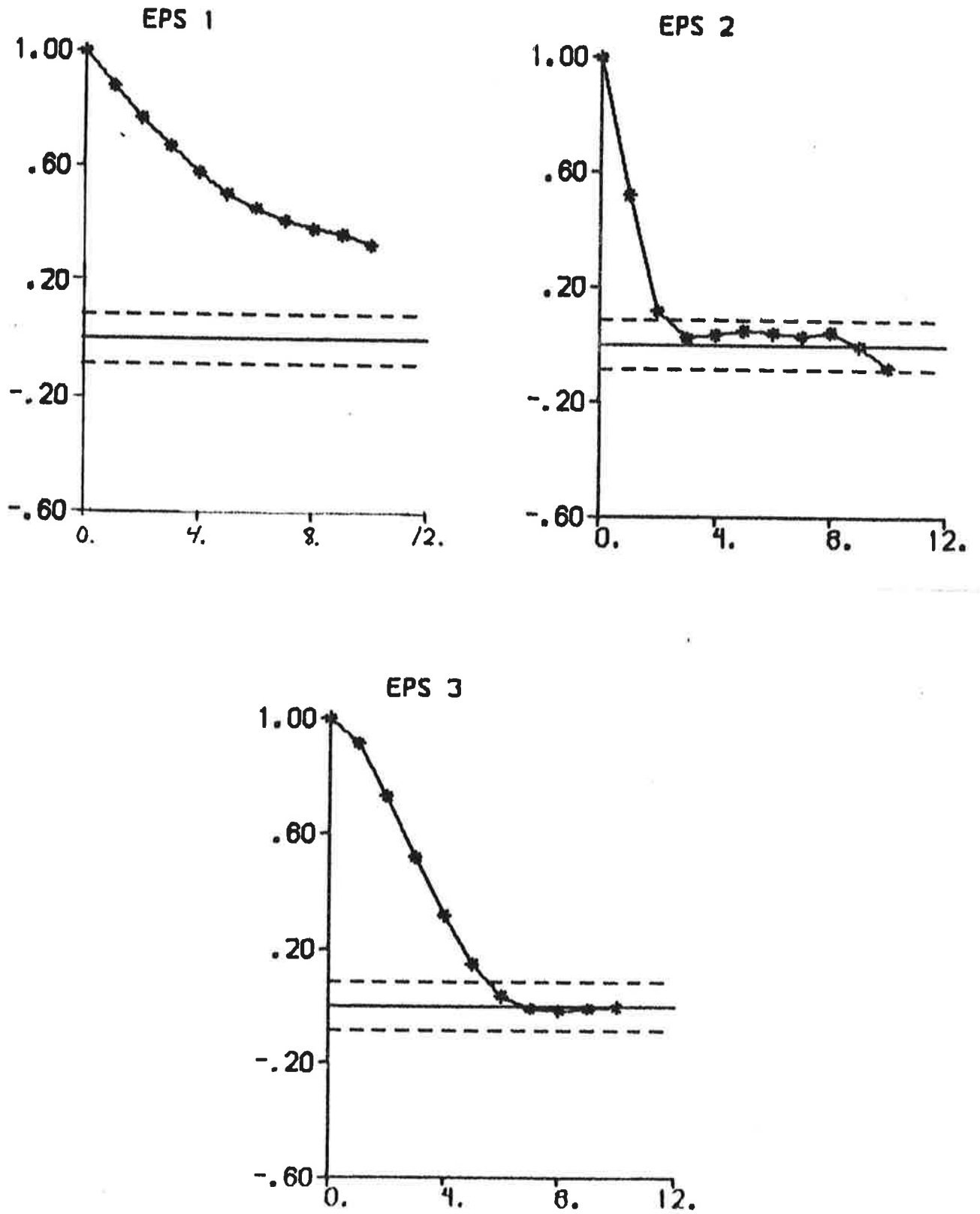
Fig. 4.10b - Prediction errors.

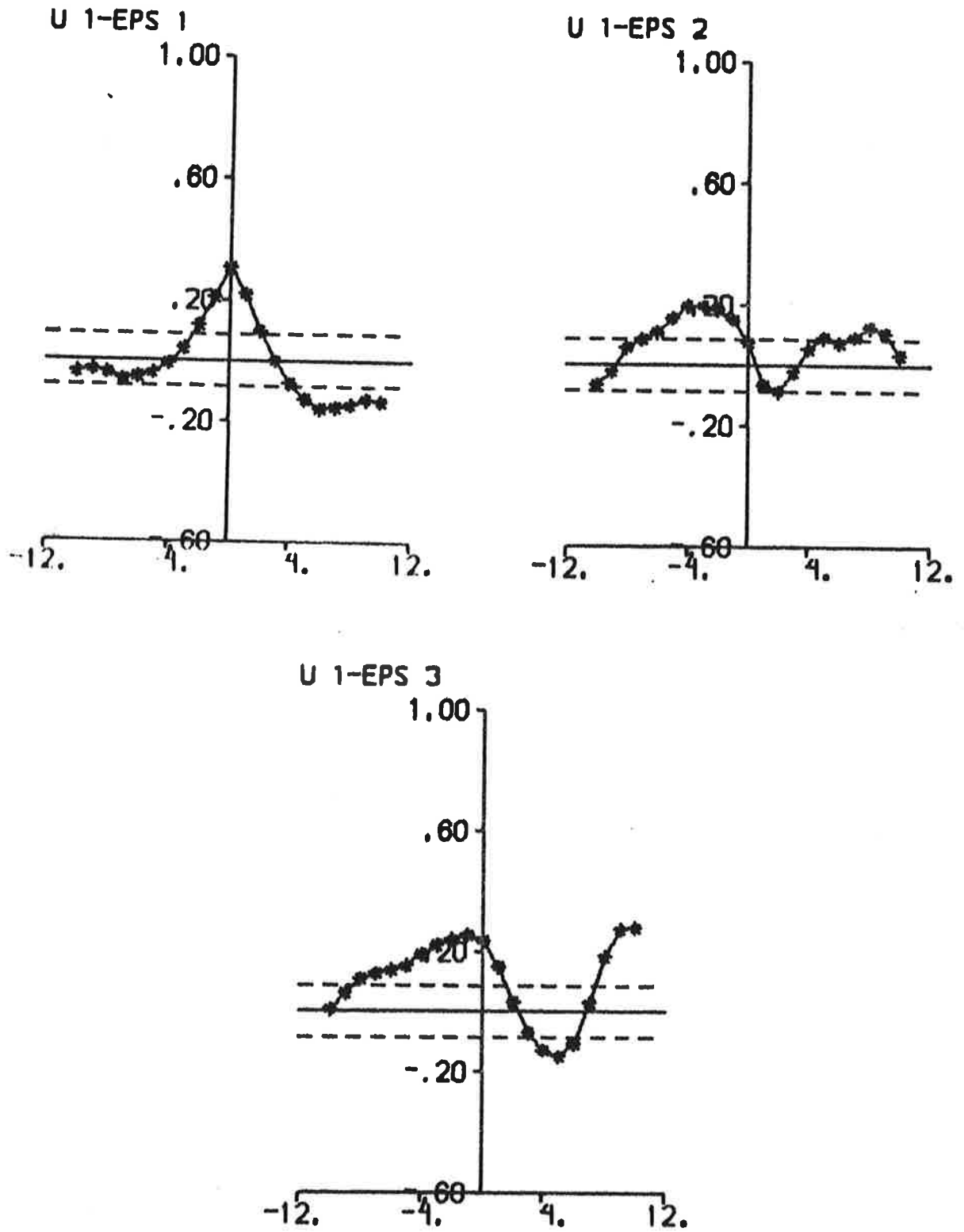Fig. 4.10c - Autocorrelation functions of prediction errors.
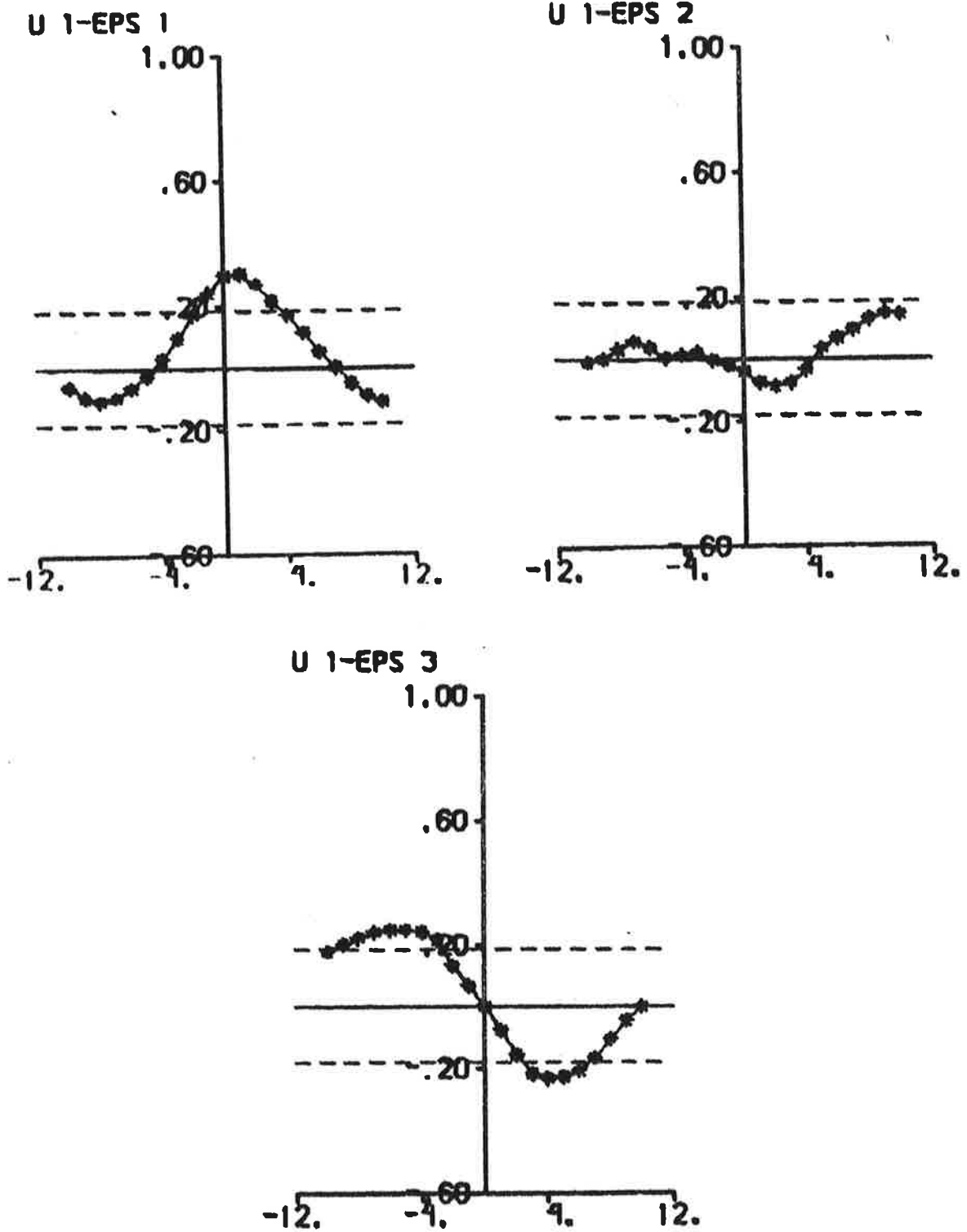
Fig. 4.10d - Cross correlation functions between rudder input and prediction errors.
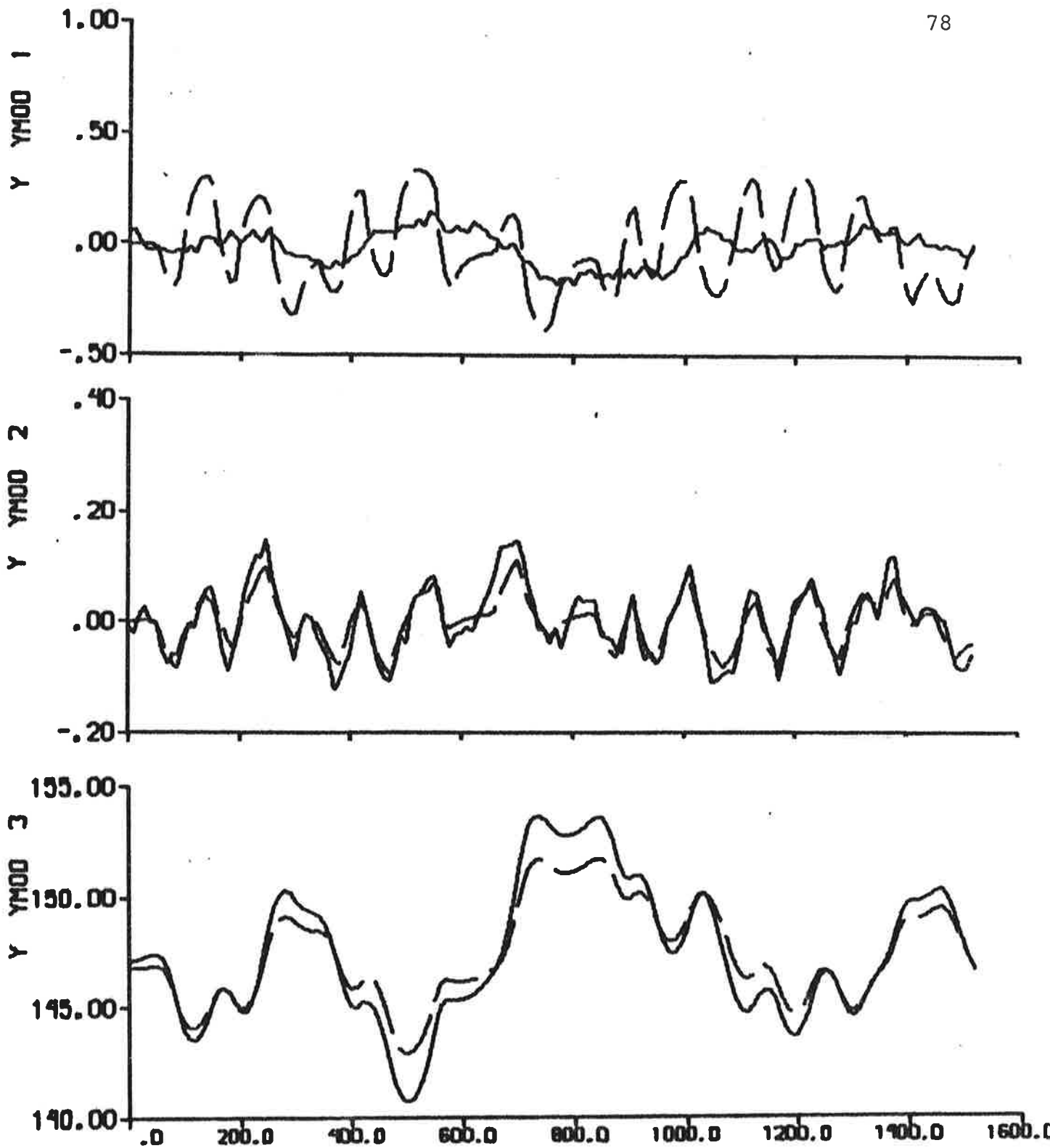
Fig. 4.11a - Result of output error identification to data from experiment E3, when the model is fixed to SSPA:s model.
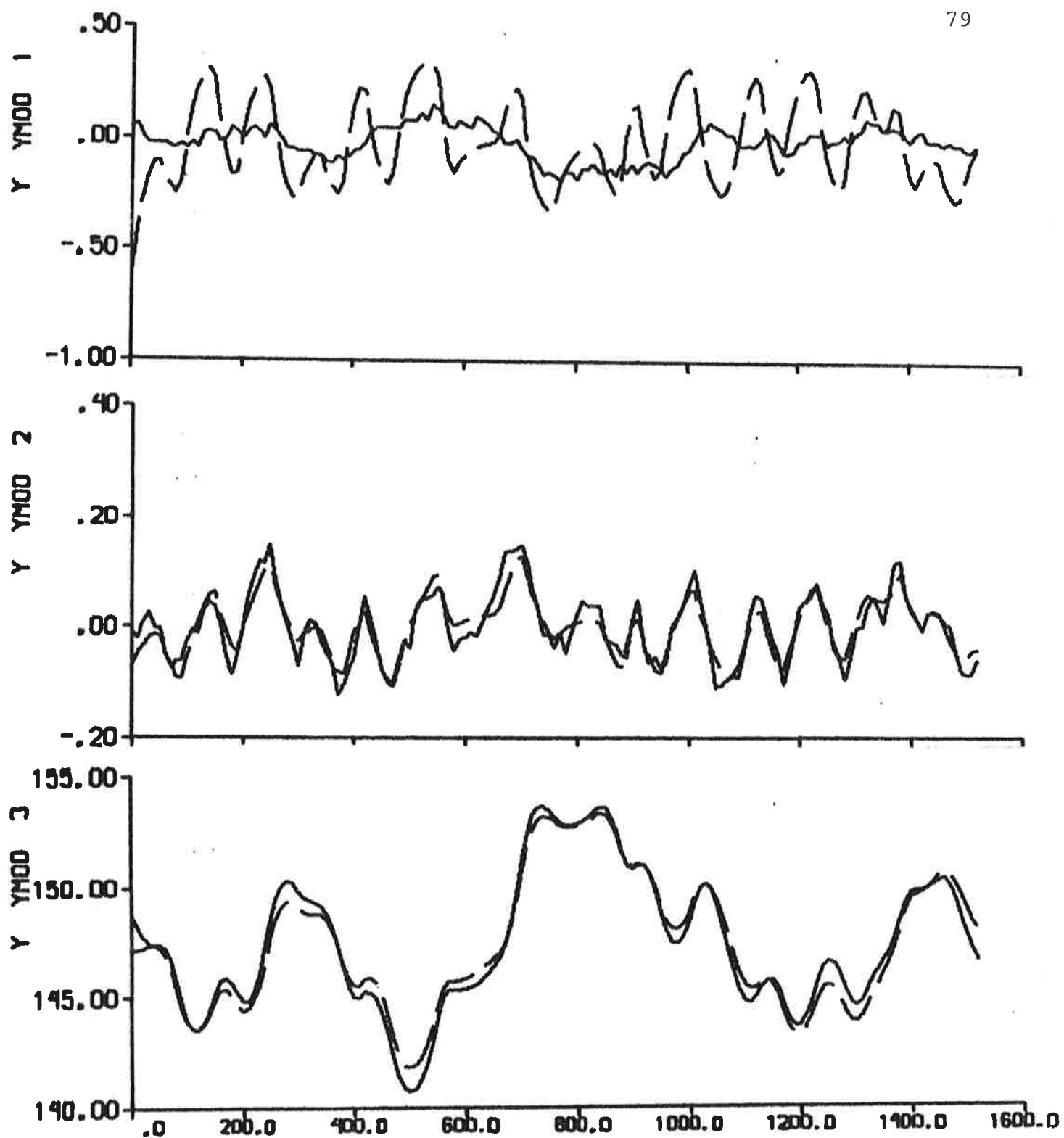
Fig. 4.11b - First part of Fig. 4.11a.

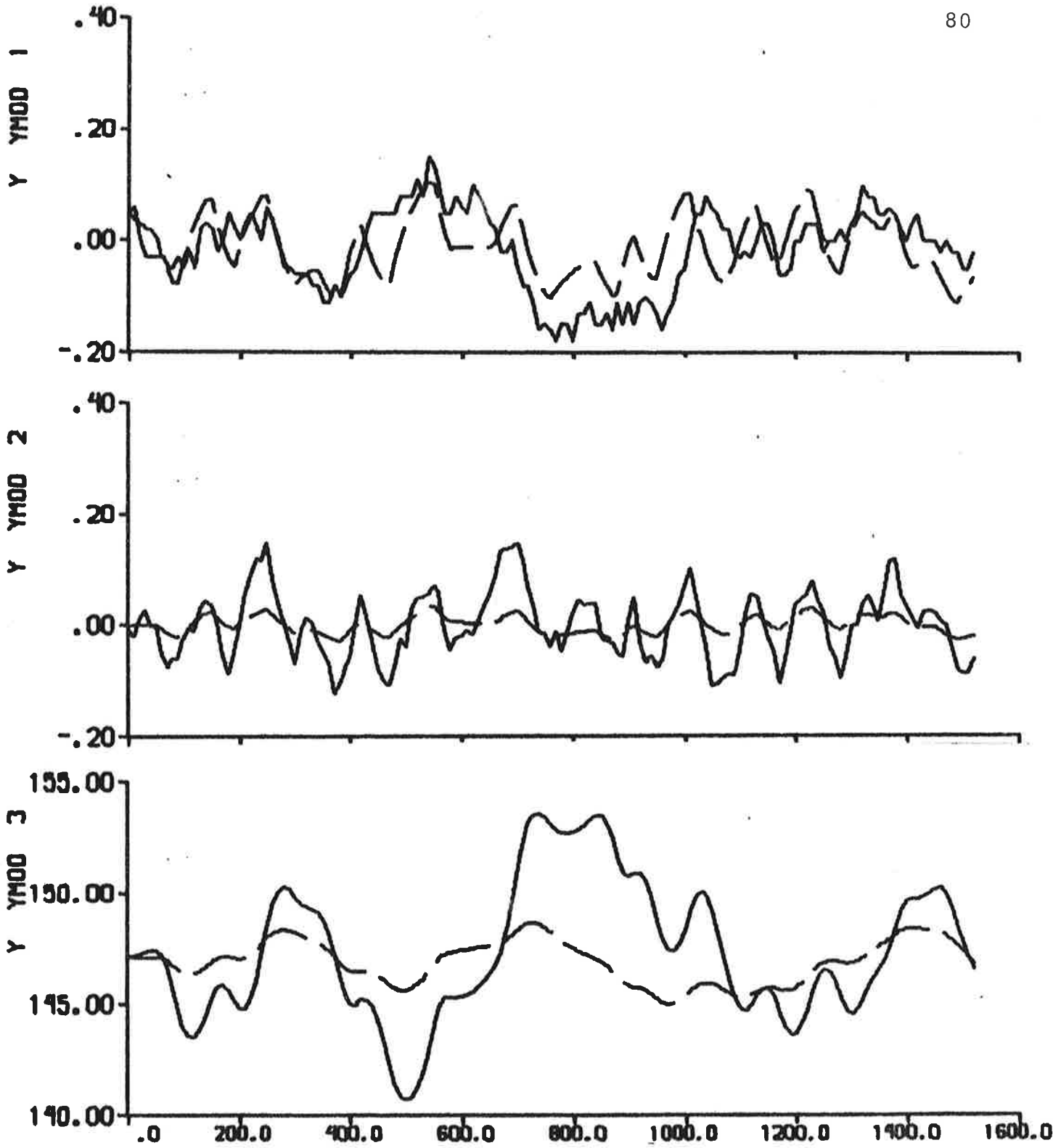Fig. 4.12 — Result of output error identification to data from experiment E3.

Fig. 4.13a - Result of ML identification to data
from experiment E3.

Fig. 4.13b - Prediction errors.

Fig. 4.13c - Autocorrelation functions of prediction errors.

Fig. 4.13d - Cross correlation functions between rudder input
and prediction errors.

Fig. 4.14a - Result of prediction error identification (p= 6)
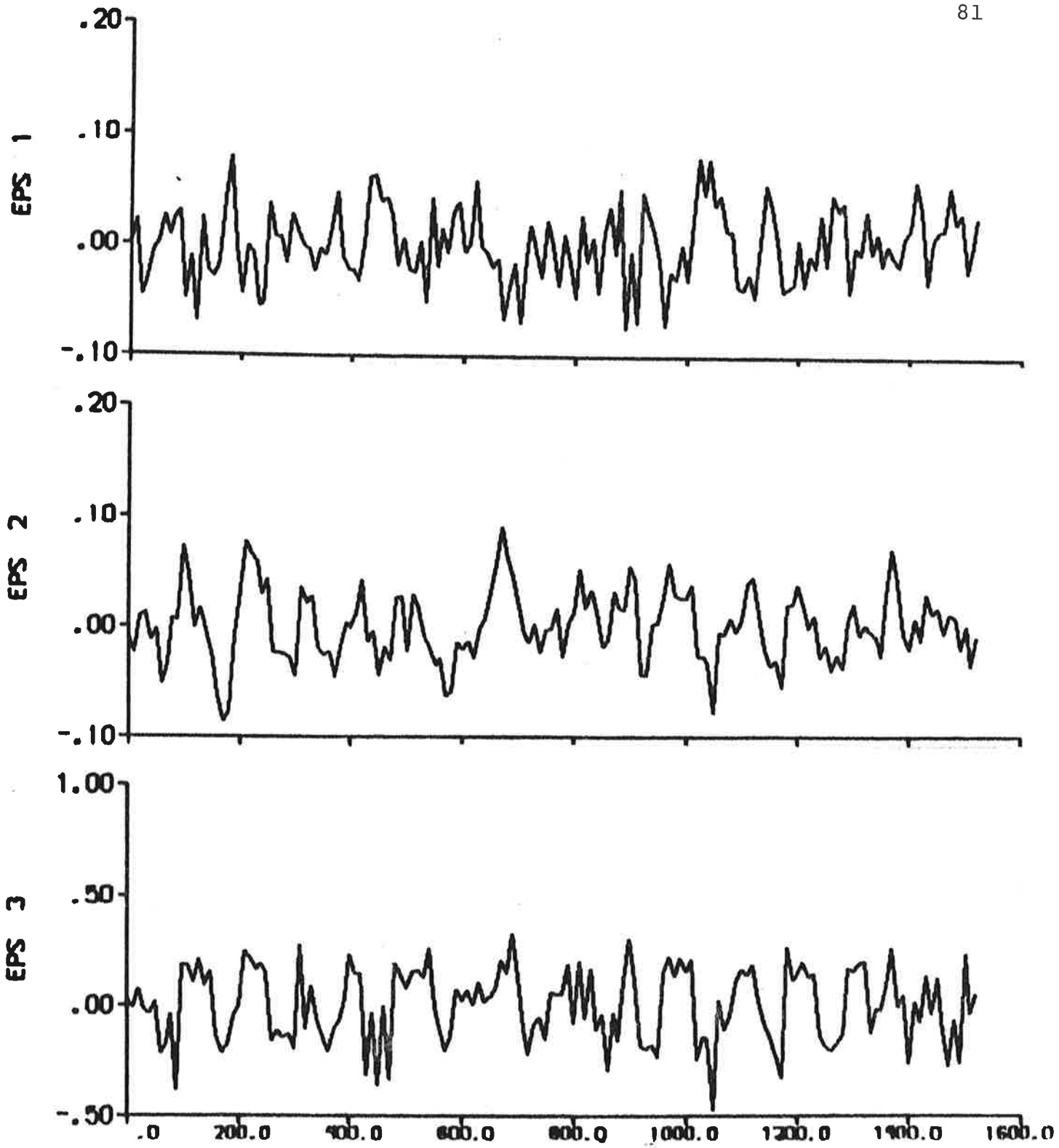to data from experiment E3.

Fig. 4.14b - Prediction errors.

Fig. 4.14c - Autocorrelation functions of prediction errors.

Fig. 4.14d - Cross correlation functions between rudder
            input and prediction errors.

Fig. 4.15a - Result of prediction error identification (p = 6) to data from experiment E3. The rudder angle is the input signal.

Fig. 4.15b - Prediction errors.

Fig. 4.15c – Autocorrelation functions of prediction errors.

Fig. 4.15d - Cross correlation functions between rudder input and prediction errors.

Fig. 4.16 - Result of output error identification to data
from experiment E4, when the model is fixed to
SSPA:s model.

Fig. 4.17 - Result of output error identification to data from experiment E4.

Fig. 4.18a - Result of ML identification to data from experiment E4.
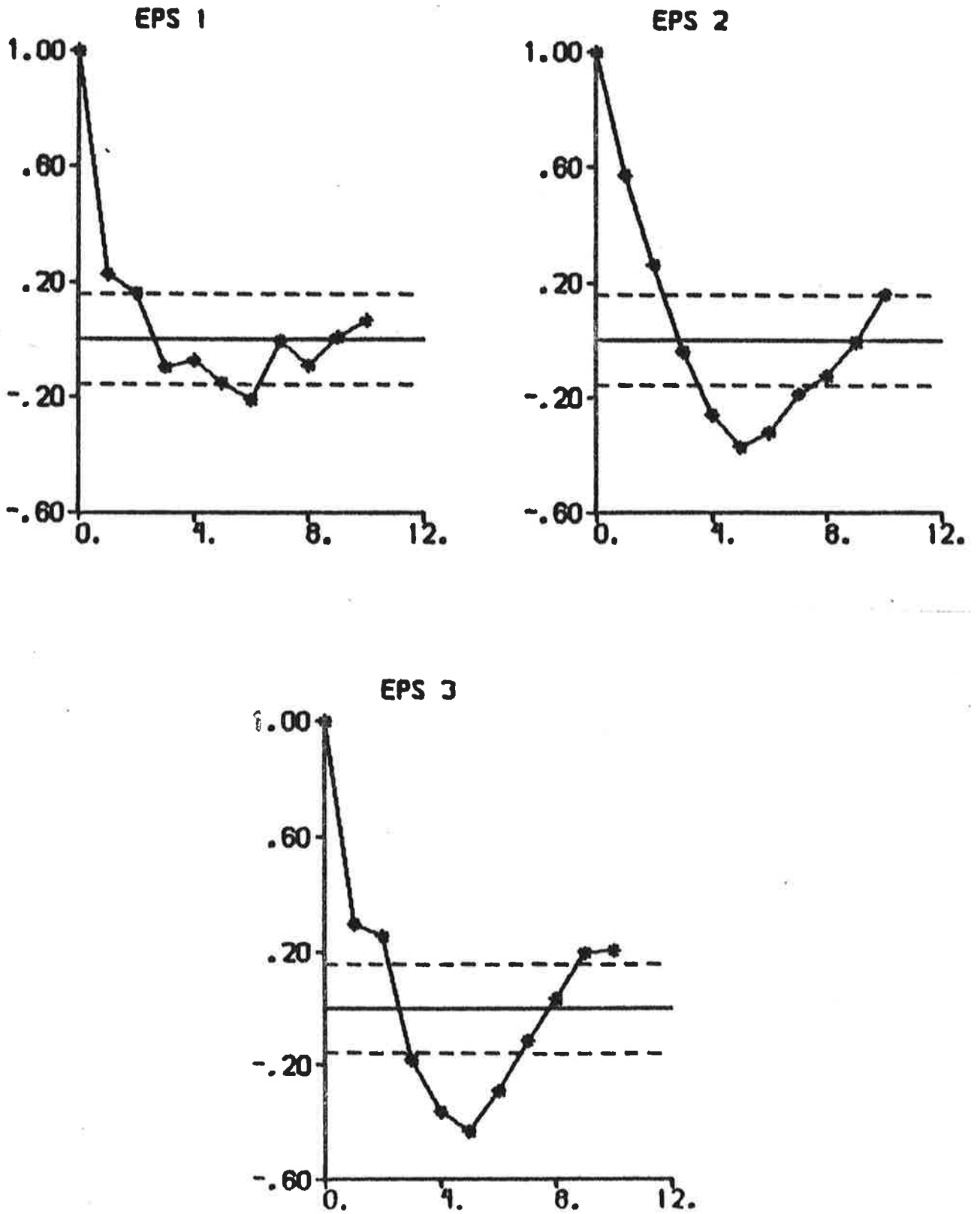
Fig. 4.18b - Prediction errors.

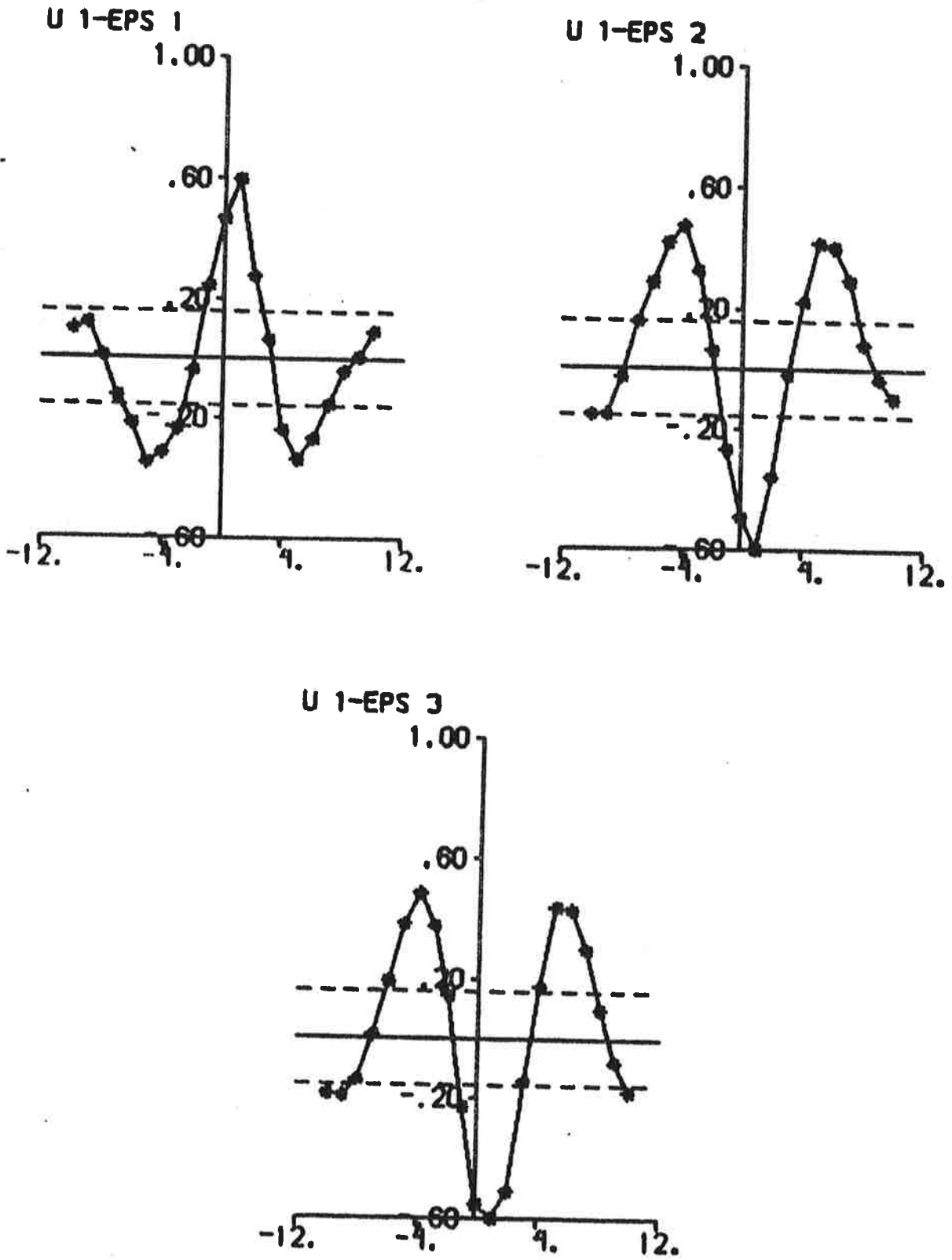Fig. 4.18c - Autocorrelation functions of prediction errors.

Fig. 4.18d – Cross correlation functions between rudder input and prediction errors.
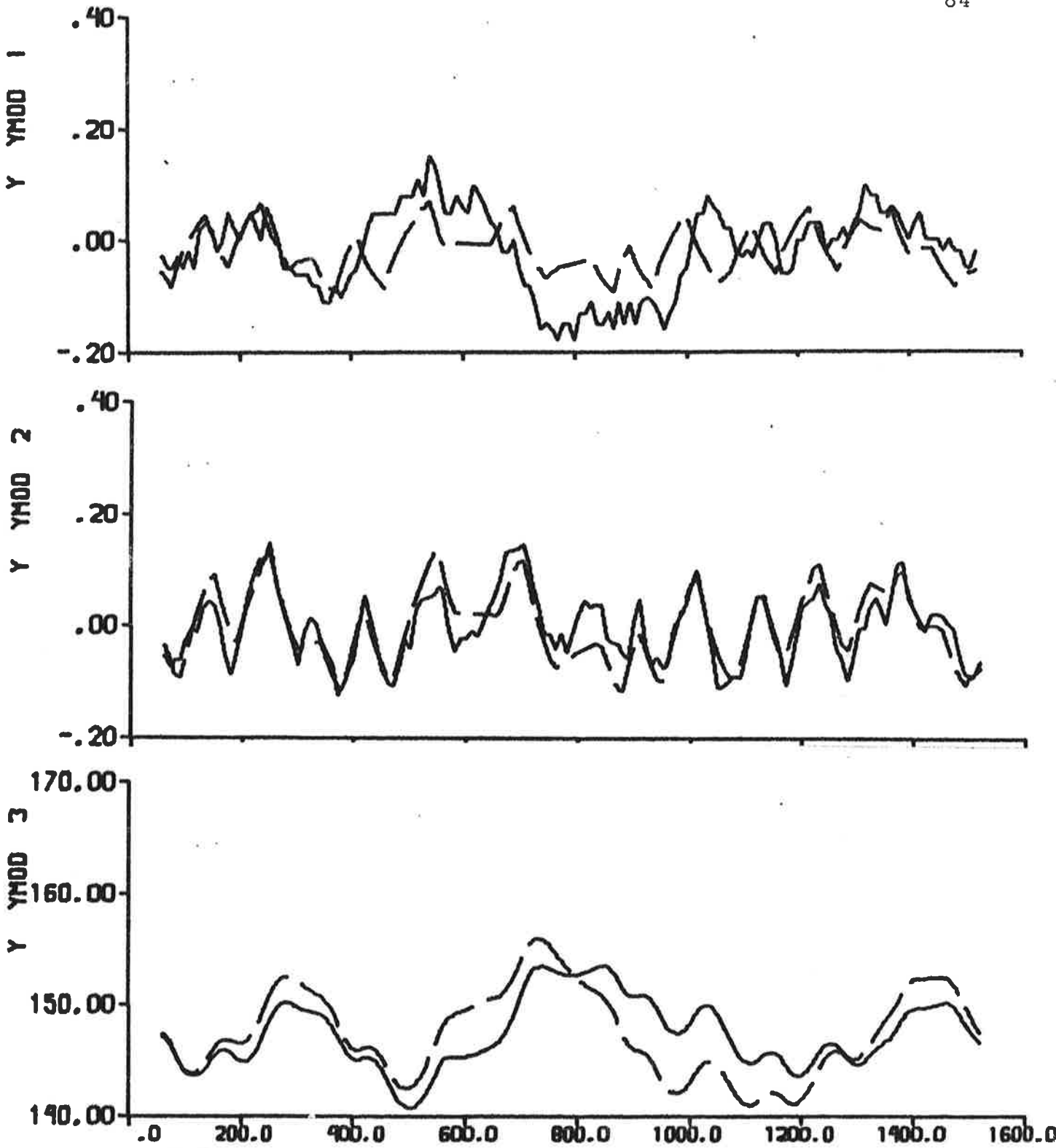
Fig. 4.19a - Result of prediction error identification (p = 6)
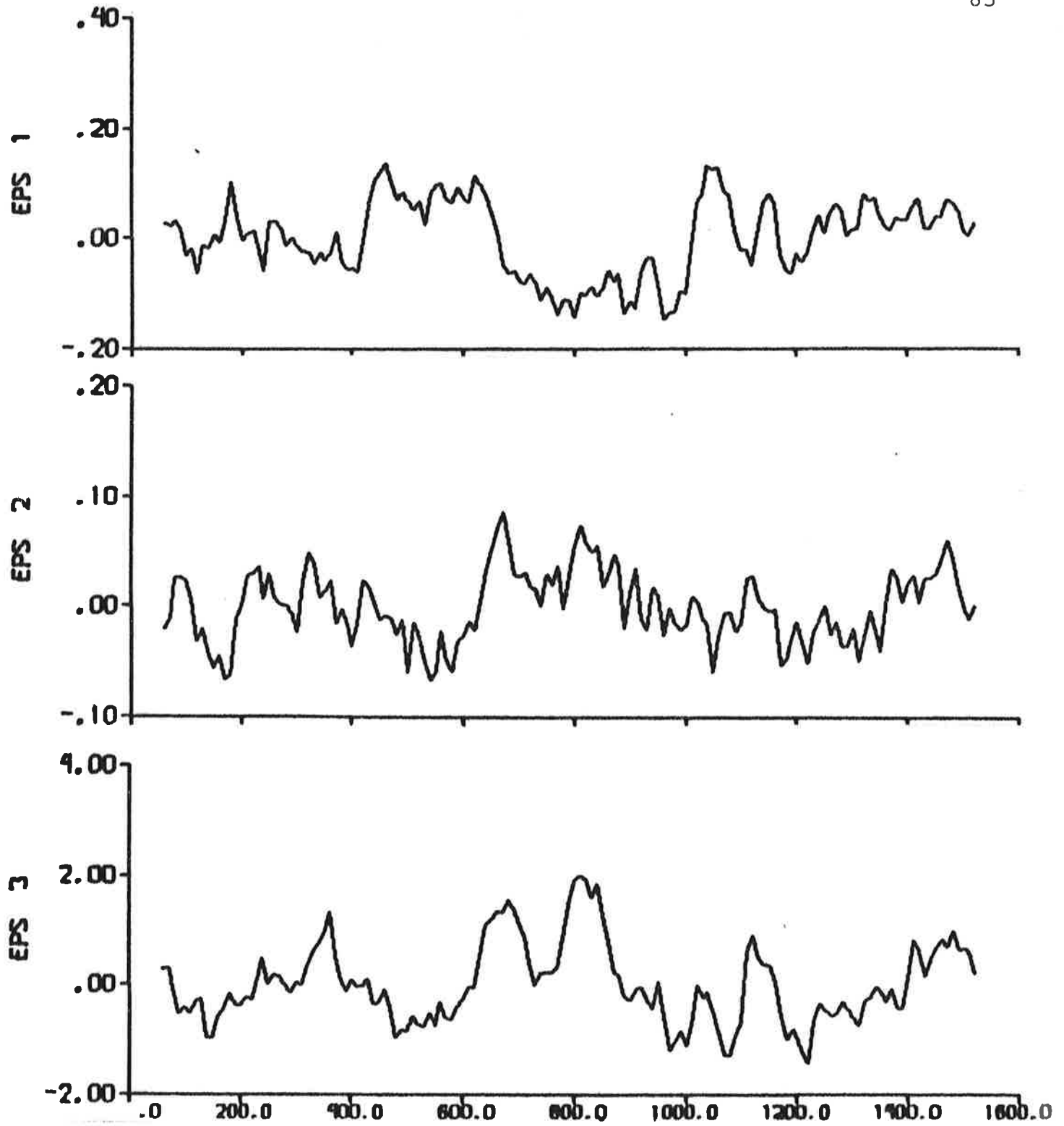to data from experiment E4.
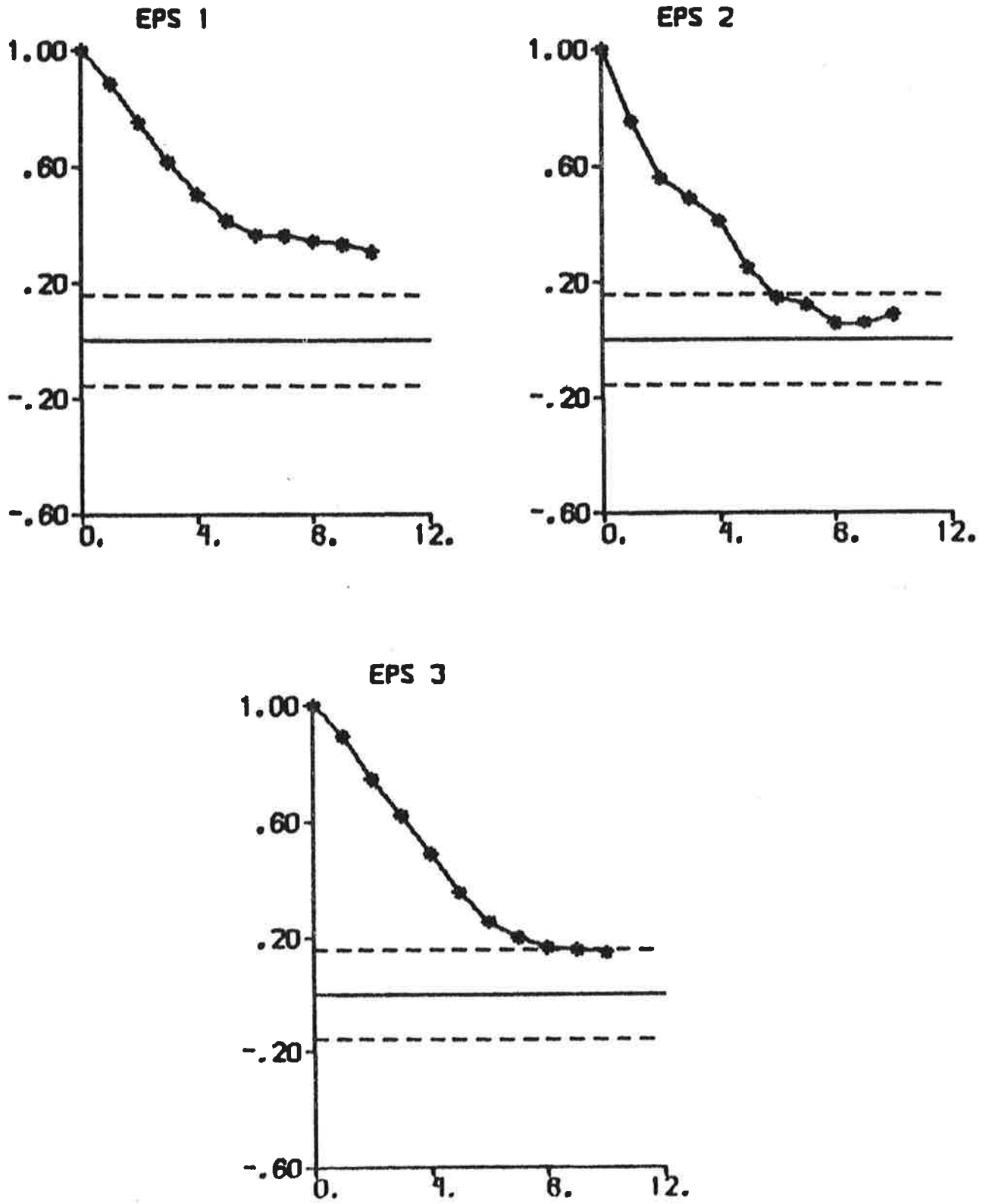
Fig. 4.19b - Prediction errors.

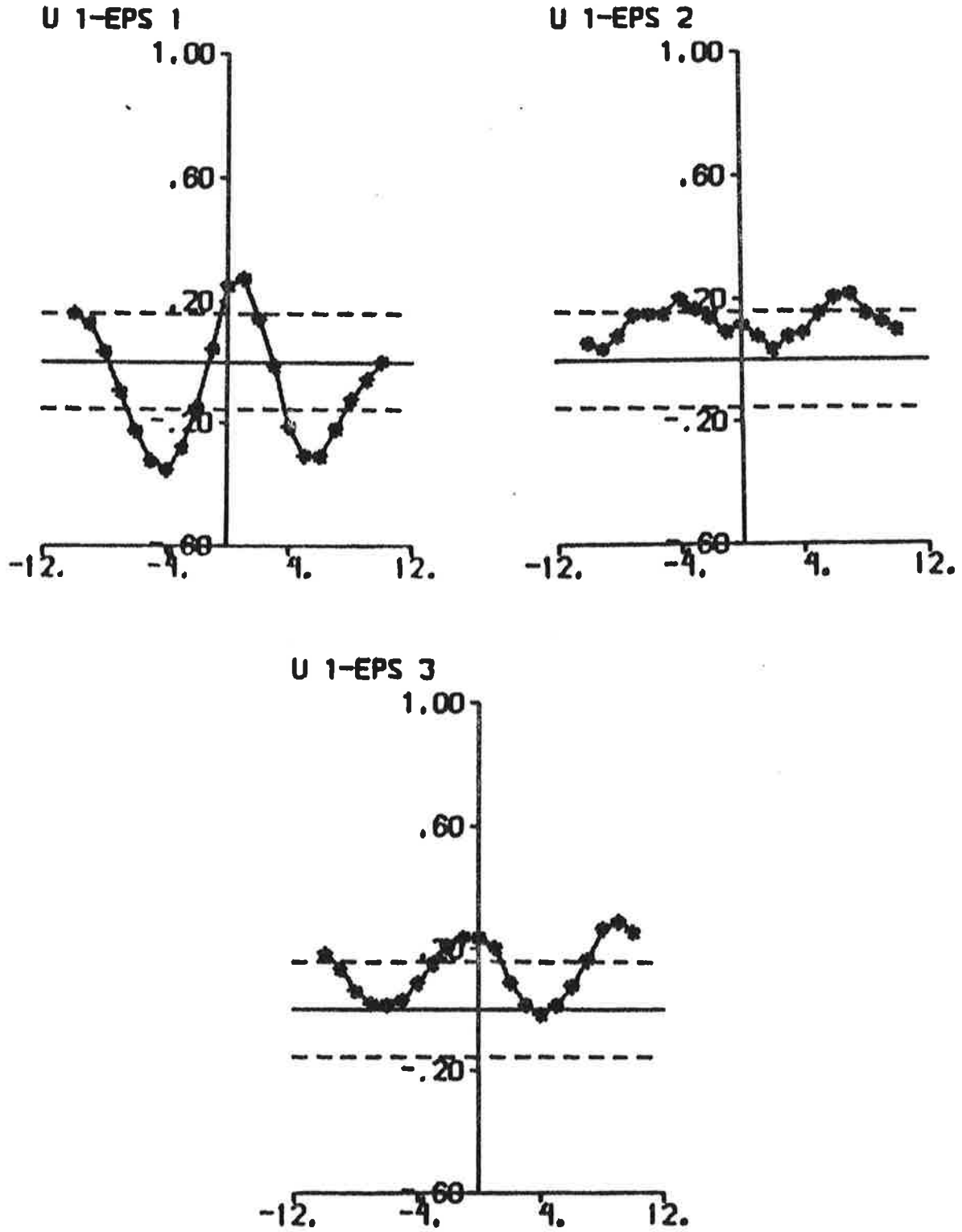Fig. 4.19c - Autocorrelation functions of prediction errors.

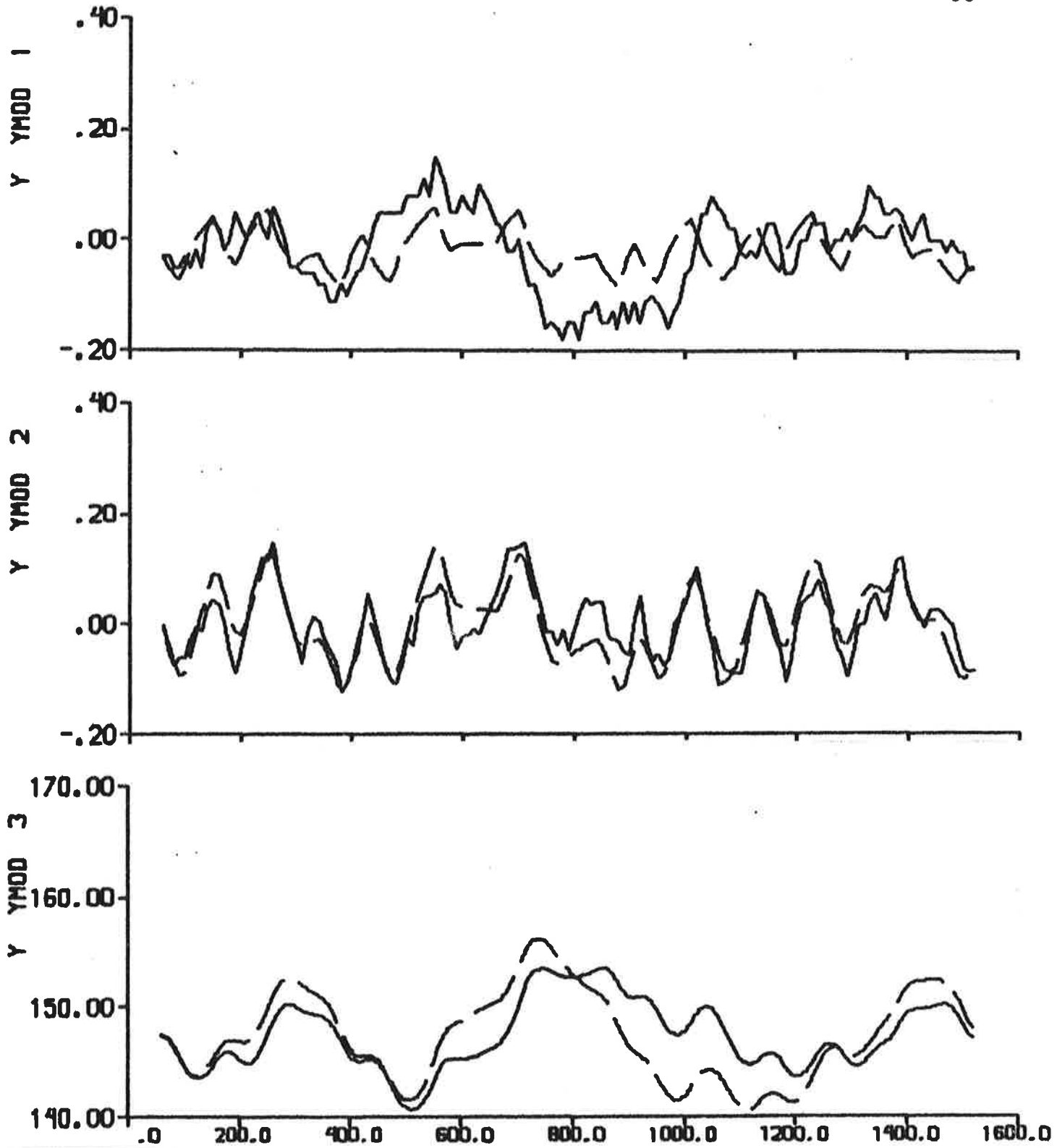Fig. 4.19d - Cross correlation functions between rudder input and prediction errors.

Fig. 4.20a - Result of prediction error identification (p = 6)
to data from experiment E4. The rudder angle is
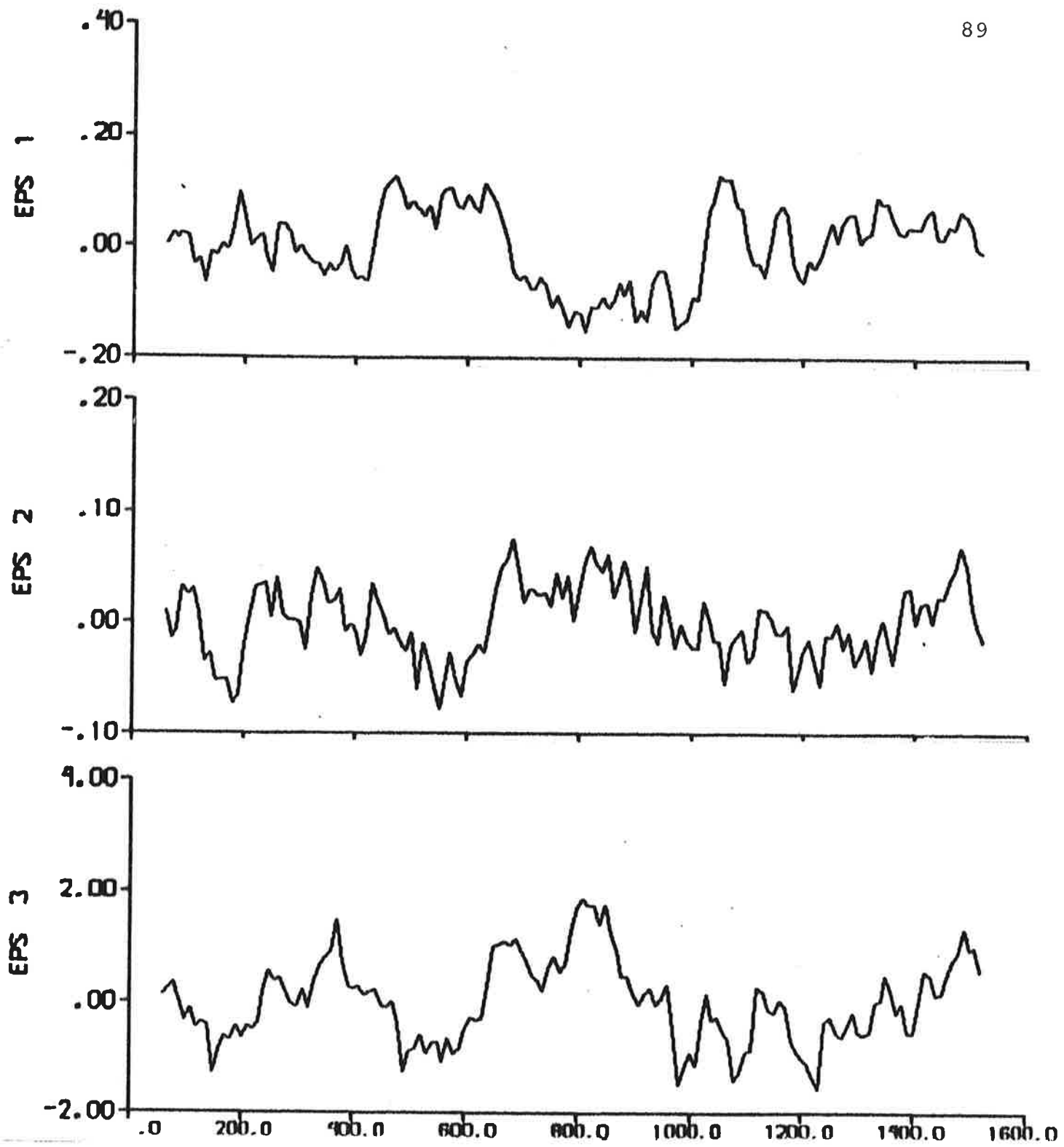the input signal.
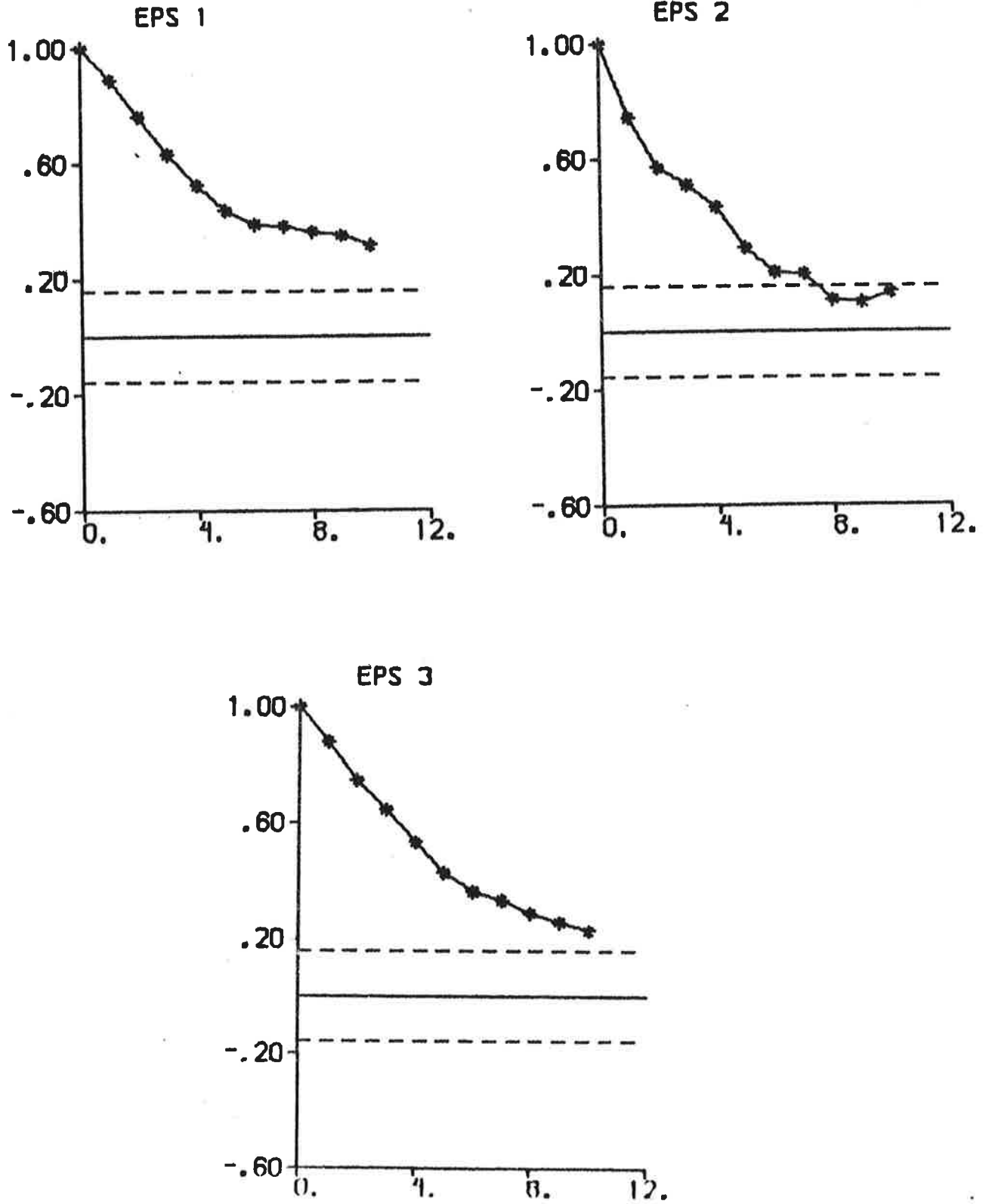
Fig. 4.20b - Prediction errors.

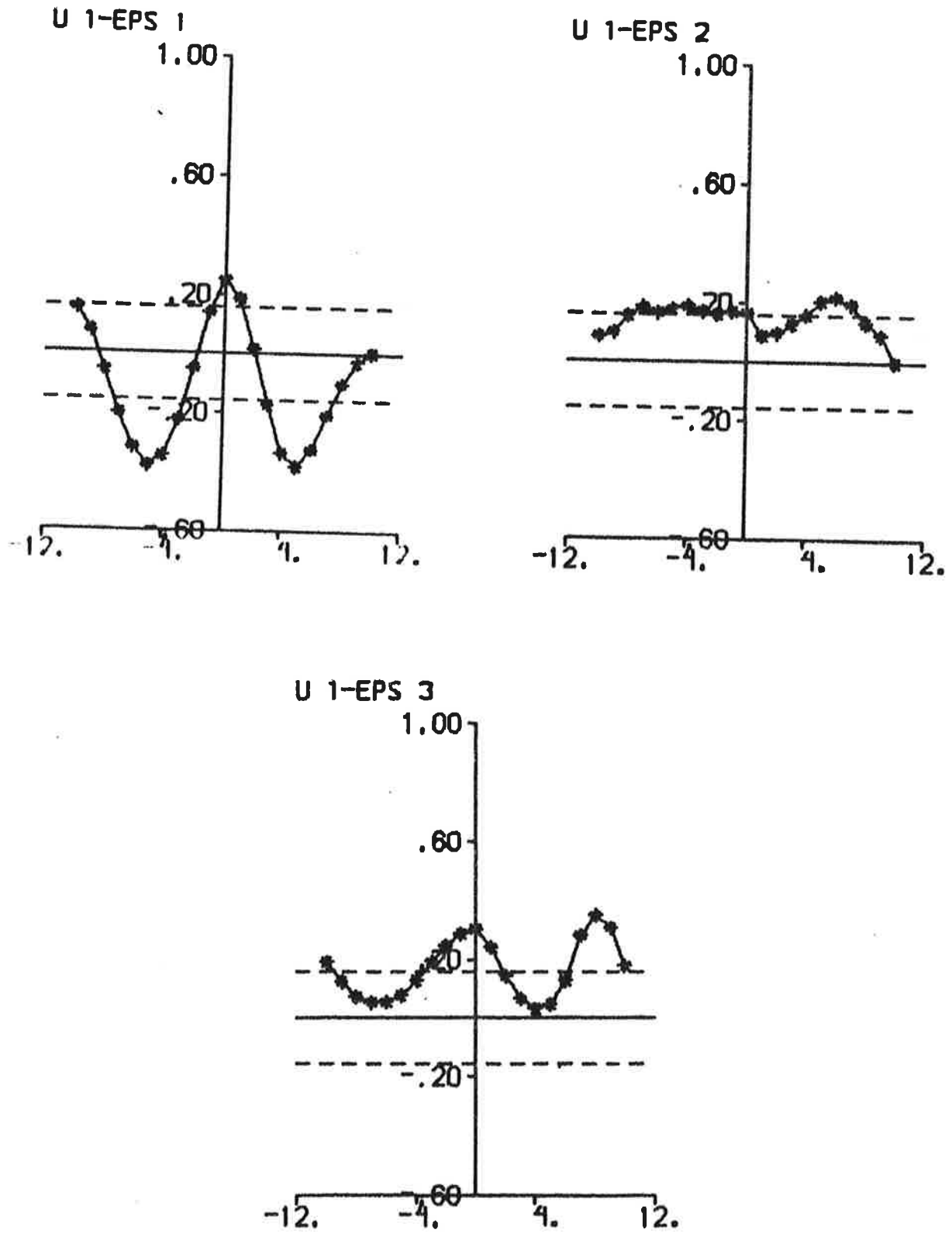Fig. 4.20c - Autocorrelation functions of prediction errors.

Fig. 4.20d - Cross correlation functions between rudder input
and prediction errors.

5. IDENTIFICATION OF NONLINEAR MODELS

Results of fitting the nonlinear model (3.1) to data from the
4 experiments are presented in this section. The fixed parameter
values (4.1) are then used, except that θ_{35} also is estimated.
The analysis performed in this section is comparable with the
analysis of Section 4.

The results are summarized in Tables 5.1 and 5.2 and in Figs.
5.1 - 5.12. The effective cross-flow drag coefficient C is
expected to be approximately 0.7 for a tanker. The values 1.99,
0.68, 28.62 and 0.52 are estimated from the 4 experiments when
the linear part of the model is fixed to SSPA:s model and the
other parameters are fitted to the data by use of the output
error method. Reasonable results are thus obtained from experi-
ments E2 and E4 only. Notice, however, that Akaike´s information
criterion AIC distinctly indicates that the nonlinear model is
appropriate to the data in all cases.

The following values of C are obtained from the output error
method when the hydrodynamic derivatives also are estimated:
C = 2.38, 0.83, 0.88 and 0.82. It is concluded by investigating
the hydrodynamic derivatives obtained that very reasonable models
are determined from experiments E2 and E4. Notice that these
models, as well as SSPA:s model, are unstable. Akaike´s information
criterion AIC indicates in all cases that the nonlinear model
should be used.

The estimated parameters from prediction error identifications
with p = 6 are summarized in Tables 5.1 and 5.2. It is concluded
that the parameter C is estimated badly in all cases except one
(C = -0.57, 0.63, -0.64 and -2.05). It is also concluded that
the parameter estimates obtained with the nonlinear model are
not changed significantly compared to the linear model (cf.
Section 4). The following filter gains K (cf. (3.4)) are obtained
from experiments E1-E4 when the prediction error method is applied
(p = 6):

$$K = \begin{pmatrix} 4.0 \cdot 10^{-1} & -1.9 \cdot 10^{-1} & -5.3 \cdot 10^{-2} \\ -4.6 \cdot 10^{-4} & 1.1 \cdot 10^{-3} & 3.2 \cdot 10^{-4} \\ -4.1 \cdot 10^{-3} & 4.6 \cdot 10^{-2} & 1.9 \cdot 10^{-2} \end{pmatrix} \qquad (5.1)$$

$$K = \begin{pmatrix} 6.8 \cdot 10^{-2} & 8.3 \cdot 10^{-2} & -3.1 \cdot 10^{-3} \\ 1.4 \cdot 10^{-4} & 1.1 \cdot 10^{-3} & 1.1 \cdot 10^{-4} \\ 4.2 \cdot 10^{-3} & 2.7 \cdot 10^{-2} & 7.4 \cdot 10^{-3} \end{pmatrix} \qquad (5.2)$$

$$K = \begin{pmatrix} 2.0 \cdot 10^{-2} & -9.4 \cdot 10^{-1} & -2.4 \cdot 10^{-2} \\ -1.2 \cdot 10^{-5} & 1.4 \cdot 10^{-3} & 2.0 \cdot 10^{-4} \\ -3.6 \cdot 10^{-4} & 4.9 \cdot 10^{-2} & 1.5 \cdot 10^{-2} \end{pmatrix} \qquad (5.3)$$

$$K = \begin{pmatrix} 1.5 \cdot 10^{-6} & -4.6 \cdot 10^{-1} & -1.1 \cdot 10^{-1} \\ -9.6 \cdot 10^{-9} & 3.0 \cdot 10^{-3} & 7.3 \cdot 10^{-4} \\ -1.9 \cdot 10^{-7} & 5.3 \cdot 10^{-2} & 2.3 \cdot 10^{-2} \end{pmatrix} \qquad (5.4)$$

Cf. (4.2) - (4.5).

It is thus concluded by comparing the results of the nonlinear
model with the results of the linear model that only experiments
E2 and E4 are influenced by nonlinear effects. It is difficult
to obtain reasonable estimates of the effective cross-flow drag
coefficient C when the "linear" experiments E1 and E3 are analysed.
Three $20^{\circ}/20^{\circ}$ zig-zag tests performed with a cargo ship of the
Mariner class were analysed in Källström (1977b). A significant
improvement by using the nonlinear model instead of the linear
model was reported in that case.

The only reasonable model obtained by the prediction error method
with p = 6 was the one obtained from experiment E2. Notice that
this model is unstable while a stable model was obtained when
a linear model was fitted to the data from experiment E2.

The model determined from experiment E2 with the prediction
error method is further investigated by fitting the wind parameters,
the biases, the initial state, and the time delay to data from
the 4 experiments by use of the output error method. The hydrodyna-
mic derivatives are then fixed. C is equal to zero when experiments
E1 and E3 are investigated, while C = 0.63 (cf. Table 5.1) when

	E 1			E 2		
	Output error (SSPA:s model)	Output error	Pred. error p = 6	Output error (SSPA:s model)	Output error	Pred. error p = 6
Figure	5.1	5.2	5.3	5.4	5.5	5.6
ν	11	16	15	11	16	15
V	88	14	0.41	1.26	$3.5 \cdot 10^{-3}$	$5.3 \cdot 10^{-3}$
AIC	250	−723	--	−56	−705	--
Y_v'	−0.00687*	−0.02577	−0.04283	−0.00687*	−0.01461	−0.02037
$Y_r'-m'$	−0.00724*	−0.00859	−0.01788	−0.00724*	−0.00853	−0.01065
N_v'	−0.00254*	−0.00108	0.00027	−0.00254*	−0.00503	−0.00300
$N_r'-m'x_G'$	−0.00161*	−0.00038	−0.00020	−0.00161*	−0.00235	−0.00138
Y_δ'	0.00201*	0.00107	0.00158	0.00201*	0.00262	0.00206
N_δ'	−0.00095*	−0.00050	−0.00074	−0.00095*	−0.00123	−0.00097
C	1.99	2.38	−0.57	0.68	0.83	0.63
θ_9	$-1.6 \cdot 10^{-5}$	$-8.0 \cdot 10^{-5}$	0*	$-2.4 \cdot 10^{-5}$	$-1.5 \cdot 10^{-5}$	0*
θ_{10}	0.066	−0.003	0*	0.218	0.107	0*
θ_{13}	$-6.4 \cdot 10^{-6}$	$1.9 \cdot 10^{-5}$	$9.4 \cdot 10^{-4}$	$-1.5 \cdot 10^{-5}$	$-6.2 \cdot 10^{-5}$	$-4.8 \cdot 10^{-4}$
θ_{14}	$-1.8 \cdot 10^{-6}$	$-4.4 \cdot 10^{-6}$	$-5.0 \cdot 10^{-7}$	$6.5 \cdot 10^{-6}$	$-8.1 \cdot 10^{-6}$	$-4.7 \cdot 10^{-5}$
θ_{15} [knots]	0.03	0.08	−0.29	0.11	0.06	0.25
θ_{17} [deg/s]	0.003	0.003	0.003	−0.002	0.002	0.003
$R_1(1,1)$ [s]	−	−	$6.9 \cdot 10^{-3}$	−	--	$3.8 \cdot 10^{-7}$
$R_1(1,2)$ [s]	−	--	$-1.3 \cdot 10^{-4}$	−	−	$3.9 \cdot 10^{-8}$
$R_1(2,2)$ [s]	−	--	$2.6 \cdot 10^{-6}$	−	--	$4.1 \cdot 10^{-9}$
$R_2(1,1)$ [knots]^2	−	--	$2.0 \cdot 10^{-8}$	−	−	$4.4 \cdot 10^{-3}$
$R_2(2,2)$ [deg/s]^2	−	--	10^{-4*}	--	−	10^{-4*}
θ_{25} [knots]	0.12	0.14	0*	0.10	0.04	0*
θ_{26} [deg/s]	0.007	−0.010	0*	0.003	−0.027	0*
θ_{27} [deg]	157.20	149.67	146.89*	143.89	144.05	144.67*
T_D [s]	8.5	6.1	1.4	0.0	0.0	1.4
K'	1.59	−35.28	−2.36	1.59	3.68	6.71
K_1'	−1.00	−0.53	−0.78	−1.00	−1.32	−1.03
K_v'	−1.38	11.80	1.02	−1.38	−1.97	−3.41
K_{1v}'	0.12	0.06	0.10	0.12	0.17	0.13
T_1'	−4.88	75.26	2.86	−4.88	−6.39	−11.08
T_2'	0.43	0.51	0.40	0.43	0.28	0.36
T_3'	1.32	0.58	0.38	1.32	0.64	0.61
T_{3v}'	0.19	0.21	0.11	0.19	0.15	0.15

* = fixed value

Table 5.1 – Estimated parameters from identifications to data from experiments E1 and E2.

	E 3			E 4		
	Output error (SSPA:s model)	Output error	Pred. error p = 6	Output error (SSPA:s model)	Output error	Pred. error p = 6
Figure	5.7	5.8	5.9	5.10	5.11	5.12
ν	11	16	15	11	16	15
V	21	5.71	0.20	0.32	0.13	$2.2\cdot10^{-2}$
AIC	-522	-1212	-	-389	-517	-
Y_v'	-0.00687^*	-0.01511	-0.26518	-0.00687^*	-0.00792	-0.41813
$Y_r'-m'$	-0.00724^*	0.00131	-0.10228	-0.00724^*	-0.00616	-0.17439
N_v'	-0.00254^*	-0.00285	0.00184	-0.00254^*	-0.00266	-0.03424
$N_r'-m'x_G'$	-0.00161^*	-0.00076	0.00001	-0.00161^*	-0.00123	-0.01567
Y_δ'	0.00201^*	0.00059	0.00166	0.00201^*	0.00208	0.00287
N_δ'	-0.00095^*	-0.00028	-0.00078	-0.00095^*	-0.00098	-0.00135
C	28.62	0.88	-0.64	0.52	0.82	-2.05
θ_9	$-4.7\cdot10^{-5}$	$1.5\cdot10^{-4}$	0^*	$-1.1\cdot10^{-5}$	$1.8\cdot10^{-5}$	0^*
θ_{10}	0.191	0.270	0^*	-0.044	0.304	0^*
θ_{13}	$1.5\cdot10^{-5}$	$1.8\cdot10^{-4}$	$-7.2\cdot10^{-4}$	$-2.8\cdot10^{-7}$	$-3.7\cdot10^{-5}$	$-5.2\cdot10^{-4}$
θ_{14}	$3.1\cdot10^{-5}$	$-2.9\cdot10^{-6}$	$1.1\cdot10^{-5}$	$3.5\cdot10^{-7}$	$-2.3\cdot10^{-7}$	$-3.3\cdot10^{-5}$
θ_{15} [knots]	0.03	-0.46	0.02	0.02	-0.03	0.00
θ_{17} [deg/s]	0.001	0.002	0.002	-0.002	0.001	0.000
$R_1(1,1)$ [s]	-	-	$1.5\cdot10^{-2}$	-	-	$1.4\cdot10^{-3}$
$R_1(1,2)$ [s]	-	-	$-1.2\cdot10^{-4}$	-	-	$1.6\cdot10^{-4}$
$R_1(2,2)$ [s]	-	-	$9.6\cdot10^{-7}$	-	-	$1.8\cdot10^{-5}$
$R_2(1,1)$ [knots]^2	-	-	$3.5\cdot10^{-1}$	-	-	901.9
$R_2(2,2)$ [deg/s]^2	-	-	10^{-4*}	-	-	10^{-4*}
θ_{25} [knots]	-0.12	0.52	0^*	-0.05	-0.14	0^*
θ_{26} [deg/s]	-0.005	-0.035	0^*	-0.013	-0.066	0^*
θ_{27} [deg]	146.23	149.28	146.58^*	146.97	148.58	147.13^*
T_D [s]	9.9	10.0	6.2	9.1	7.0	7.9
K'	1.59	-0.39	-1.09	1.59	2.01	-1.14
K_1'	-1.00	-	-0.86	-1.00	-1.03	-1.57
K_v'	-1.38	0.01	0.43	-1.38	-1.30	0.48
K_{1v}'	0.12	-	0.11	0.12	0.13	0.22
T_1'	-4.88	}complex	1.27	-4.88	-4.64	1.09
T_2'	0.43	}poles	0.06	0.43	0.50	0.02
T_3'	1.32	0.77	0.06	1.32	1.19	0.03
T_{3v}'	0.19	6.58	0.02	0.19	0.23	0.01

* = fixed value

Table 5.2 - Estimated parameters from identification to data from experiments E3 and E4.
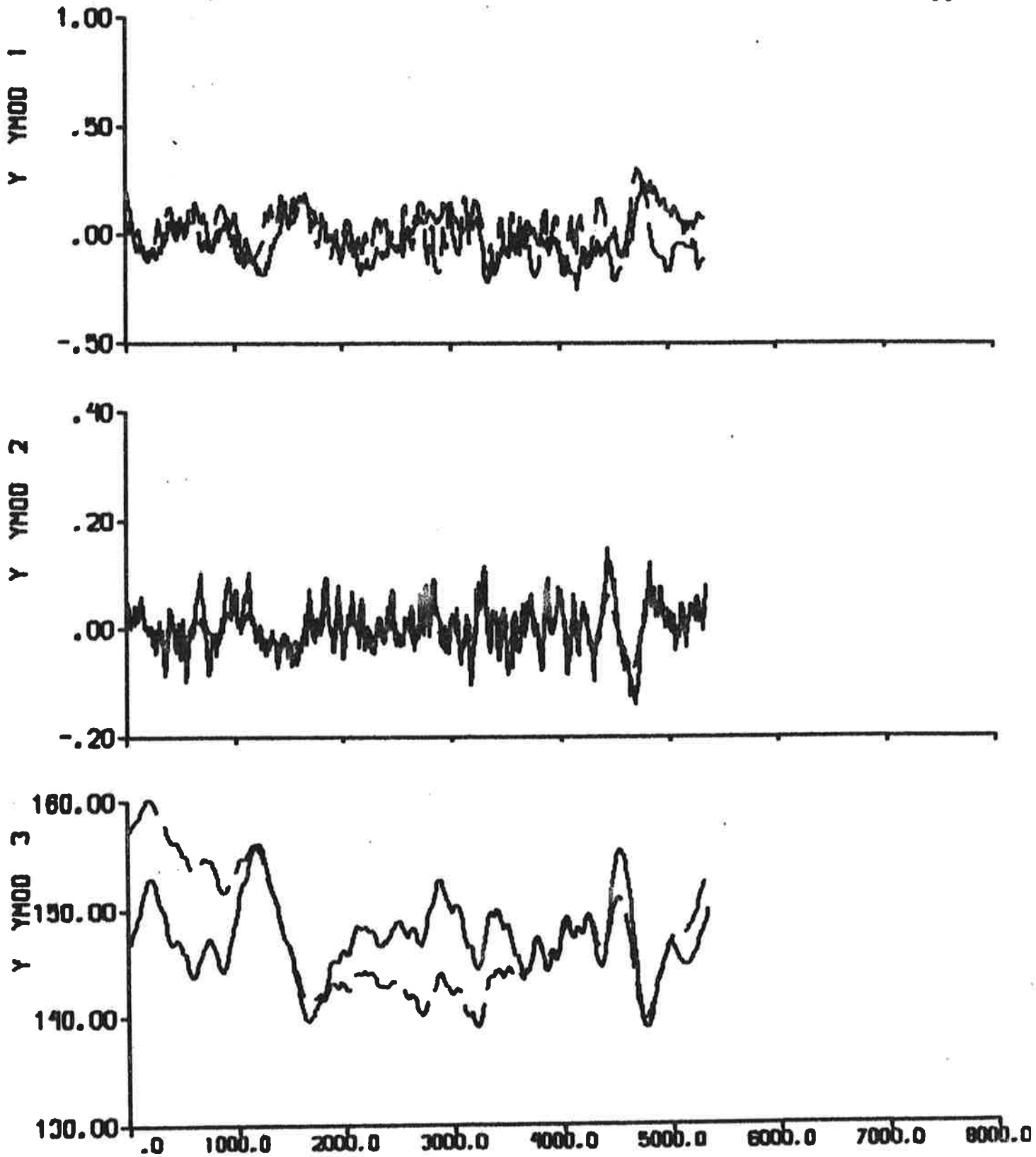
Fig. 5.1a – Result of output error identification to data from experiment E1,
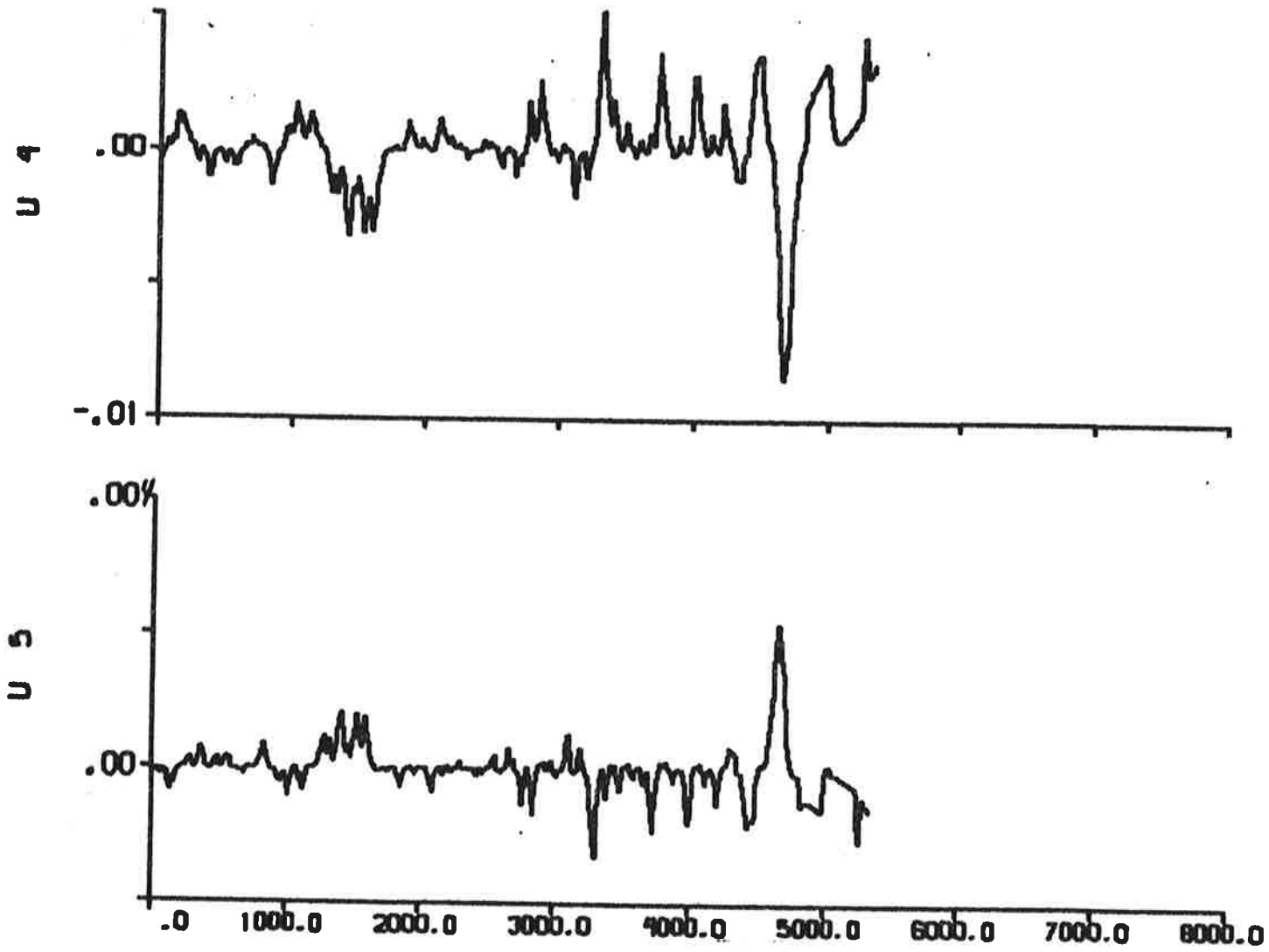when the linear part of the model is fixed to SSPA:s model

Fig. 5.1b - Additional inputs U4 = f_Y/m' and U5 = f_N/m'
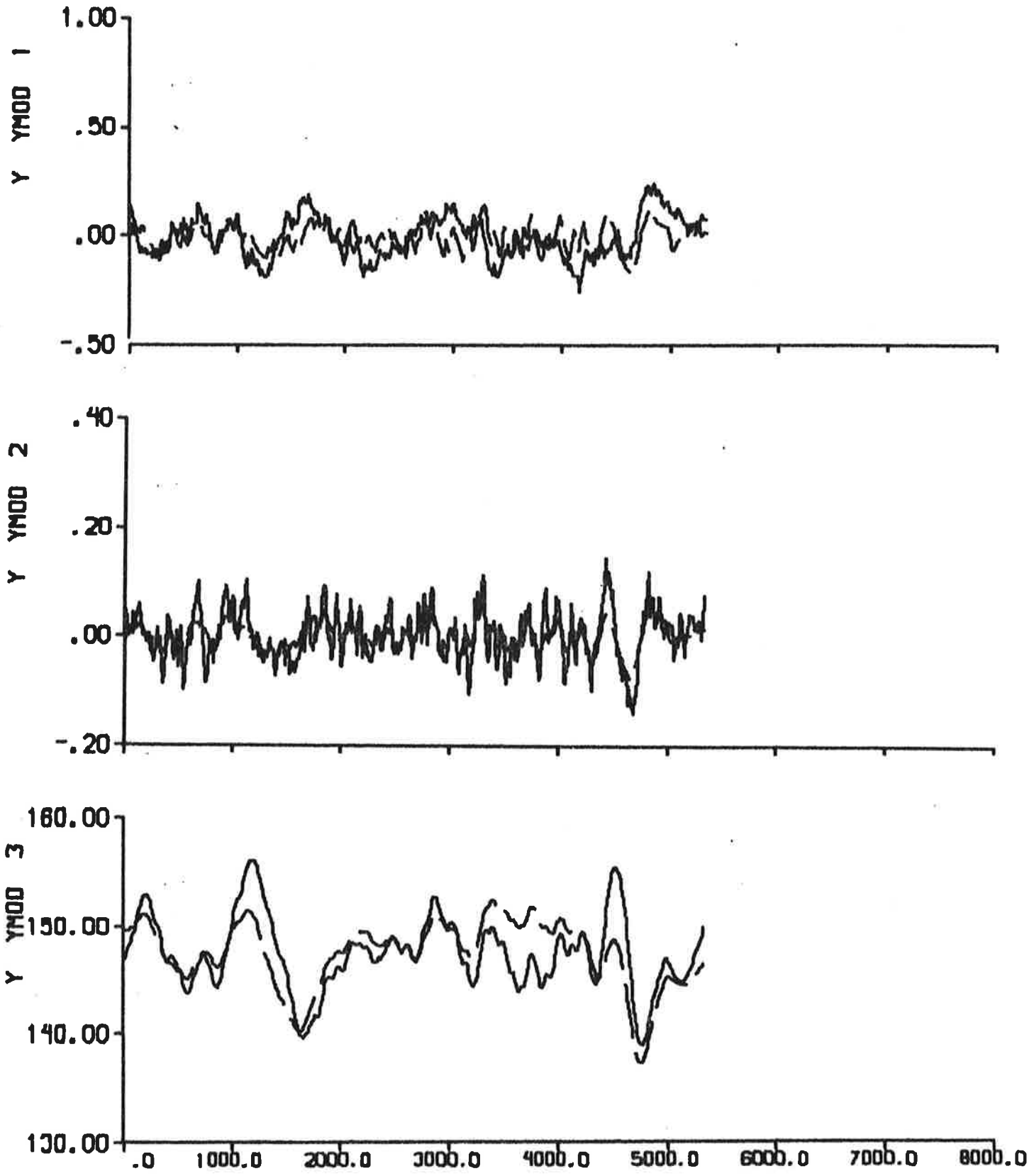describing the nonlinear contributions.

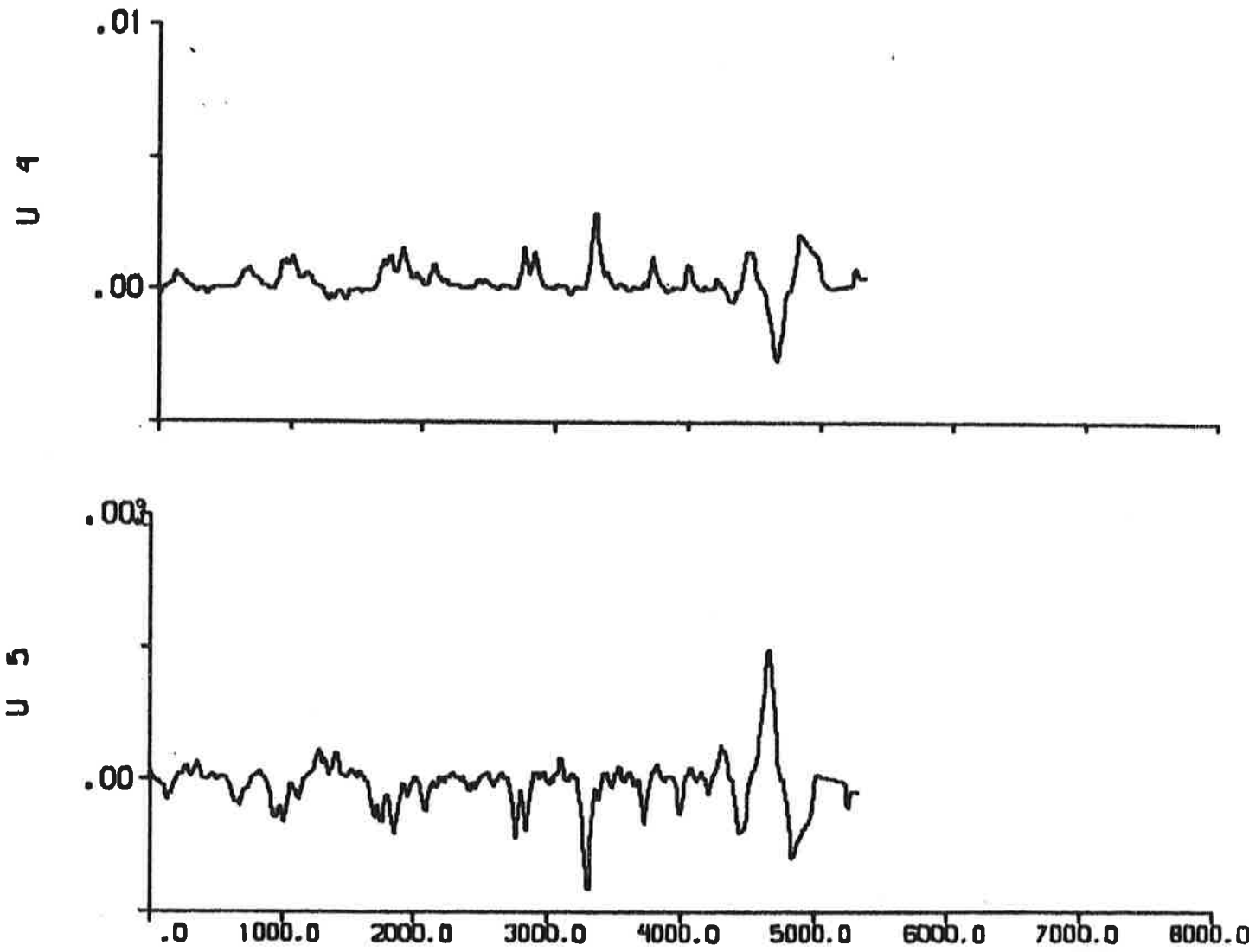Fig. 5.2a - Result of output error identification
to data from experiment E1.

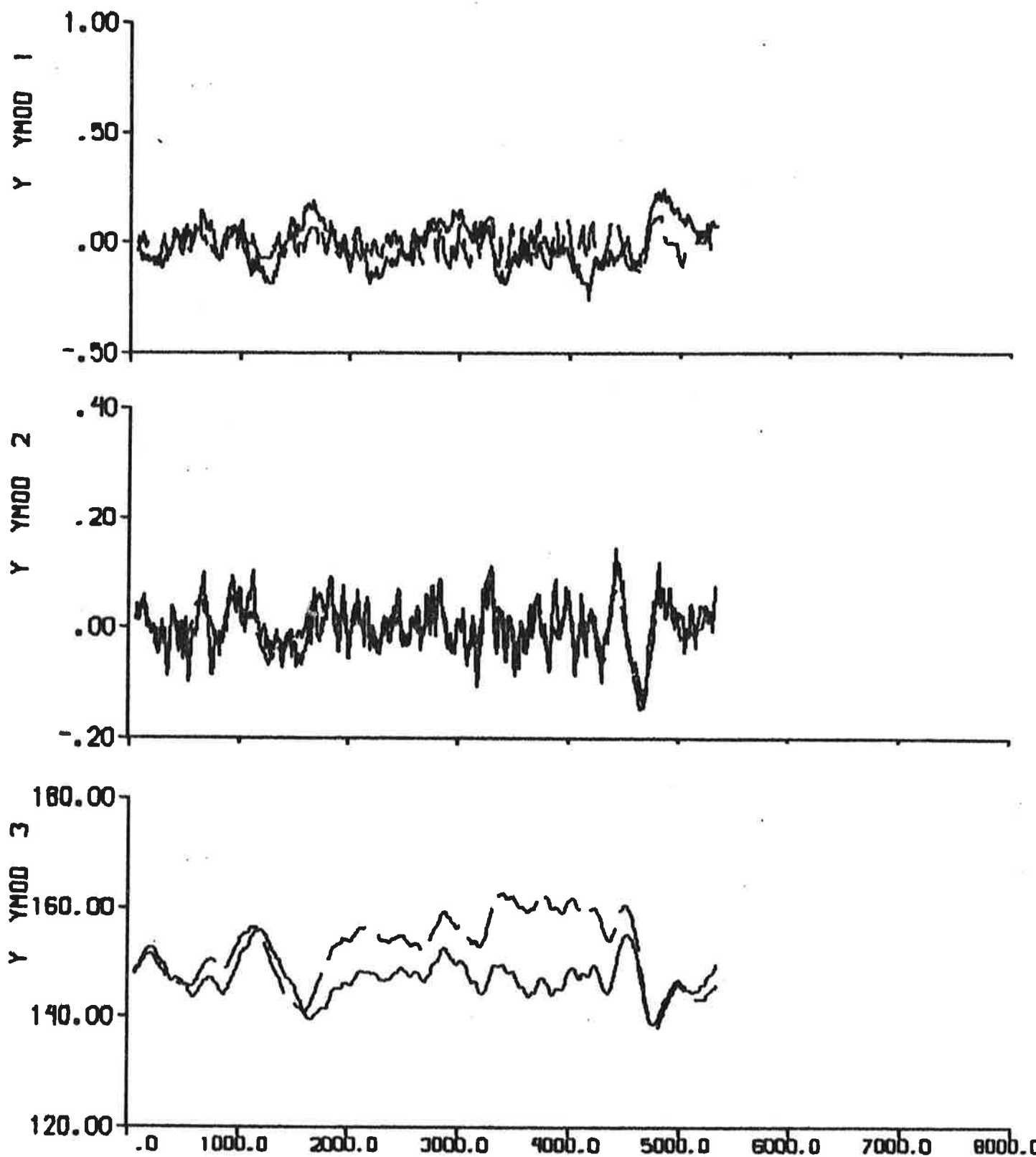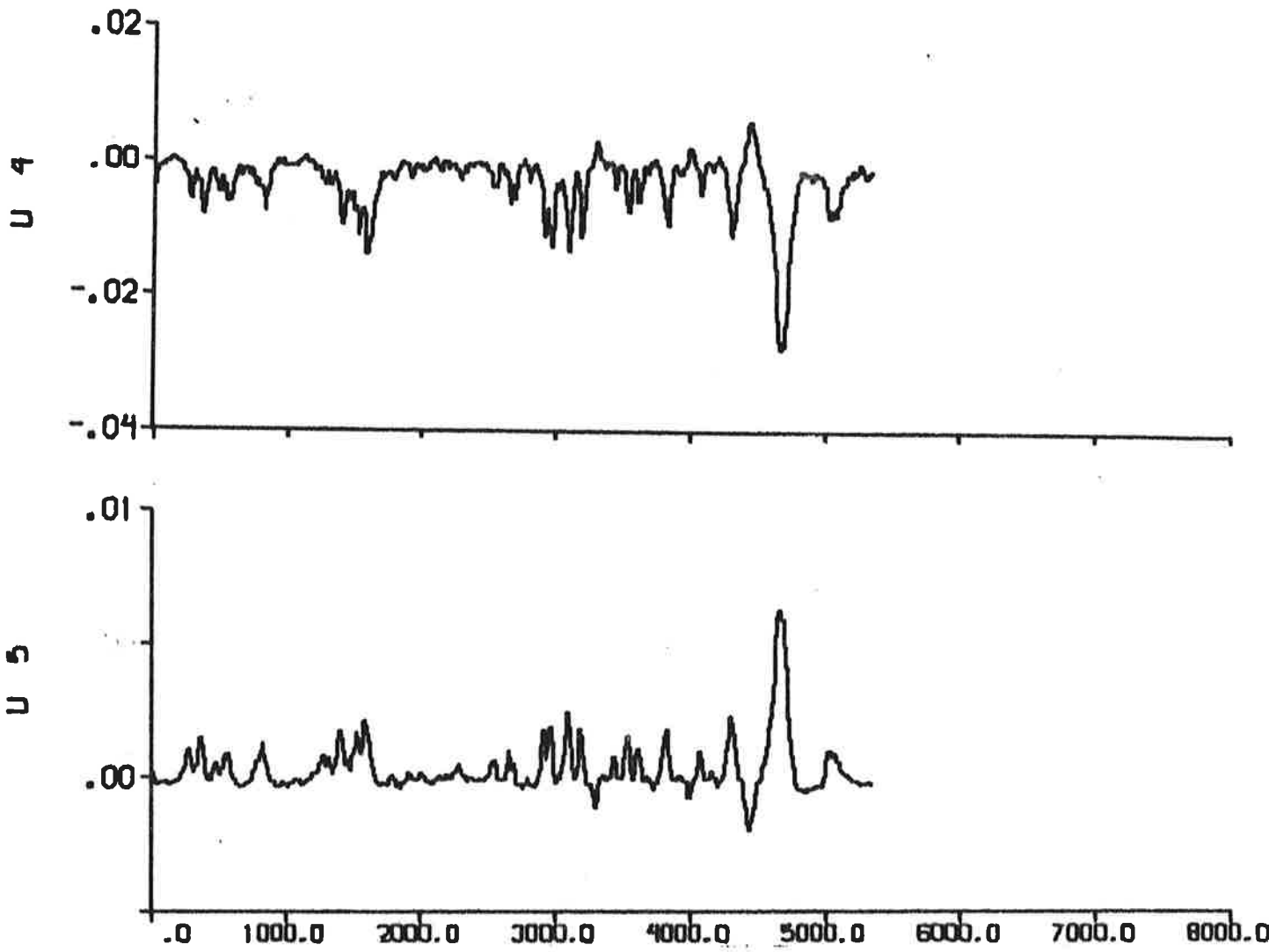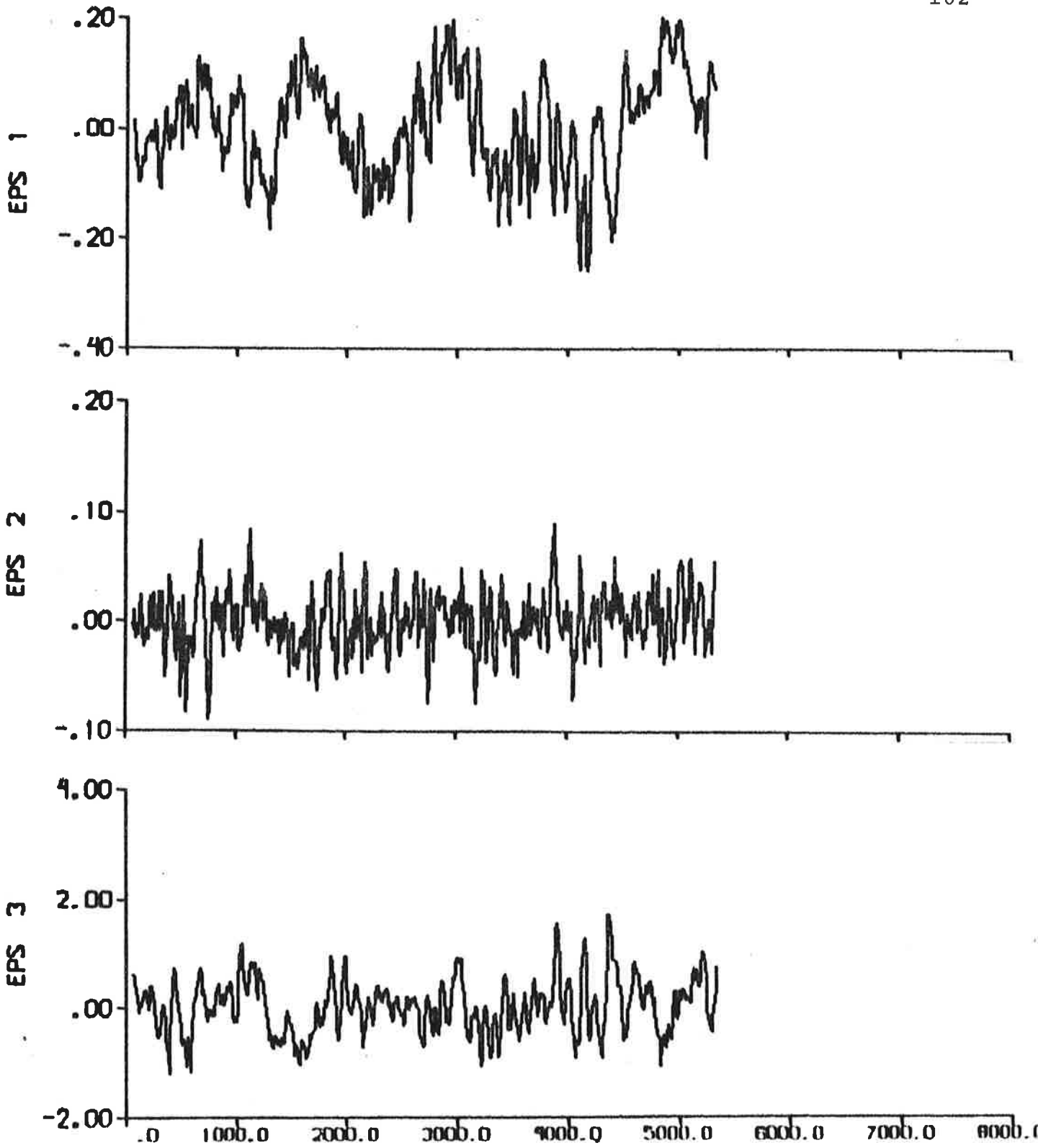Fig. 5.2b - Additional inputs U4 = f_Y/m' and U5 = f_N/m' describing the nonlinear contributions.
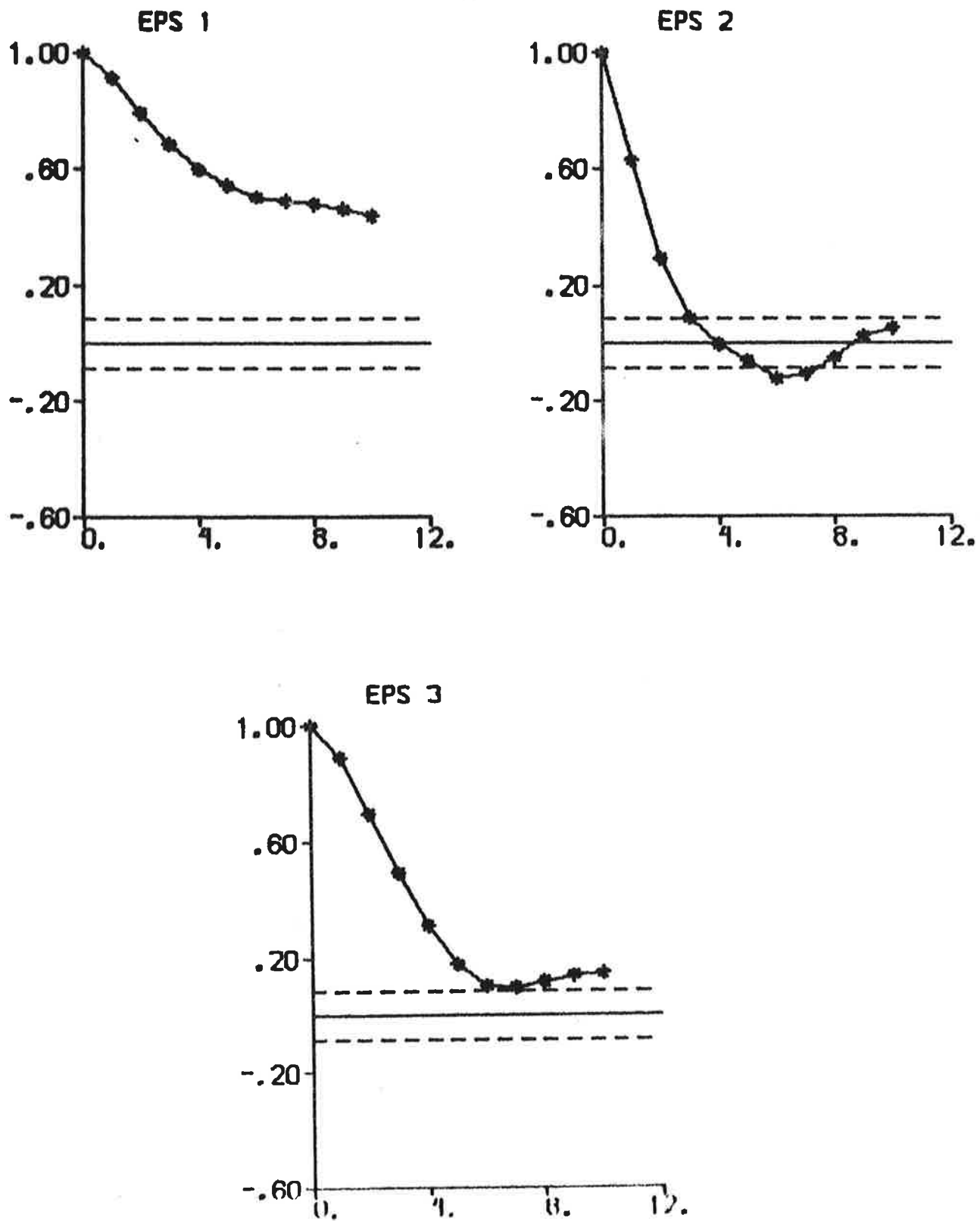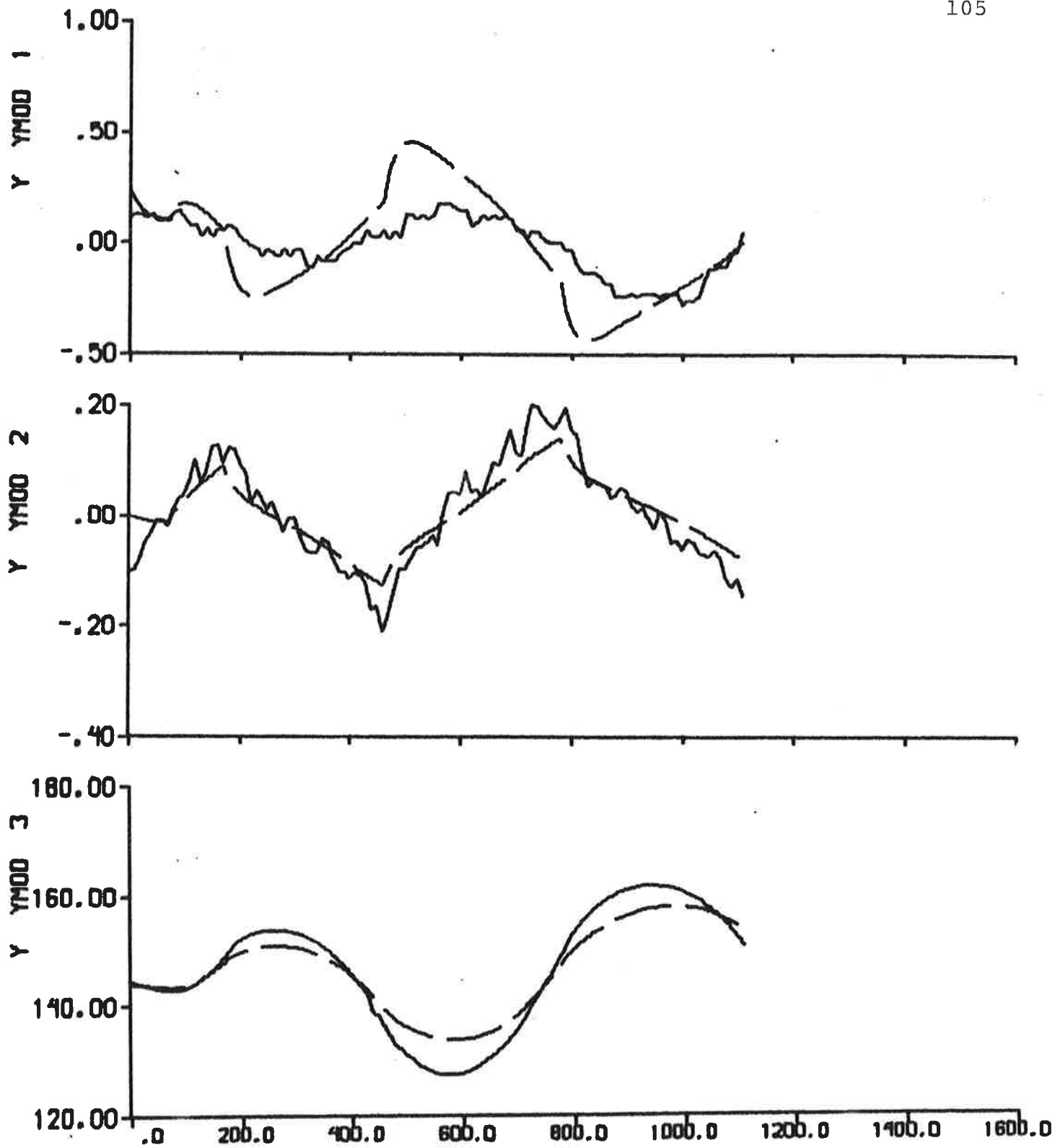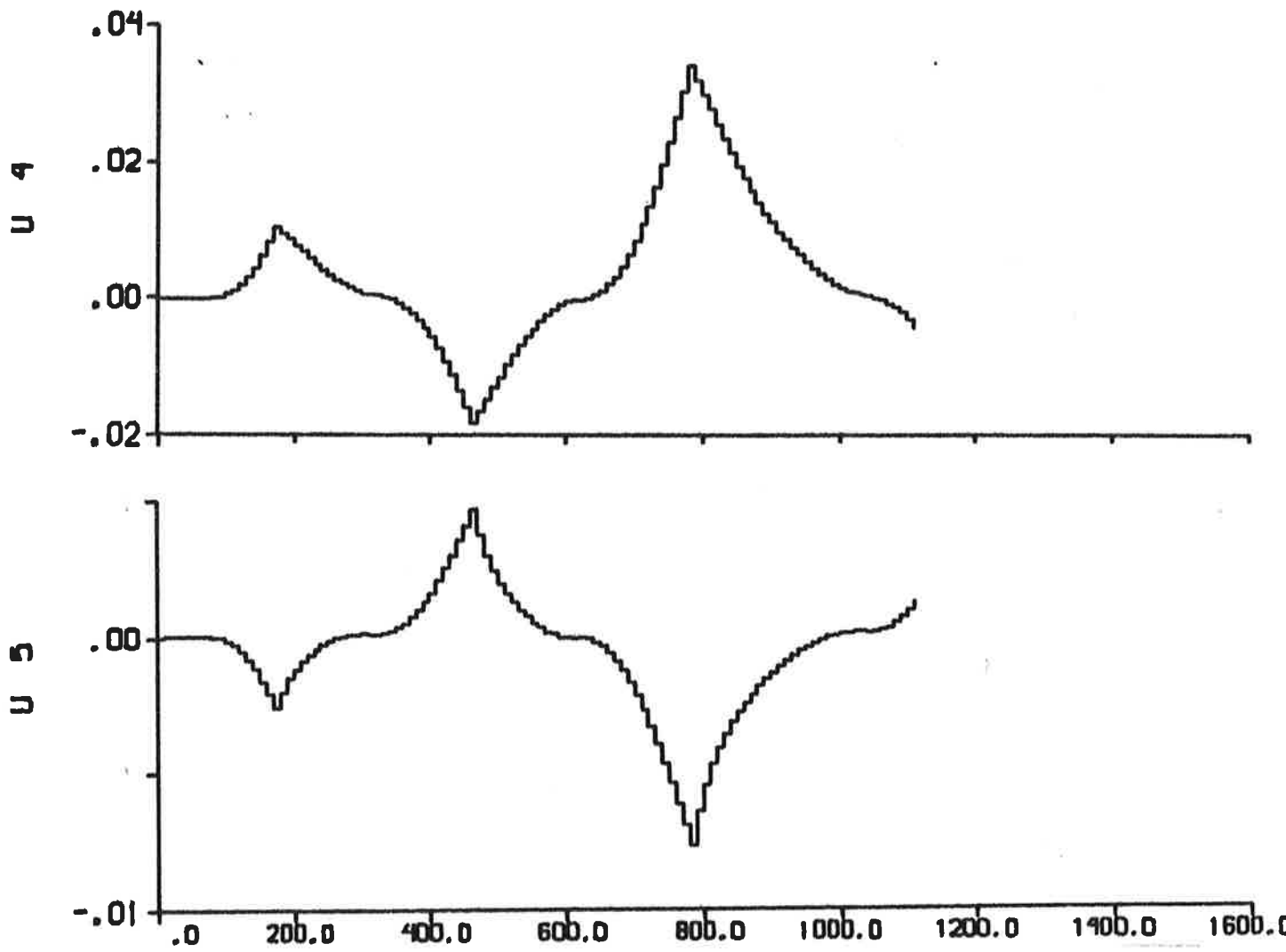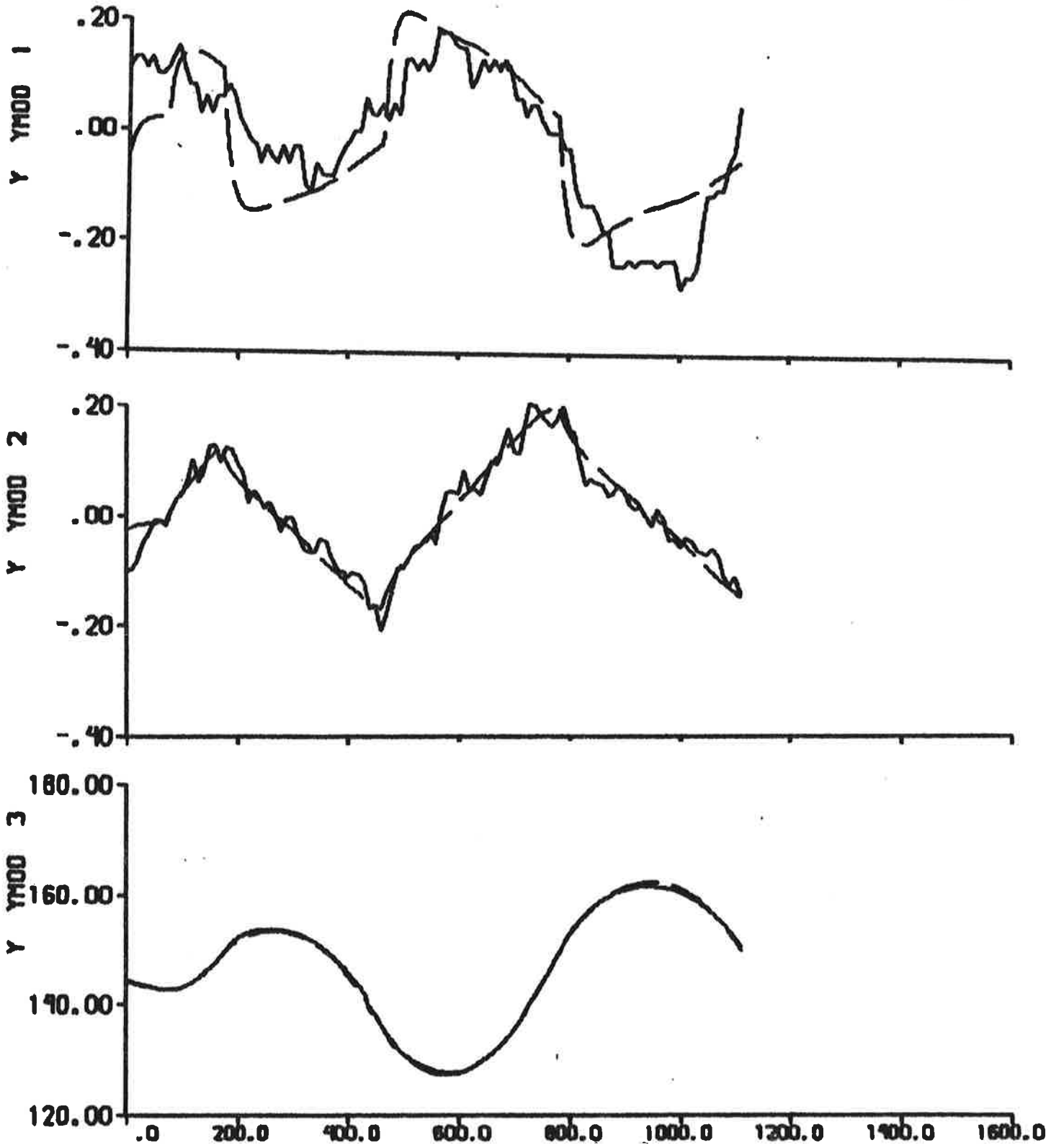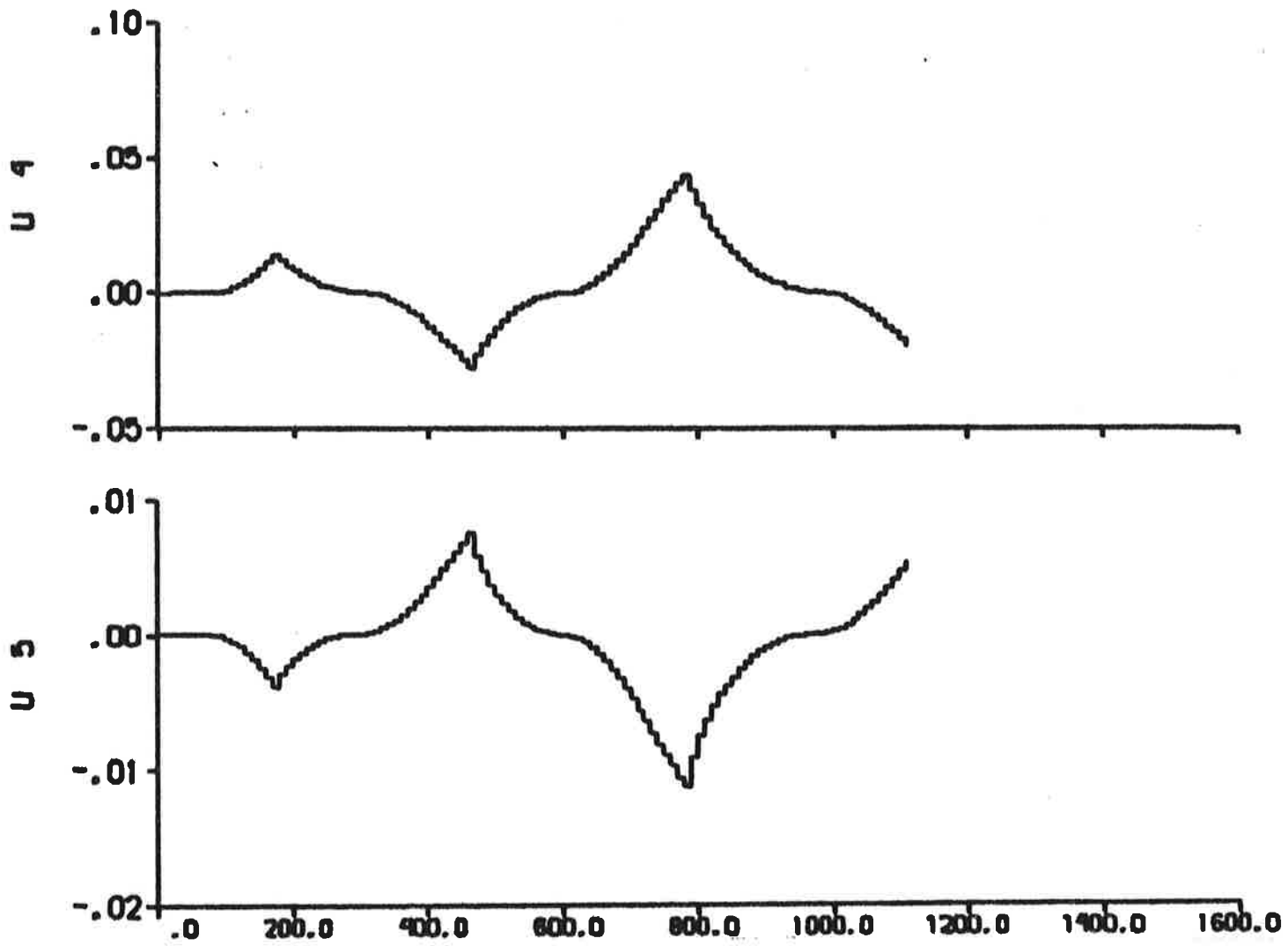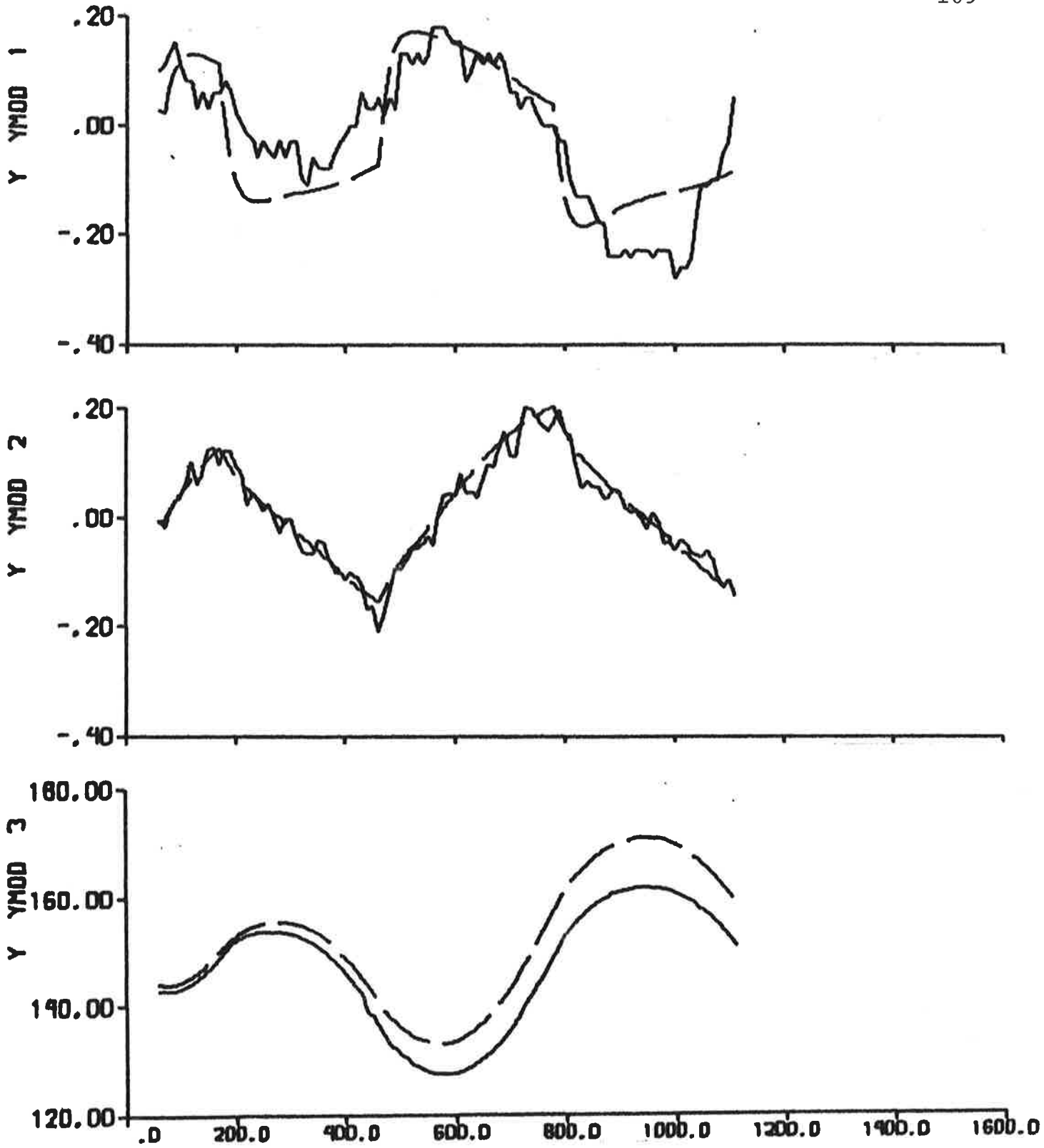
Fig. 5.3a - Result of prediction error identification (p = 6)
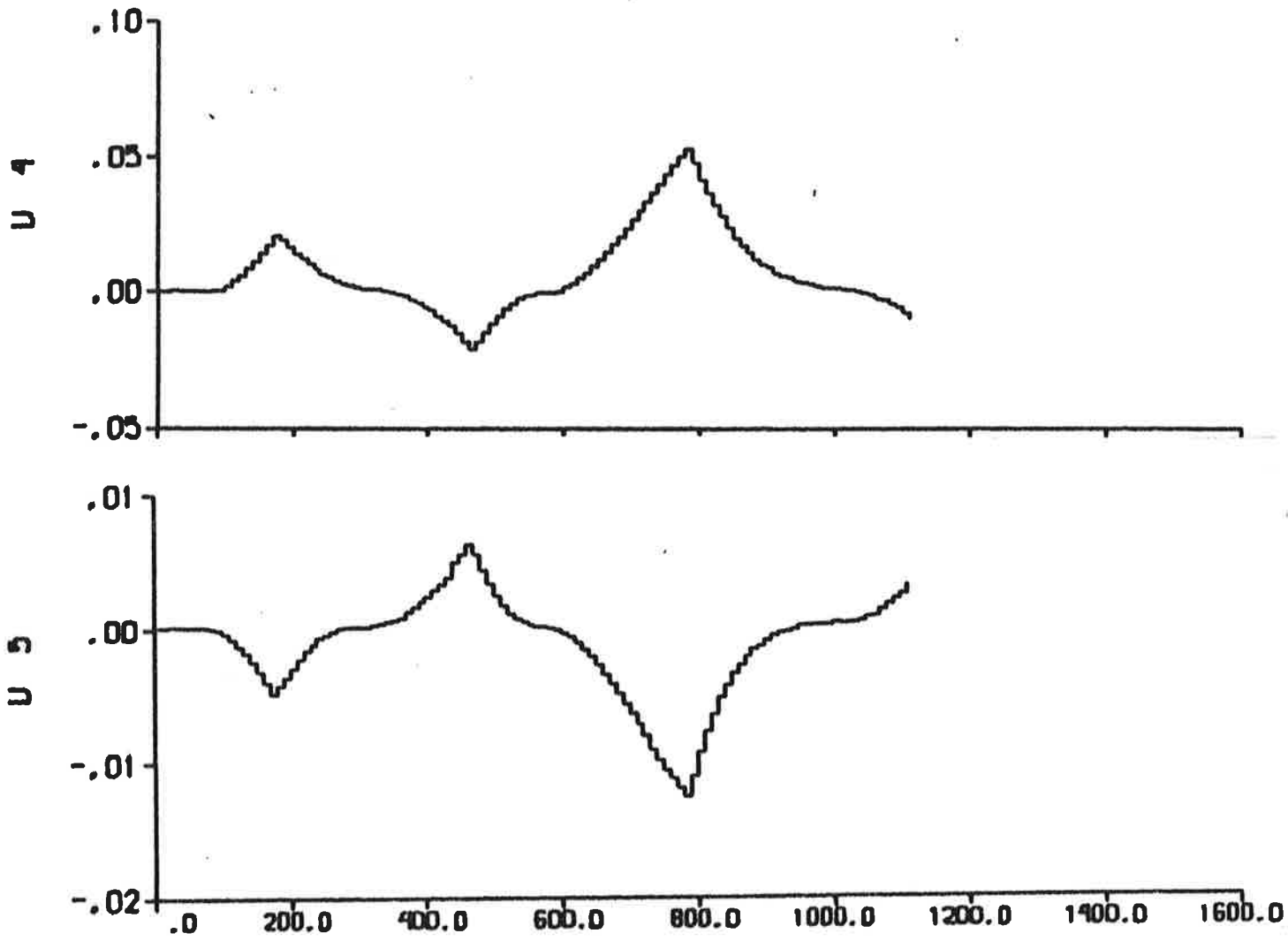to data from experiment E1.

Fig. 5.3 b - Additional inputs U4 = f_Y/m' and U5 = f_N/m'
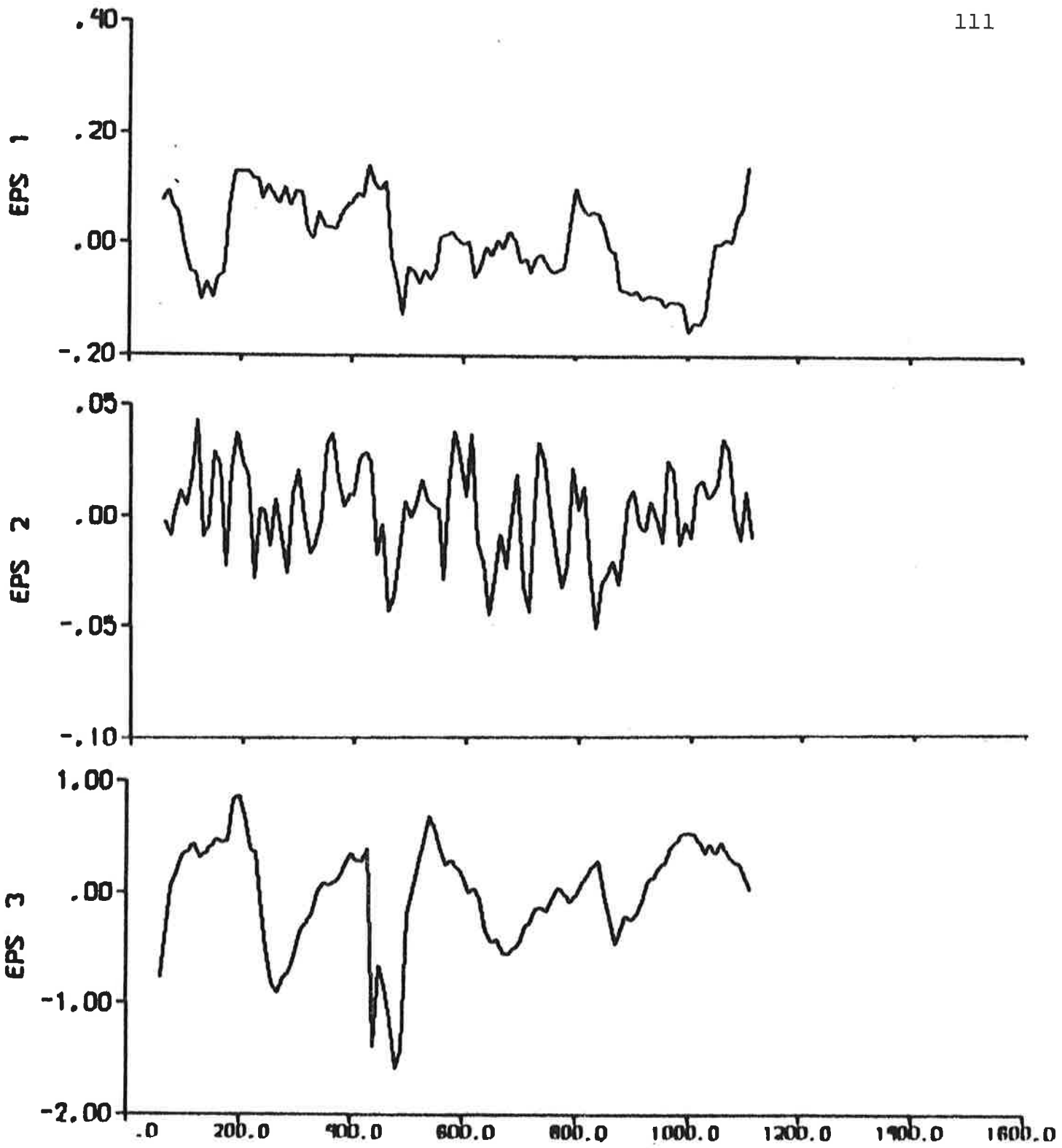describing the nonlinear contributions.

Fig. 5.3c - Prediction errors.

Fig. 5.3d - Autocorrelation functions of prediction errors.
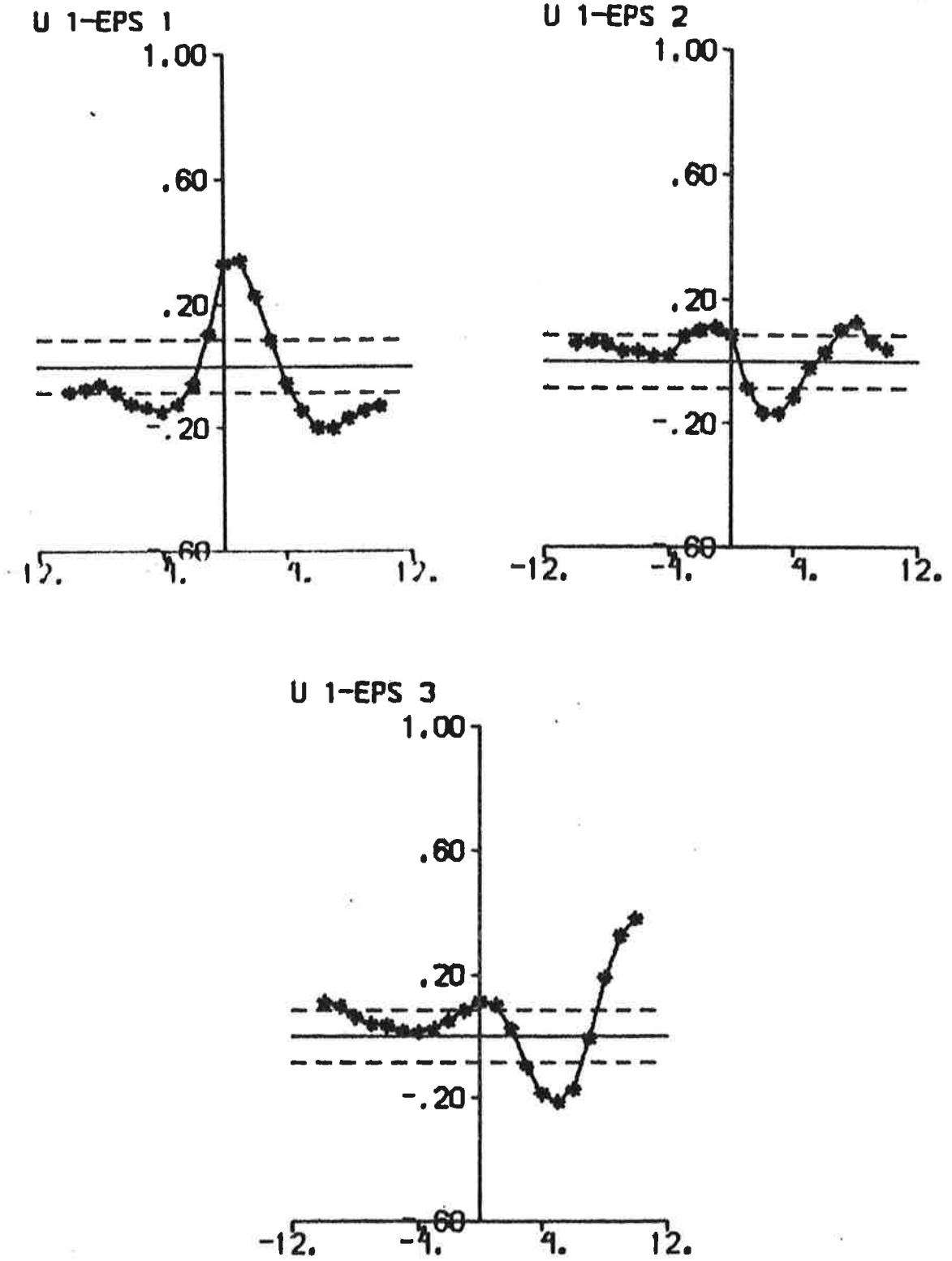
Fig. 5.3e - Cross correlation functions between rudder input and prediction errors.

Fig. 5.4a — Result of output error identification to data from experiment E2, when the linear part of the model is fixed to SSPA:s model.

Fig. 5.4b - Additional inputs U4 = f_Y/m' and U5 = f_N/m' describing the nonlinear contributions.

Fig. 5.5a - Result of output error identification to data from experiment E2.

Fig. 5.5b - Additional inputs U4 = f_Y/m' and U5 = f_N/m' describing the nonlinear contributions.

Fig. 5.6a - Result of prediction error identification (p = 6)
to data from experiment E2.

Fig. 5.6b - Additional inputs U4 = f_Y/m' and U5 = f_N/m' describing the nonlinear contributions.
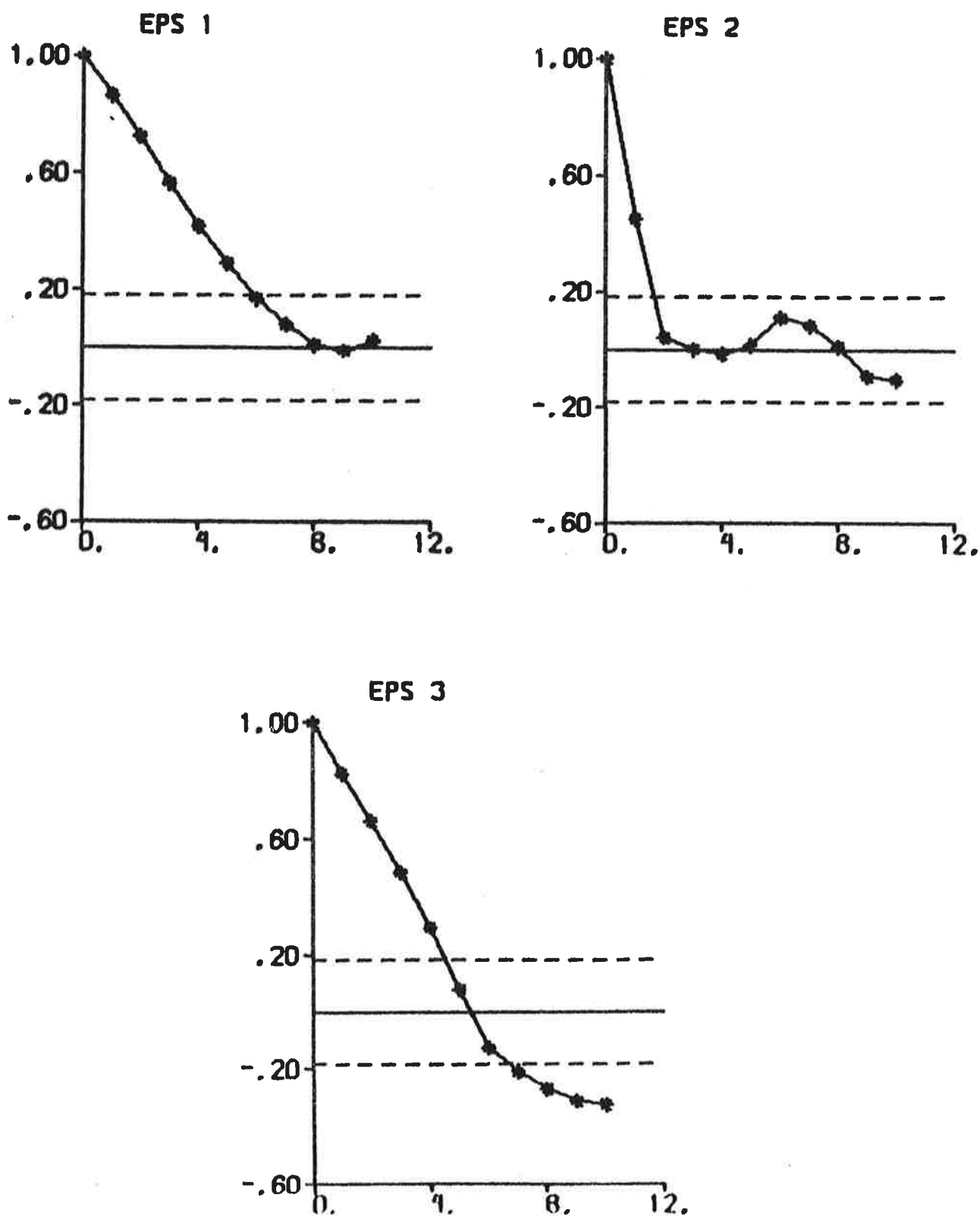
Fig. 5.6c - Prediction errors.

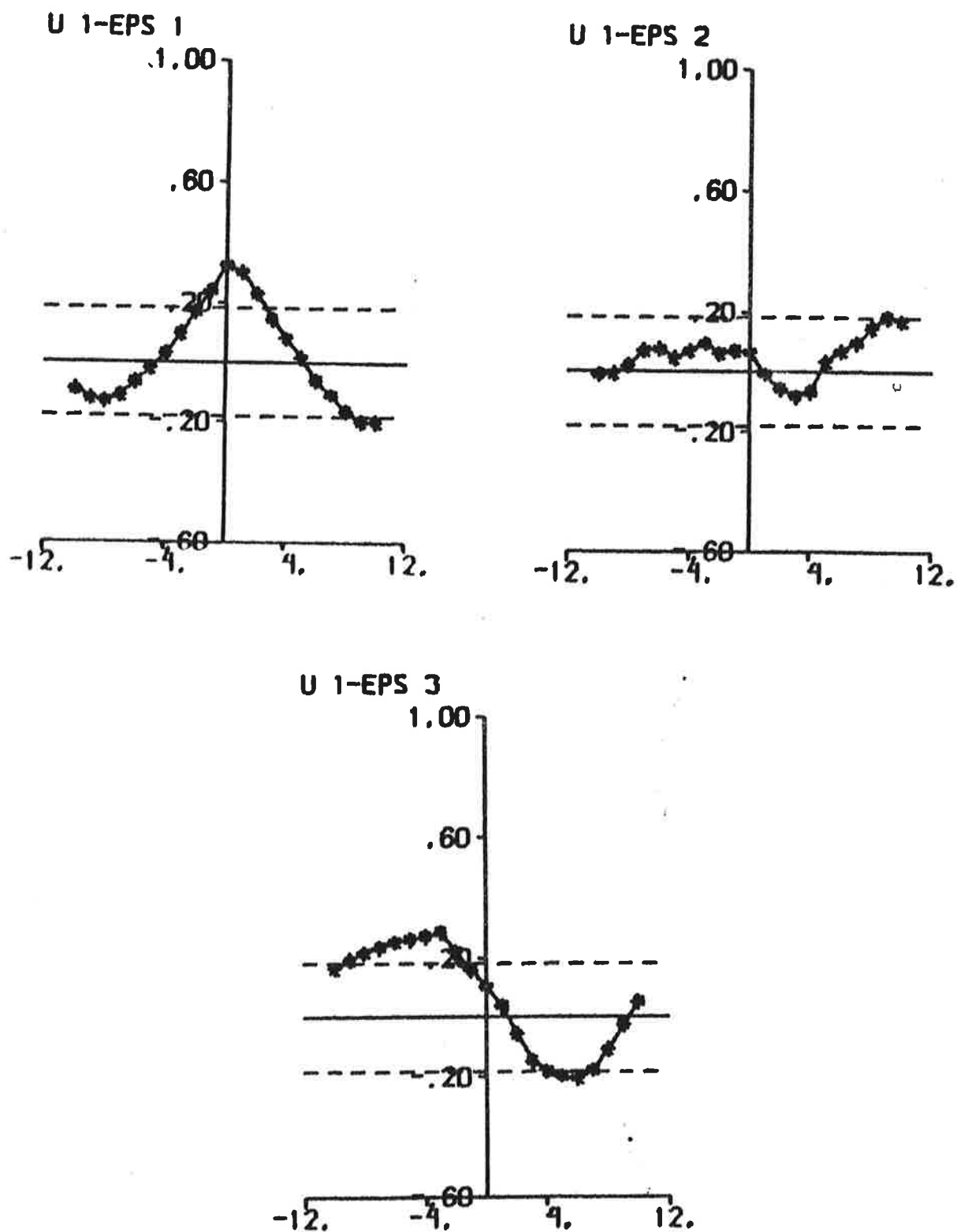Fig. 5.6d – Autocorrelation functions of prediction errors.

Fig. 5.6e - Cross correlation functions between rudder input and prediction errors.
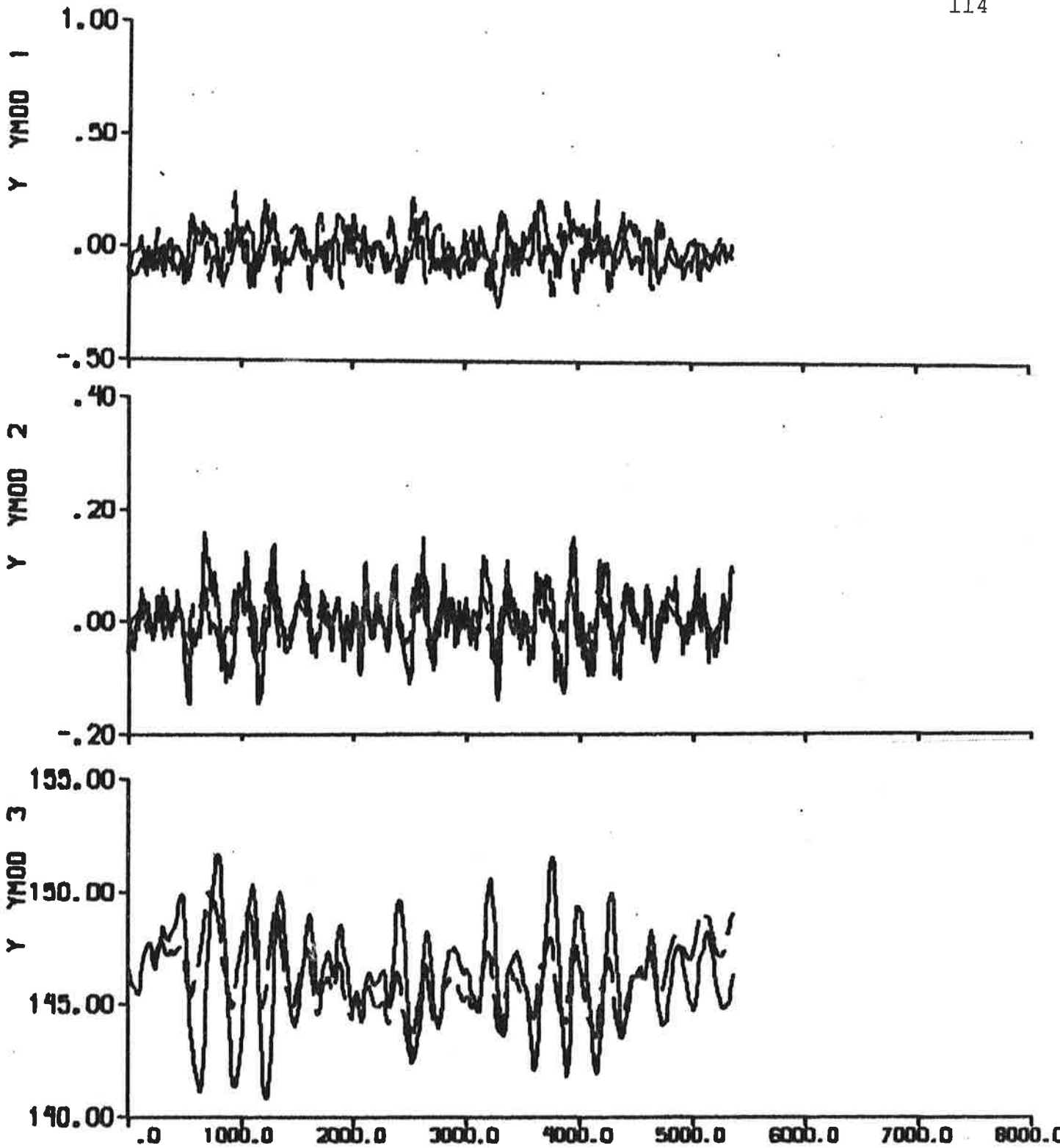
Fig. 5.7a - Result of output error identification to data from
experiment E3, when the linear part of the model
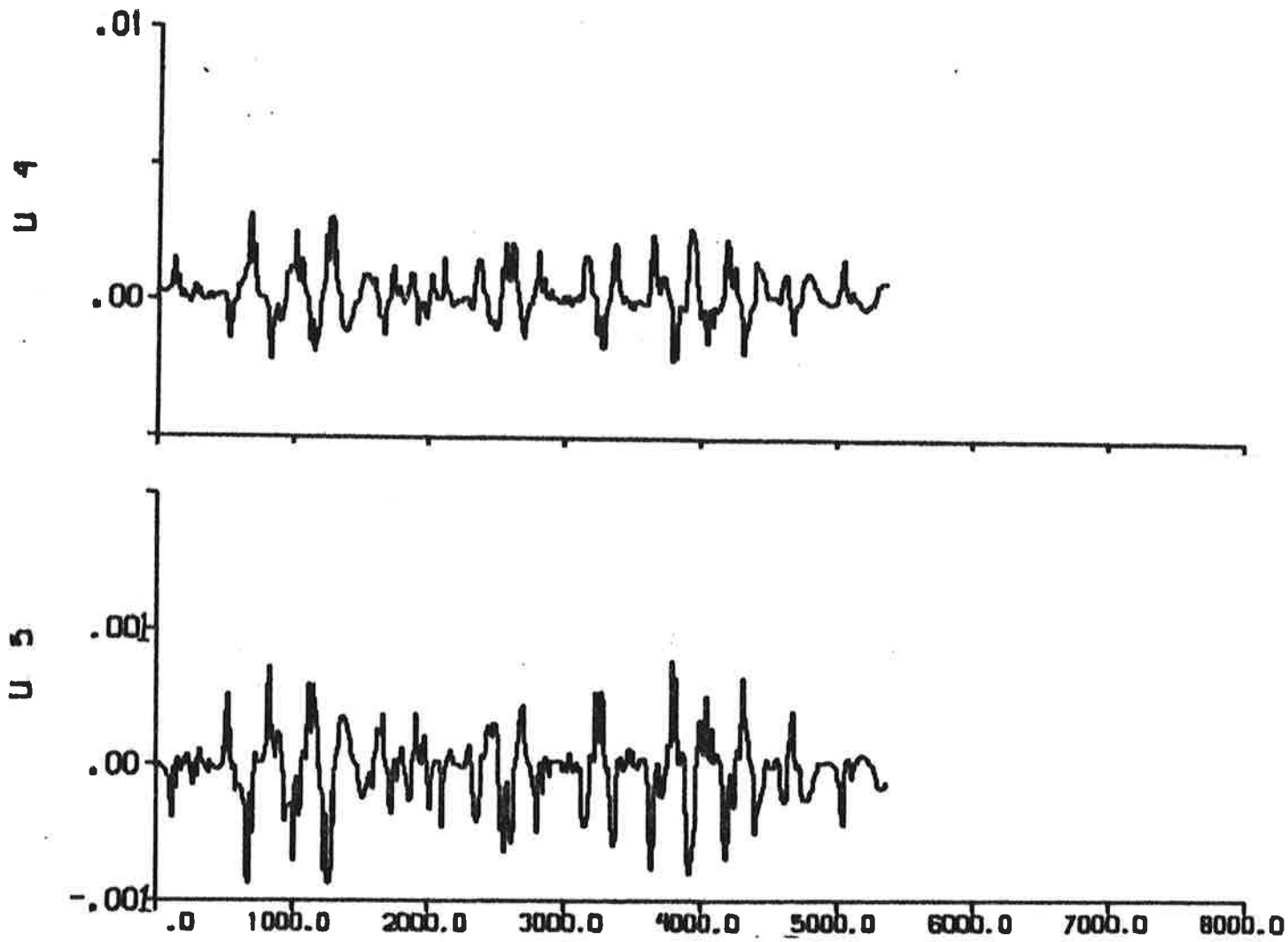is fixed to SSPA:s model.

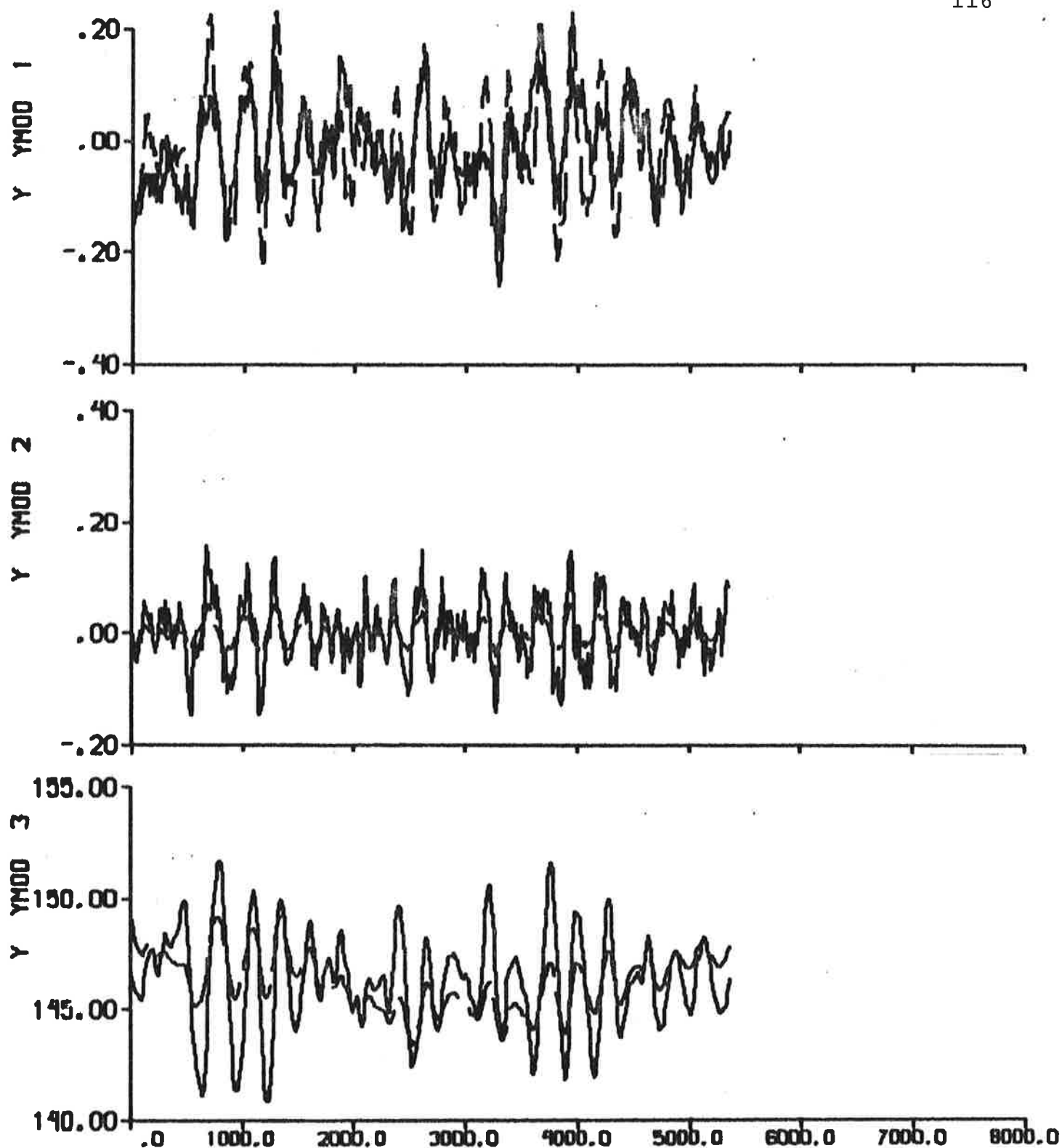Fig. 5.7b - Additional inputs U4 = f_Y/m' and U5 = f_N/m' describing the nonlinear contributions.

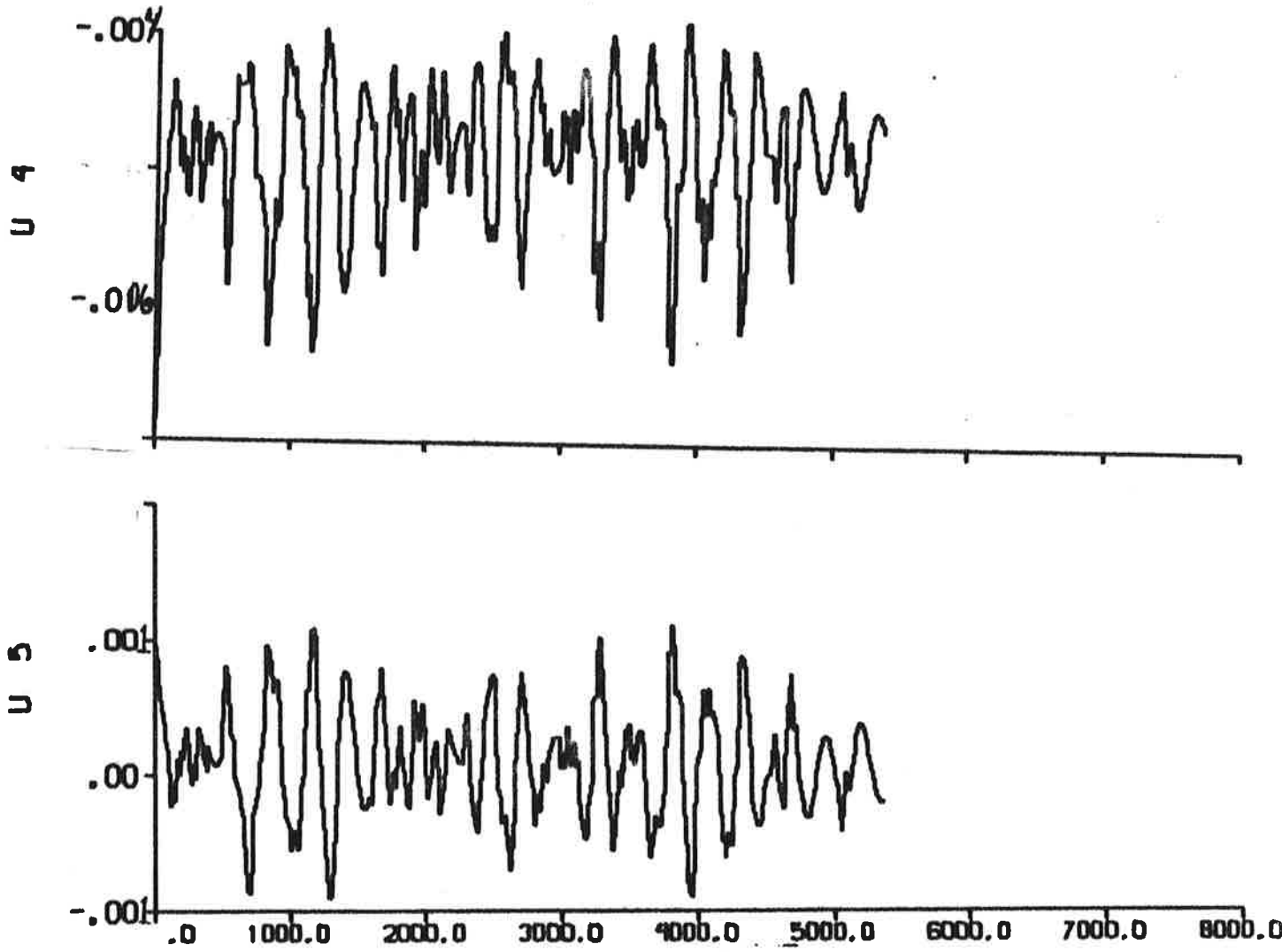Fig. 5.8a - Result of output error identification to data from experiment E3.

Fig. 5.8 b - Additional inputs U4 = f_Y/m' and U5 = f_N/m'
describing the nonlinear contributions.

Fig. 5.9a – Result of prediction error identification (p = 6)
to data from experiment E3.

Fig. 5.9b - Additional inputs U4 = f_Y/m' and U5 = f_N/m' describing the nonlinear contributions.

Fig. 5.9c - Prediction errors.

Fig. 5.9d - Autocorrelation functions of prediction errors.

U 1-EPS 1

U 1-EPS 2

U 1-EPS 3

Fig. 5.9e – Cross correlation functions between rudder
input and prediction errors.
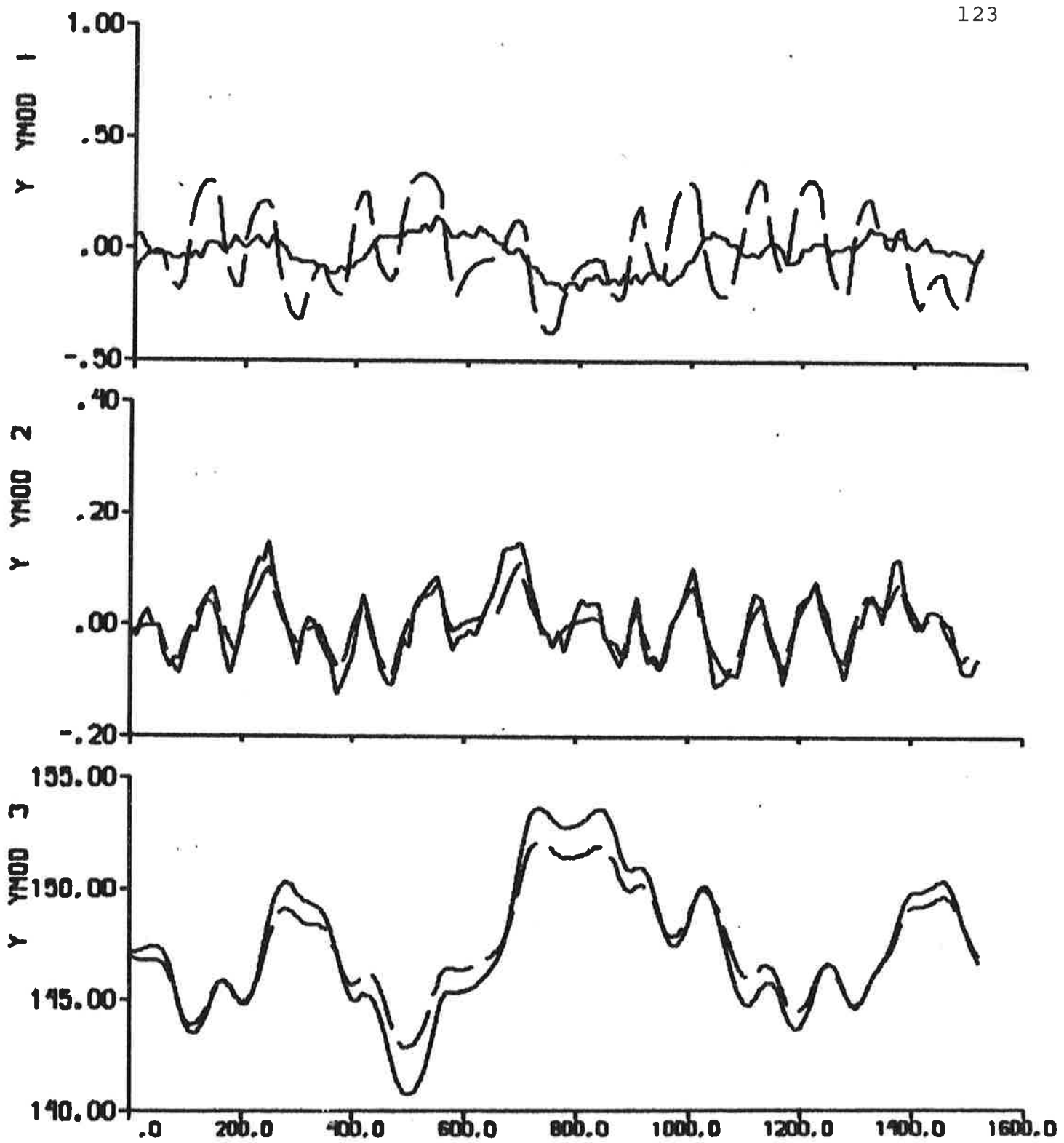
Fig. 5.10a - Result of output error identification to data
from experiment E4, when the linear part of the
model is fixed to SSPA:s model.
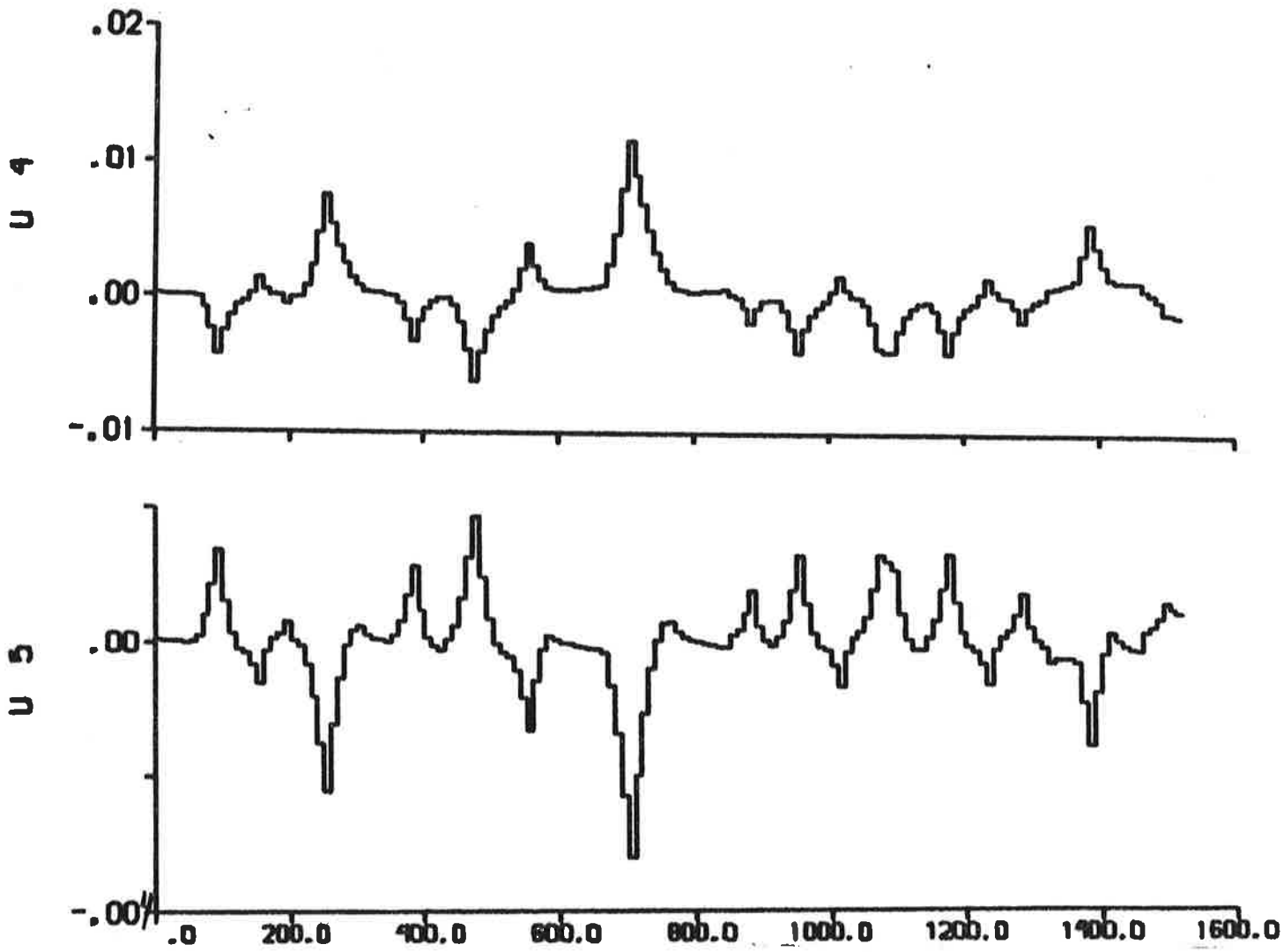
Fig. 5.10b - Additional inputs U4 = f_Y/m' and U5 = f_N/m' describing the nonlinear contributions.
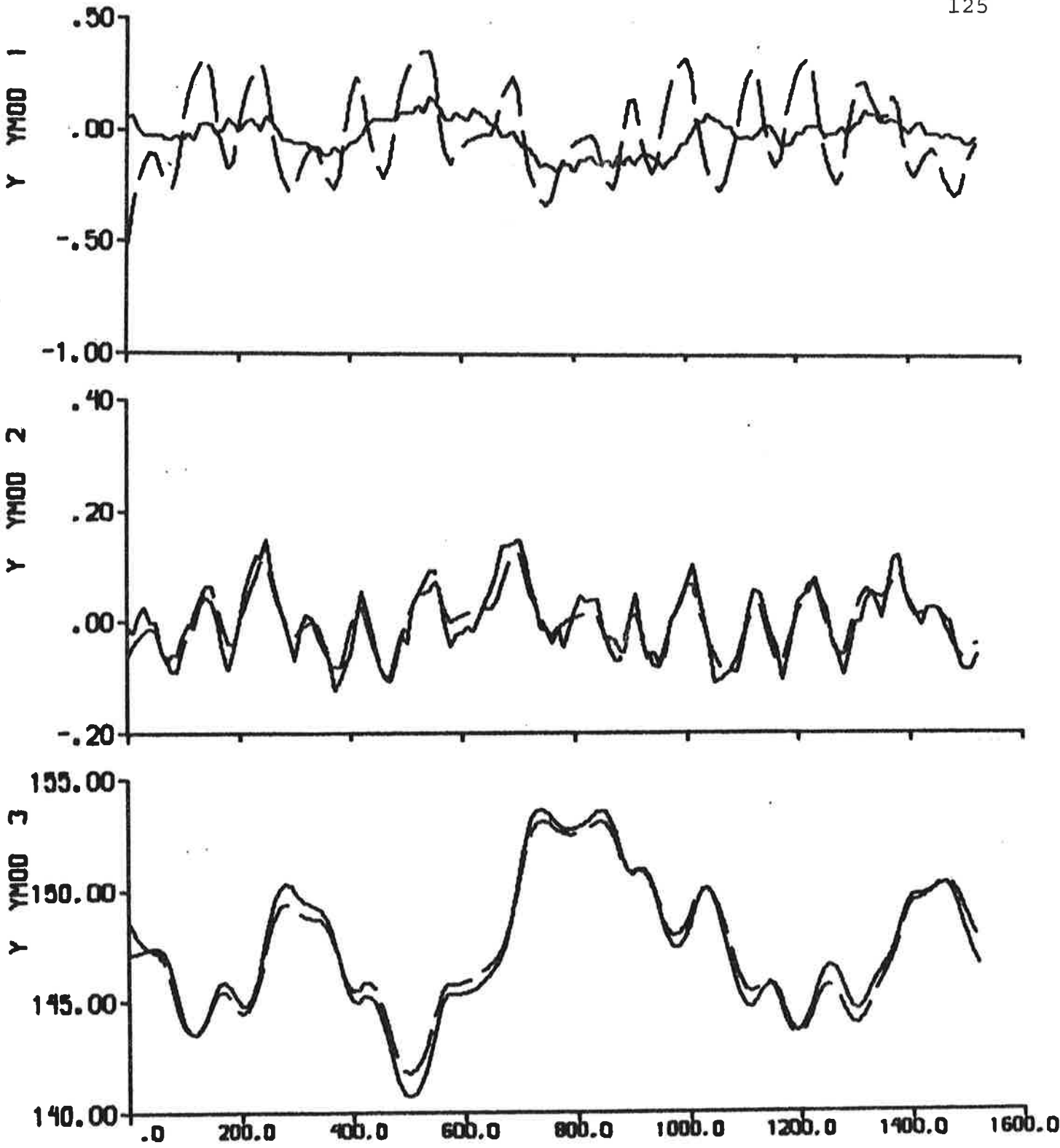
Fig. 5.11a - Result of output error identification to data
from experiment E4.

Fig. 5.11b - Additional inputs U4 = f_Y/m' and U5 = f_N/m'
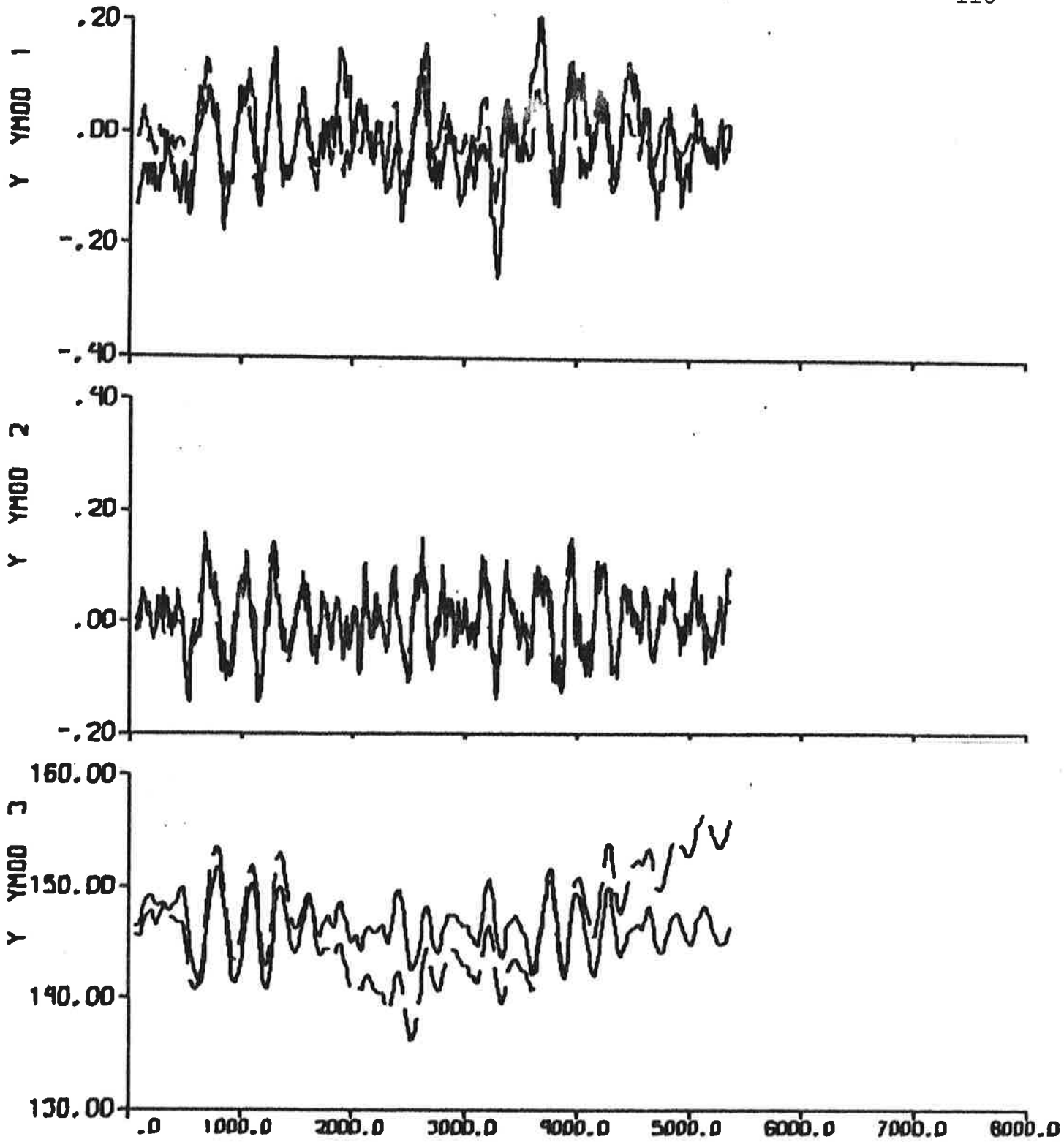describing the nonlinear contributions.

Fig. 5.12a - Result of prediction error identification
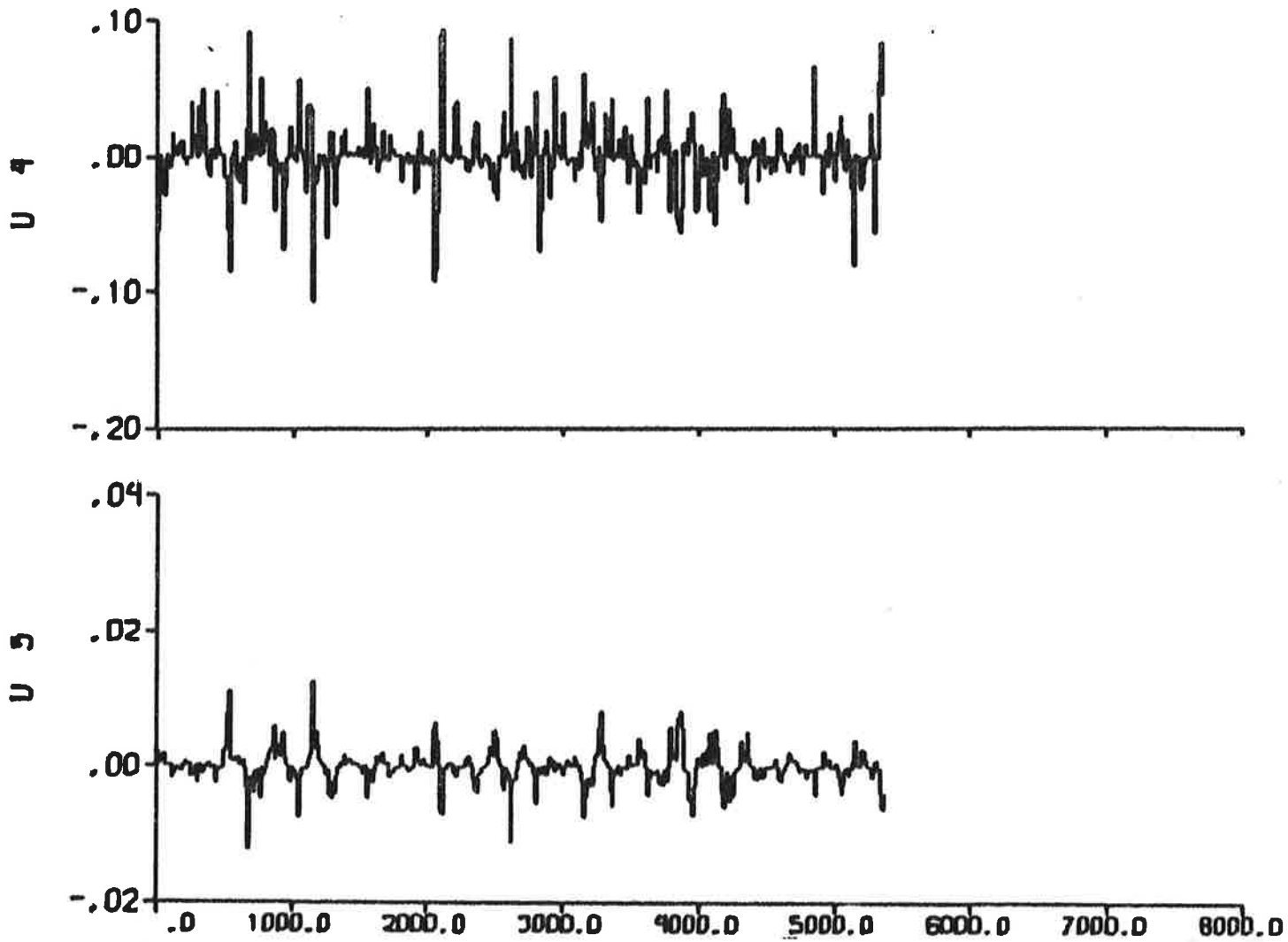(p = 6) to data from experiment E4.

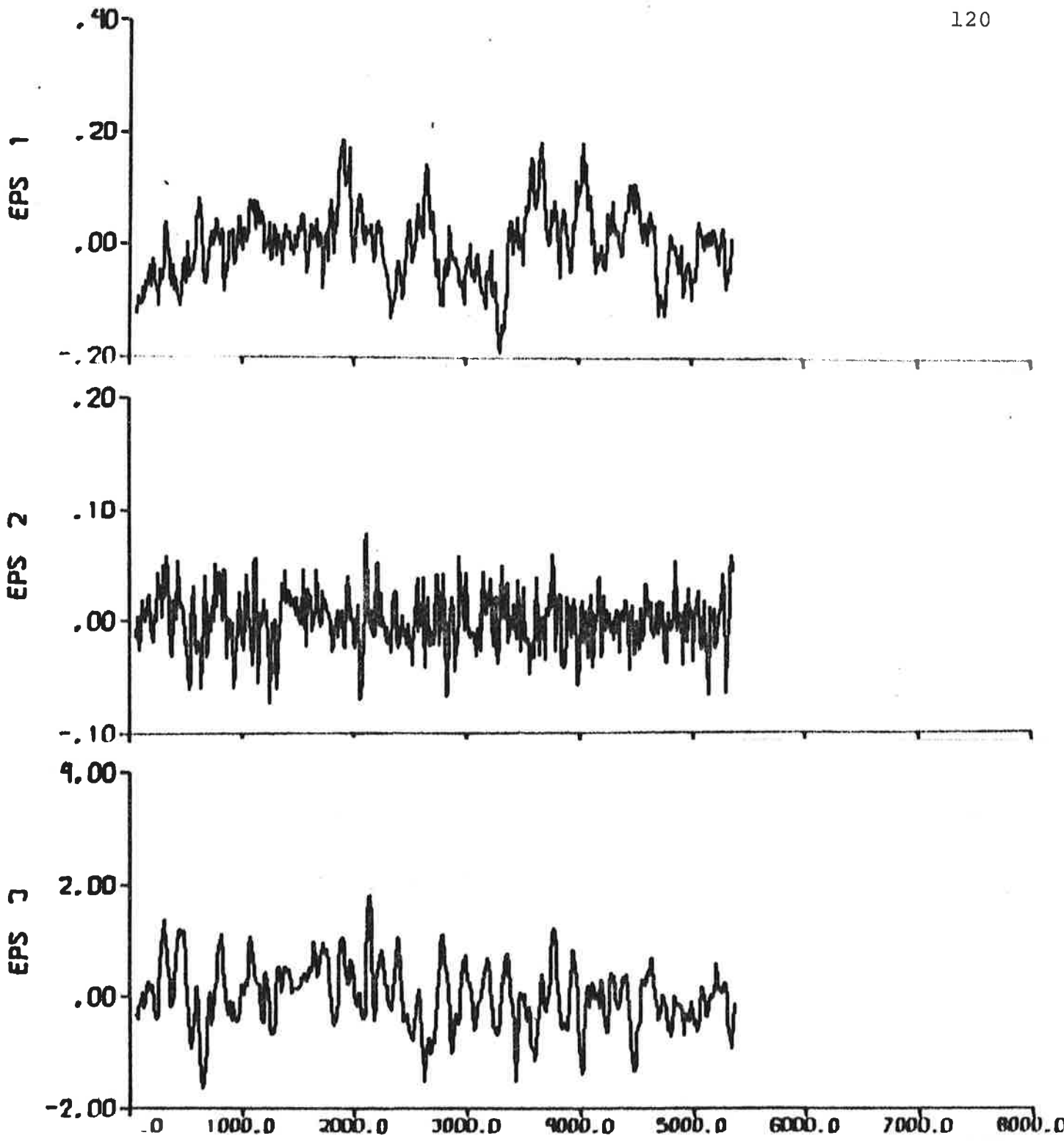Fig. 5.12b – Additional inputs U4 = f_Y/m' and U5 = f_N/m' describing the nonlinear contributions.
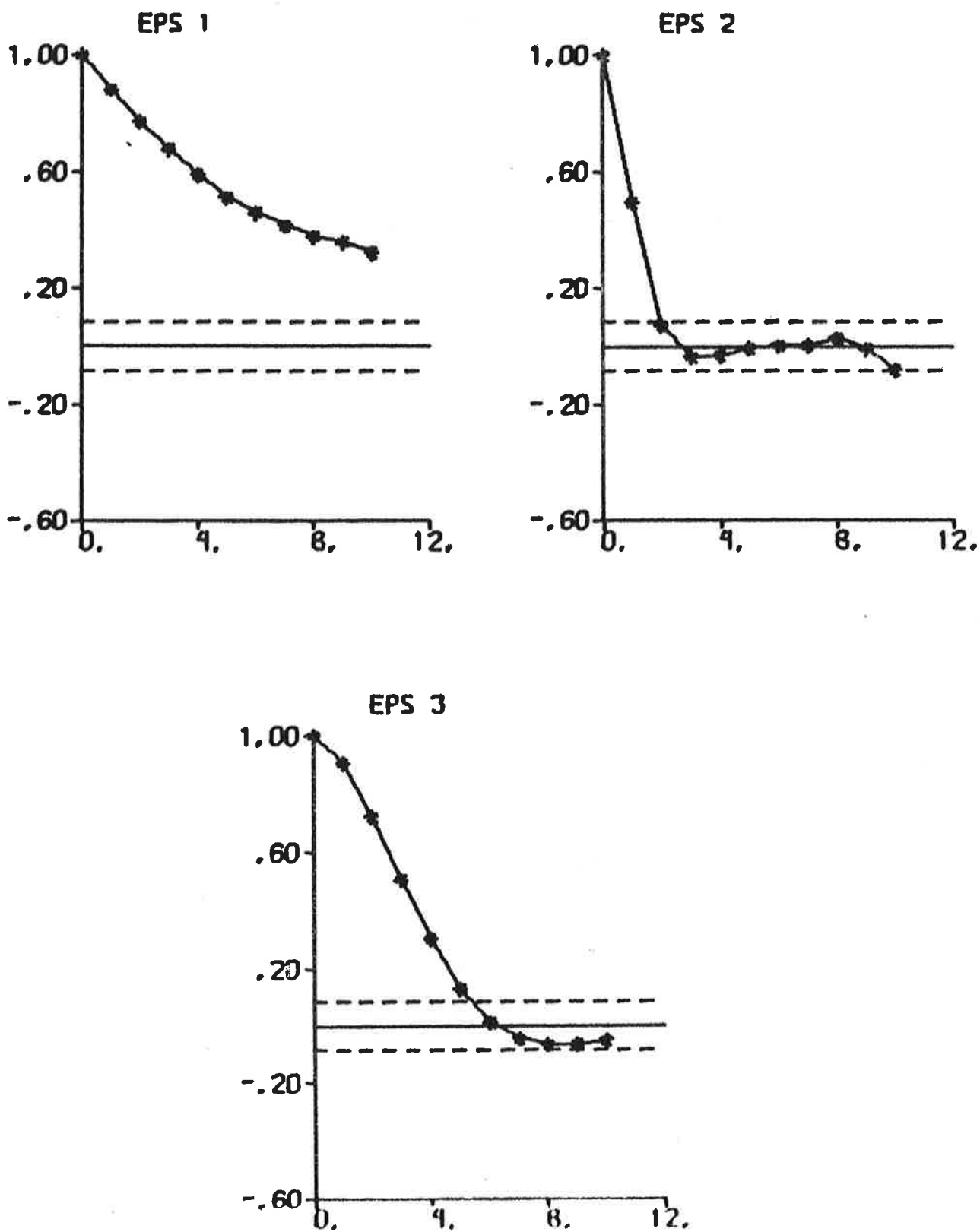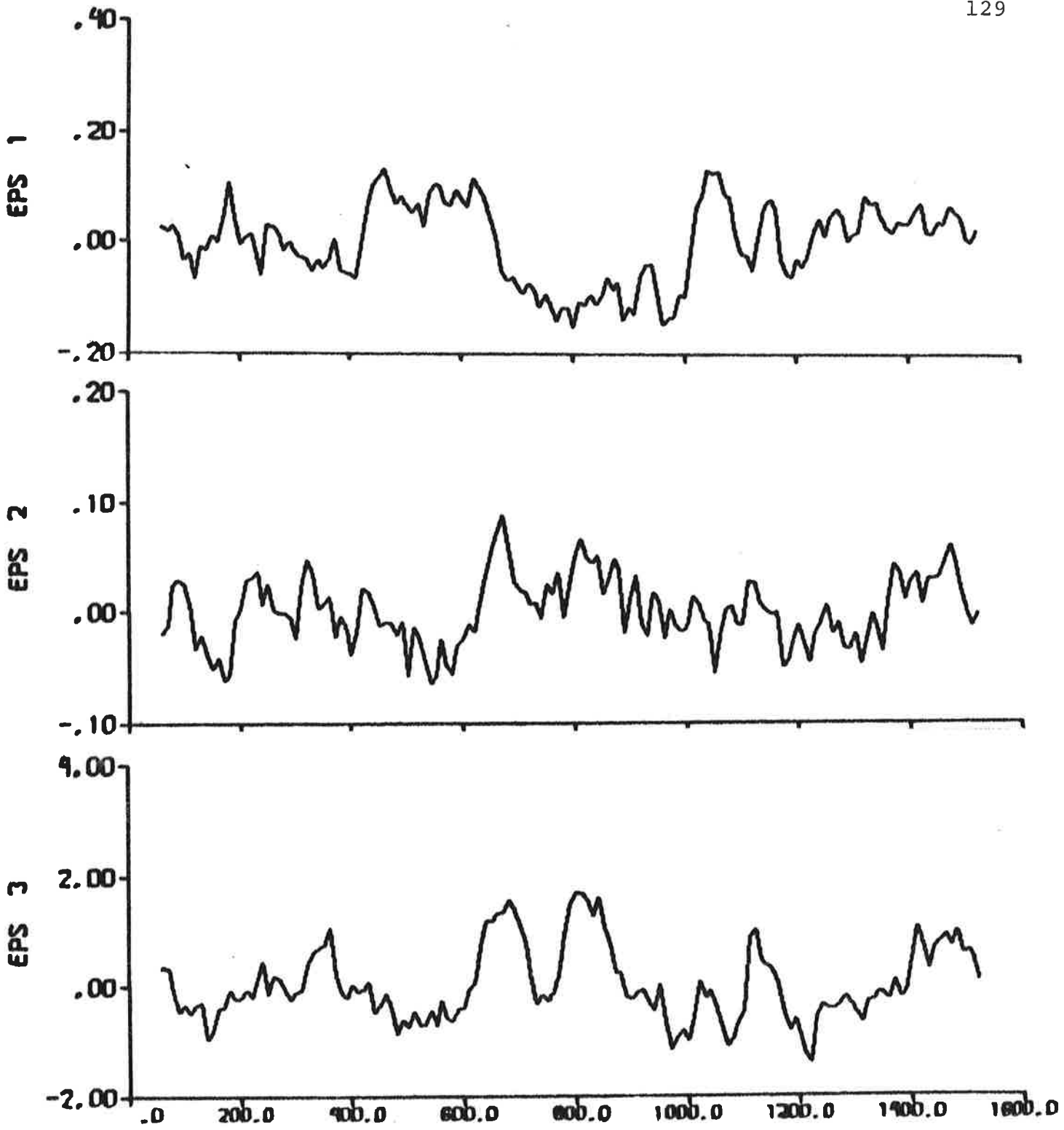
Fig. 5.12c - Prediction errors.
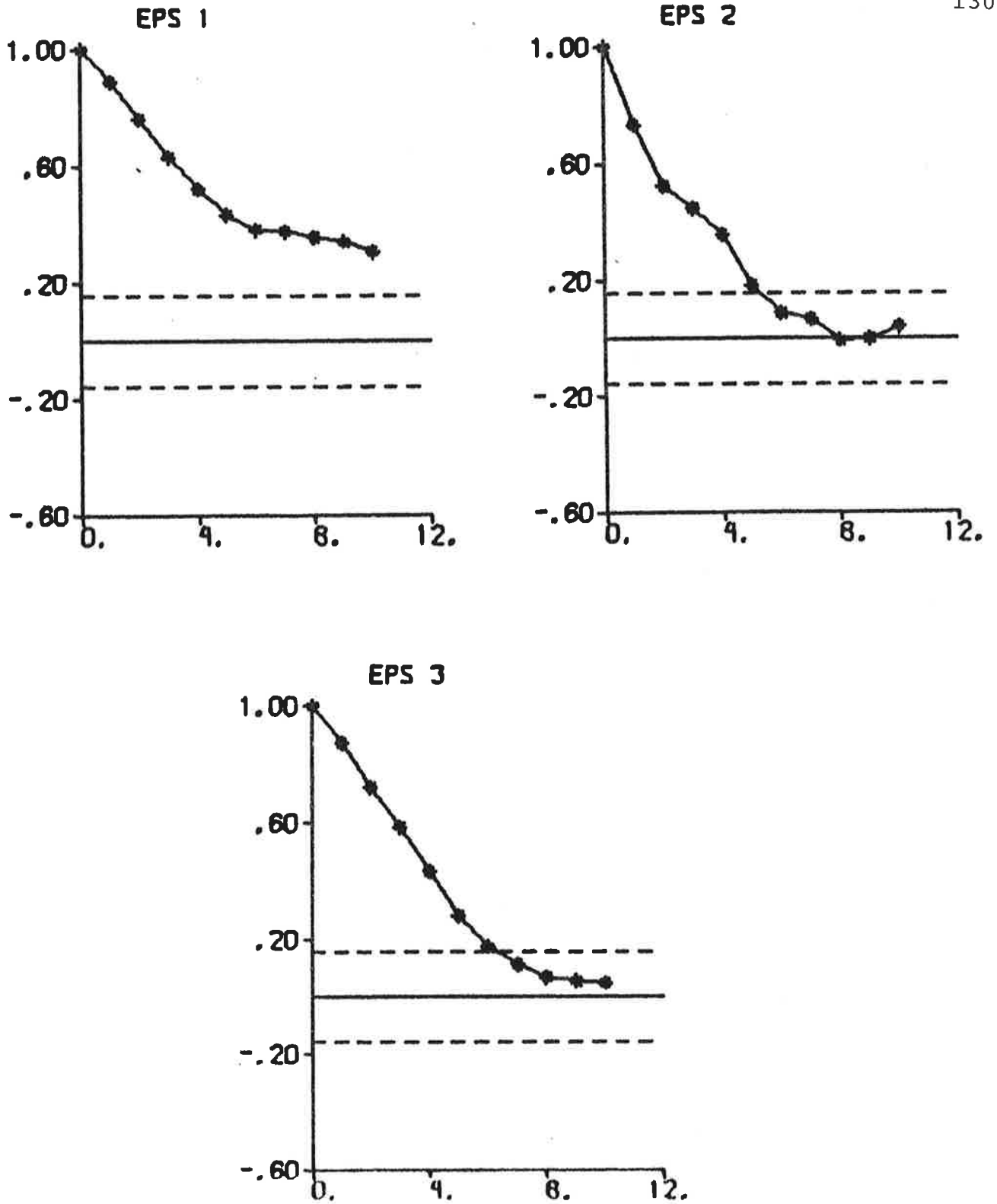
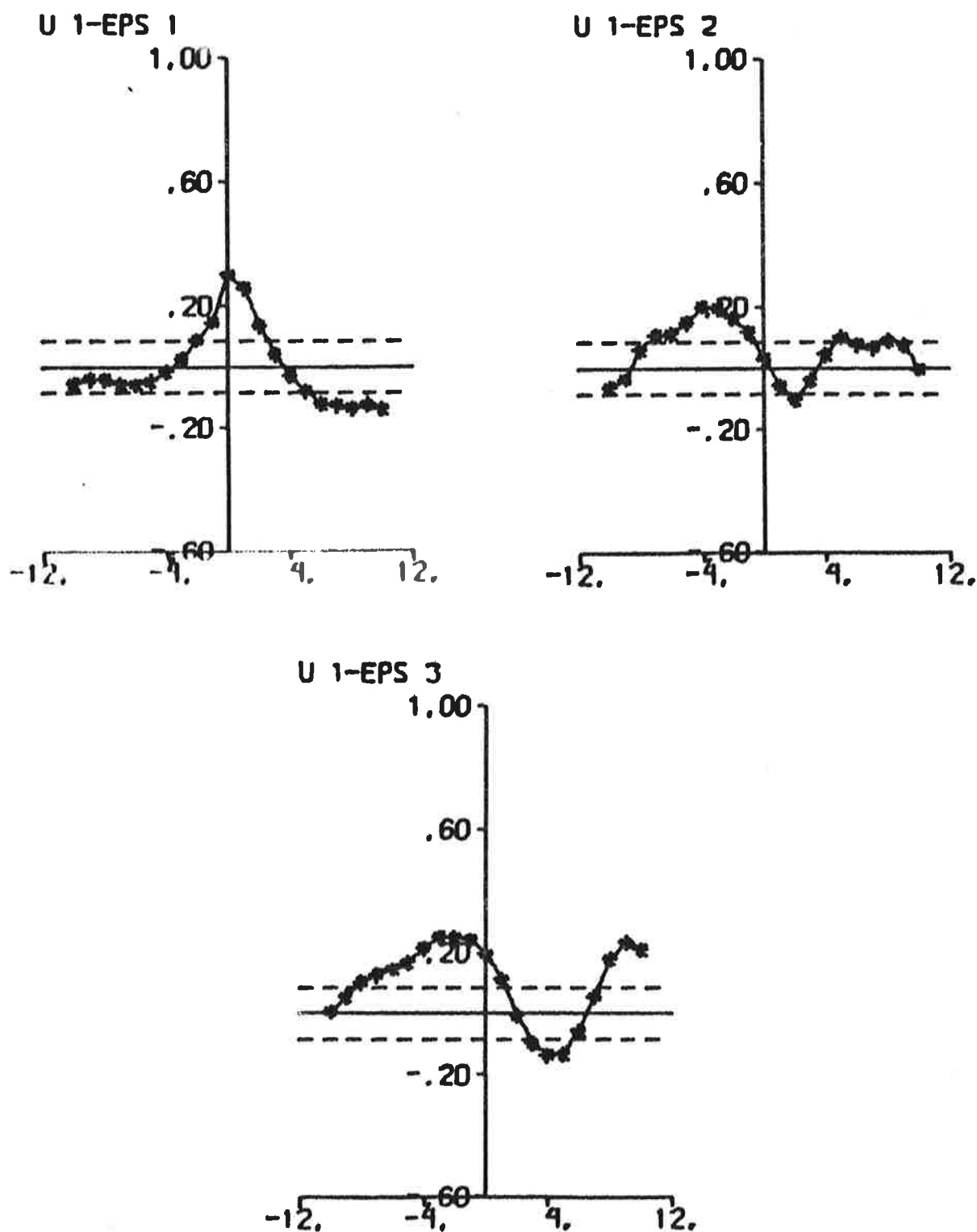Fig. 5.12d - Autocorrelation functions of prediction errors.

U 1-EPS 1

U 1-EPS 2

U 1-EPS 3
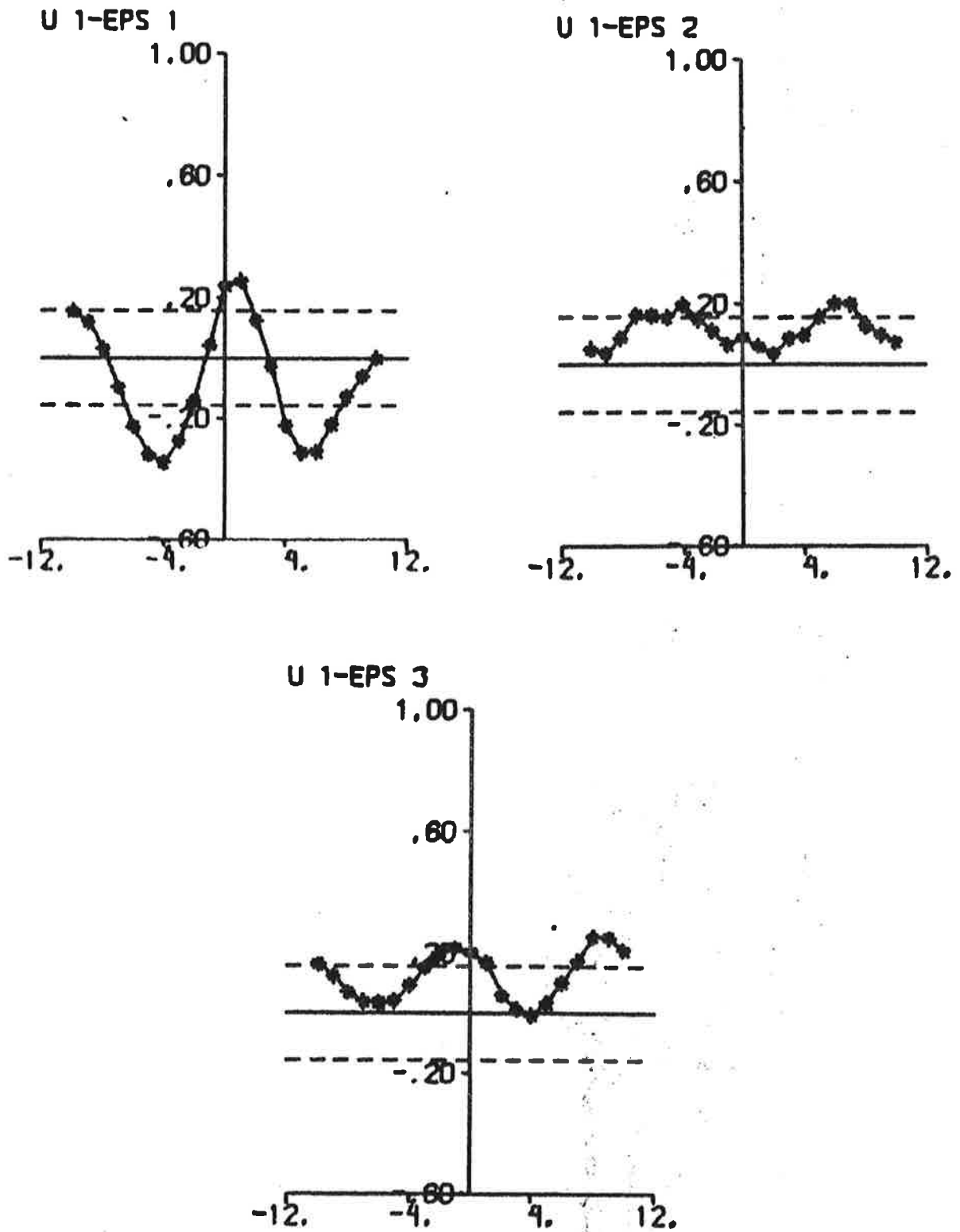
Fig. 5.12e - Cross correlation functions between rudder
input and prediction errors.

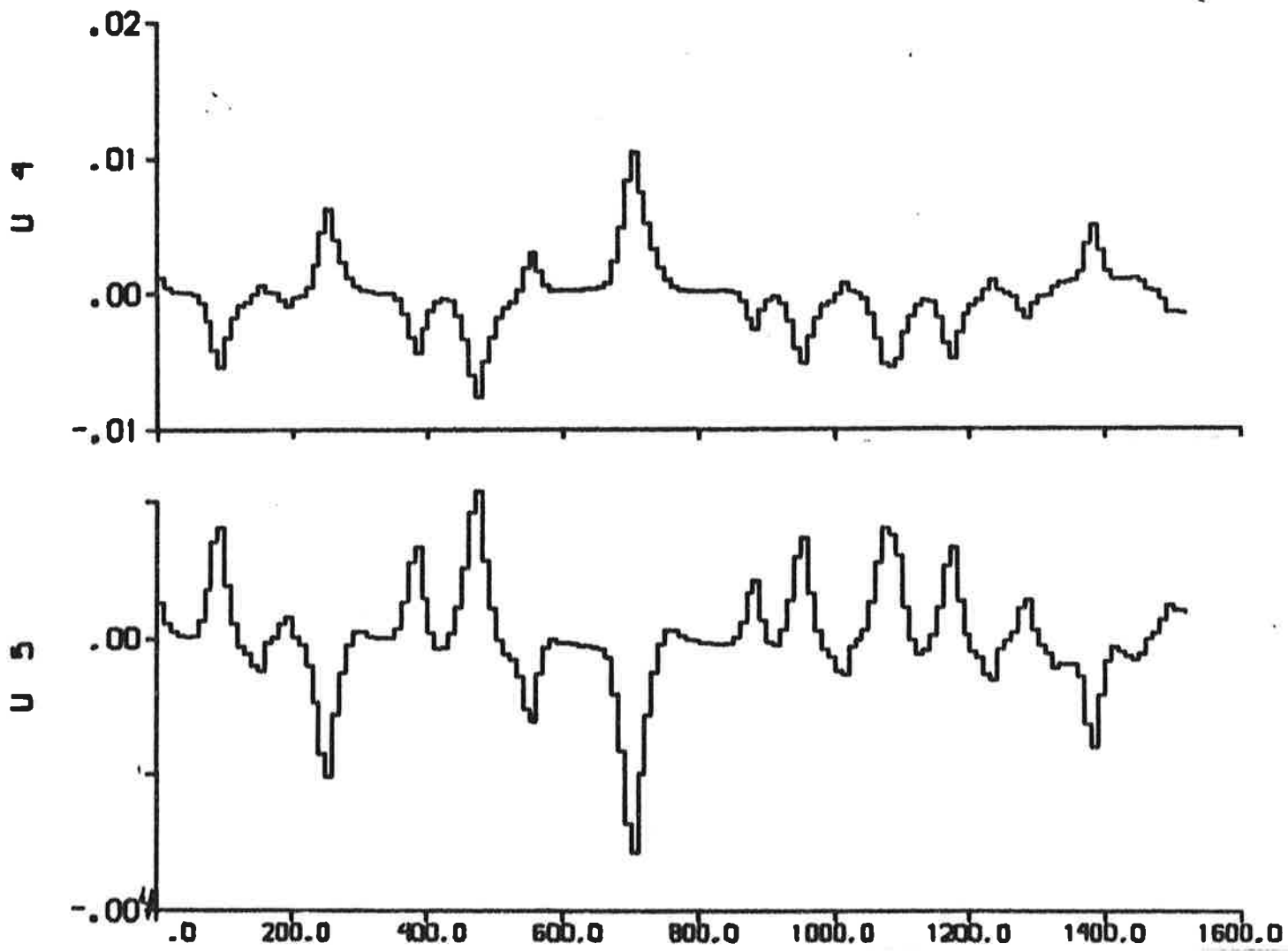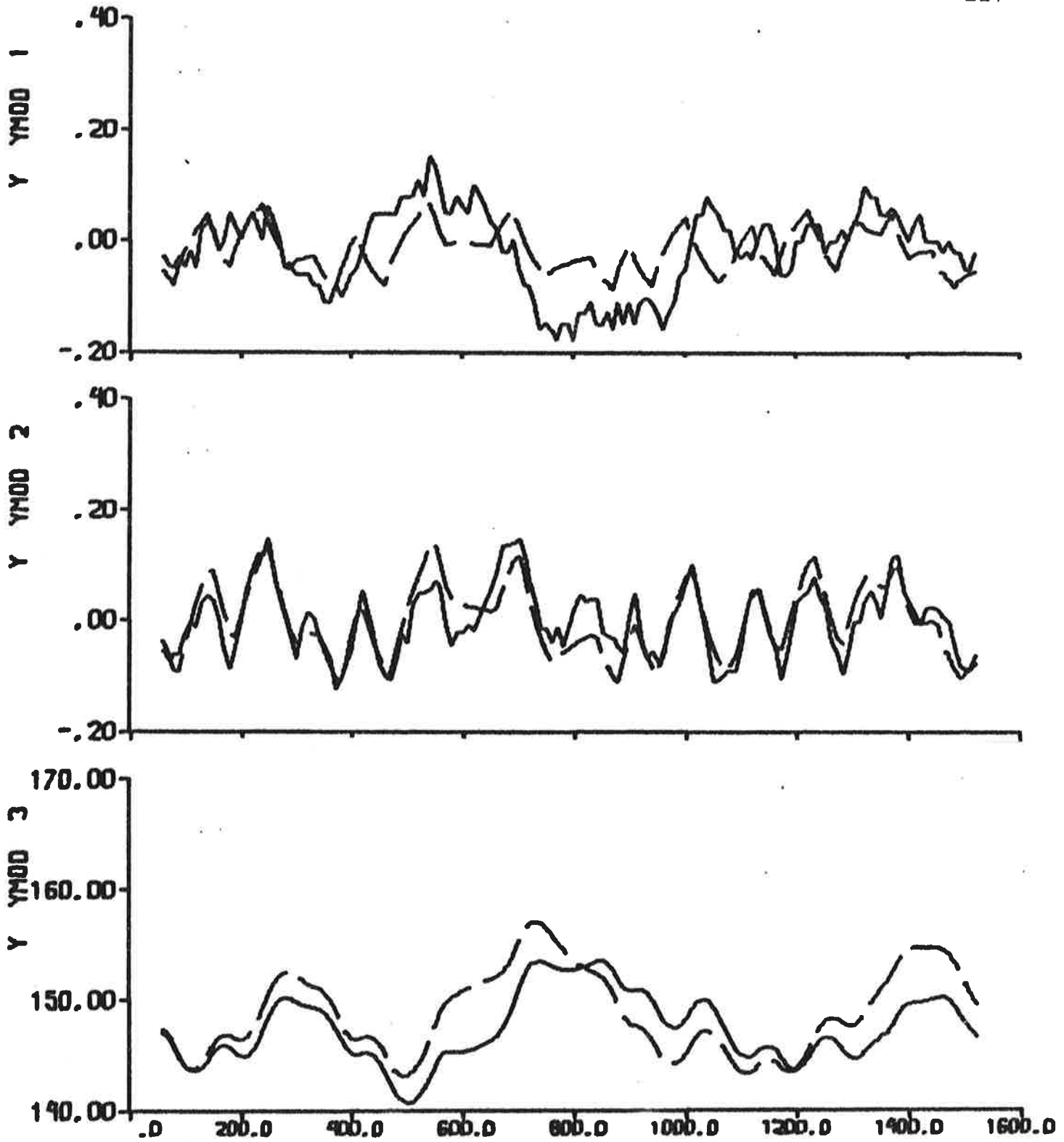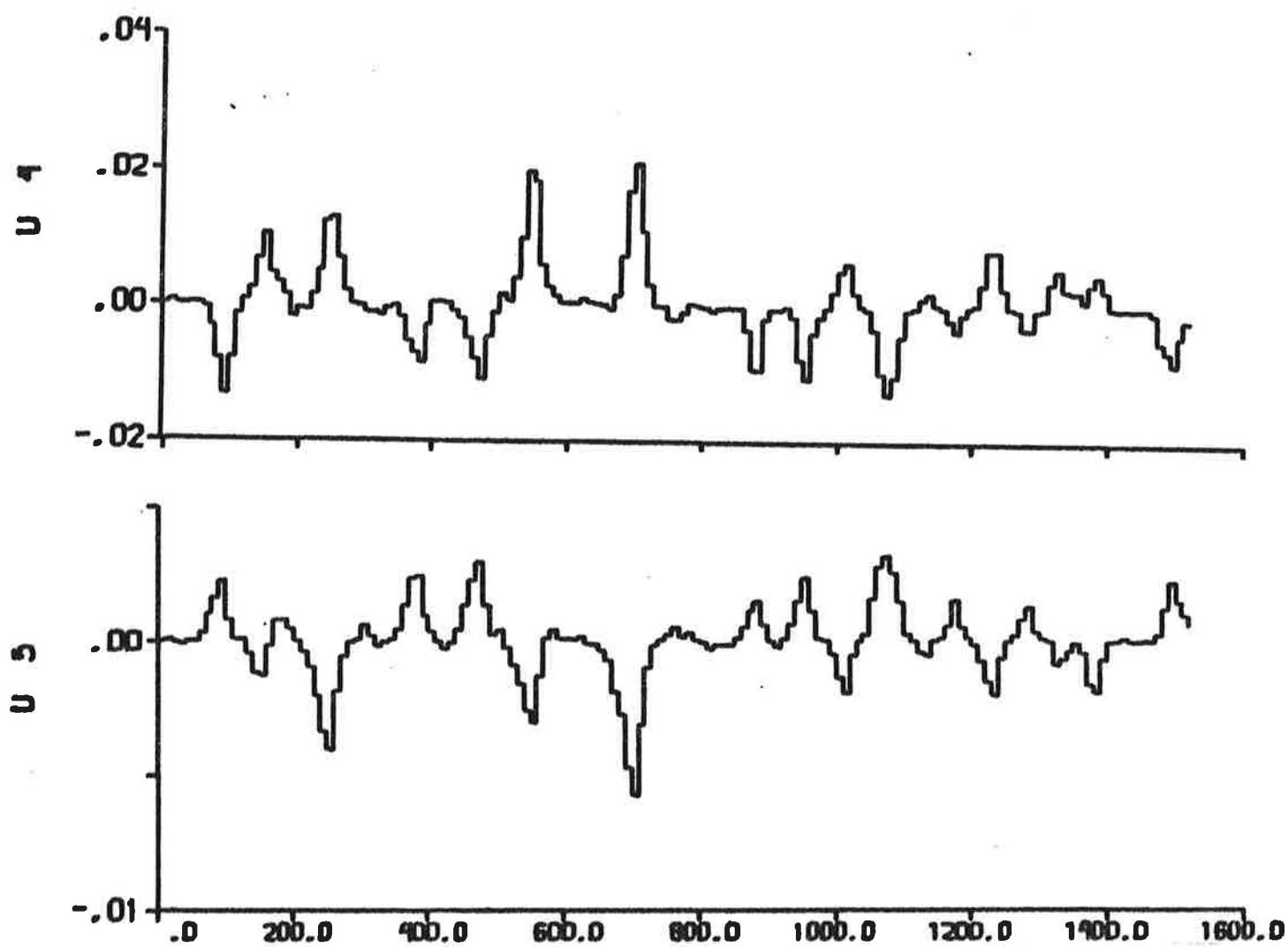experiments E2 and E4 are analysed. However, experiment E4 is also analysed by using C = 0 and by estimating C. The results are summarized in Table 5.3 and in Figs. 5.13 - 5.18.

The analysis shows that the prediction error model from experiment E2 is a reasonable model. It can be concluded that this model also is somewhat better than SSPA:s model. The identifications indicate that it is questionable if a nonlinear model is appropriate to the data from experiment E4 in this case.

6. DETERMINATION OF THE TRANSFER FUNCTION RELATING HEADING TO RUDDER ANGLE

Results of fitting the model (3.10) to data from the 4 experiments by use of the program LISPID are presented in this section. The output error method, the maximum likelihood method and the prediction error method are then applied. Maximum likelihood identifications based on the model (3.15) are also performed with the program IDPAC. Notice that the only measurement signal used in this section is the heading.

Parameters of Nomoto's model (see (3.13) and (3.17)) are first estimated by using the program LISPID. The identifications are based on the model (3.10), and the following fixed parameter values are then used:

$$
\begin{aligned}
\varphi_2 &= 0 \\
\varphi_3 &= 0 \\
\varphi_5 &= 0 \\
\varphi_6 &= 0 \\
\varphi_9 &= 0 \\
\varphi_{11} &= 0 \\
\varphi_{13} &= 0.01 \text{ deg}^2 \\
\varphi_{15} &= 0 \\
\varphi_{16} &= 0
\end{aligned}
\tag{6.1}
$$

The initial state φ_{17} is always fixed to the initial heading measurement, i.e. to 146.89, 144.67, 146.58 or 147.13 deg

| | E 1 | E 2 | E 3 | E 4 | | |
	Linear model	Nonlinear model	Linear model	Linear model	Nonlinear model	Nonlinear model
Figure	5.13	5.14	5.15	5.16	5.17	5.18
ν	10	10	10	10	10	11
V	44	$7.7 \cdot 10^{-3}$	371	0.22	0.33	0.20
AIC	−123	−628	1018	−448	−386	−461
C	0^*	0.63^*	0^*	0^*	0.63^*	−0.18
θ_9	$-1.6 \cdot 10^{-5}$	$1.5 \cdot 10^{-5}$	$-4.9 \cdot 10^{-5}$	$-2.2 \cdot 10^{-5}$	$-4.4 \cdot 10^{-5}$	$-5.1 \cdot 10^{-5}$
θ_{10}	0.029	0.246	−0.226	−0.073	−0.045	−0.052
θ_{13}	$-5.7 \cdot 10^{-6}$	$4.6 \cdot 10^{-7}$	$4.8 \cdot 10^{-6}$	$-1.3 \cdot 10^{-5}$	$3.3 \cdot 10^{-4}$	$3.5 \cdot 10^{-4}$
θ_{14}	$1.0 \cdot 10^{-6}$	$4.8 \cdot 10^{-6}$	$-3.3 \cdot 10^{-5}$	$-5.2 \cdot 10^{-6}$	$3.5 \cdot 10^{-5}$	$3.5 \cdot 10^{-5}$
θ_{15} [knots]	0.01	−0.03	0.09	0.02	−0.16	−0.16
θ_{17} [deg/s]	0.004	0.002	−0.013	−0.002	−0.002	−0.002
θ_{25} [knots]	0.12	0.08	0.12	0.03	0.23	0.14
θ_{26} [deg/s]	0.003	−0.020	0.000	0.001	0.002	−0.012
θ_{27} [deg]	148.35	143.81	151.12	147.48	147.28	147.70
T_D [s]	6.1	2.0	8.7	7.2	8.3	6.8

* = fixed value

Table 5.3 - Estimated parameters from output error identifications. The hydrodynamic derivatives are fixed to the values obtained from prediction error identification (p = 6) to data from experiment E2 (see Table 5.1).

Fig. 5.13a - Result of output error identification to data
from experiment E1, when the model is fixed to
the model obtained from prediction error
identification (p = 6) to data from E2. C = 0.

Fig. 5.13b - First part of Fig. 5.13a.

Fig. 5.14a - Result of output error identification to data from
experiment E2, when the model is fixed to the model
obtained from prediction error identification (p = 6)
to data from E2. C = 0.63.

Fig. 5.14b - Additional inputs U4 = f_Y/m' and U5 = f_N/m' describing the nonlinear contributions.

Fig. 5.15a - Result of output error identification to data
from experiment E3, when the model is fixed
to the model obtained from prediction error
identification (p = 6) to data from E2. C = 0.

Fig. 5.15b - First part of Fig. 5.15a.

Fig. 5.16 - Result of output error identification to data from experiment E4, when the model is fixed to the model obtained from prediction error identification (p = 6) to data from E2. C = 0.

Fig. 5.17a - Result of output error identification to data from experiment E4, when the model is fixed to the model obtained from prediction error identification (p = 6) to data from E2. C = 0.63.

Fig. 5.17b - Additional inputs U4 = f_Y/m' and U5 = f_N/m'
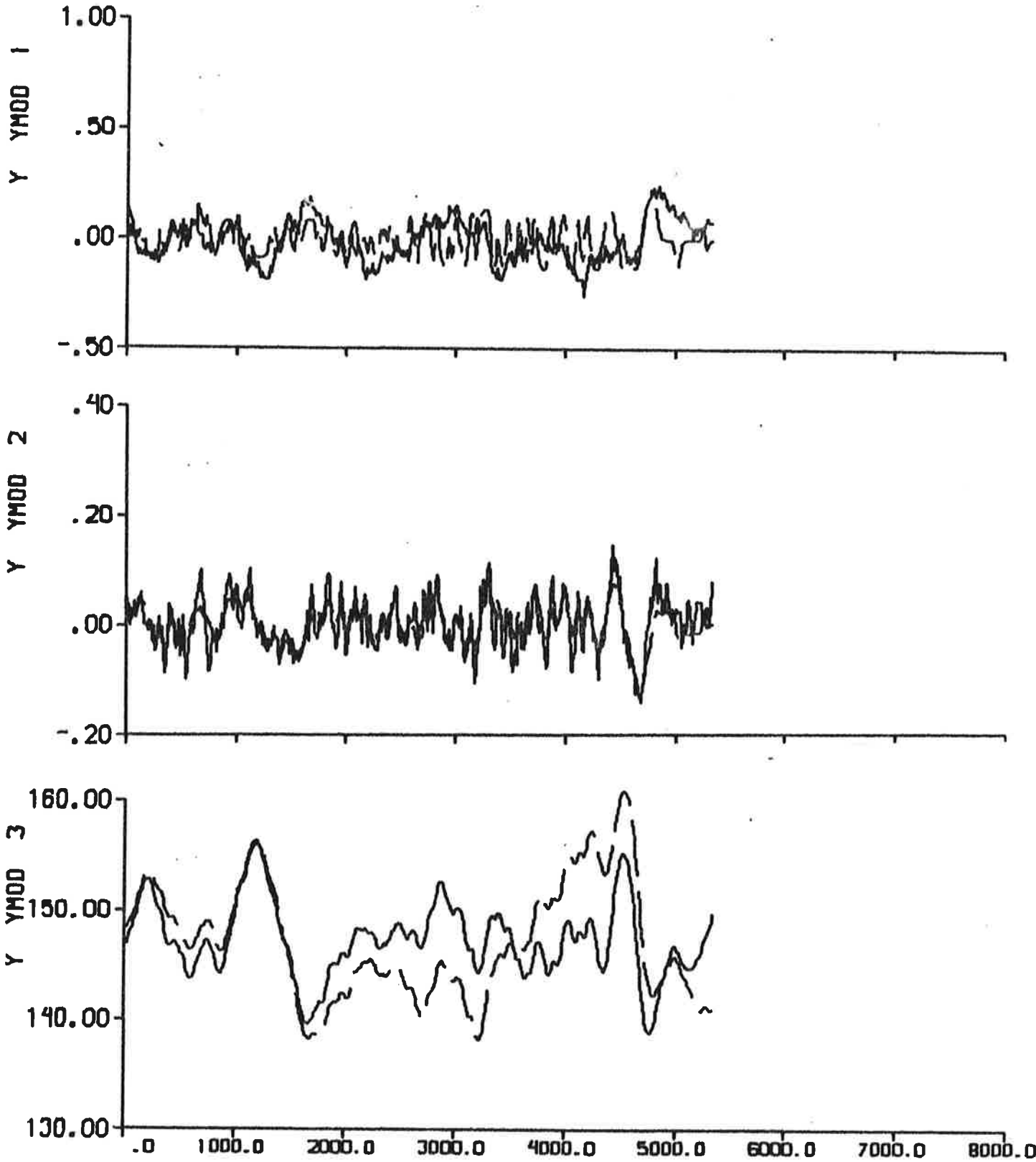describing the nonlinear contributions.

Fig. 5.18a - Result of output error identification to data from
experiment E4, when the model is fixed to the model
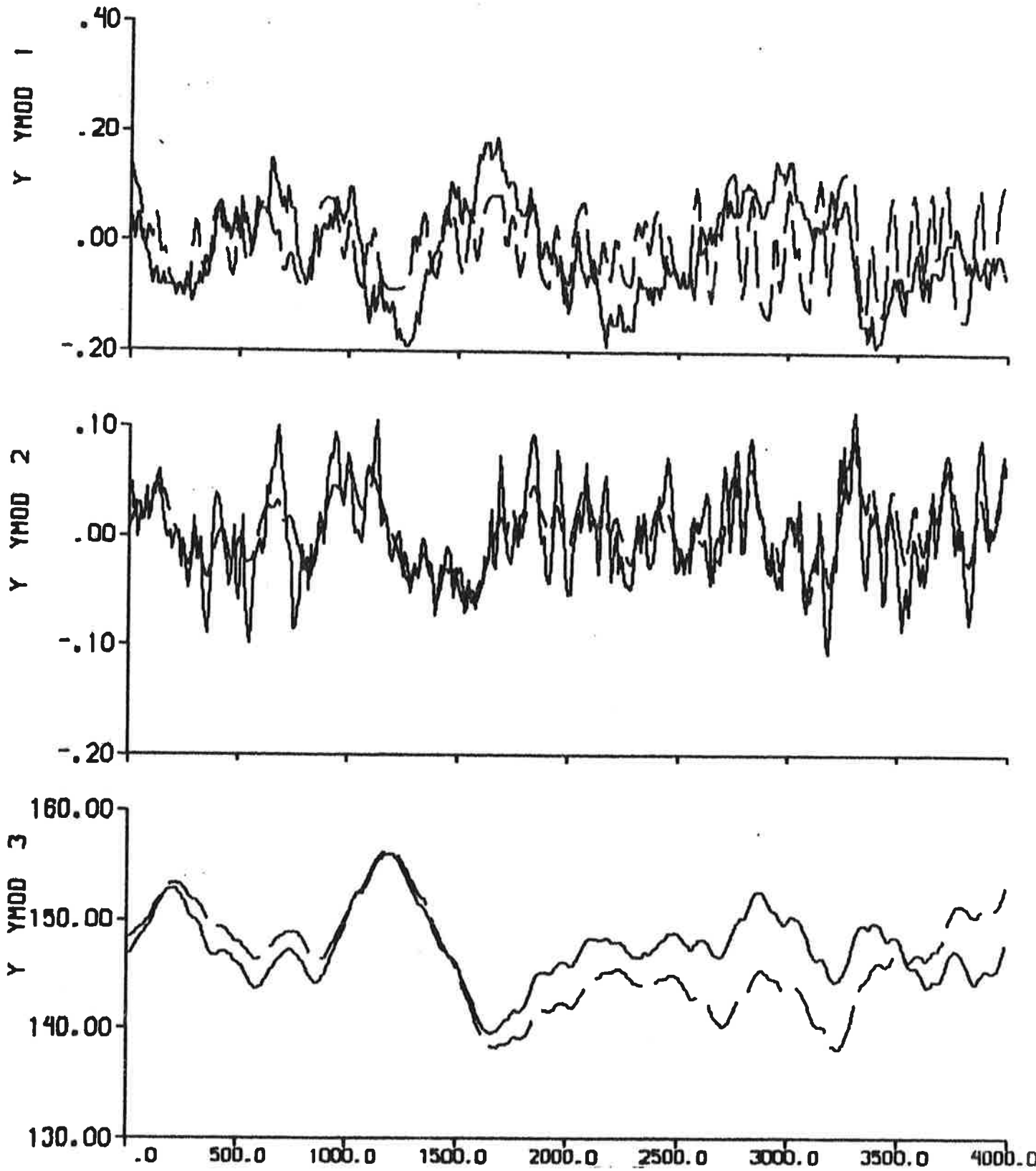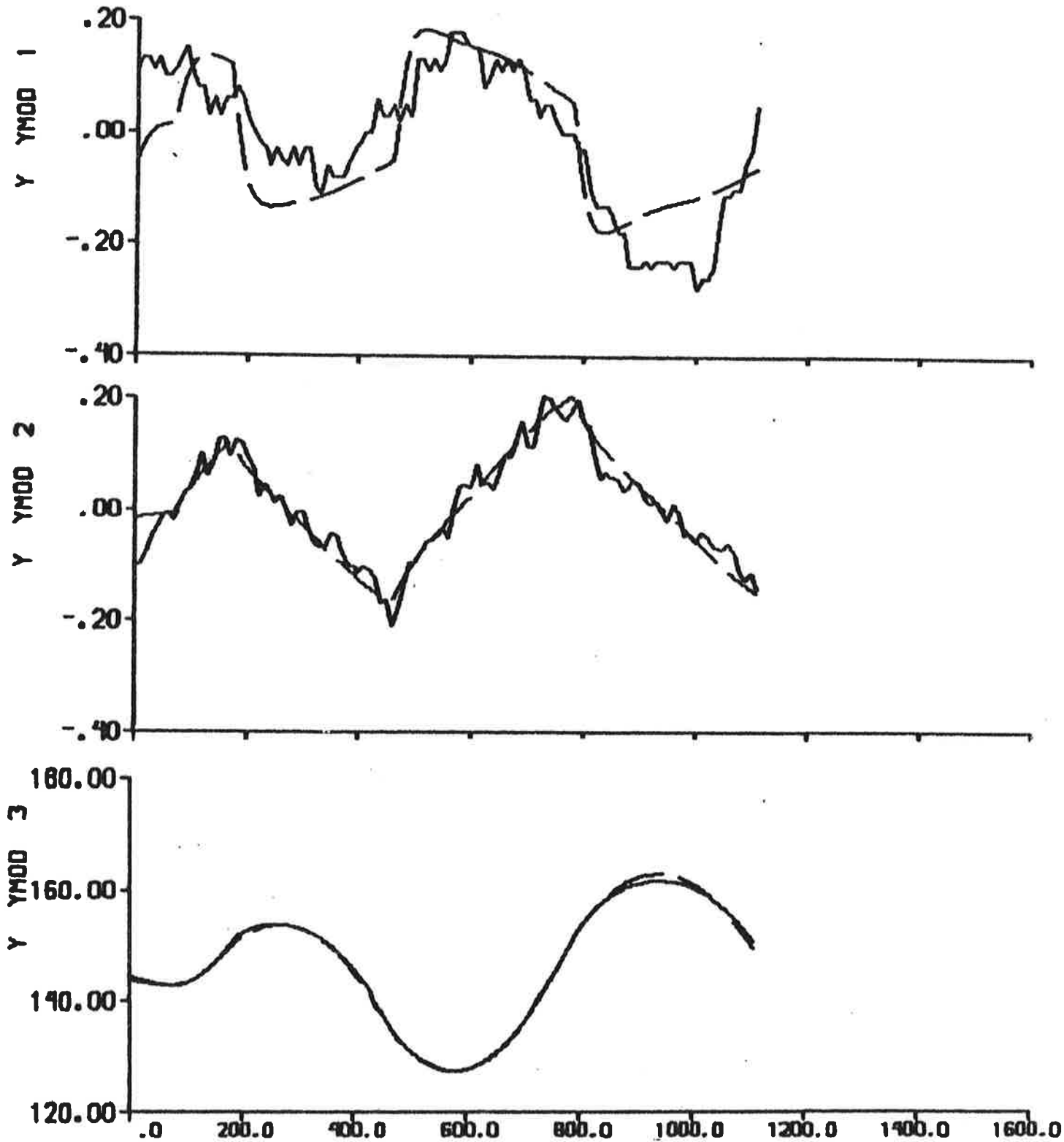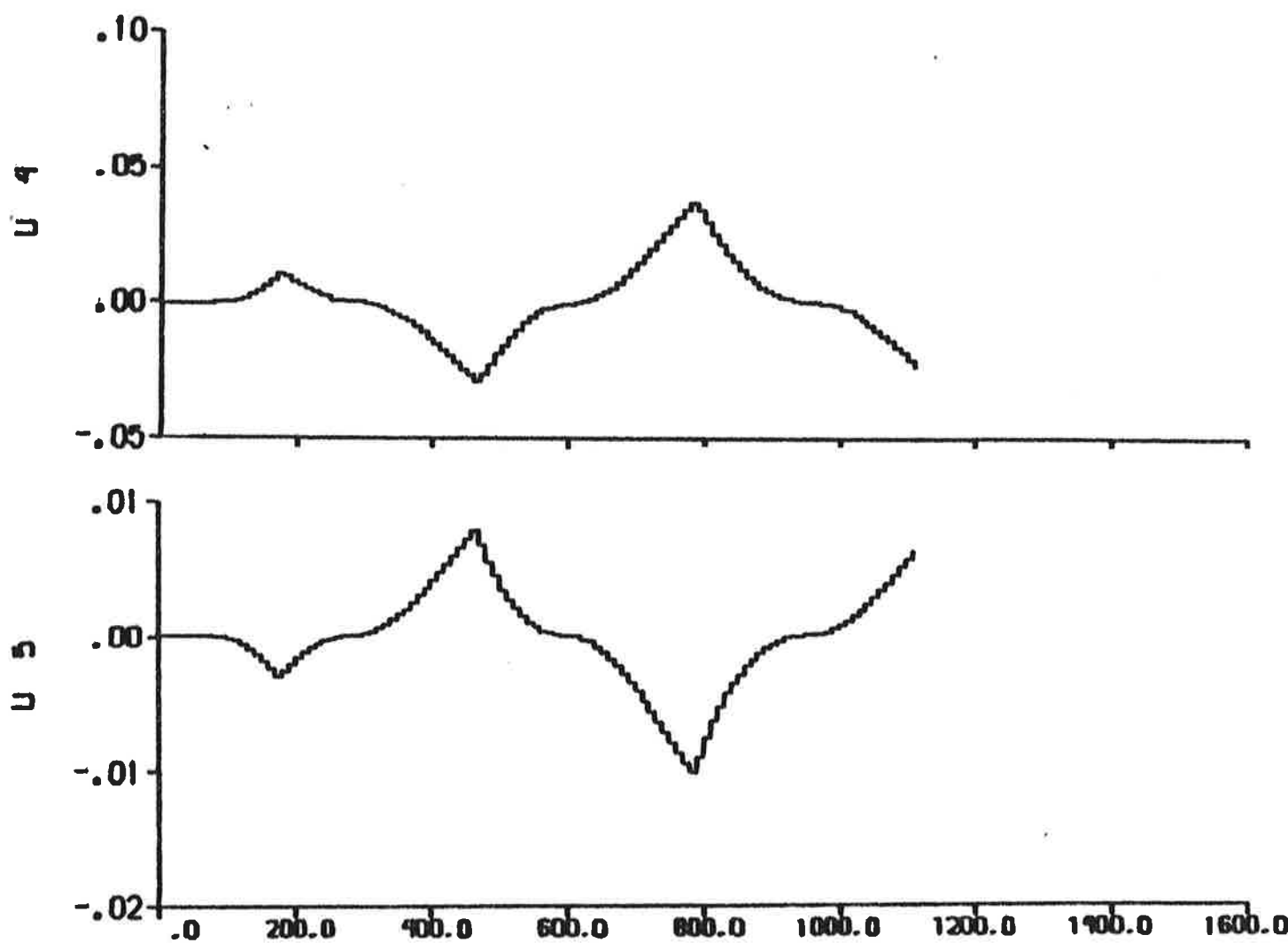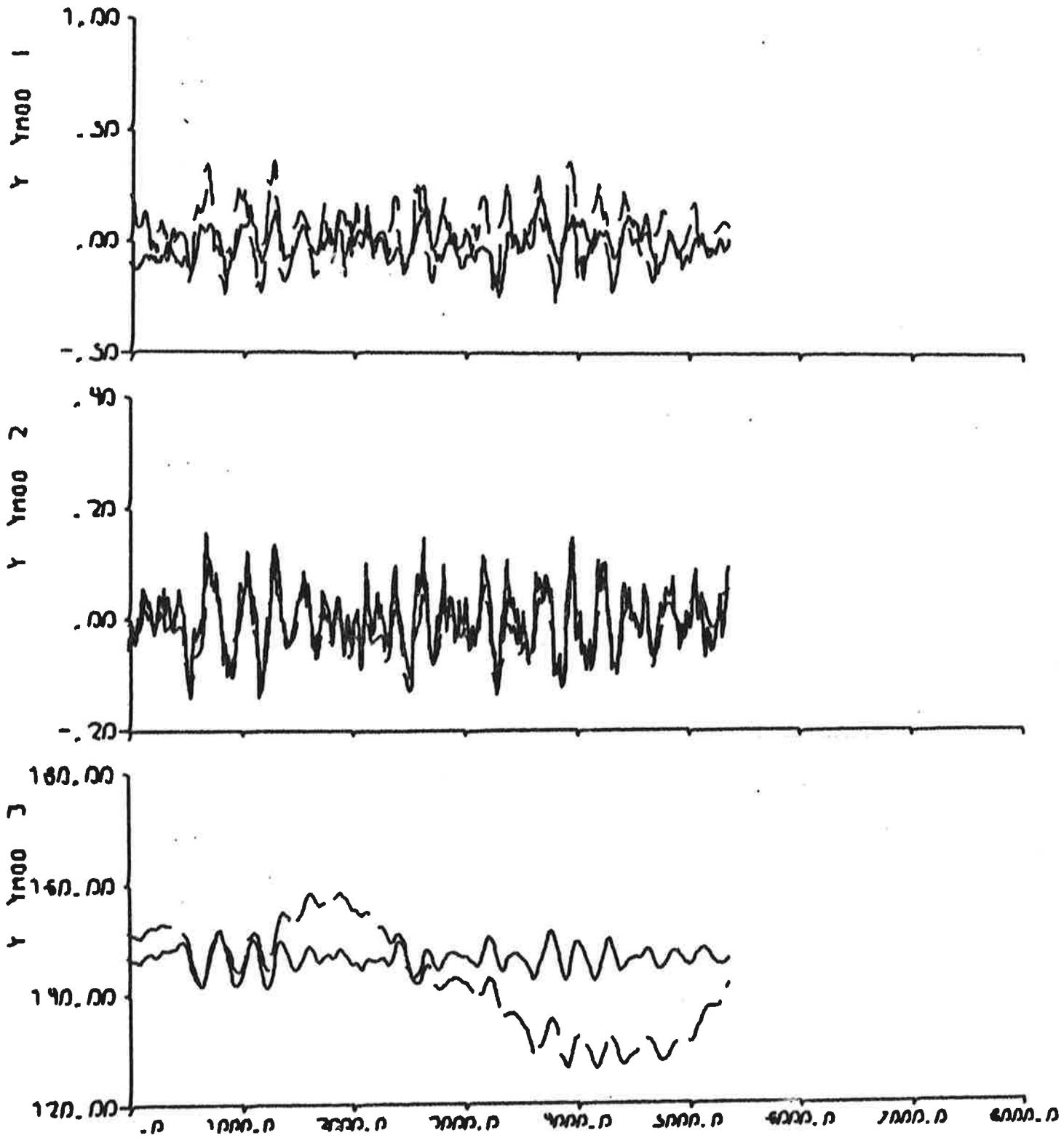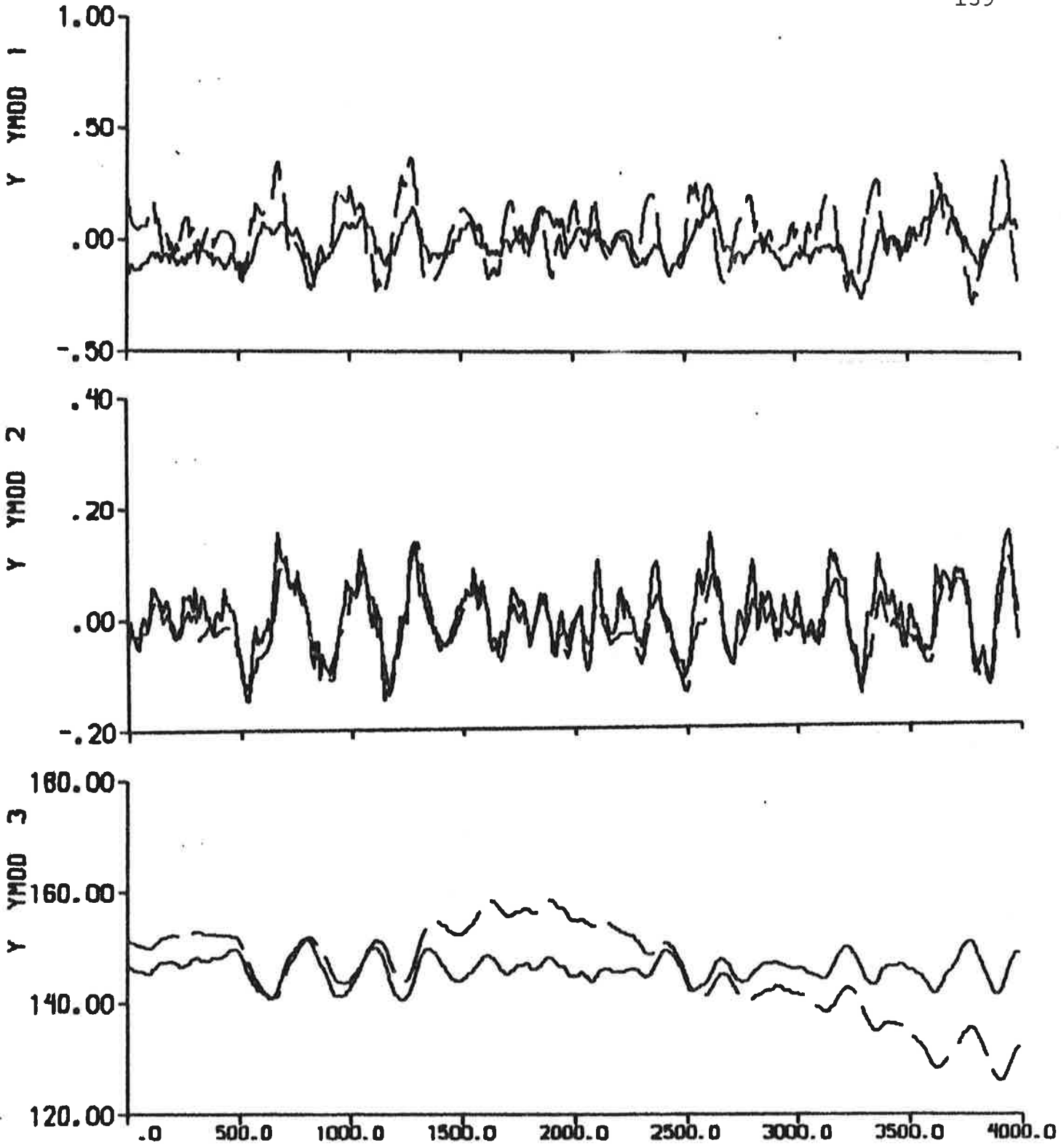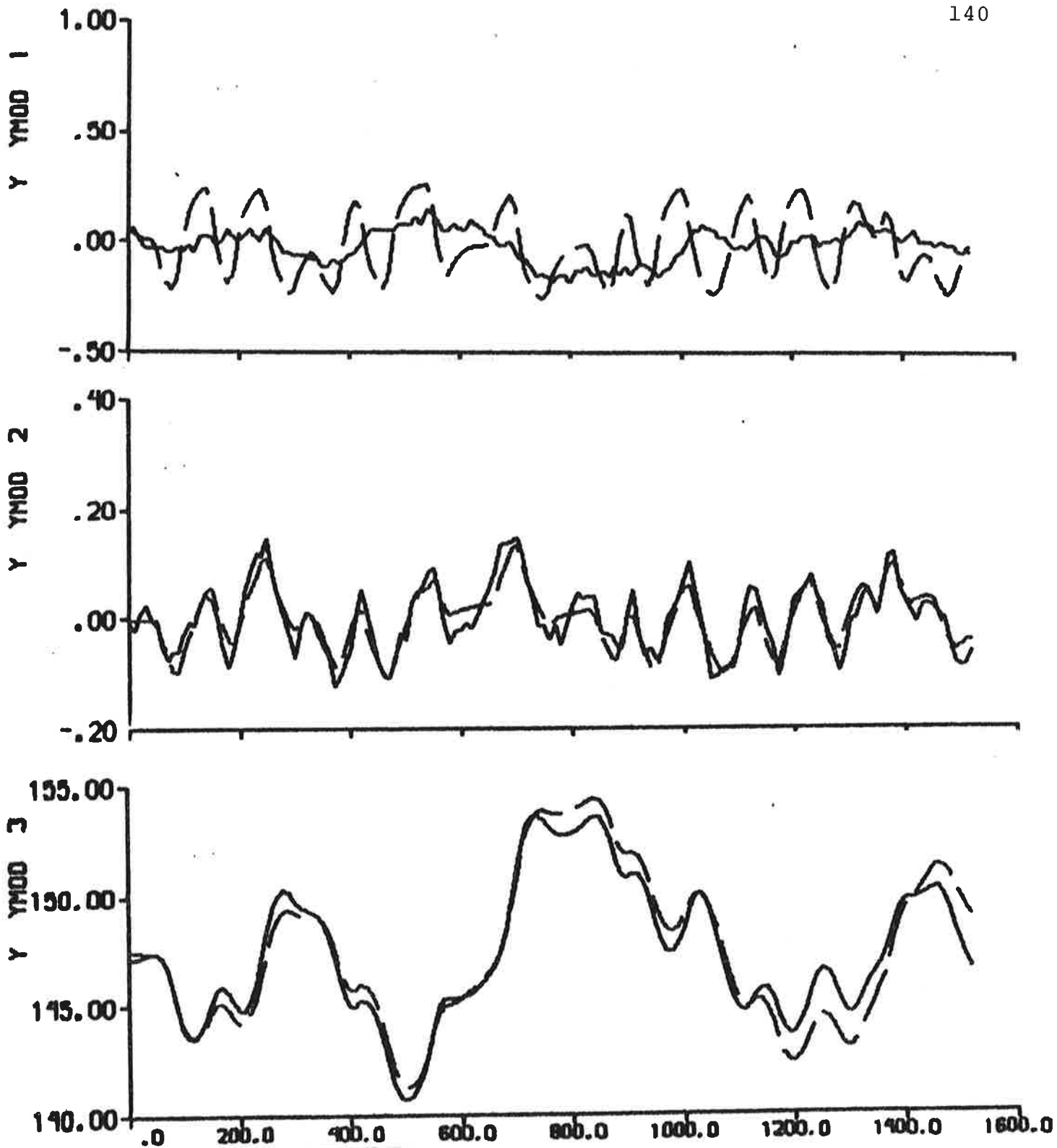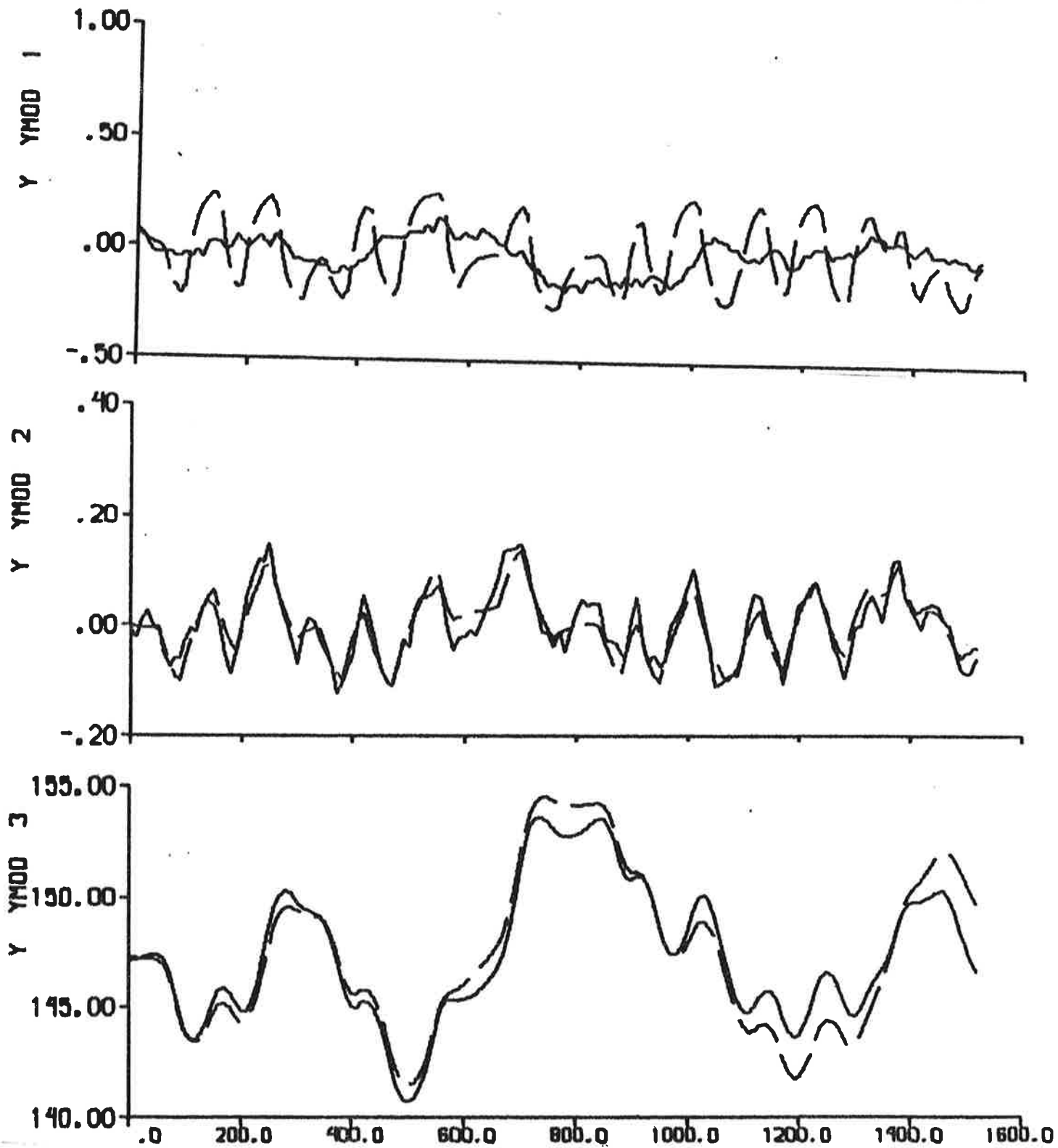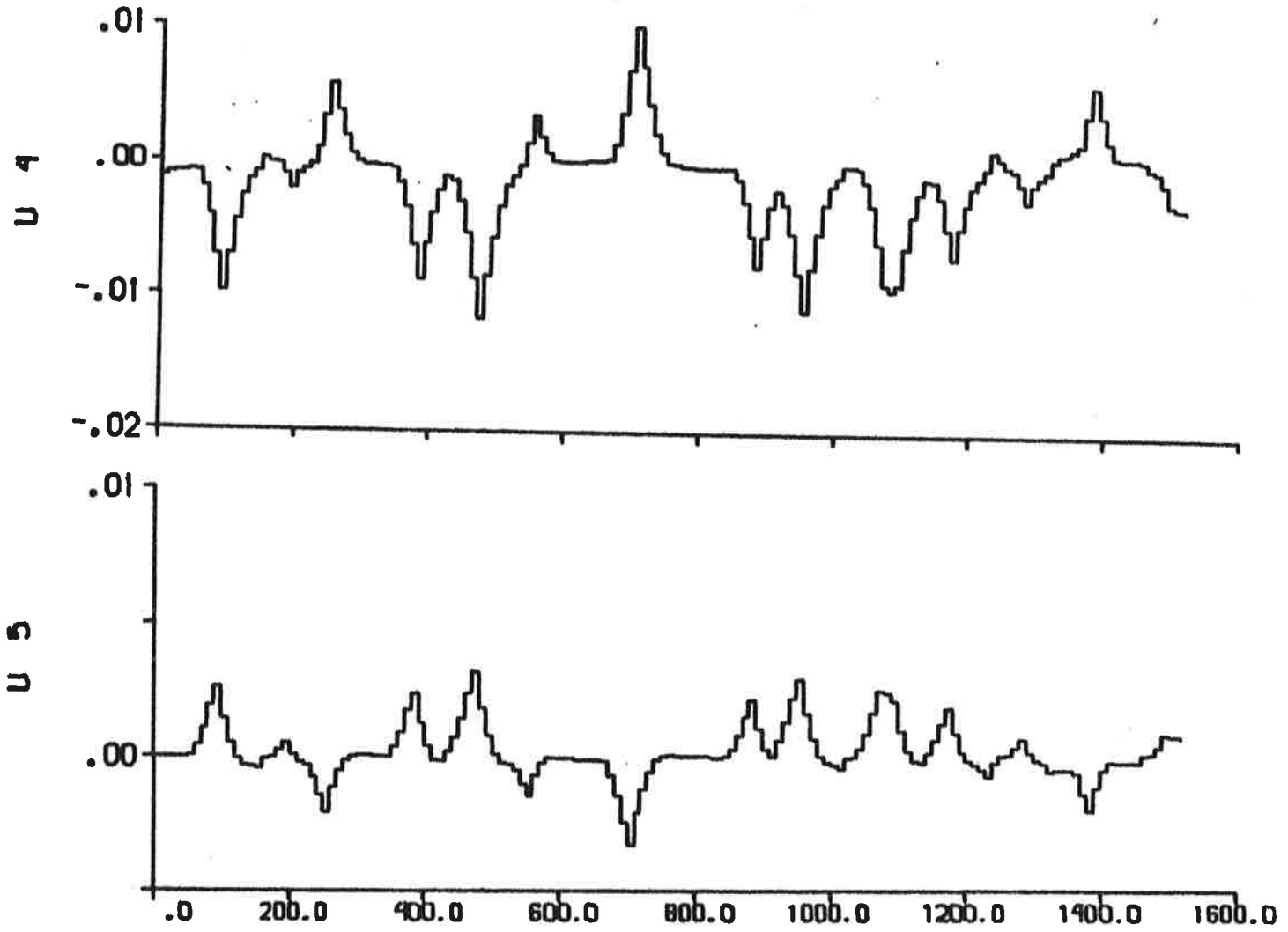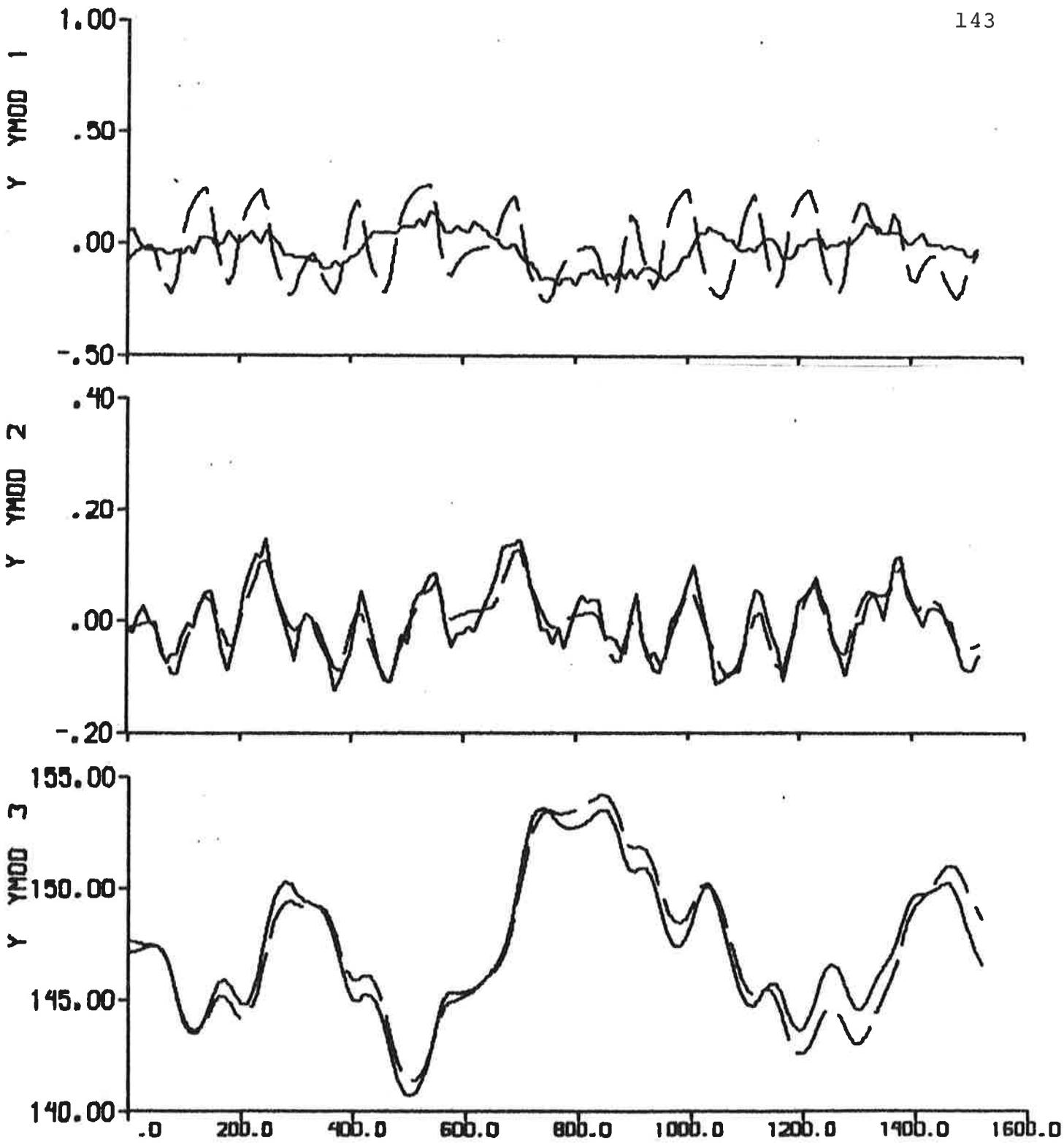obtained from prediction error identification (p = 6)
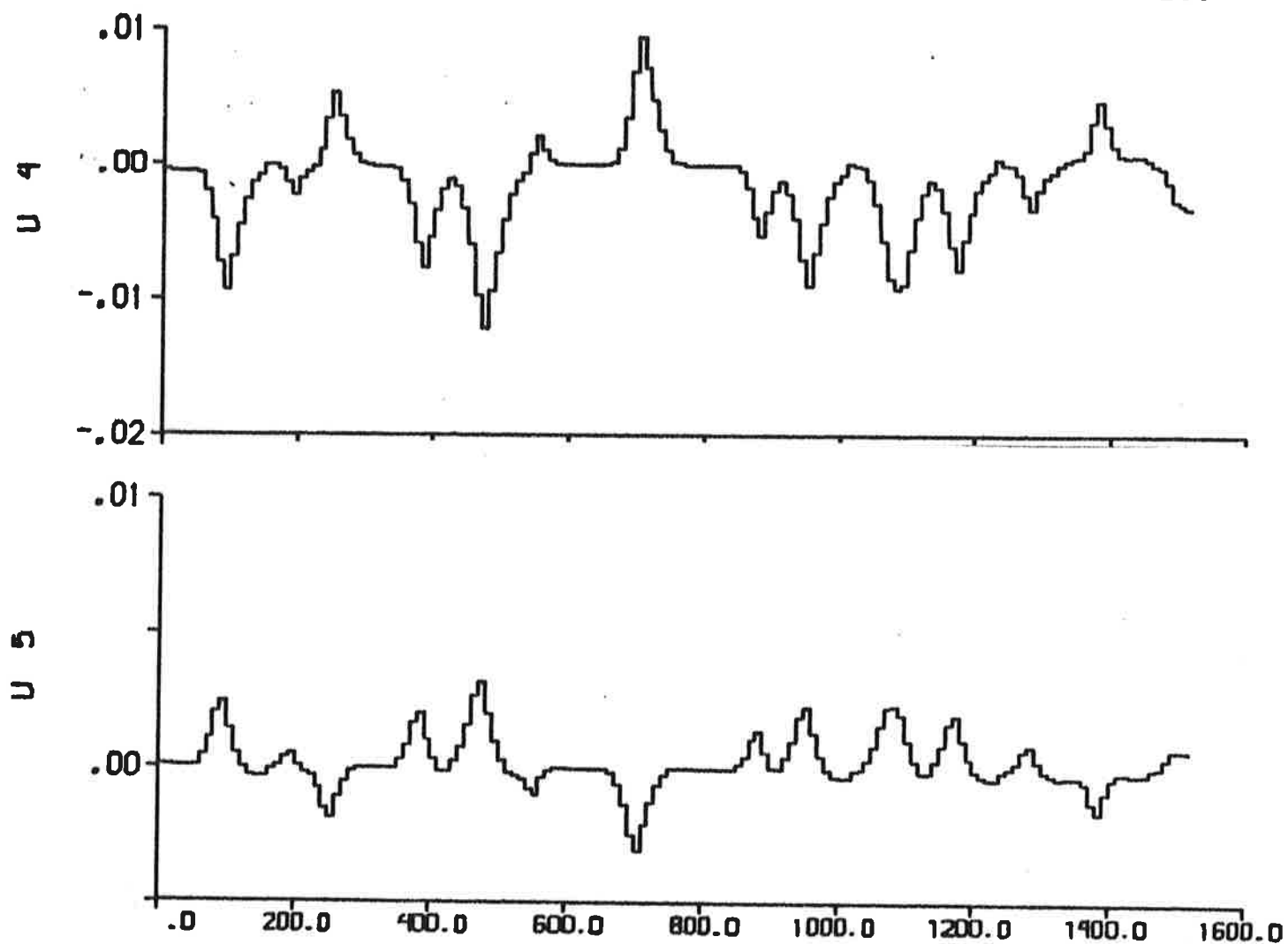to data from E2. C is estimated.

Fig. 5.18b - Additional inputs U4 = f_Y/m' and U5 = $\ddot{f}_N/m'$ describing the nonlinear contributions.

dependent on the experiment. The results are summarized in Table 6.1, and the plots are shown in Figs. 6.1 - 6.16. The heading measurements (the continuous line) and the model output (the dashed line) are shown in the uppermost diagram of each page. The next diagram shows the prediction errors. The auto-correlation function of prediction errors and the cross correlation function between rudder input and prediction errors are also shown. Notice that the dashed lines in these diagrams are the $\pm 2\sigma$ limits. SSPA:s model given in Table 6.1 is derived from the model in Table 3.1 by assuming $T' = T_1' + T_2' - T_3'$ (cf. (3.12) and (3.13)). The consistency between the parameter estimates obtained from the output error identifications to data from the 4 experiments is rather bad. The residuals obtained from the output error identifications are not white and they are correlated to the rudder inputs. The following estimated standard deviations are obtained when the output error method is applied to data from experiments E1, E2 and E3 (cf. Table 6.1):

$$
\begin{aligned}
\varphi_1 &= 0.22 \pm 0.03 & 0.16 \pm 0.02 & & 1.50 \pm 0.10 \\
\varphi_4 &= -0.31 \pm 0.03 & -0.69 \pm 0.01 & & -0.43 \pm 0.04 \\
\varphi_7 &= (5.3 \pm 0.4) \cdot 10^{-7} & (1.24 \pm 0.02) \cdot 10^{-6} & & (1.3 \pm 0.1) \cdot 10^{-6} \\
\varphi_{24} &= 2.8 \pm 0.2 & 3.4 \pm 0.3 & & 3.14 \pm 0.01
\end{aligned} \tag{6.2}
$$

The parameter $\varphi_4 = K_1'$ is estimated to -0.99, -0.72, -0.94 and -1.03 when the ML method is applied to data from the 4 experiments. Notice, however, that the estimates of $\varphi_1 = 1/T'$ obtained from the different experiments differ somewhat more. It is concluded from Figs. 6.2, 6.6, 6.10 and 6.14 that the prediction errors are almost white and almost uncorrelated to the rudder inputs. Akaike's information criterion AIC also indicates distinctly that process noise should be modelled. The following estimated standard deviations are obtained when the ML method is applied to data from experiments E1, E2, E3 and E4:

$$
\begin{aligned}
\varphi_1 &= 0.41 \pm 0.05 & 0.19 \pm 0.04 & 0.65 \pm 0.04 & 0.65 \pm 0.08 \\
\varphi_4 &= -0.99 \pm 0.02 & -0.72 \pm 0.04 & -0.94 \pm 0.02 & -1.03 \pm 0.02 \\
\varphi_7 &= (1.9 \pm 0.5) \cdot 10^{-6} & (2.5 \pm 1.4) \cdot 10^{-6} & (2.5 \pm 0.6) \cdot 10^{-6} & (2.7 \pm 1.1) \cdot 10^{-6} \\
\varphi_{10} &= (4.4 \pm 0.9) \cdot 10^{-8} & (1.0 \pm 0.4) \cdot 10^{-9} & (1.8 \pm 0.3) \cdot 10^{-8} & (6.0 \pm 1.9) \cdot 10^{-8} \\
\varphi_{24} &= 2.69 \pm 0.04 & 1.6 \pm 0.8 & 2.72 \pm 0.04 & 0.21 \pm 0.04
\end{aligned} \tag{6.3}
$$

The following filter gains K (cf. (3.4)) are obtained from
applying the ML method to data from experiments E1, E2, E3
and E4:

$$K = \begin{pmatrix} 0 \\ 1.5 \cdot 10^{-3} \\ 3.2 \cdot 10^{-2} \end{pmatrix}, \begin{pmatrix} 0 \\ 0.5 \cdot 10^{-3} \\ 1.7 \cdot 10^{-2} \end{pmatrix}, \begin{pmatrix} 0 \\ 1.2 \cdot 10^{-3} \\ 2.8 \cdot 10^{-2} \end{pmatrix}, \begin{pmatrix} 0 \\ 1.5 \cdot 10^{-3} \\ 3.2 \cdot 10^{-2} \end{pmatrix} \quad (6.4)$$

The results of prediction error identifications with p = 4
and 6 indicate no significant changes compared to the ML results.
A prediction interval of 10 s is is thus not unreasonable in this
case. The following filter gains K (cf. (3.4)) are obtained when
p = 4:

$$K = \begin{pmatrix} 0 \\ 1.4 \cdot 10^{-3} \\ 3.1 \cdot 10^{-2} \end{pmatrix}, \begin{pmatrix} 0 \\ 0.5 \cdot 10^{-3} \\ 1.5 \cdot 10^{-2} \end{pmatrix}, \begin{pmatrix} 0 \\ 1.1 \cdot 10^{-3} \\ 2.7 \cdot 10^{-2} \end{pmatrix}, \begin{pmatrix} 0 \\ 1.6 \cdot 10^{-3} \\ 3.4 \cdot 10^{-2} \end{pmatrix} \quad (6.5)$$

The corresponding filter gains for p = 6 are:

$$K = \begin{pmatrix} 0 \\ 1.3 \cdot 10^{-3} \\ 2.9 \cdot 10^{-2} \end{pmatrix}, \begin{pmatrix} 0 \\ 0.4 \cdot 10^{-3} \\ 1.4 \cdot 10^{-2} \end{pmatrix}, \begin{pmatrix} 0 \\ 1.1 \cdot 10^{-3} \\ 2.6 \cdot 10^{-2} \end{pmatrix}, \begin{pmatrix} 0 \\ 1.7 \cdot 10^{-3} \\ 3.4 \cdot 10^{-2} \end{pmatrix} \quad (6.6)$$

It is concluded by comparing (6.4), (6.5) and (6.6) that the filter
gains do not differ much.

Notice that only one unstable model is obtained in Table 6.1.
In all cases, except when the output error method is applied
to experiment E4, stable models are determined.

The parameters of the transfer function (3.12) are also estimated
by using the program LISPID. The identifications are based on the
model (3.10) with the following fixed parameter values (cf. (6.1)):

$\varphi_3 = 0$

$\varphi_{11} = 0$

$\varphi_{13} = 0.01 \text{ deg}^2$

$\varphi_{15} = 0$

$\varphi_{16} = 0$

$\varphi_{17} = 146.89, 144.67\ 146.58 \text{ or } 147.13 \text{ deg}$

$$(6.7)$$

The results of output error identifications, maximum likelihood identifications and prediction error identifications are shown in Figs. 6.17 - 6.32. A summary of the results is given in Table 6.2. SSPA:s model given in this table is derived from the model in Table 3.1 (cf. (3.14)).

Strange models are obtained when the output error method is applied to data from experiments E1 and E3. An improved model is determined from experiment E2. Finally, experiment E4 gave parameter values close to SSPA:s estimates. An unstable model is obtained in this case. Akaike´s information criterion selects the third-order transfer function (3.12) instead of Nomoto´s model (3.13) in all cases, when the output error method is used.

Reasonable parameter estimates are obtained when the ML method is applied to experiments E1 and E4. Akaike´s information criterion AIC also indicates that the third-order model should be selected instead of Nomoto´s model in these two cases. The following estimated standard deviations are obtained when the ML method is applied to data from experiment E1 (cf. Table 6.2):

$$
\begin{aligned}
\varphi_1 &= 3.70 \pm 0.10 \\
\varphi_2 &= 0.26 \pm 0.01 \\
\varphi_4 &= -1.40 \pm 0.05 \\
\varphi_5 &= -2.38 \pm 0.08 \\
\varphi_6 &= (8.3 \pm 1.3) \cdot 10^{-8} \\
\varphi_7 &= (2.3 \pm 0.2) \cdot 10^{-4} \\
\varphi_9 &= (5.6 \pm 2.4) \cdot 10^{-3} \\
\varphi_{10} &= 18.8 \pm 8.3 \\
\varphi_{24} &= 0.19 \pm 0.04
\end{aligned}
\tag{6.8}
$$

The models determined from experiments E2 and E3 with the ML method are strange. Nomoto´s model is thus to be preferred in these two cases instead of the third-order model. This is also verified by Akaike´s information criterion. Notice that all ML models are stable except the one obtained from experiment E4. Notice also that it is concluded from analysis of the prediction errors and from Akaike´s information criterion that the process noise should be modelled in all ceses. The following filter gains K (cf. (3.4)) are obtained from applying the ML method to data from experiments E1-E4:
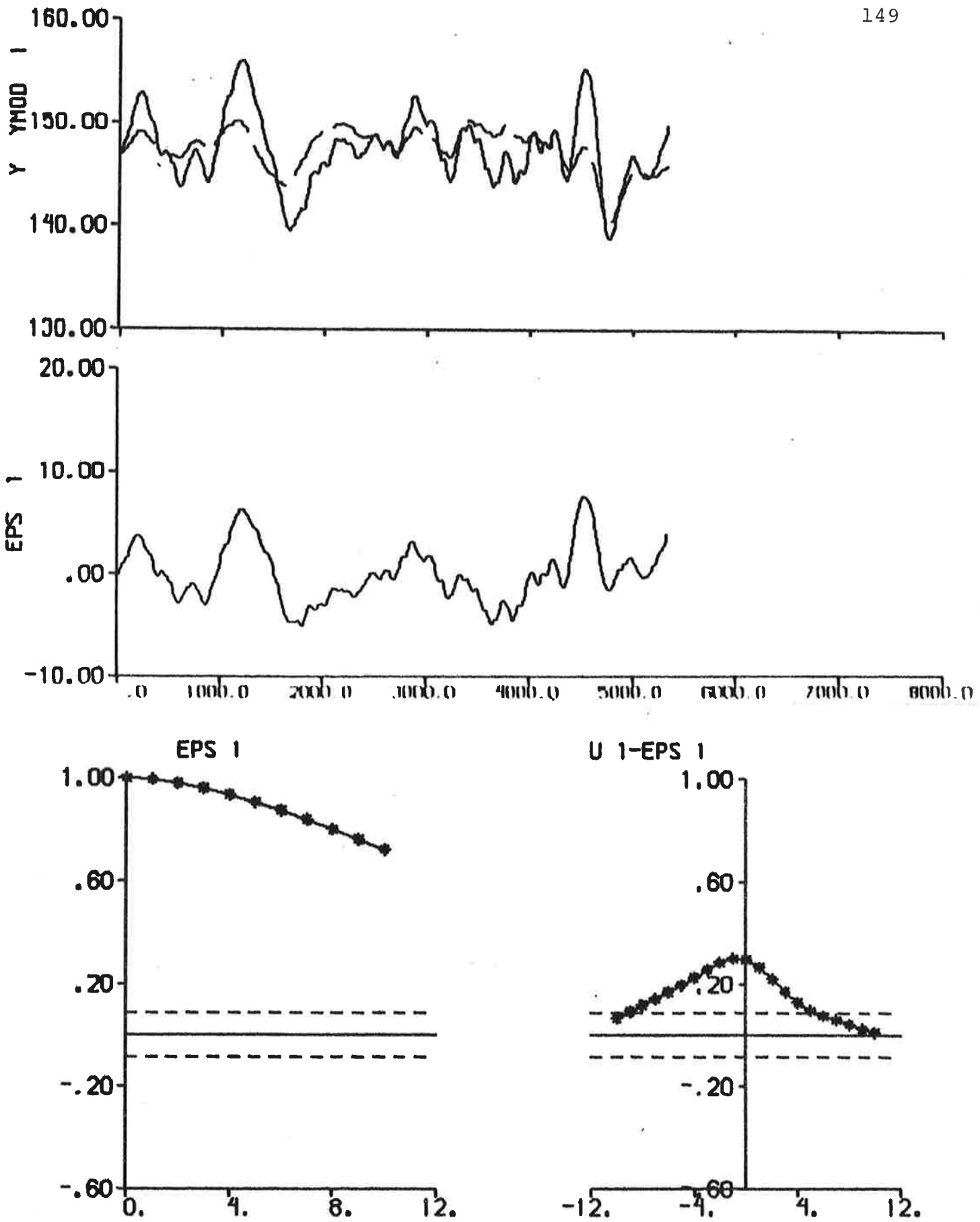
	SSPA:s model	E 1				E 2				E 3				E 4			
		Output error	ML	Pred. error $p=4$	Pred. error $p=6$	Output error	ML	Pred. error $p=4$	Pred. error $p=6$	Output error	ML	Pred. error $p=4$	Pred. error $p=6$	Output error	ML	Pred. error $p=4$	Pred. error $p=6$
Figure		6.1	6.2	6.3	6.4	6.5	6.6	6.7	6.8	6.9	6.10	6.11	6.12	6.13	6.14	6.15	6.16
ν		4	5	5	5	4	5	5	5	4	5	5	5	4	5	5	5
V		7.56	$4.2 \cdot 10^{-3}$	$9.3 \cdot 10^{-2}$	0.25	1.97	$5.5 \cdot 10^{-2}$	0.31	0.65	3.35	$7.6 \cdot 10^{-3}$	0.12	0.30	1.67	$5.9 \cdot 10^{-3}$	0.16	0.47
AIC		2608	−1400	−	−	402	3	−	−	2181	−1086	−	−	521	−341	−	−
φ_1	−0.17	0.22	0.41	0.35	0.31	0.16	0.19	0.19	0.18	1.50	0.65	0.59	0.56	−0.21	0.65	0.54	0.49
φ_4 [s^{-2}]	−0.28	−0.31	−0.99	−0.95	−0.90	−0.69	−0.72	−0.71	−0.70	−0.43	−0.94	−0.90	−0.87	−0.51	−1.03	−1.01	−0.99
φ_7 [s^{-3}]		$5.3 \cdot 10^{-7}$	$1.9 \cdot 10^{-6}$	$1.8 \cdot 10^{-6}$	$1.6 \cdot 10^{-6}$	$1.2 \cdot 10^{-6}$	$2.5 \cdot 10^{-6}$	$2.5 \cdot 10^{-6}$	$2.5 \cdot 10^{-6}$	$1.3 \cdot 10^{-6}$	$2.5 \cdot 10^{-6}$	$2.4 \cdot 10^{-6}$	$2.3 \cdot 10^{-6}$	$1.1 \cdot 10^{-6}$	$2.7 \cdot 10^{-6}$	$2.4 \cdot 10^{-6}$	$2.3 \cdot 10^{-6}$
$R_1(2,2)$	−	−	$4.4 \cdot 10^{-8}$	$3.2 \cdot 10^{-8}$	$2.0 \cdot 10^{-8}$	−	$1.0 \cdot 10^{-9}$	$7.0 \cdot 10^{-10}$	$5.0 \cdot 10^{-10}$	−	$1.8 \cdot 10^{-8}$	$1.5 \cdot 10^{-8}$	$1.1 \cdot 10^{-8}$	−	$6.0 \cdot 10^{-8}$	$8.4 \cdot 10^{-8}$	$1.0 \cdot 10^{-7}$
T_D [s]	6.6	6.6	5.6	4.5	3.6	7.4	0.0	0.0	0.0	10.0	5.9	5.2	5.0	0.0	7.9	7.0	6.7
K'	1.59	−1.41	−2.41	−2.71	−2.90	−4.31	−3.79	−3.74	−3.89	−0.29	−1.45	−1.53	−1.55	2.43	−1.58	−1.87	−2.02
K_1'	−0.28	−0.31	−0.99	−0.95	−0.90	−0.69	−0.72	−0.71	−0.70	−0.43	−0.94	−0.90	−0.87	−0.51	−1.03	−1.01	−0.99
T'	−5.77	4.55	2.44	2.86	3.23	6.25	5.26	5.26	5.56	0.67	1.54	1.69	1.79	−4.76	1.54	1.85	2.04

Table 6.1 – Parameter values from identifications of Nomoto's model (see (3.13) and (3.17)).

Fig. 6.1 - Result of output error identification to data
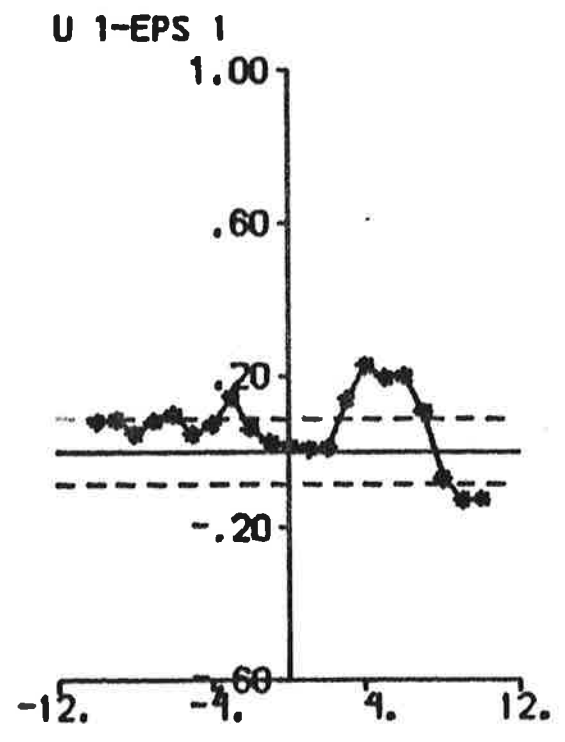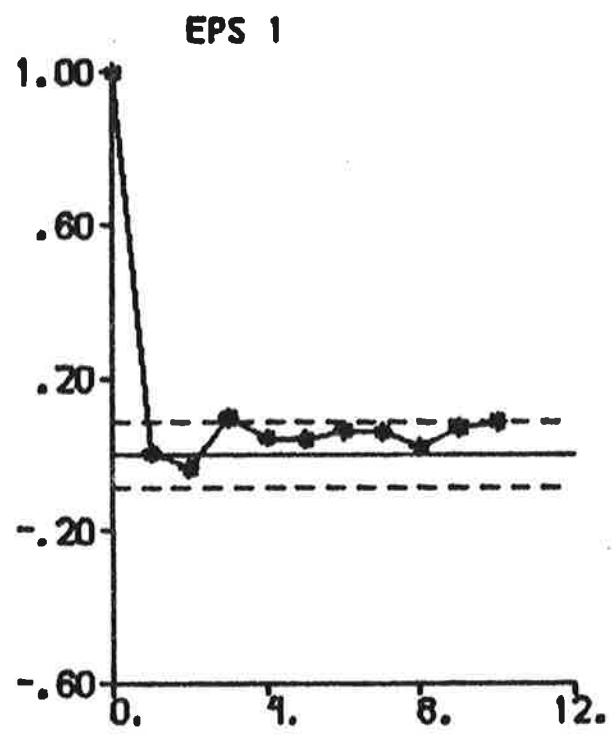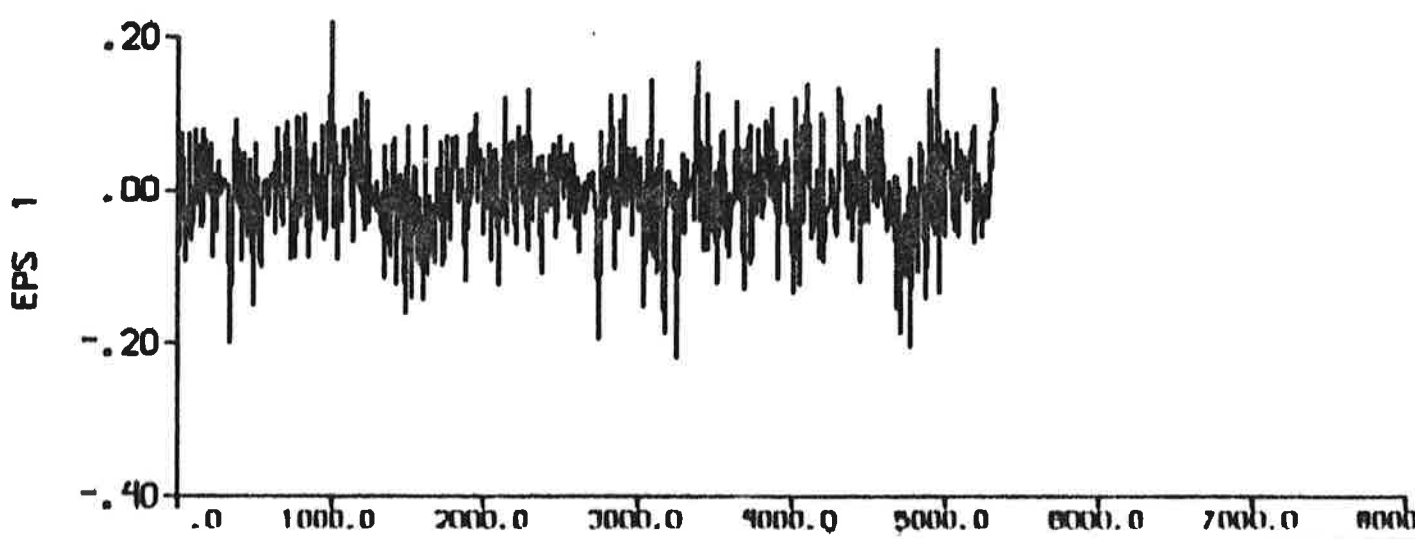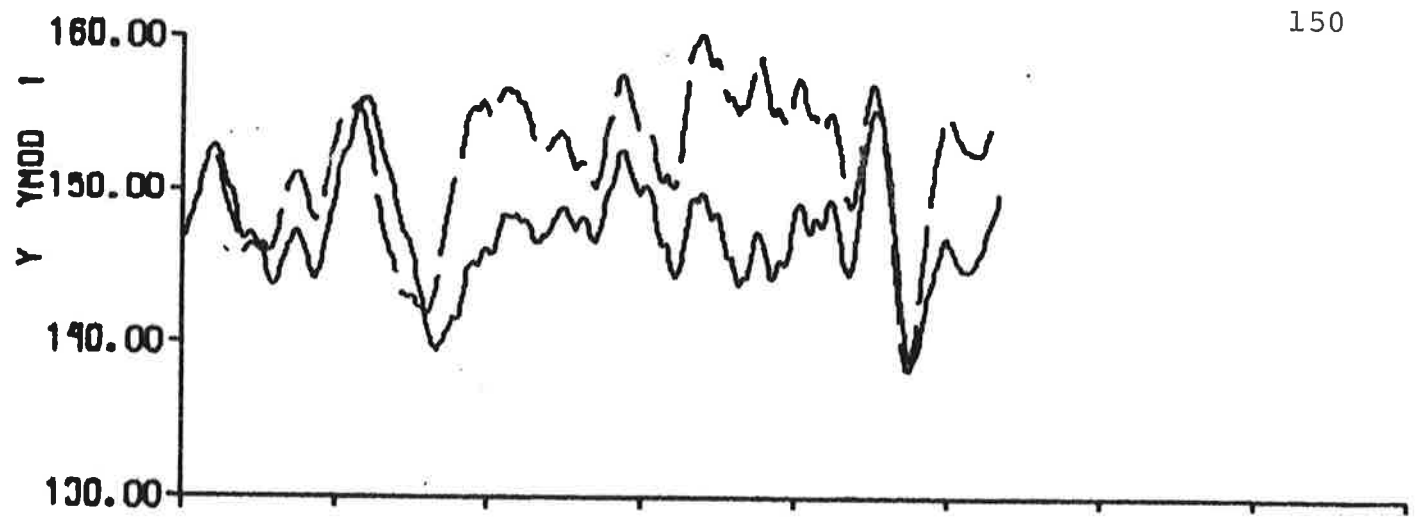from experiment E1.
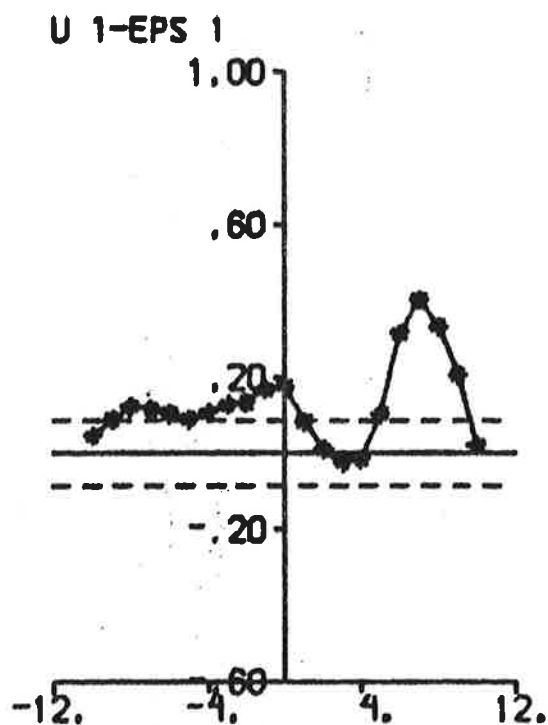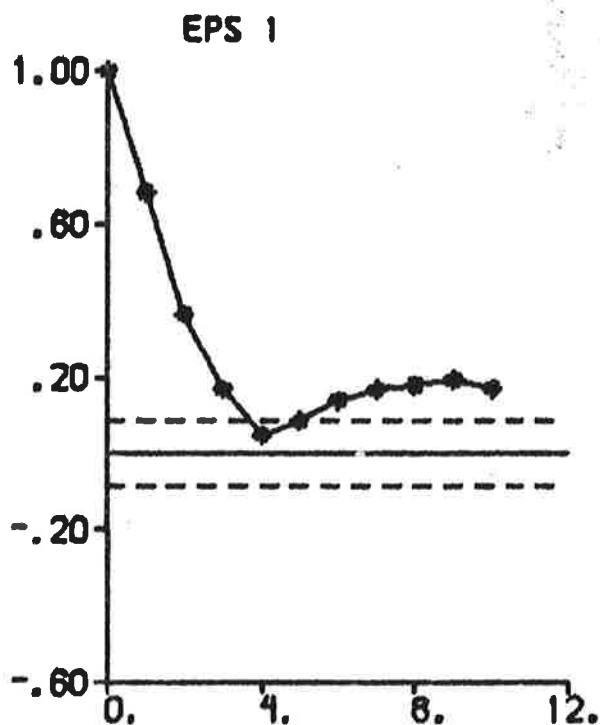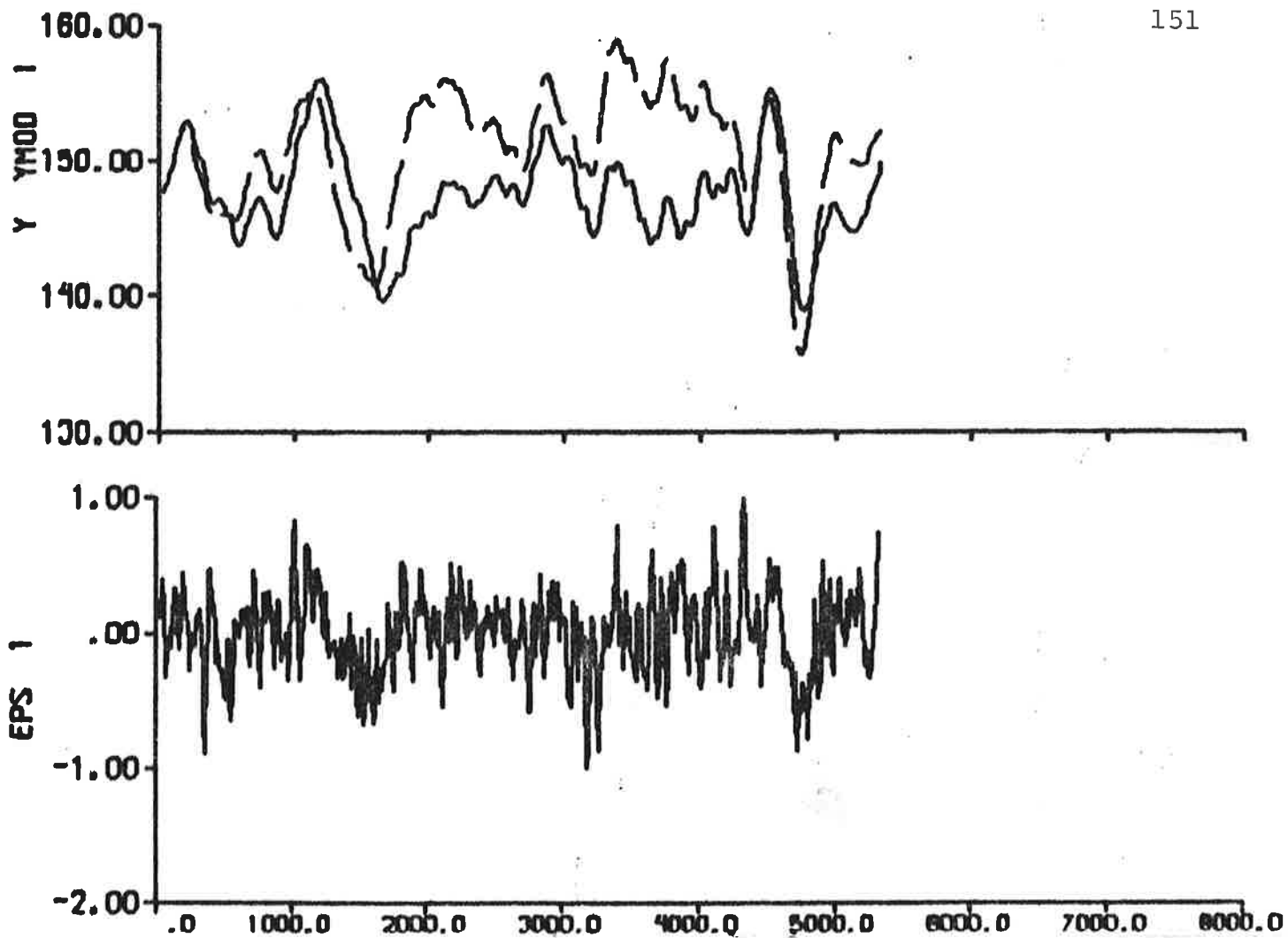
Fig. 6.2 - Result of ML identification to data
from experiment E1.

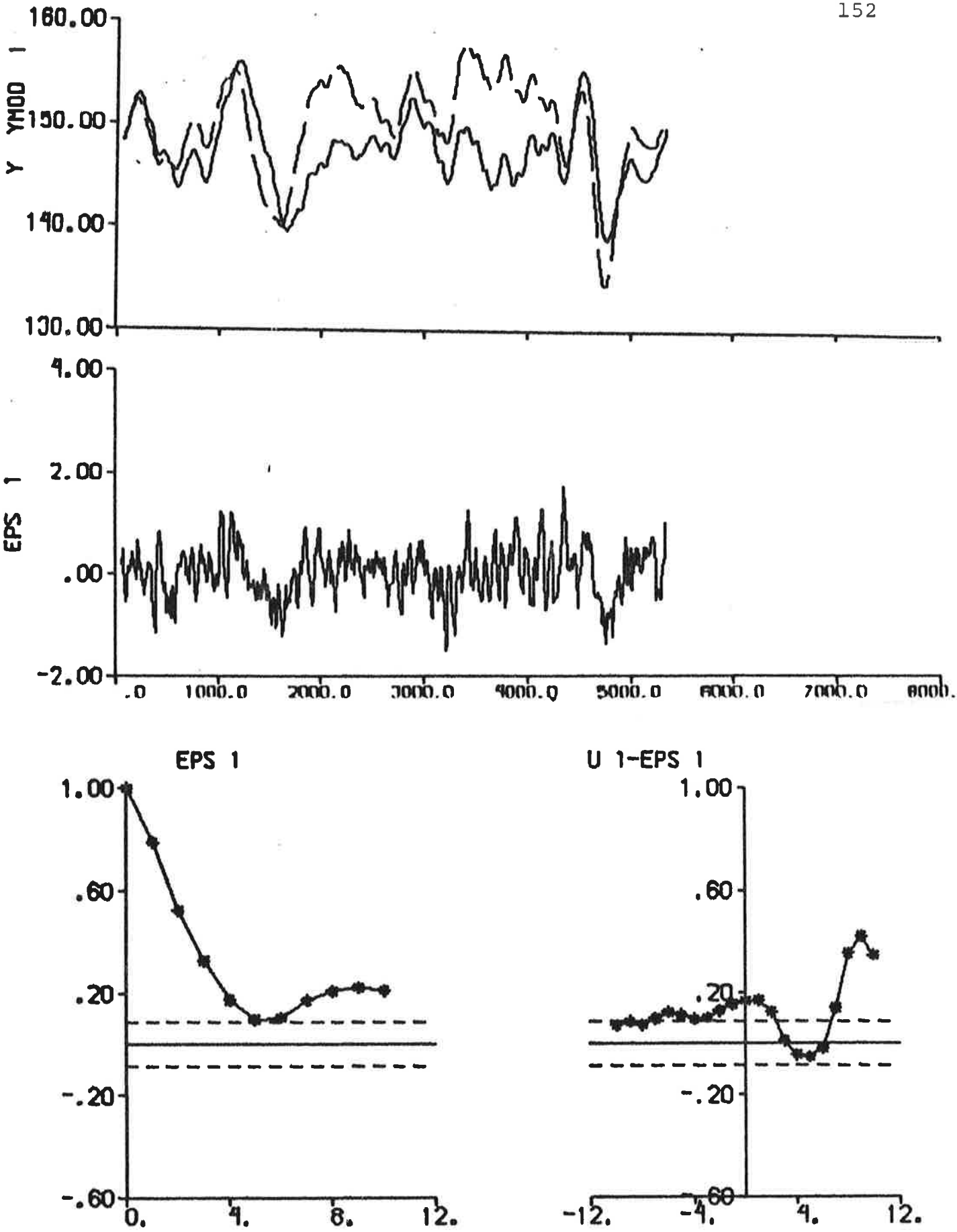Fig. 6.3 - Result of prediction error identification (p = 4) to data from experiment E1.

Fig. 6.4 - Result of prediction error identification (p = 6) to data from experiment E1.
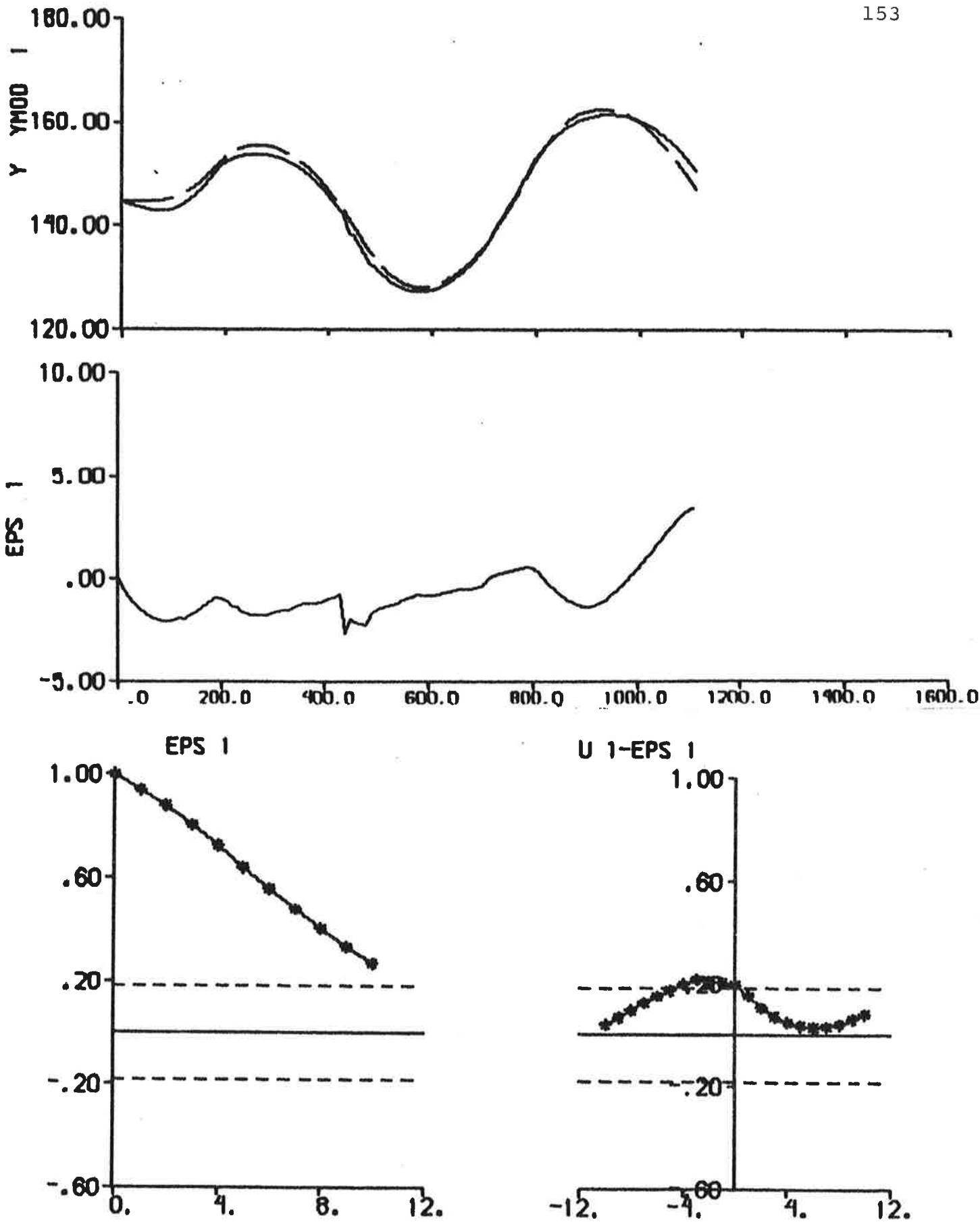
Fig. 6.5 – Result of output error identification to data
from experiment E2.

Fig. 6.6 – Result of ML identification to data
from experiment E2.

Fig. 6.7 - Result of prediction error identification (p = 4) to data from experiment E2.

Fig. 6.8 - Result of prediction error identification (p = 6) to data from experiment E2.

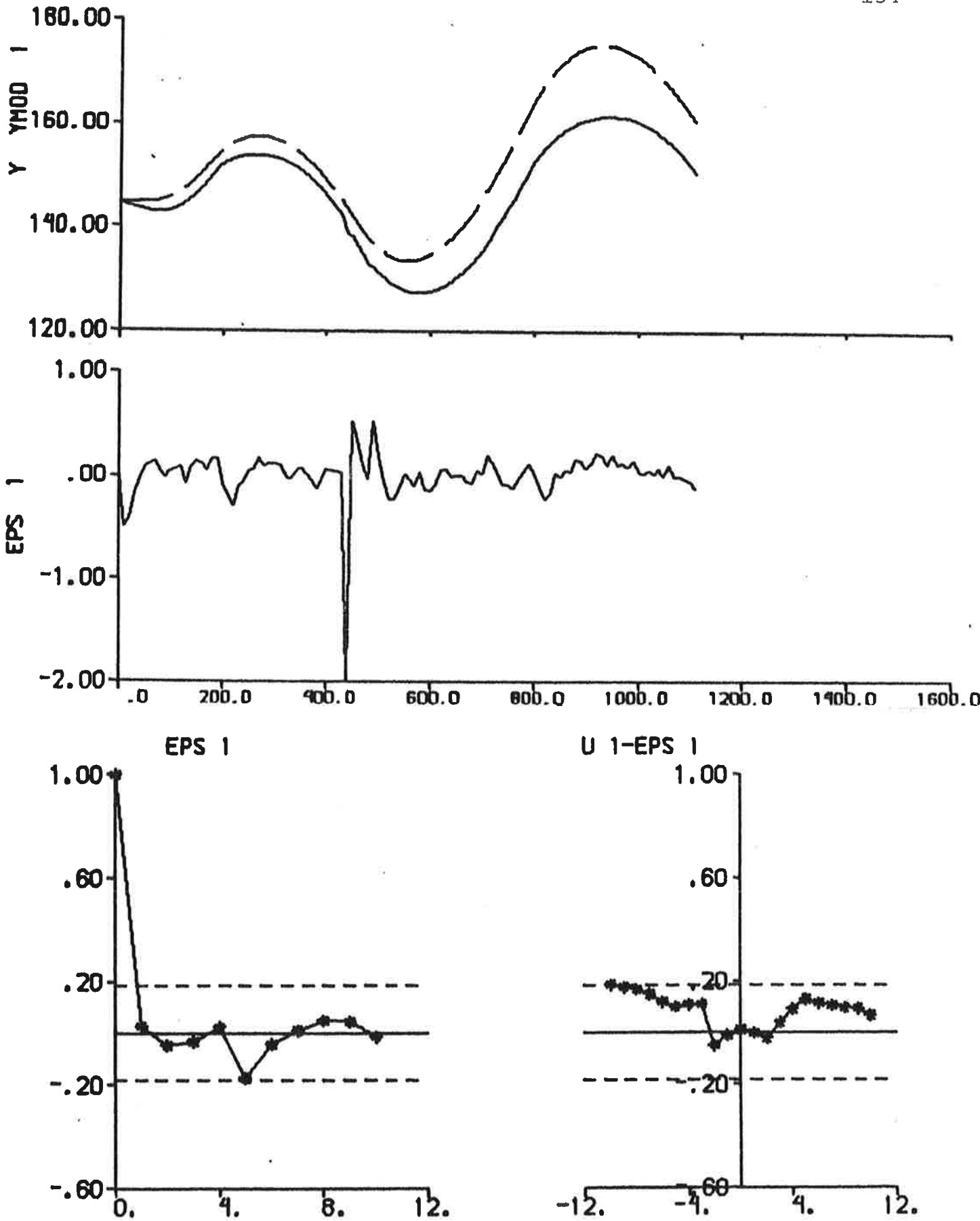Fig. 6.9 - Result of output error identification to data
from experiment E3.

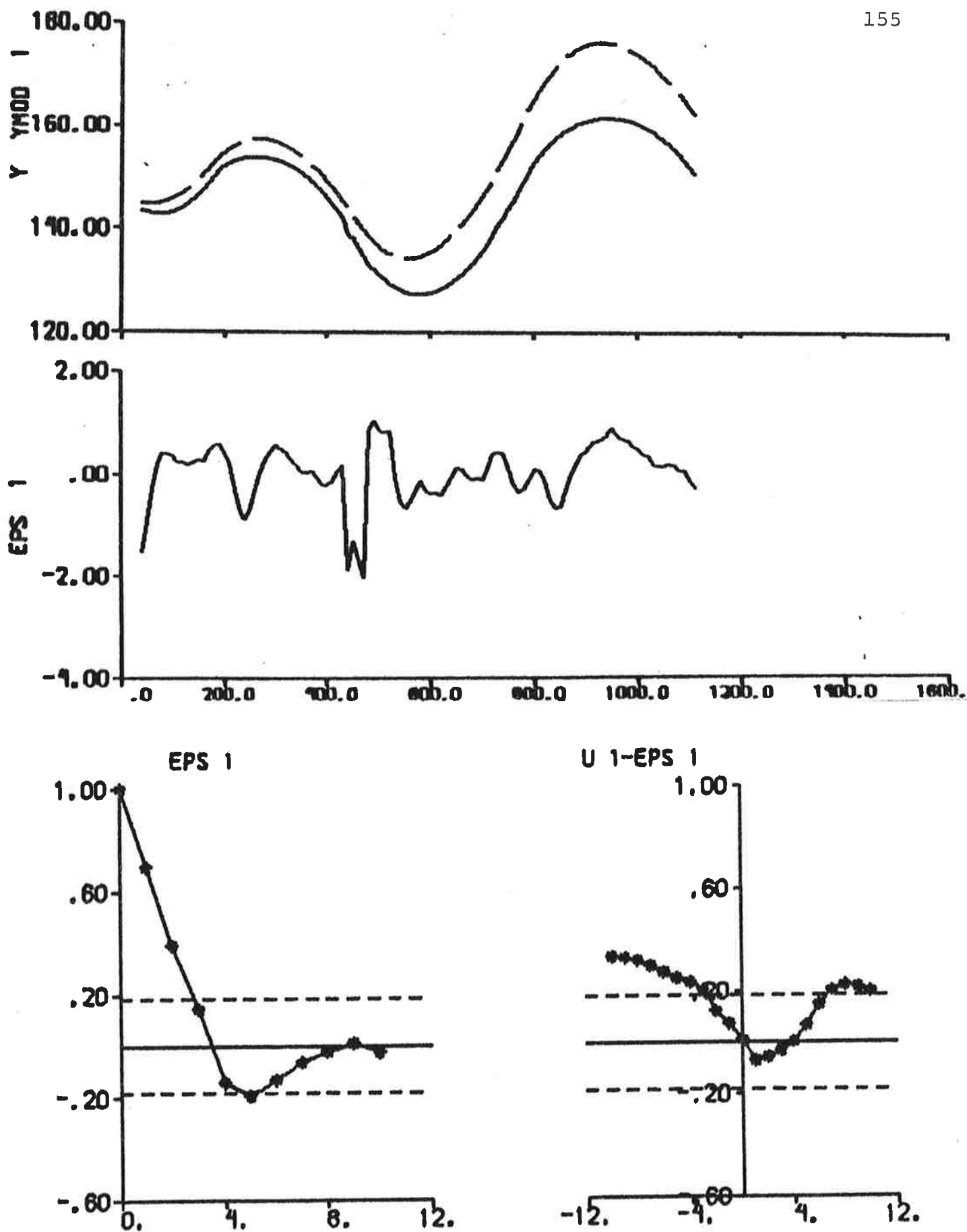Fig. 6.10 - Result of ML identification to data
from experiment E3.

Fig. 6.11 - Result of prediction error identification (p = 4) to data from experiment E3.
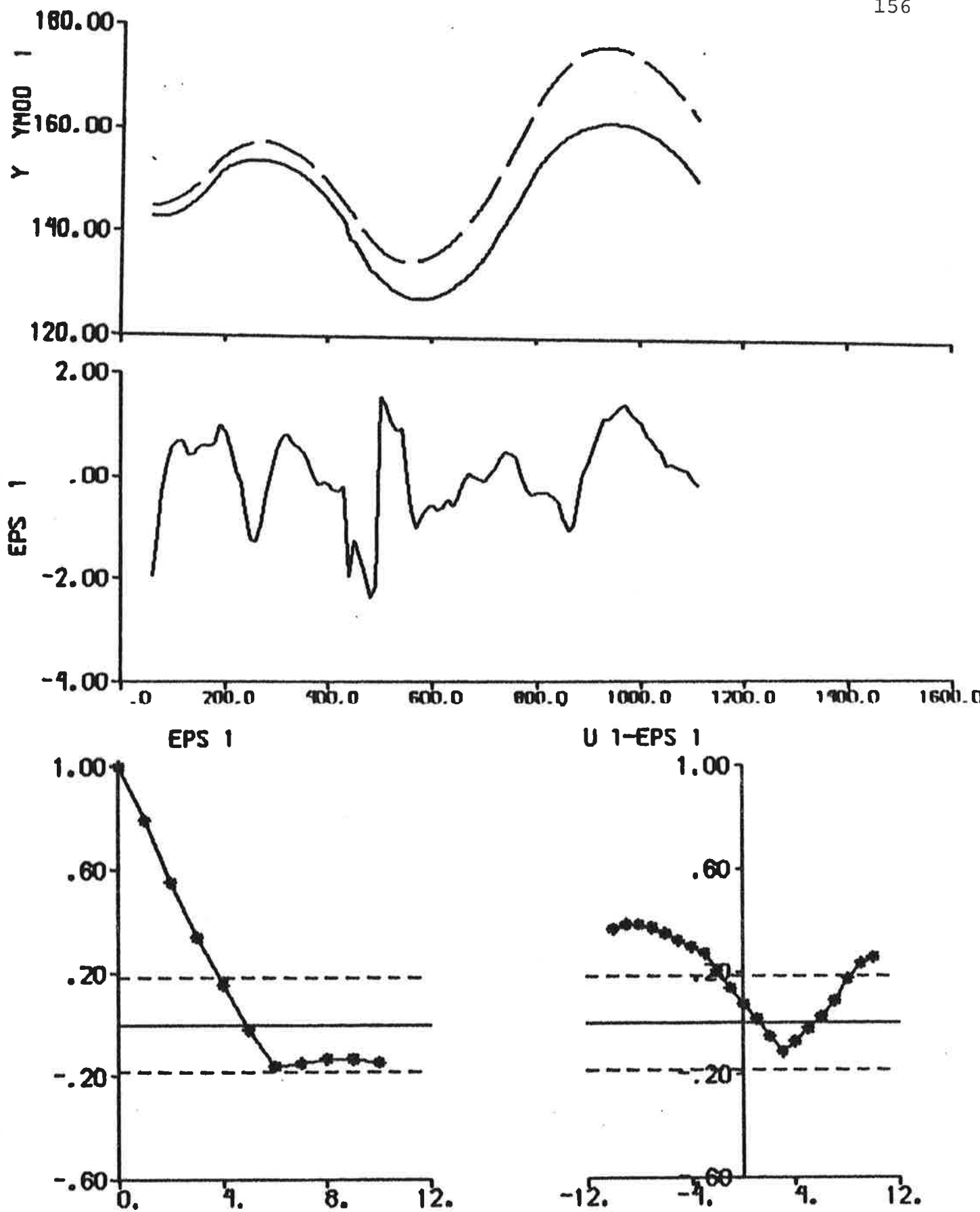
Fig. 6.12 - Result of prediction error identification (p = 6)
to data from experiment E3.

Fig. 6.13 - Result of output error identification to data
from experiment E4.

Fig. 6.14 - Result of ML identification to data from experiment E4.

Fig. 6.15 - Result of prediction error identification (p = 4)
to data from experiment E4.

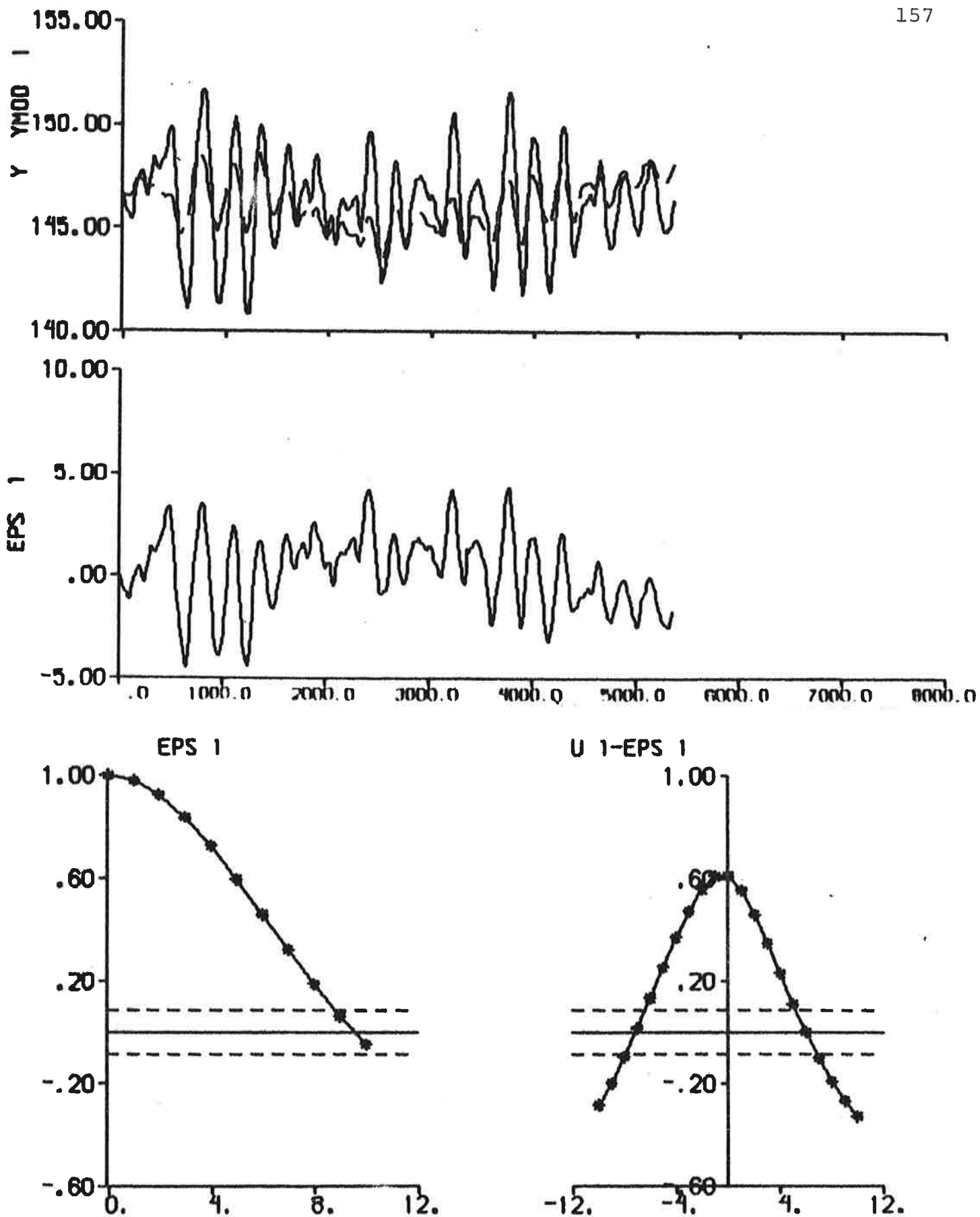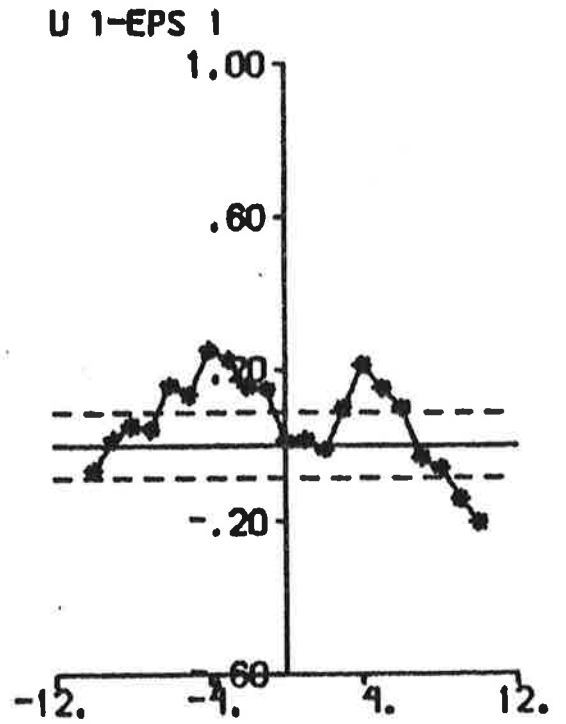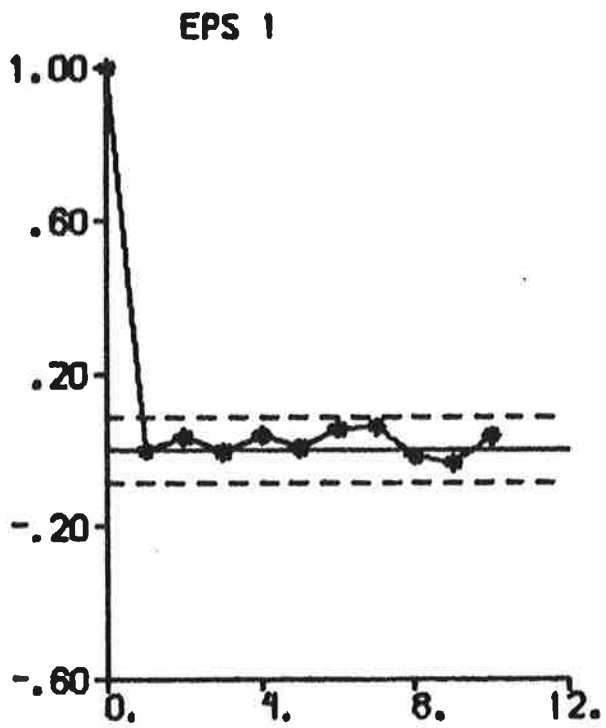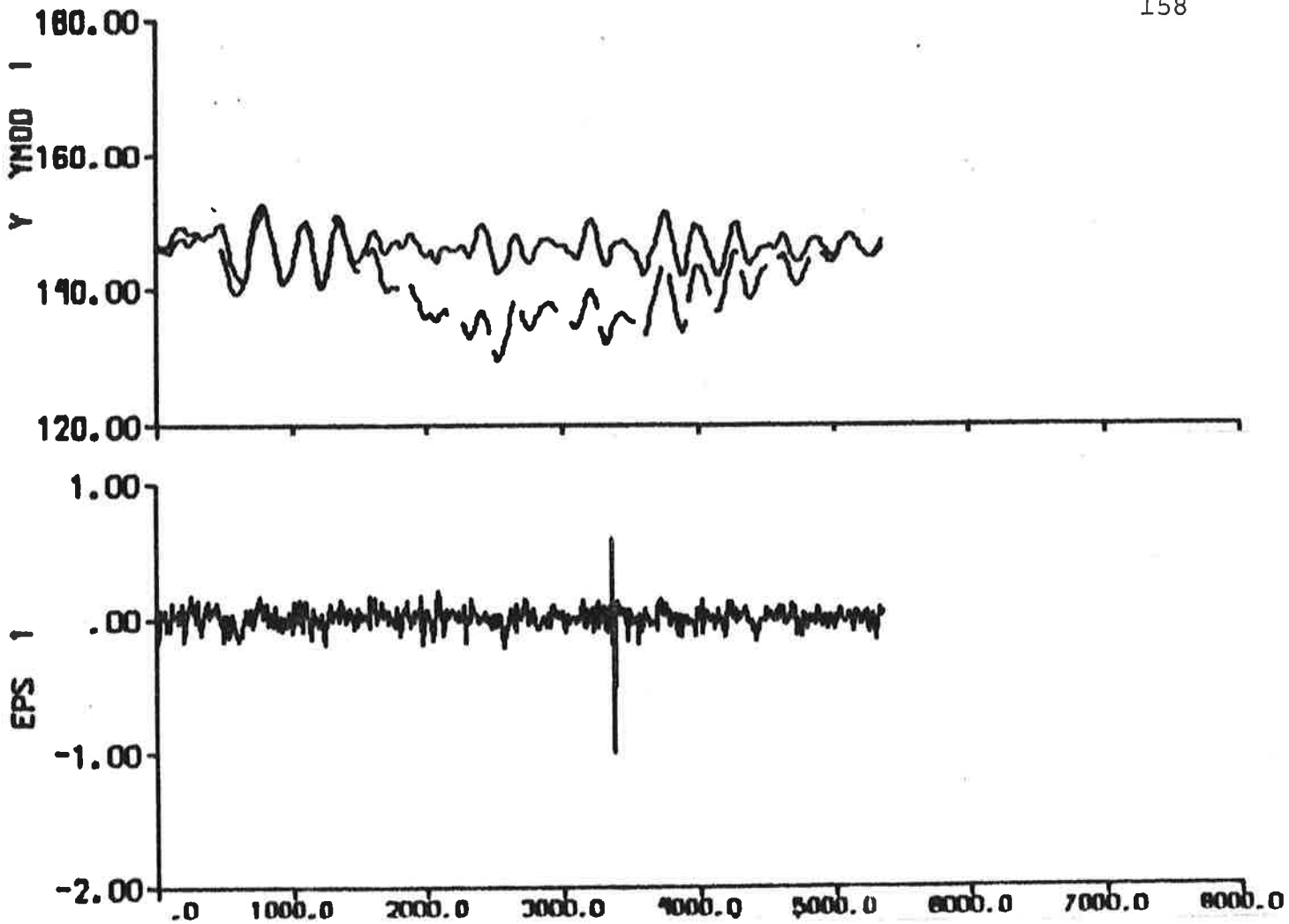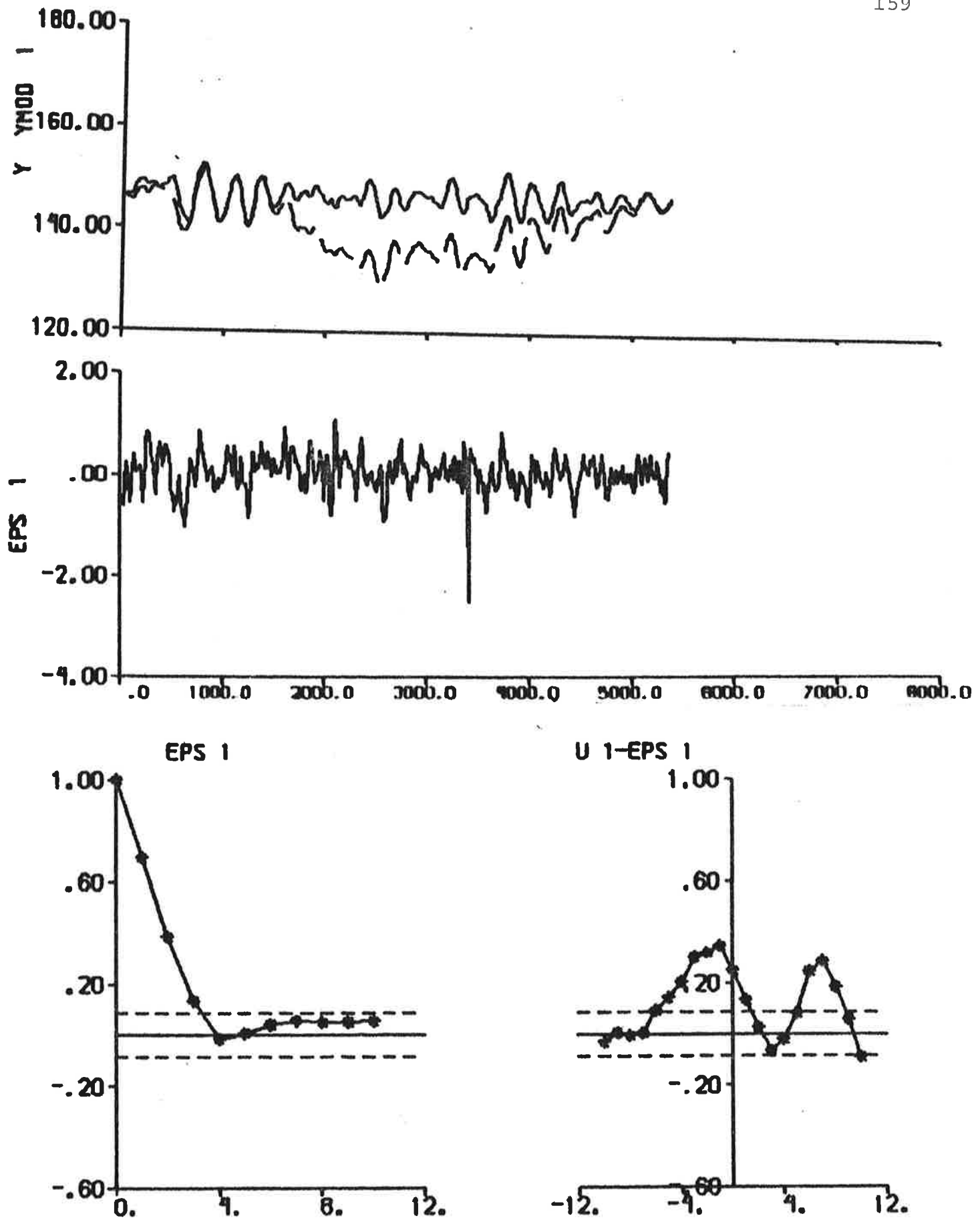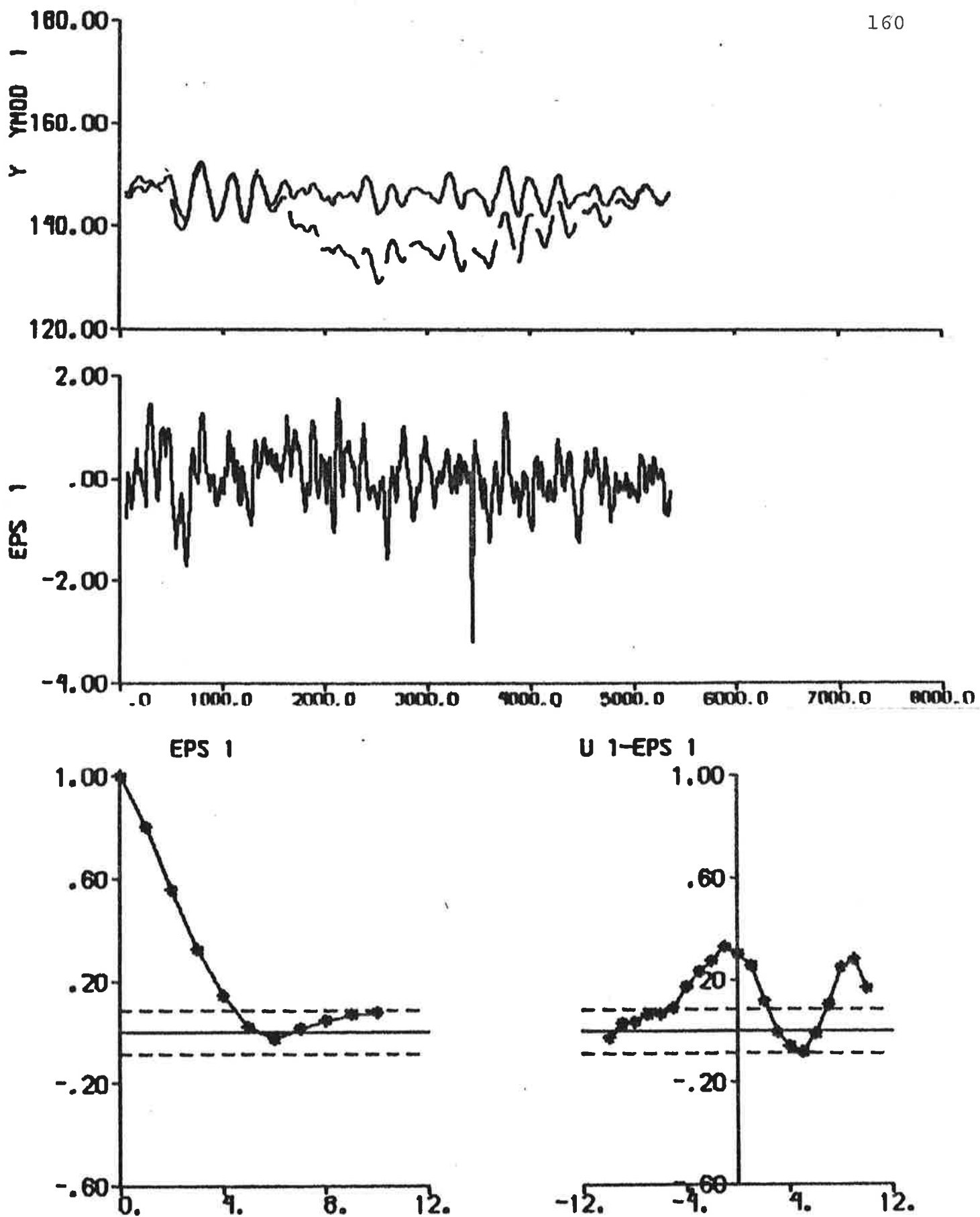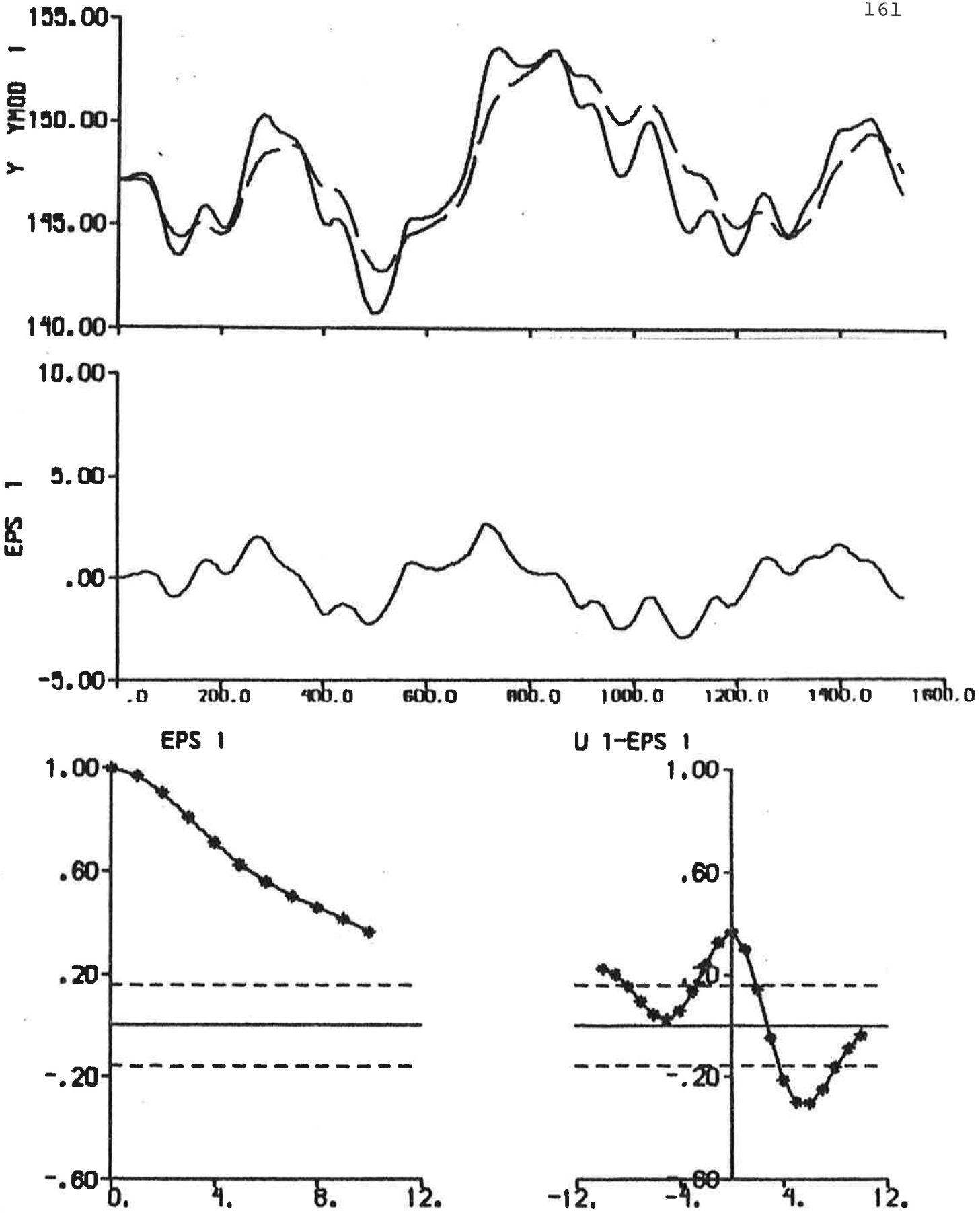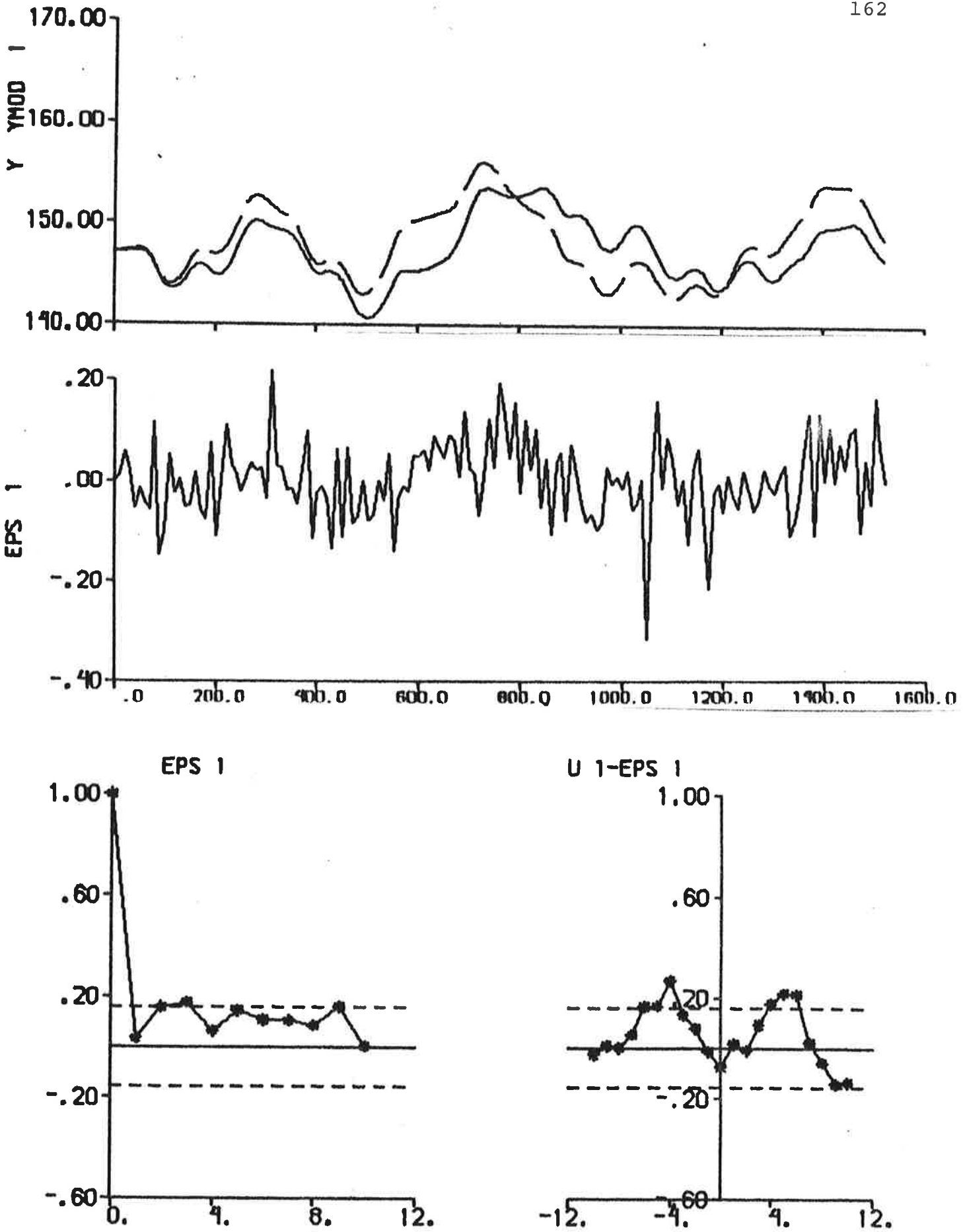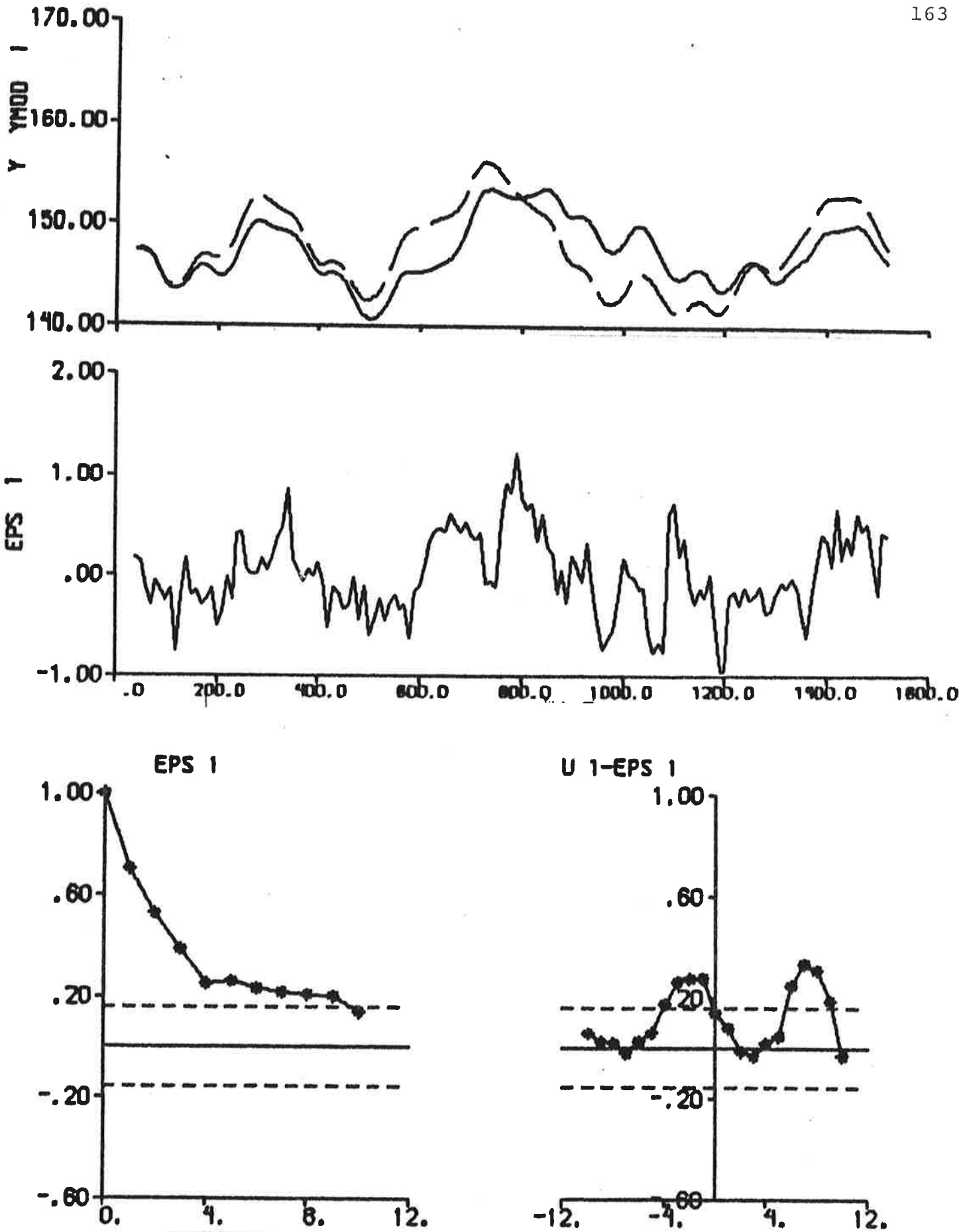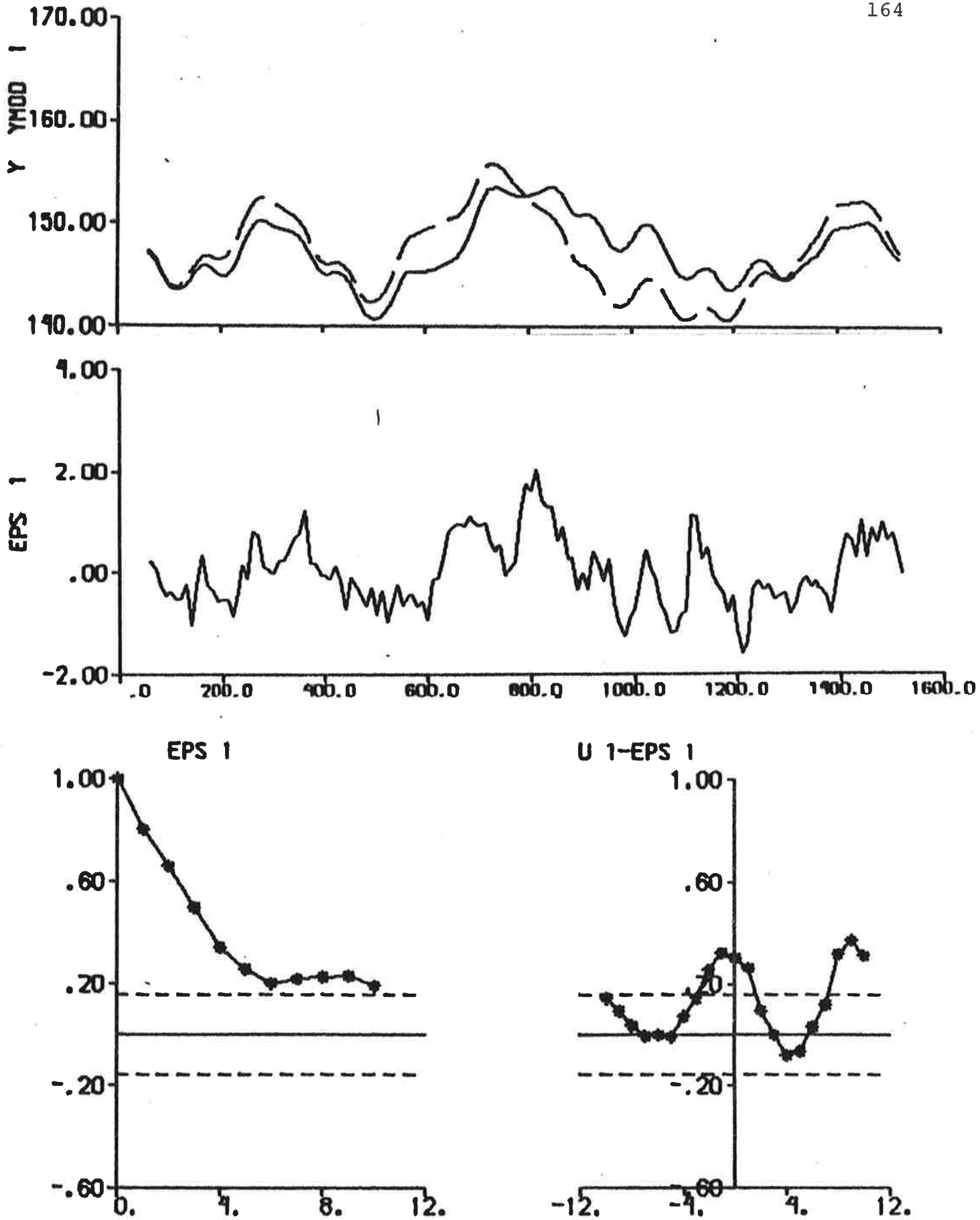Fig. 6.16 - Result of prediction error identification (p = 6)
to data from experiment E4.

$$
K = \begin{bmatrix} 4.8 \cdot 10^{-5} \\ 1.3 \cdot 10^{-3} \\ 3.3 \cdot 10^{-2} \end{bmatrix}, \quad \begin{bmatrix} 6.4 \cdot 10^{-8} \\ -2.1 \cdot 10^{-5} \\ 1.9 \cdot 10^{-2} \end{bmatrix}, \quad \begin{bmatrix} 3.8 \cdot 10^{-4} \\ 8.2 \cdot 10^{-4} \\ 2.8 \cdot 10^{-2} \end{bmatrix}, \quad \begin{bmatrix} 8.3 \cdot 10^{-10} \\ 1.3 \cdot 10^{-3} \\ 3.4 \cdot 10^{-2} \end{bmatrix} \quad (6.9)
$$

Cf. (6.4).

The results of prediction error identifications with p = 4 are
improved compared to the ML results. Reasonable models are
obtained in all cases. However, the models from experiments
E2 and E3 are stable while experiments E1 and E4 gave unstable
models. Especially the parameter values obtained from experiment
E4 are close to SSPA:s estimates. The following filter gains K
(cf. (3.4)) are obtained when p = 4:

$$
K = \begin{bmatrix} 3.3 \cdot 10^{-5} \\ 1.5 \cdot 10^{-3} \\ 3.5 \cdot 10^{-2} \end{bmatrix}, \quad \begin{bmatrix} 2.1 \cdot 10^{-8} \\ 9.0 \cdot 10^{-5} \\ 2.2 \cdot 10^{-2} \end{bmatrix}, \quad \begin{bmatrix} 9.6 \cdot 10^{-5} \\ 1.1 \cdot 10^{-3} \\ 3.1 \cdot 10^{-2} \end{bmatrix}, \quad \begin{bmatrix} 3.3 \cdot 10^{-11} \\ 1.4 \cdot 10^{-3} \\ 3.4 \cdot 10^{-2} \end{bmatrix} \quad (6.10)
$$

Cf. (6.5) and (6.9).

The results of prediction error identifications with p = 6 are
not changed much compared to the results with p = 4. A prediction
interval of approximately 40 s is thus reasonable when a third-
order transfer function is fitted to the data. The following
filter gains are obtained when p = 6:

$$
K = \begin{bmatrix} 3.0 \cdot 10^{-5} \\ 1.6 \cdot 10^{-3} \\ 3.5 \cdot 10^{-2} \end{bmatrix}, \quad \begin{bmatrix} 2.8 \cdot 10^{-10} \\ 2.1 \cdot 10^{-4} \\ 2.4 \cdot 10^{-2} \end{bmatrix}, \quad \begin{bmatrix} 8.0 \cdot 10^{-5} \\ 1.2 \cdot 10^{-3} \\ 3.3 \cdot 10^{-2} \end{bmatrix}, \quad \begin{bmatrix} 6.6 \cdot 10^{-12} \\ 1.4 \cdot 10^{-3} \\ 3.4 \cdot 10^{-2} \end{bmatrix} \quad (6.11)
$$

The experiments have also been analysed using the rudder angle
instead of the rudder command as input signal. The parameter
values obtained by fitting Nomoto´s model (3.13) and the transfer
function (3.12) to data from the 4 experiments by use of the
output error method and the prediction error method with p = 6
are summarized in Table 6.3. The plots are shown in Figs. 6.33 -
6.48.

There is no significant difference between the results obtained
by using the rudder angle instead of the rudder command, when

Table 6.2 – Parameter values from identifications of the transfer function (3.12)

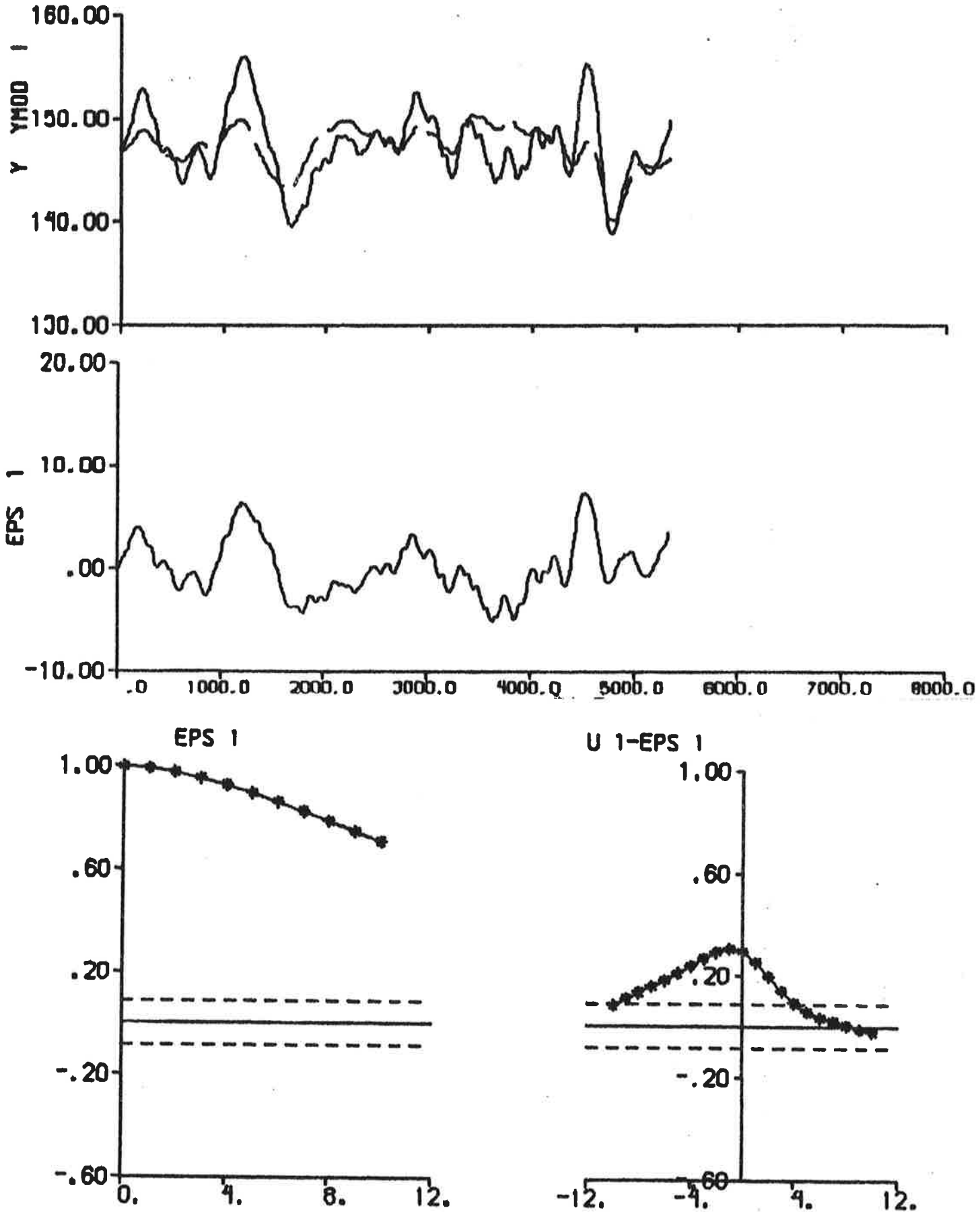|	SSPA:s model	E1				E2				E3				E4			
		Output error	ML	Pred. error p=4	Pred. error p=6	Output error	ML	Pred. error p=4	Pred. error p=6	Output error	ML	Pred.error p=4	Pred.error p=6	Output error	ML	Pred.error p=4	Pred.error p=6
Figure		6.17	6.18	6.19	6.20	6.21	6.22	6.23	6.24	6.25	6.26	6.27	6.28	6.29	6.30	6.31	6.32
ν		7	9	9	9	7	9	9	9	7	9	9	9	7	9	9	9
V		7.36	$3.9 \cdot 10^{3}$	$5.9 \cdot 10^{2}$	0.14	0.42	$5.1 \cdot 10^{2}$	0.17	0.28	1.62	$7.6 \cdot 10^{3}$	$8.4 \cdot 10^{2}$	0.20	0.20	$5.0 \cdot 10^{3}$	$5.6 \cdot 10^{2}$	0.11
AIC		2600	-1431	–	–	235	3	–	–	1797	-1078	–	–	202	-358	–	–
φ_1	2.14	1.26	3.70	2.51	2.32	8.60	40.96	13.50	10.05	37.31	19.83	6.22	5.06	1.49	2.27	2.05	2.04
φ_2	-0.48	0.25	0.26	-0.01	-0.04	0.78	2.63	0.69	0.51	127.26	9.83	1.07	0.60	-0.24	-0.17	-0.22	-0.23
φ_4	-1.01	-0.23	-1.40	-1.36	-1.34	-2.31	-11.57	-4.69	-3.66	41.23	-2.58	-1.93	-1.80	-1.09	-1.23	-1.24	-1.25
φ_5	-0.76	-0.38	-2.38	-1.47	-1.34	-5.15	-24.50	-7.90	-5.84	-24.57	-16.17	-4.01	-3.09	-0.74	-1.15	-1.00	-0.99
$\varphi_6\ [s^{-3}]$		$1.2 \cdot 10^{-8}$	$8.3 \cdot 10^{-8}$	$5.1 \cdot 10^{-8}$	$4.7 \cdot 10^{-8}$	$2.4 \cdot 10^{-7}$	$1.2 \cdot 10^{-6}$	$3.8 \cdot 10^{-7}$	$2.8 \cdot 10^{-7}$	$1.2 \cdot 10^{-6}$	$8.1 \cdot 10^{-7}$	$2.0 \cdot 10^{-7}$	$1.5 \cdot 10^{-7}$	$3.3 \cdot 10^{-8}$	$5.1 \cdot 10^{-8}$	$4.4 \cdot 10^{-8}$	$4.3 \cdot 10^{-8}$
$\varphi_7\ [s^{-2}]$		$2.2 \cdot 10^{-4}$	$2.3 \cdot 10^{-4}$	$6.0 \cdot 10^{-6}$	$-3.7 \cdot 10^{-5}$	$6.5 \cdot 10^{-4}$	$2.1 \cdot 10^{-3}$	$5.5 \cdot 10^{-4}$	$4.1 \cdot 10^{-4}$	0.11	$8.5 \cdot 10^{-3}$	$9.2 \cdot 10^{-4}$	$5.2 \cdot 10^{-4}$	$-2.1 \cdot 10^{-4}$	$-1.5 \cdot 10^{-4}$	$-1.9 \cdot 10^{-4}$	$-2.0 \cdot 10^{-4}$
$R_1(1,1)[s^{-5}]$	–	–	$5.6 \cdot 10^{-3}$	$2.0 \cdot 10^{-3}$	$2.2 \cdot 10^{-3}$	–	$1.4 \cdot 10^{-4}$	$9.8 \cdot 10^{-4}$	0.41	–	1.5	$5.4 \cdot 10^{-2}$	0.14	–	$2.3 \cdot 10^{-5}$	$8.2 \cdot 10^{-5}$	$6.1 \cdot 10^{-5}$
$R_1(2,2)[s^{-3}]$	–	–	18.8	13.0	15.7	–	2981.1	$1.2 \cdot 10^{6}$	$3.0 \cdot 10^{8}$	–	349.3	60.5	193.1	–	$3.7 \cdot 10^{6}$	$1.1 \cdot 10^{6}$	$5.3 \cdot 10^{6}$
$T_D\ [s]$	10.0	10.0	8.1	7.5	7.1	10.0	10.0	10.0	10.0	0.0	10.0	10.0	9.9	6.0	9.1	9.1	9.1
K'	1.59	-1.50	-9.26	244.15	33.81	-6.57	-9.33	-11.39	-11.56	-0.19	-1.65	-3.75	-5.15	3.02	6.77	4.52	4.23
K_1'	-1.00	-0.23	-1.38	-1.35	-1.34	-2.27	-14.08	-4.95	-3.68	40.92	-2.68	-1.87	-1.81	-1.08	-1.22	-1.26	-1.24
T_1'	-4.88	4.02	14.13	-416.41	-58.67	10.85	15.57	19.40	19.78	0.26	1.97	5.65	8.24	-6.71	-13.81	-9.77	-9.21
T_2'	0.43	0.99	0.28	0.40	0.43	0.12	0.02	0.07	0.10	0.03	0.05	0.17	0.20	0.61	0.43	0.46	0.47
T_3'	1.32	0.61	0.59	0.92	1.00	0.45	0.47	0.59	0.63	-1.68	0.16	0.48	0.58	1.47	1.07	1.25	1.27

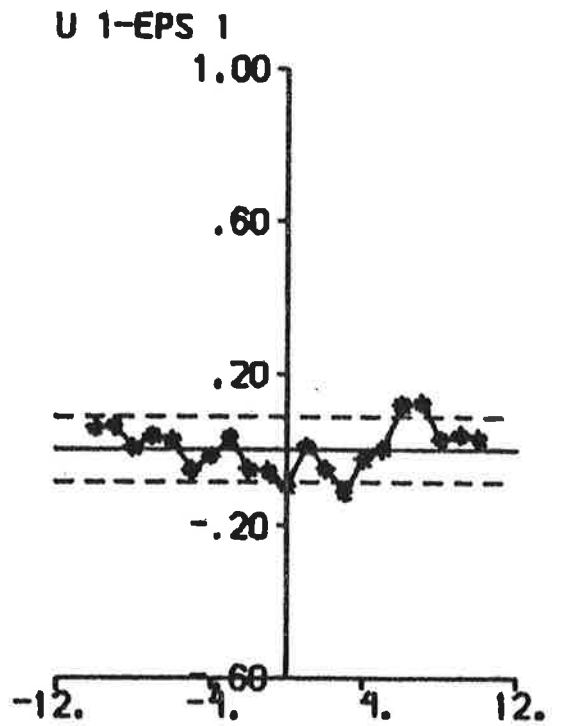Fig. 6.17 - Result of output error identification to data from experiment E1.
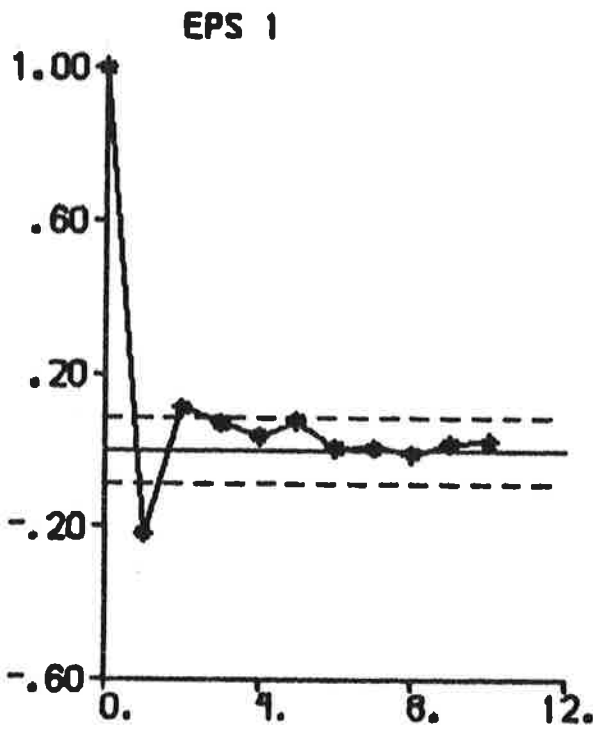
Fig. 6.18 - Result of ML identification to data
           from experiment E1.

Fig. 6.19 - Result of prediction error identification (p = 4)
to data from experiment El.

Fig. 6.20 - Result of prediction error identification (p = 6) to data from experiment E1.

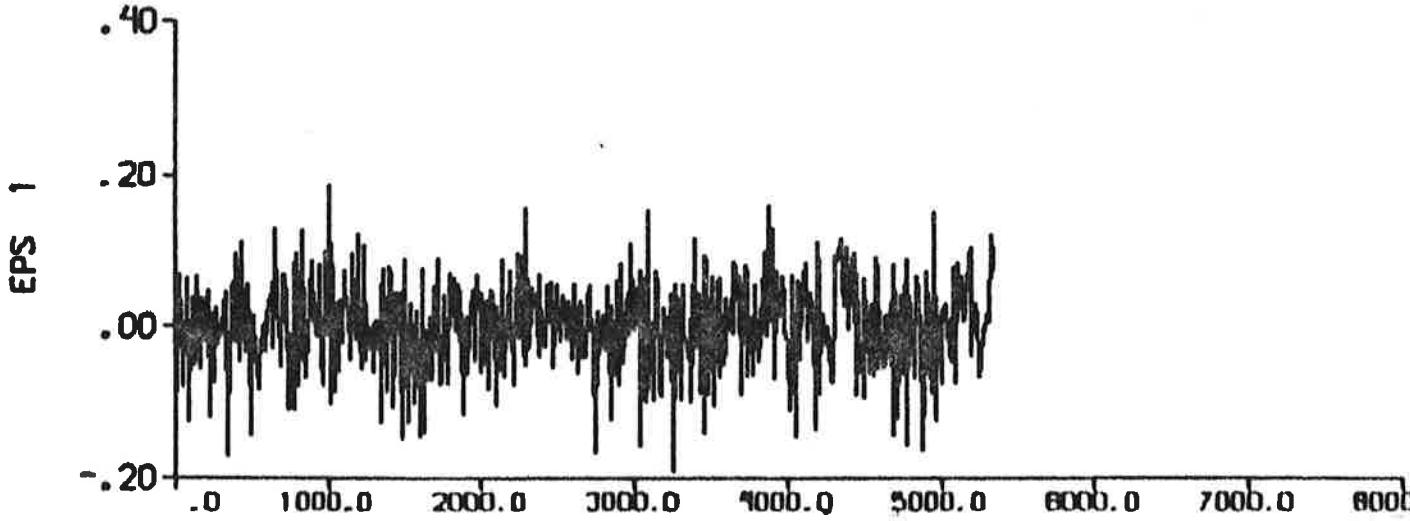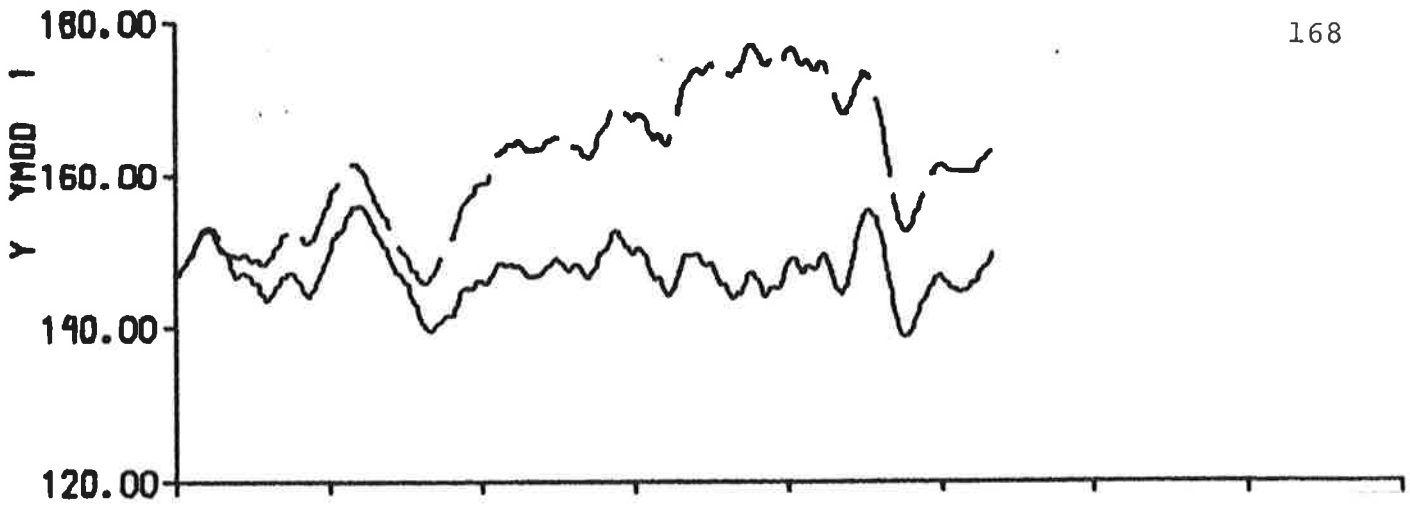Fig. 6.21 - Result of output error identification to data from experiment E2.

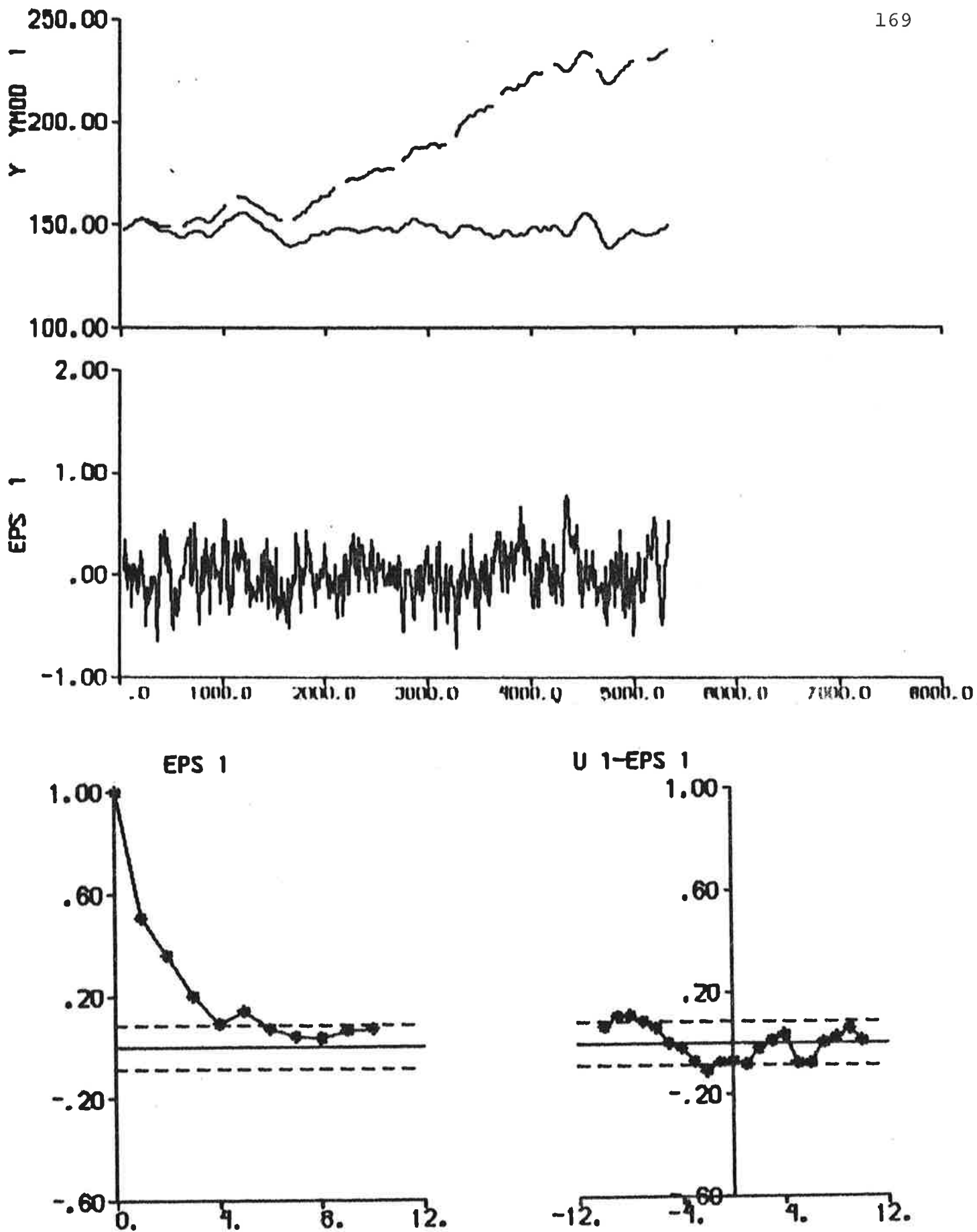Fig. 6.22 - Result of ML identification to data from experiment E2.

Fig. 6.23 - Result of prediction error identification (p = 4) to data from experiment E2.

Fig. 6.24 - Result of prediction error identification (p = 6) to data from experiment E2.

Fig. 6.25 - Result of output error identification to data from experiment E3.

Fig. 6.26 - Result of ML identification to data from experiment E3.

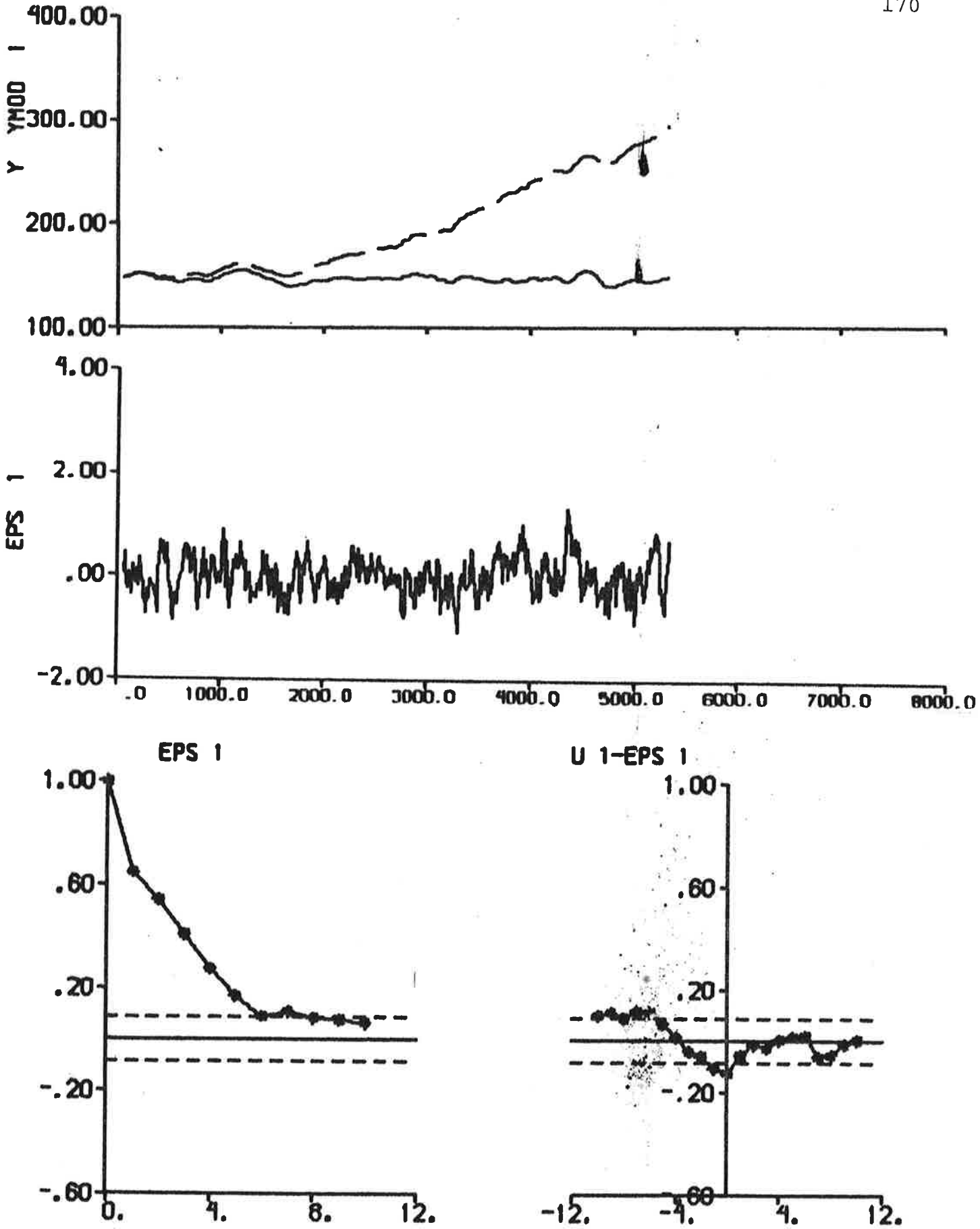Fig. 6.27 - Result of prediction error identification (p = 4) to data from experiment E3.

Fig. 6.28 - Result of prediction error identification (p = 6) to data from experiment E3.

Fig. 6.29 - Result of output error identification to data
from experiment E4.

Fig. 6.30 - Result of ML identification to data
from experiment E4.

Fig. 6.31 – Result of prediction error identification (p = 4) to data from experiment E4.

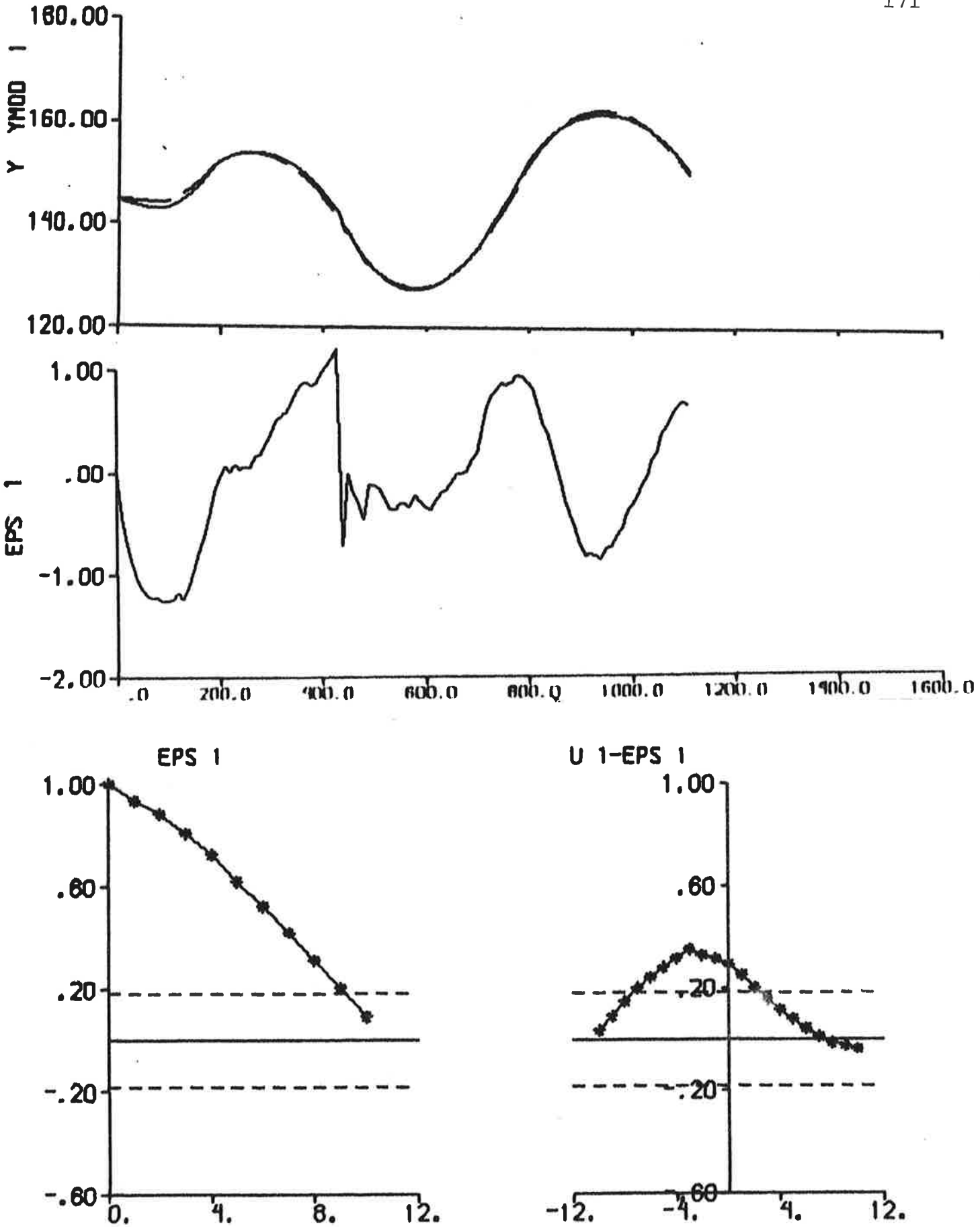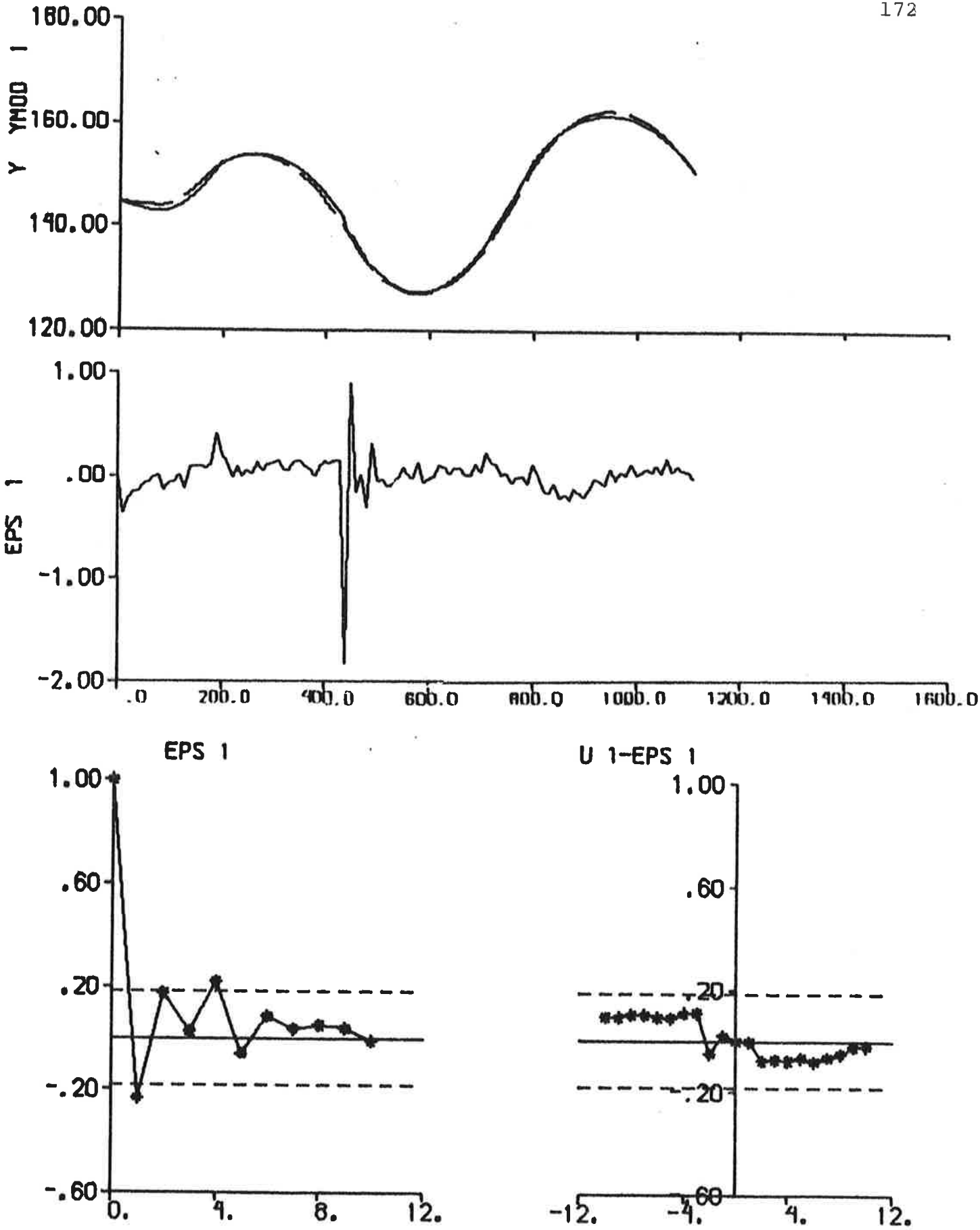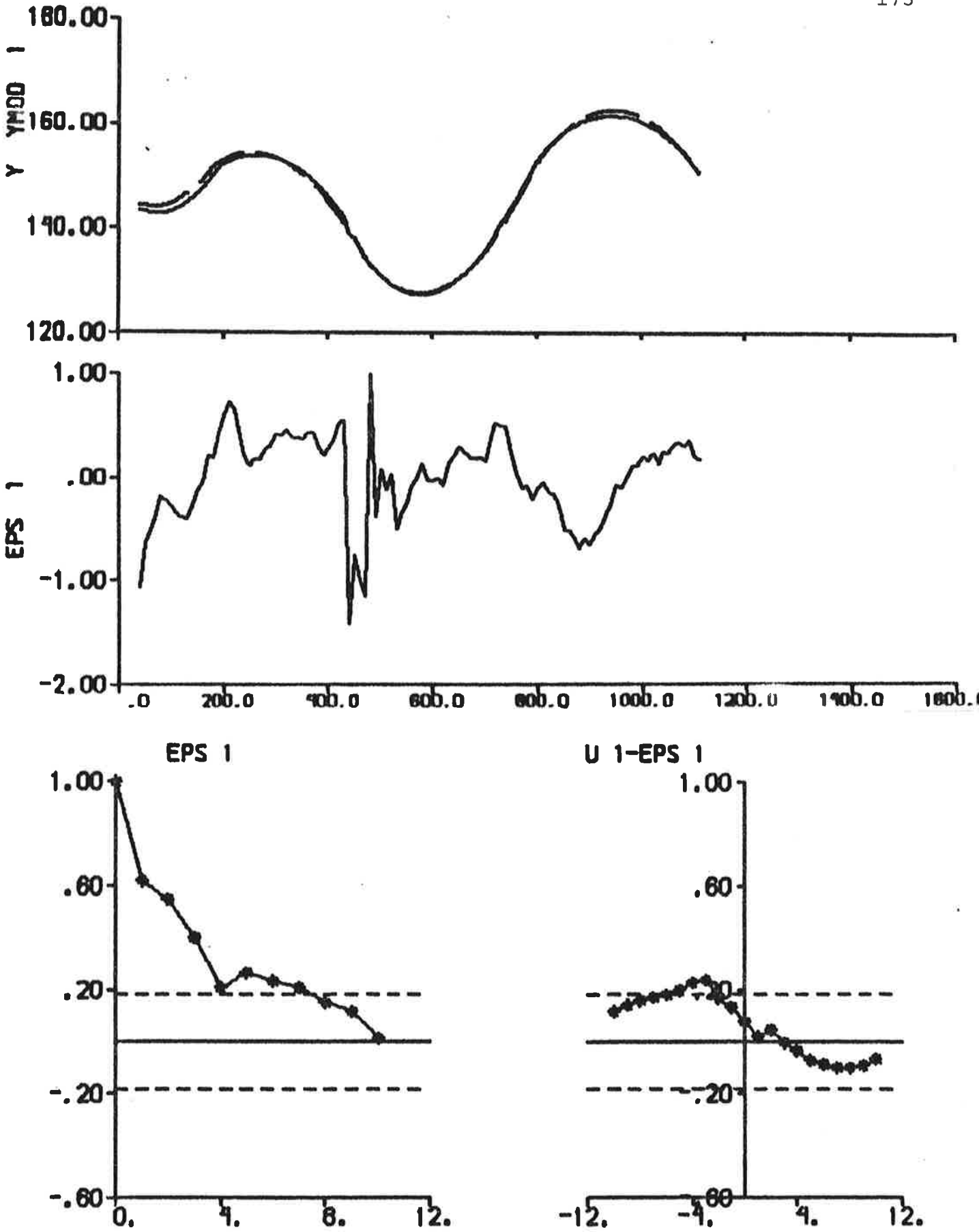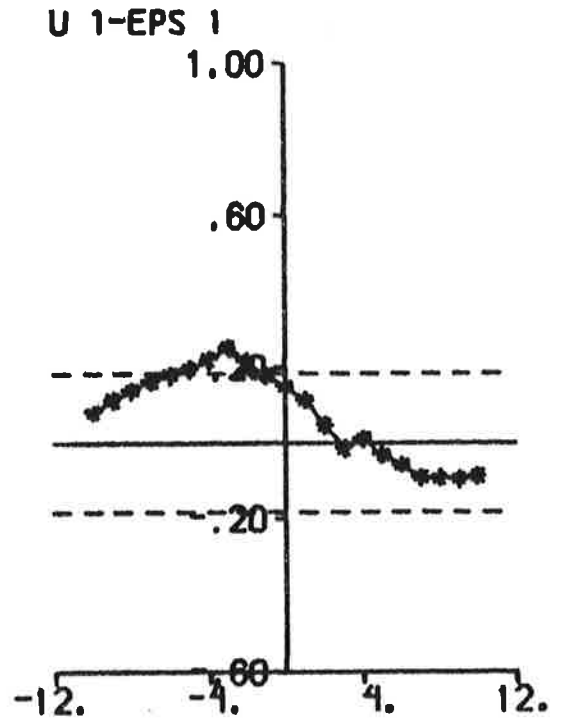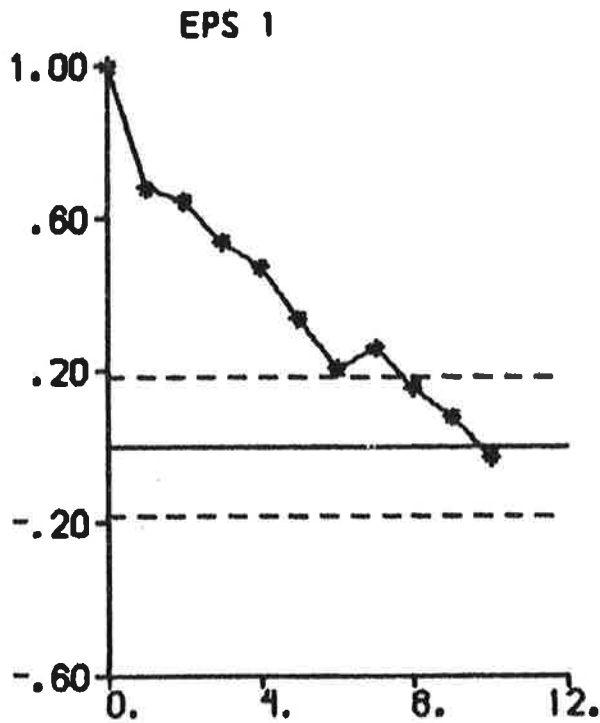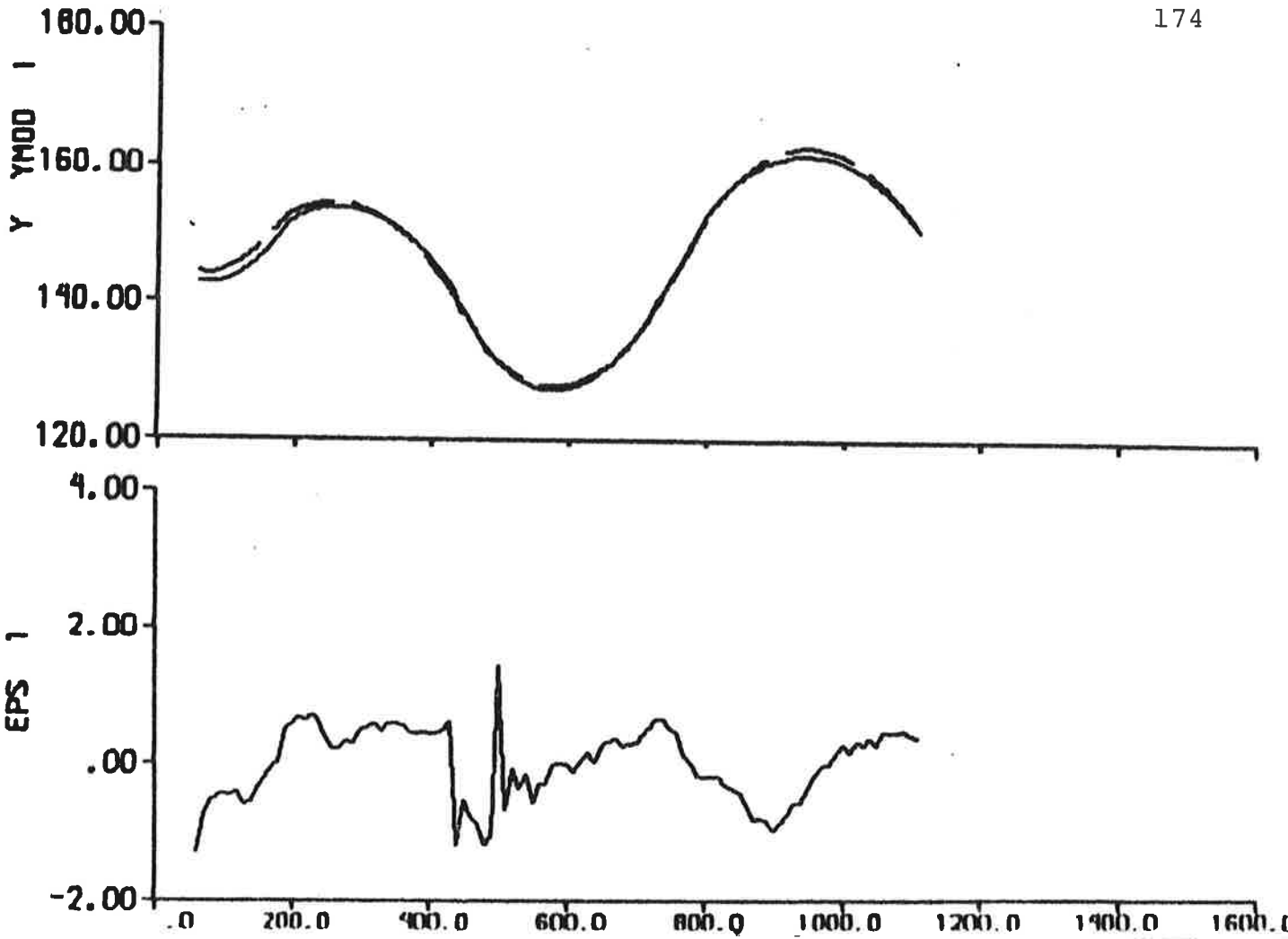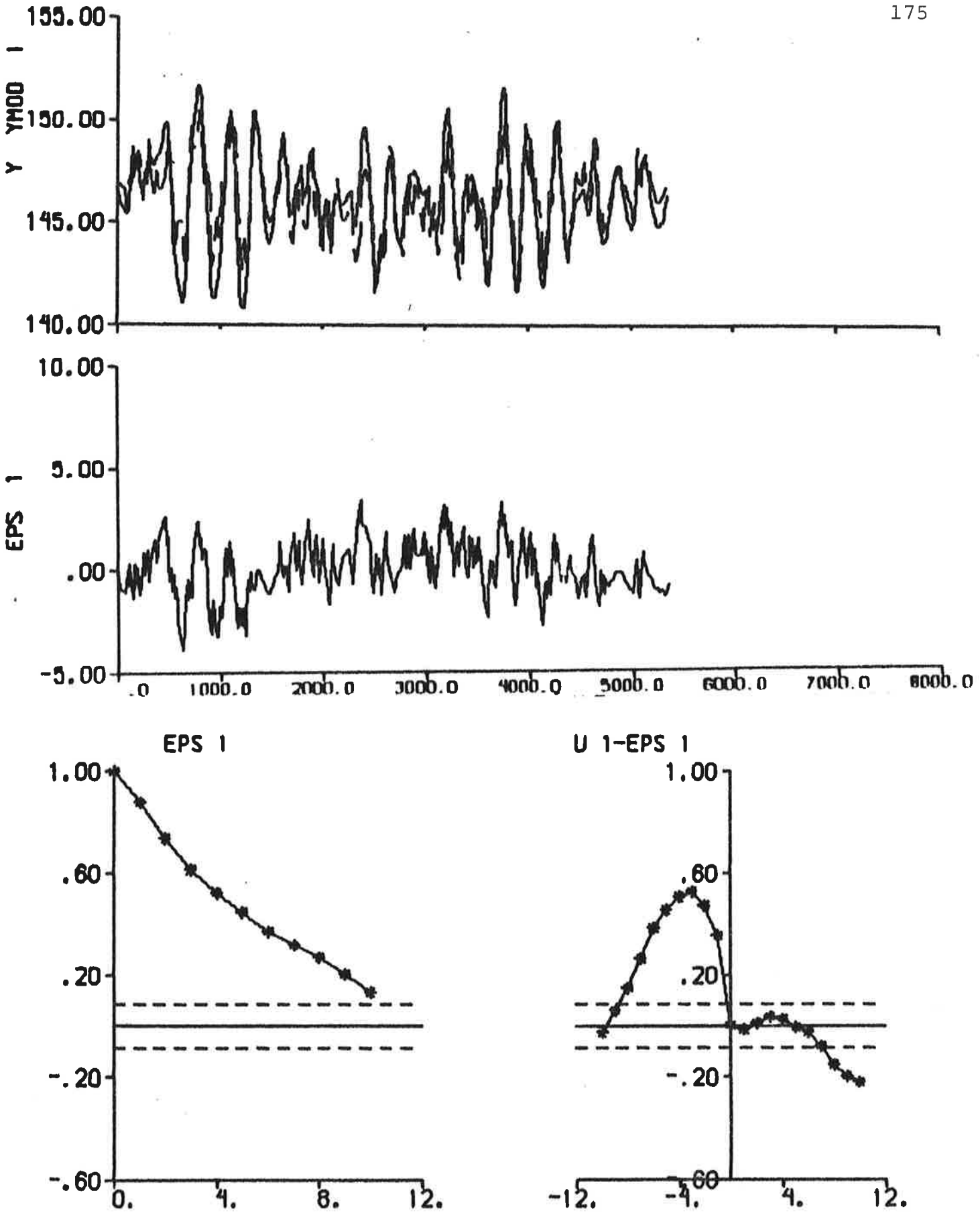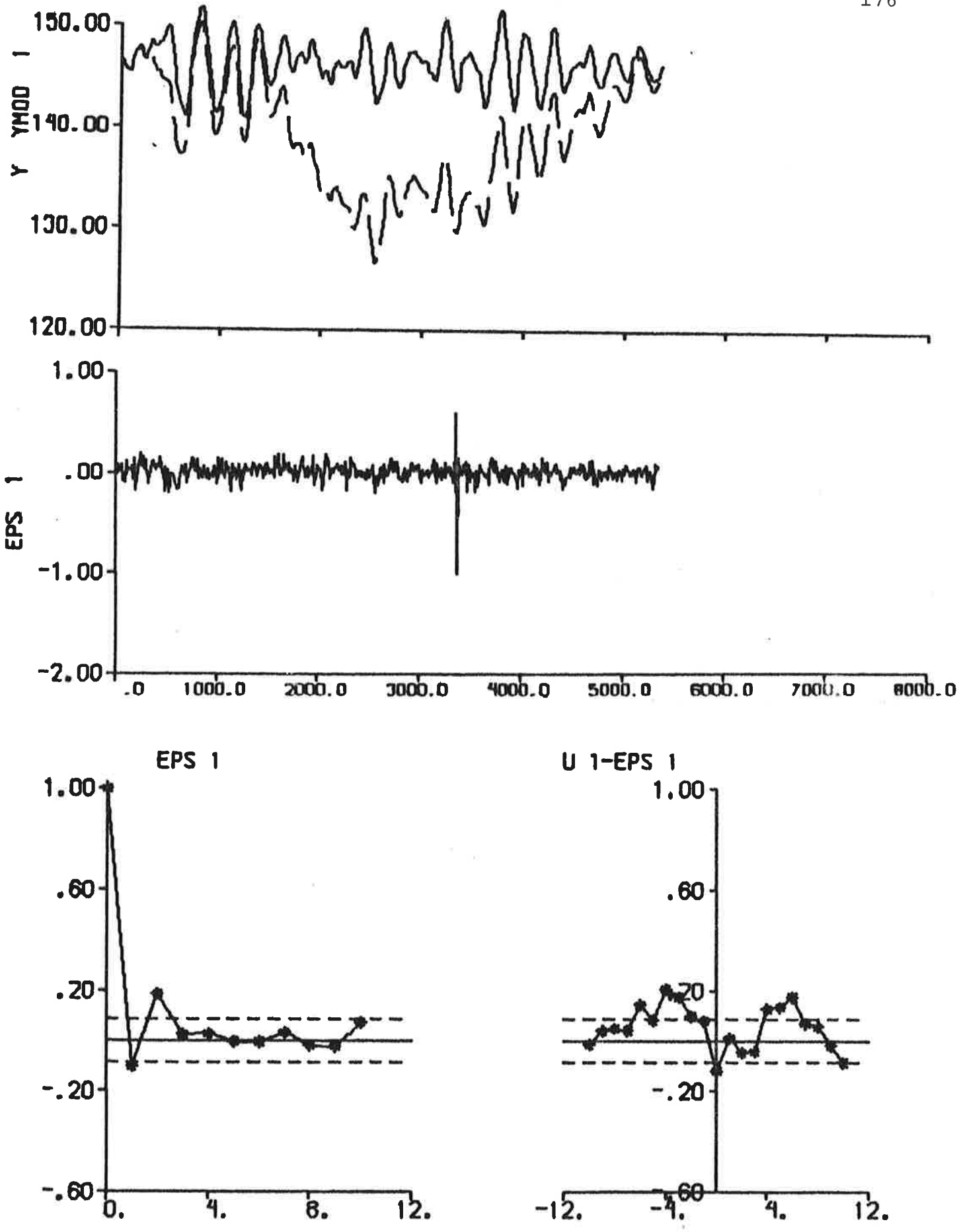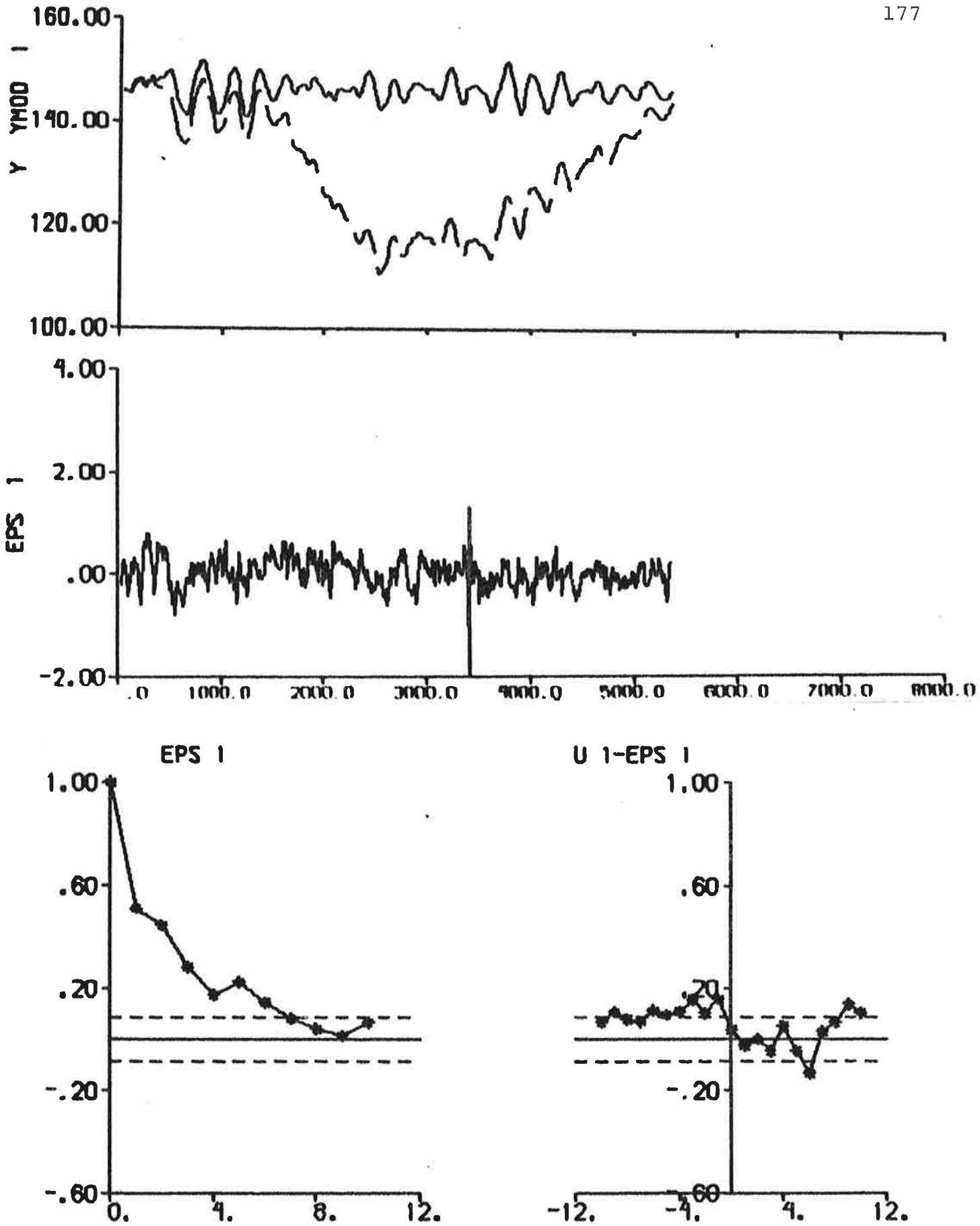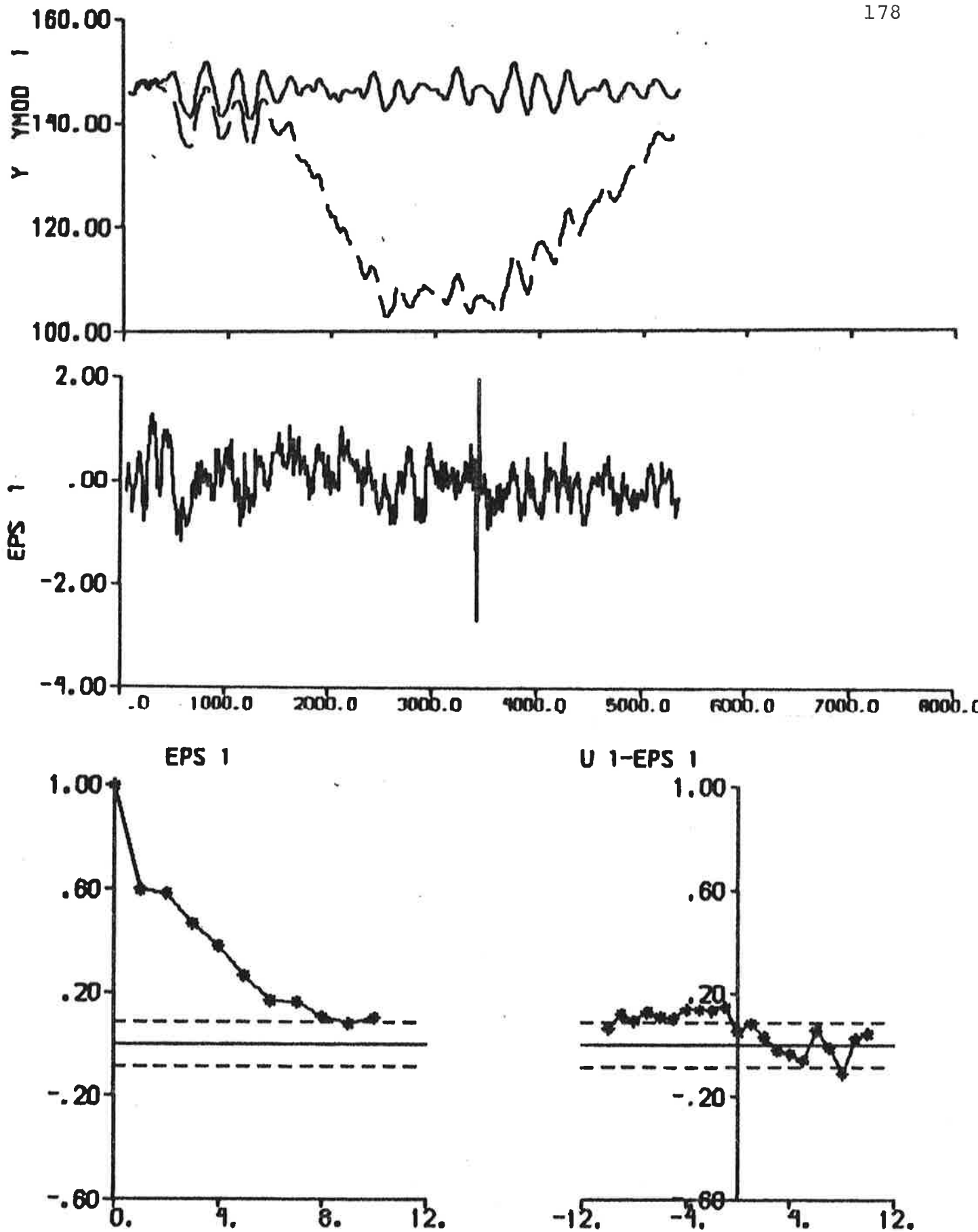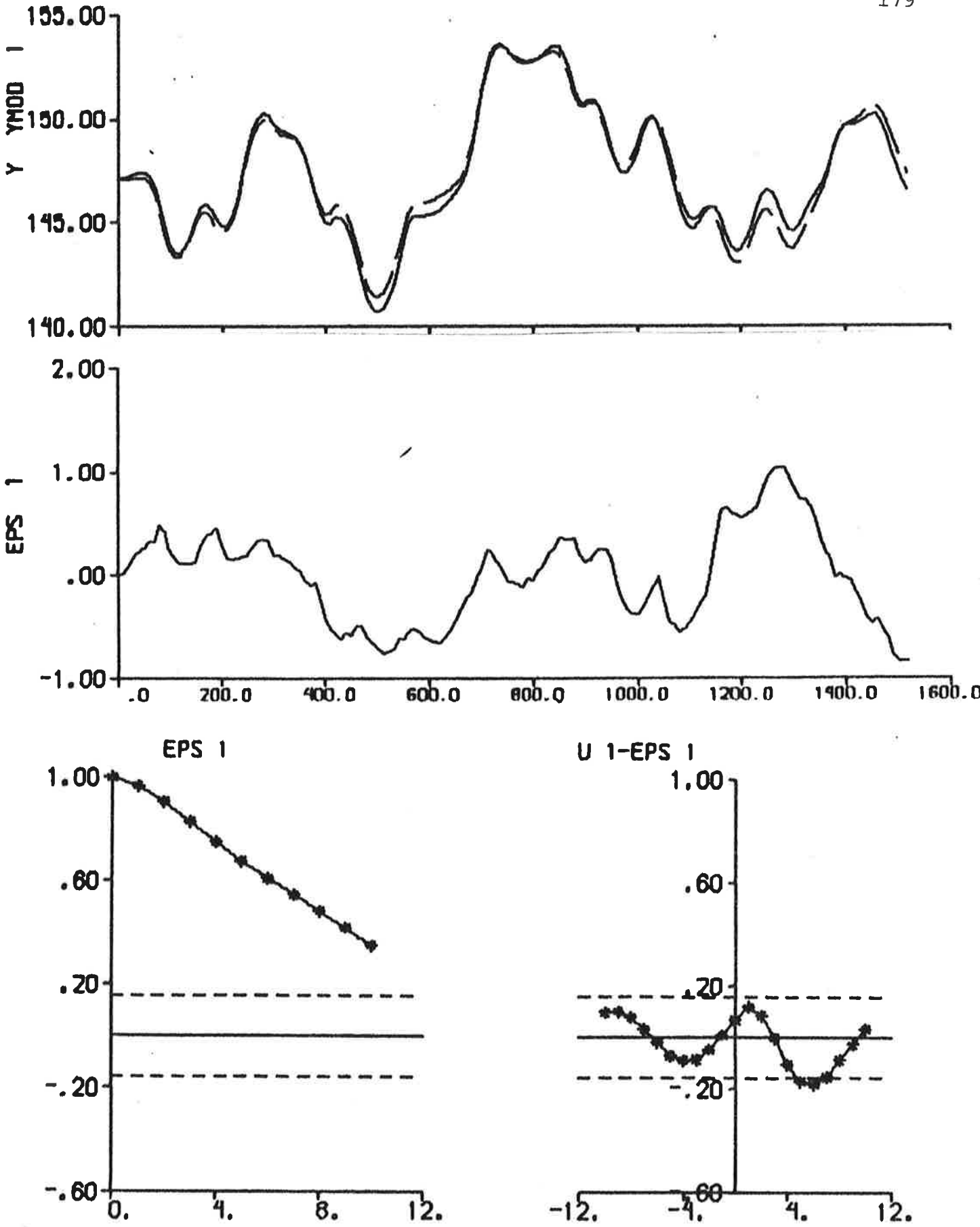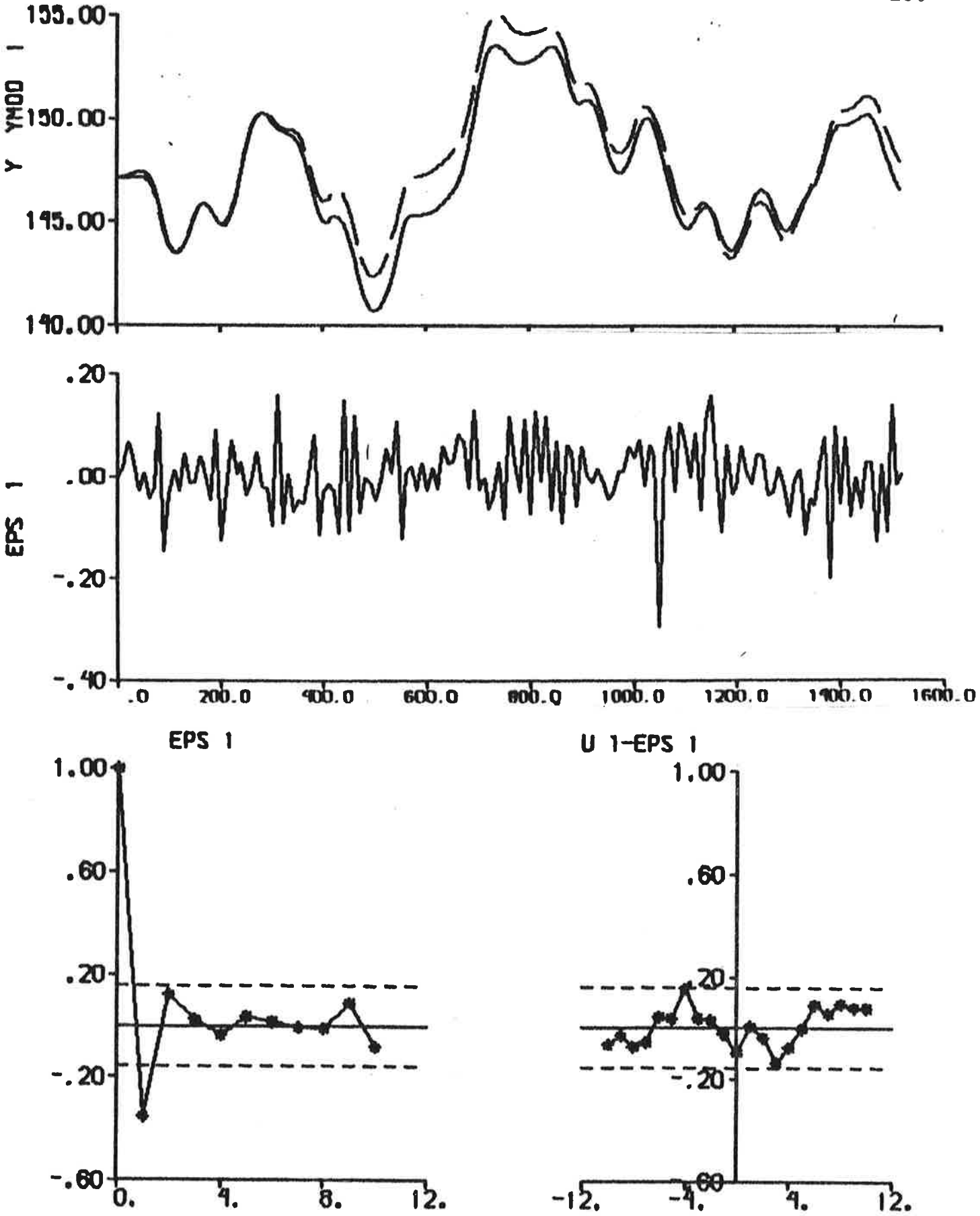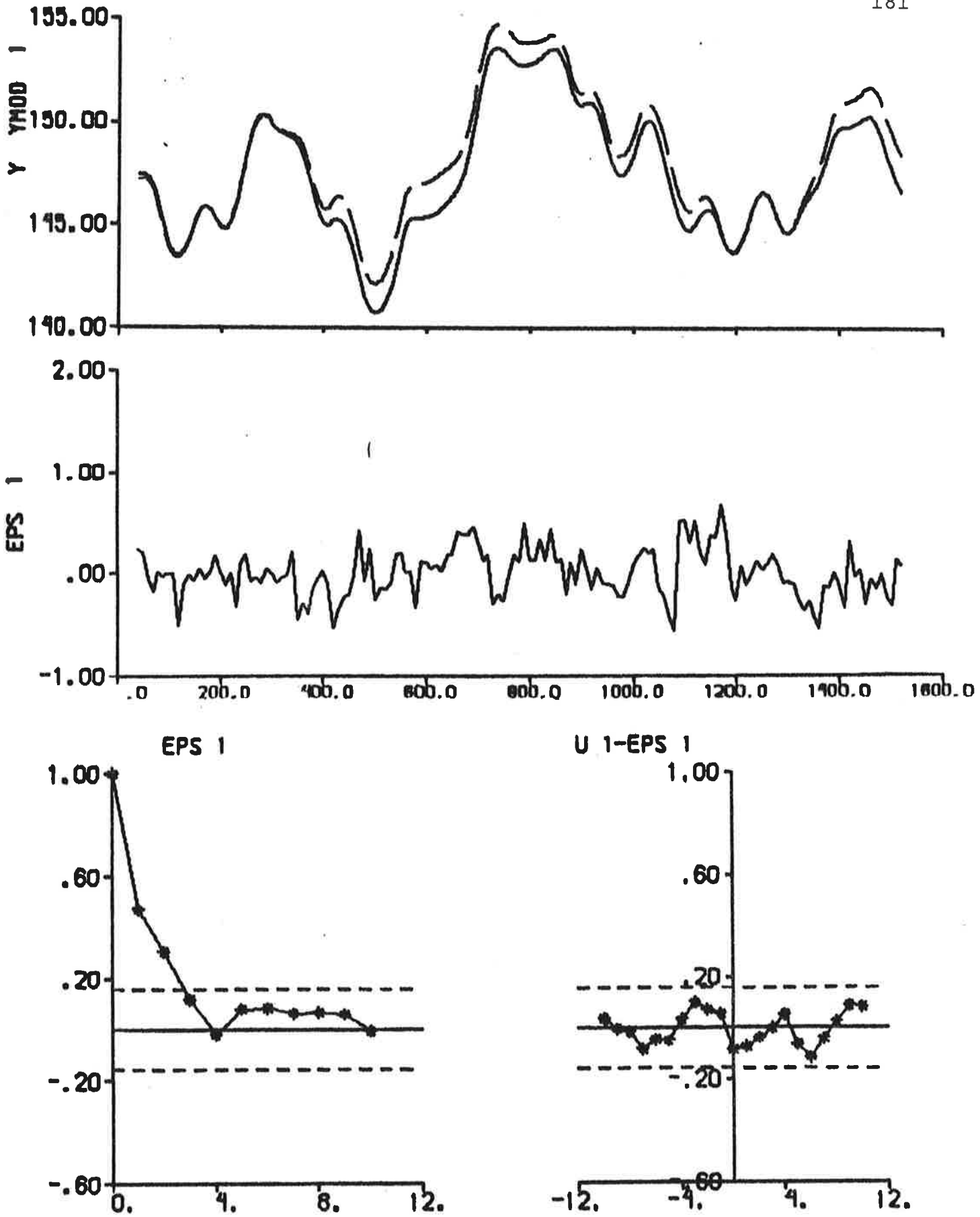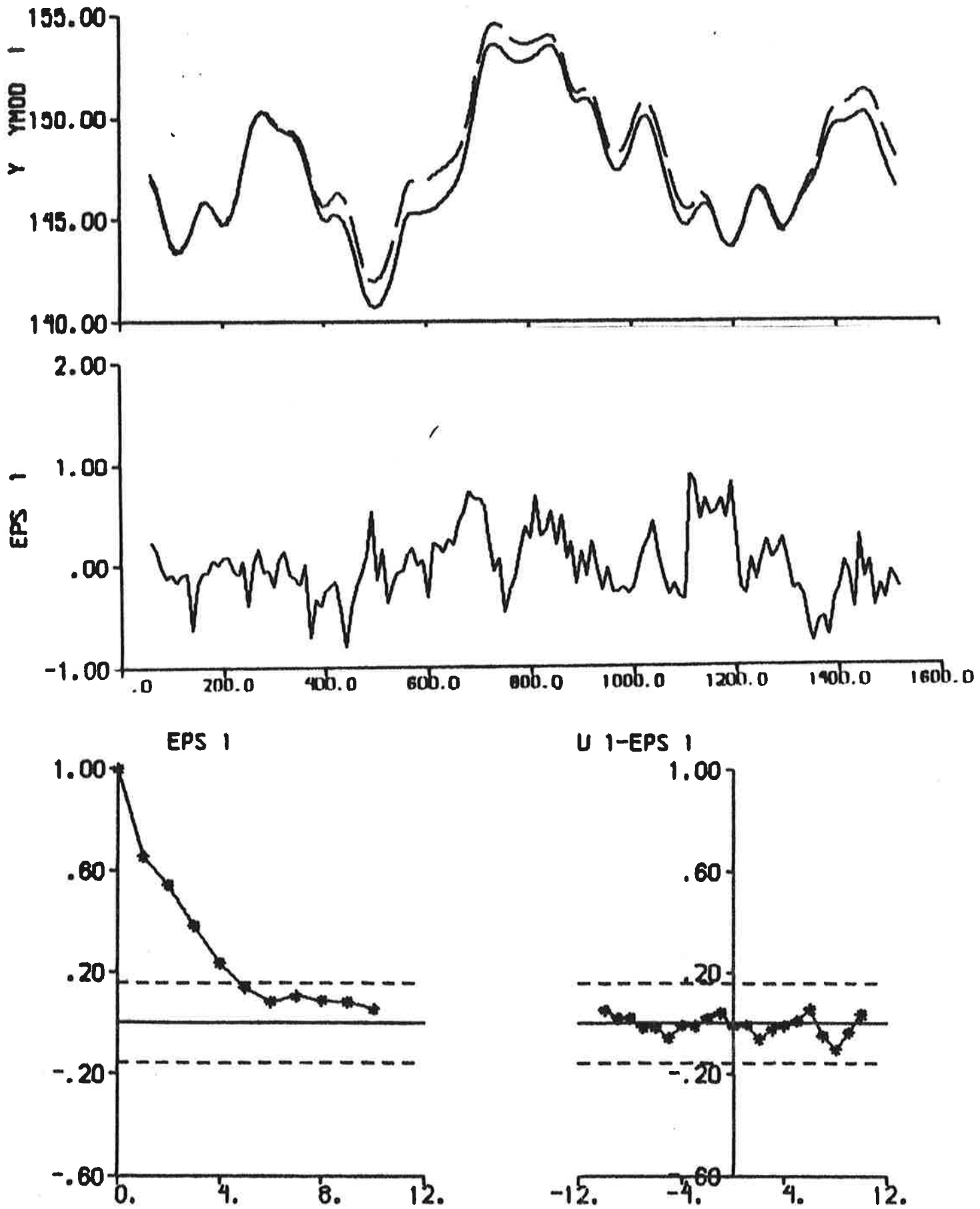Fig. 6.32 - Result of prediction error identification (p = 6) to data from experiment E4.

	E 1 — Model A, Output error	E 1 — Model A, Pred. error p=6	E 1 — Model B, Output error	E 1 — Model B, Pred. error p=6	E 2 — Model A, Output error	E 2 — Model A, Pred. error p=6	E 2 — Model B, Output error	E 2 — Model B, Pred. error p=6	E 3 — Model A, Output error	E 3 — Model A, Pred. error p=6	E 3 — Model B, Output error	E 3 — Model B, Pred. error p=6	E 4 — Model A, Output error	E 4 — Model A, Pred. error p=6	E 4 — Model B, Output error	E 4 — Model B, Pred. error p=6
Figure	6.33	6.34	6.35	6.36	6.37	6.38	6.39	6.40	6.41	6.42	6.43	6.44	6.45	6.46	6.47	6.48
ν	4	5	7	9	4	5	7	9	4	5	7	9	4	5	7	9
V	8.35	0.30	9.41	0.13	5.17	0.86	0.33	0.30	2.87	0.31	1.72	0.17	2.03	0.51	0.13	$5.7 \cdot 10^{2}$
AIC	2662	–	2732	–	510	–	208	–	2098	–	1829	–	551	–	136	–
φ_1	0.25	0.30	40.34	3.06	0.16	0.15	10.15	11.22	1.51	0.56	0.68	10.82	0.05	0.59	2.32	2.35
φ_2	0*	0*	0.25	-0.20	0*	0*	0.30	0.26	0*	0*	1.06	1.64	0*	0*	-0.28	-0.28
φ_4	-0.23	-0.86	-5.16	-1.56	-0.69	-0.67	-3.40	-3.98	-0.58	-0.89	-0.35	-3.45	-0.46	-1.06	-1.41	-1.44
φ_5 [s^{-3}]	0*	0*	-3.53	-1.70	0*	0*	-5.71	-6.36	0*	0*	-0.24	-7.03	0*	0*	-1.11	-1.10
φ_6 [s^{-2}]	$-1.5 \cdot 10^{-6}$	$-5.6 \cdot 10^{-6}$	$-4.3 \cdot 10^{-7}$	$-2.0 \cdot 10^{-7}$	$-5.2 \cdot 10^{-6}$	$-3.7 \cdot 10^{-6}$	$-6.6 \cdot 10^{-7}$	$-7.3 \cdot 10^{-7}$	$-3.5 \cdot 10^{-6}$	$-5.7 \cdot 10^{-6}$	$-2.8 \cdot 10^{-8}$	$-8.2 \cdot 10^{-7}$	$-2.8 \cdot 10^{-6}$	$-6.6 \cdot 10^{-6}$	$-1.3 \cdot 10^{-7}$	$-1.3 \cdot 10^{-7}$
φ_7 [s^{-5}]	0*	0*	$1.6 \cdot 10^{-4}$	$-1.9 \cdot 10^{-4}$	0*	0*	$1.6 \cdot 10^{-4}$	$1.1 \cdot 10^{-4}$	0*	0*	$9.3 \cdot 10^{-4}$	$1.4 \cdot 10^{-3}$	0*	0*	$-2.5 \cdot 10^{-4}$	$-2.6 \cdot 10^{-4}$
$R_1(1,1)$ [s^{-5}]	–	0	–	$7.0 \cdot 10^{-4}$	–	0*	–	3.5	–	0*	–	0.33	–	0*	–	$5.1 \cdot 10^{5}$
$R_1(2,2)$ [s^{-3}]	–	$2.0 \cdot 10^{-8}$	–	3.1	–	$5.3 \cdot 10^{-10}$	–	$2.1 \cdot 10^{8}$	–	$8.1 \cdot 10^{-9}$	–	188.9	–	$1.2 \cdot 10^{-7}$	–	$7.7 \cdot 10^{6}$
T_D [s]	10.0	0.0	10.0	4.8	0.0	0.0	10.0	10.0	10.0	1.6	10.0	10.0	6.1	1.4	4.4	4.4
K'	-0.92	-2.87	-14.25	8.70	-4.31	-4.47	-18.95	-24.42	-0.38	-1.59	-0.22	-4.28	-9.20	-1.80	4.03	3.91
K_1	-0.23	-0.86	-6.39	-1.57	-0.69	-0.67	-3.38	-3.98	-0.58	-0.89	–	-3.59	-0.46	-1.06	-1.41	-1.43
T_1	4.00	3.33	162.75	-15.98	6.25	6.67	33.60	42.96	0.66	1.79	complex poles	6.49	20.00	1.69	-8.84	-8.73
T_2	–	–	0.02	0.32	–	–	0.10	0.09	–	–	0.09	0.09	–	–	0.41	0.41
T_3	–	–	1.46	0.92	–	–	0.60	0.63	–	–	1.48	0.49	–	–	1.27	1.31

* = fixed value

Table 6.3 — Parameter values from identifications of Nomoto's model (see (3.13) and (3.17), model A, and the transfer function (3.12), model B. The rudder angle is used as input signal.

Fig. 6.33 - Result of output error identification to data from experiment El. Nomoto's model is used and the rudder angle is the input signal.

Fig. 6.34 - Result of prediction error identification (p = 6)
to data from experiment El. Nomoto's model is used
and the rudder angle is the input signal.

Fig. 6.35 - Result of output error identification to data from experiment El. The transfer function (3.12) is used and the rudder angle is the input signal.

Fig. 6.36 - Result of prediction error identification (p = 6)
          to data from experiment E1. The transfer function
          (3.12) is used and the rudder angle is the input signal.

Fig. 6.37 - Result of output error identification to data from experiment E2. Nomoto´s model is used and the rudder angle is the input signal.

Fig. 6.38 - Result of prediction error identification (p = 6) to data from experiment E2. Nomoto´s model is used and the rudder angle is the input signal.

Fig. 6.39 - Result of output error identification to data
from experiment E2. The transfer function (3.12)
is used and the rudder angle is the input signal.

Fig. 6.40 - Result of prediction error identification (p = 6) to data from experiment E2. The transfer function (3.12) is used and the rudder angle is the input signal.
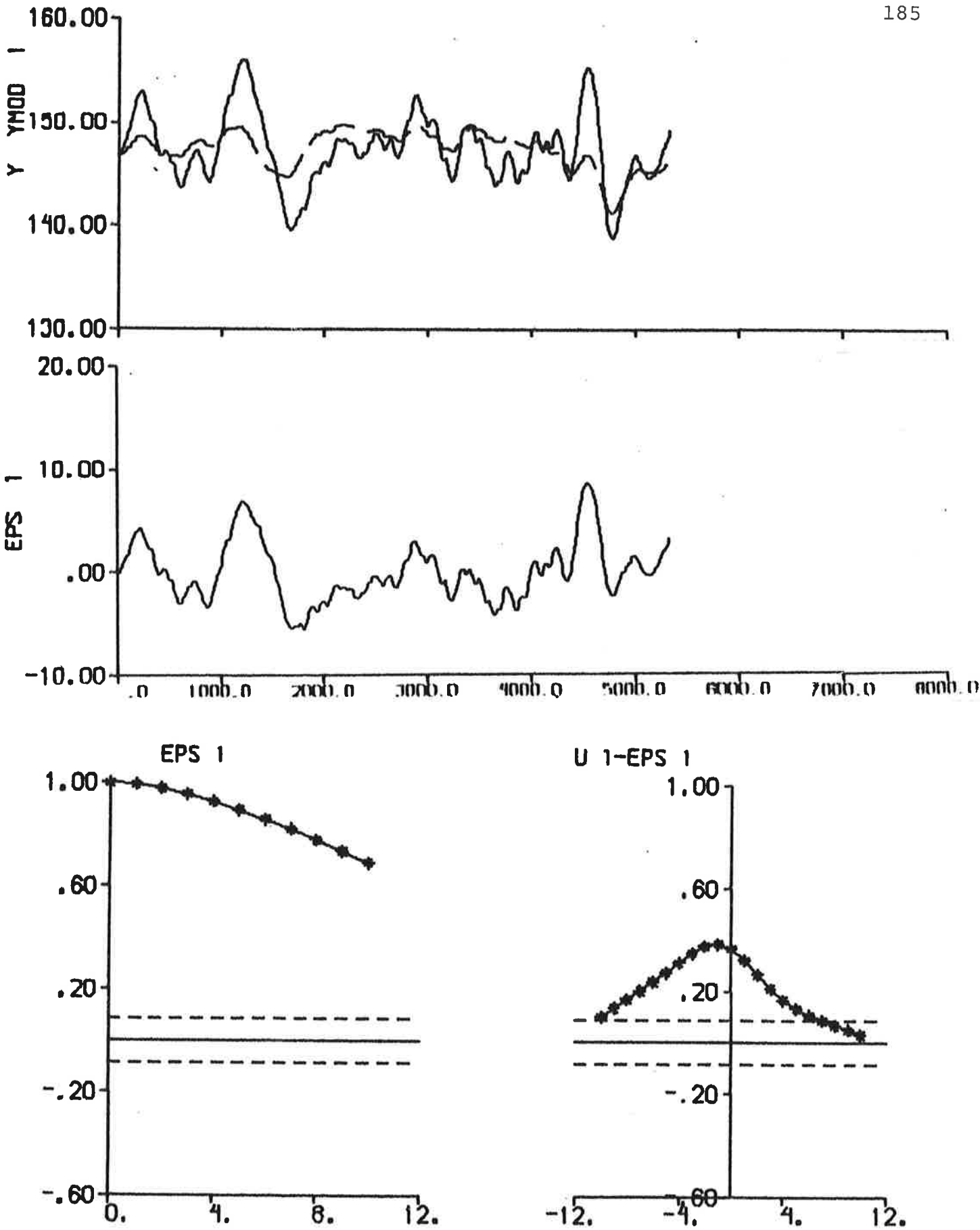
Fig. 6.41 - Result of output error identification to data
from experiment E3. Nomoto's model is used and
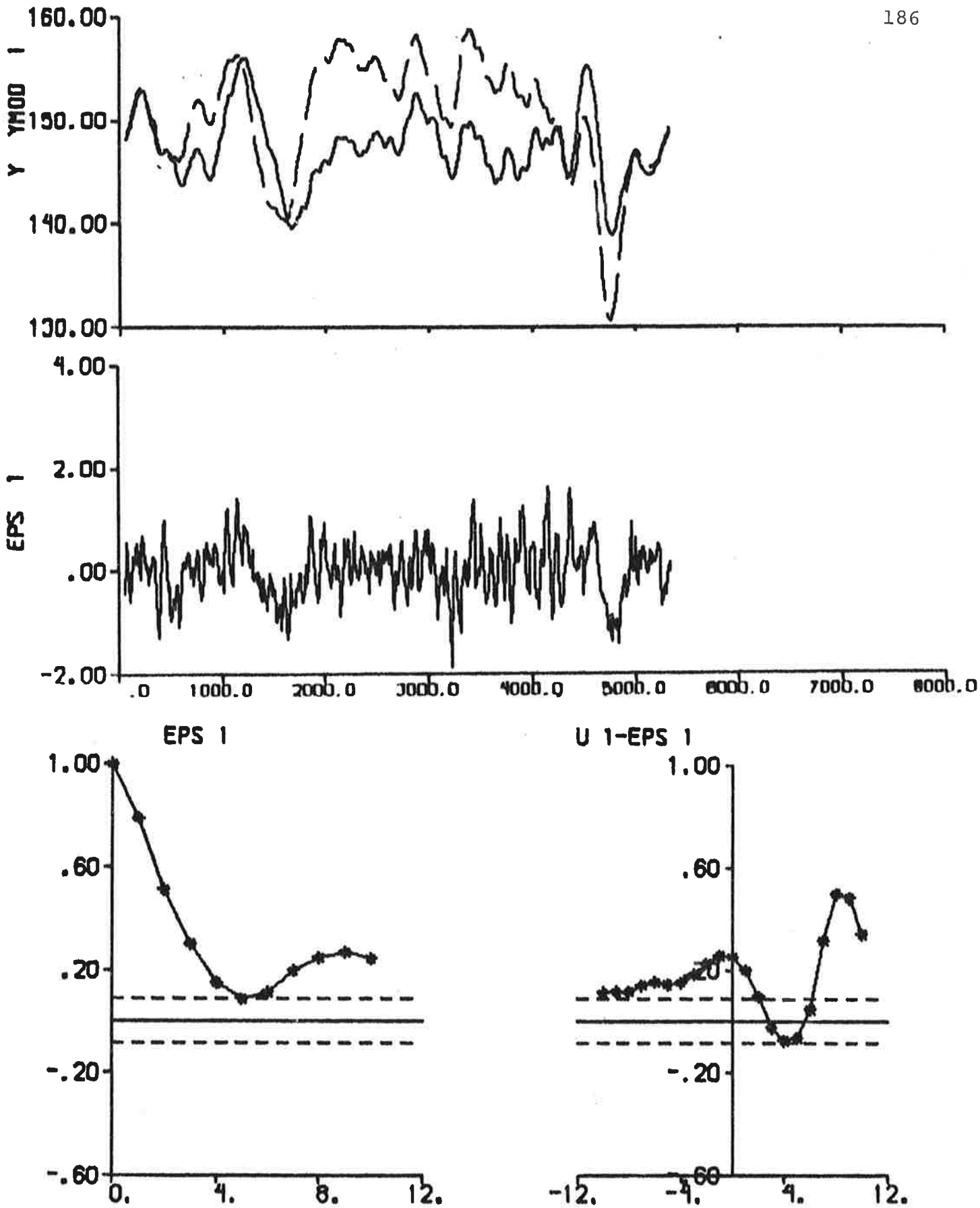the rudder angle is the input signal.
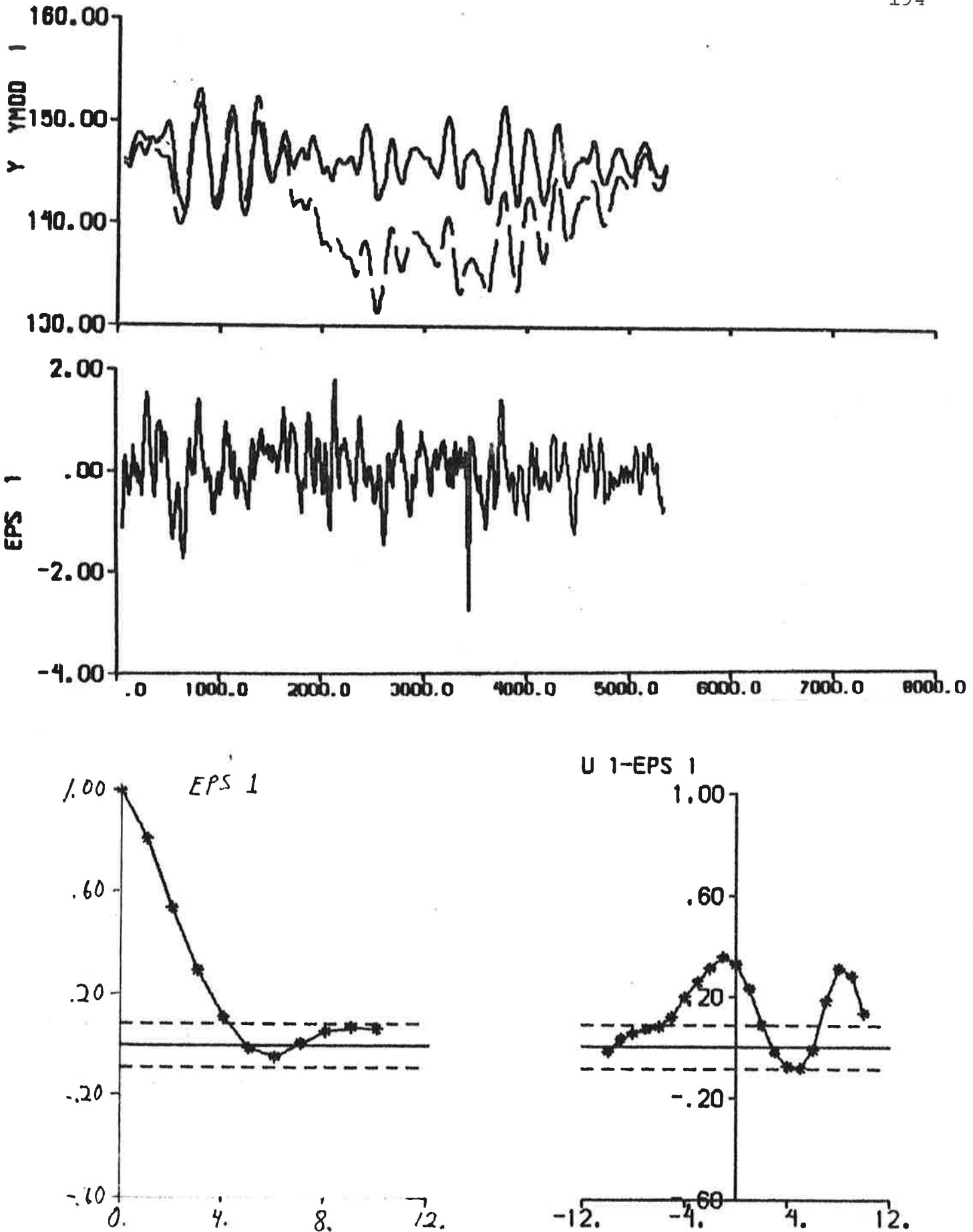
Fig. 6.42 - Result of prediction error identification (p = 6)
to data from experiment E3. Nomoto's model is used
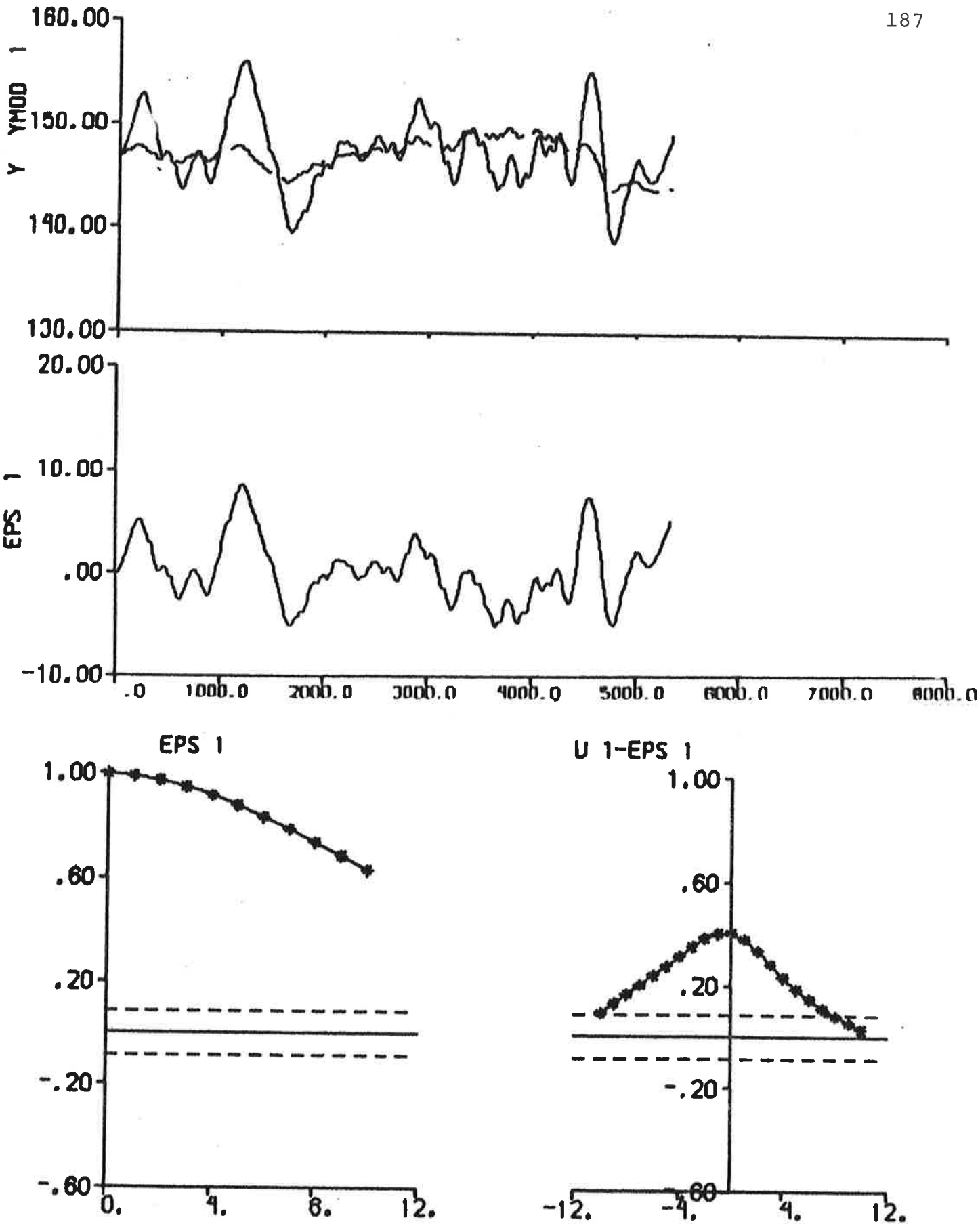and the rudder angle is the input signal.

Fig. 6.43 - Result of output error identification to data
from experiment E3. The transfer function (3.12)
is used and the rudder angle is the input signal.

Fig. 6.44 - Result of prediction error identification (p = 6)
           to data from experiment E3. The transfer function (3.12)
           is used and the rudder angle is the input signal.

Fig. 6.45 - Result of output error identification to data from experiment E4. Nomoto´s model is used and the rudder angle is the input signal.
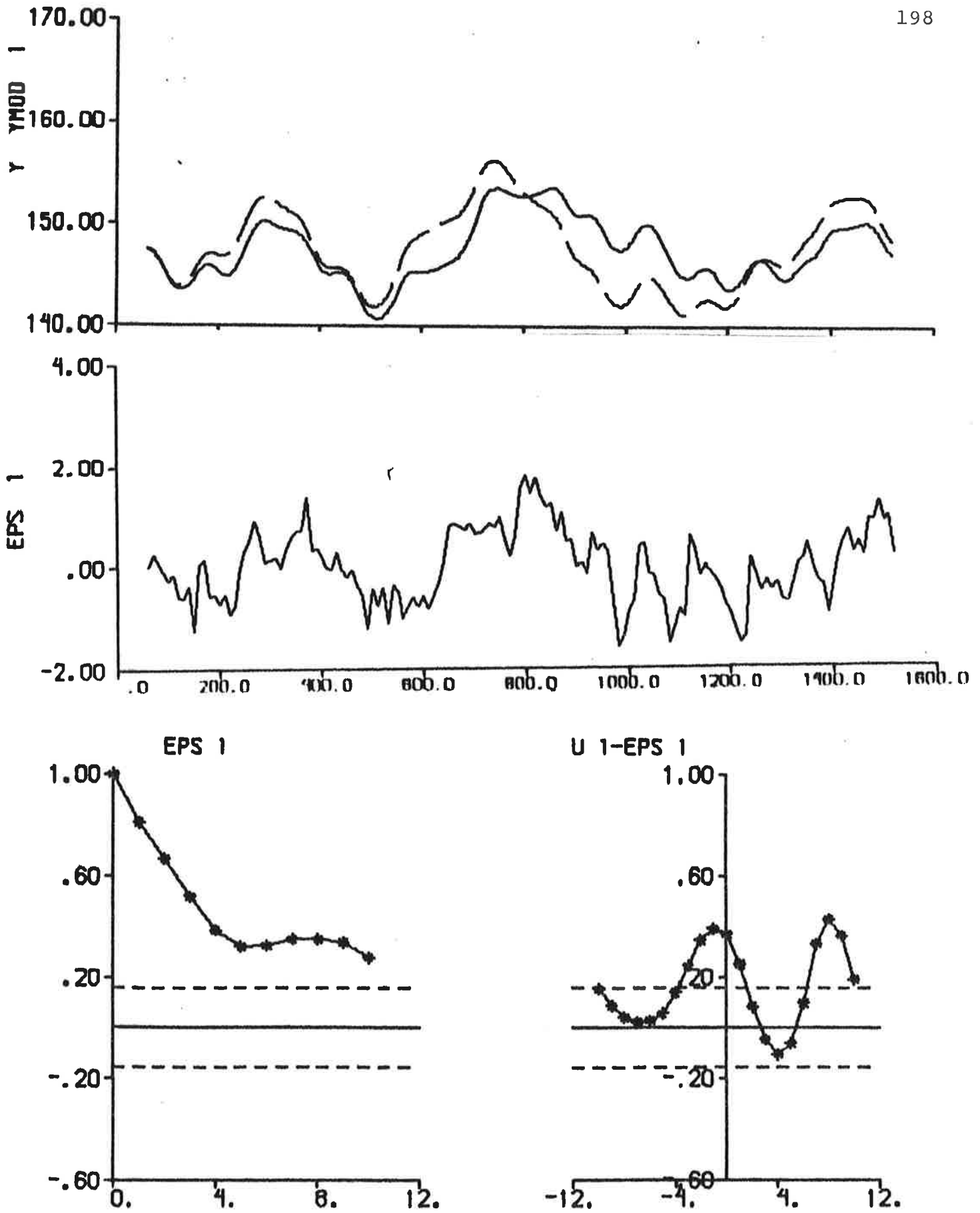
Fig. 6.46 - Result of prediction error identification (p = 6)
to data from experiment E4. Nomoto´s model is used
and the rudder angle is the input signal.
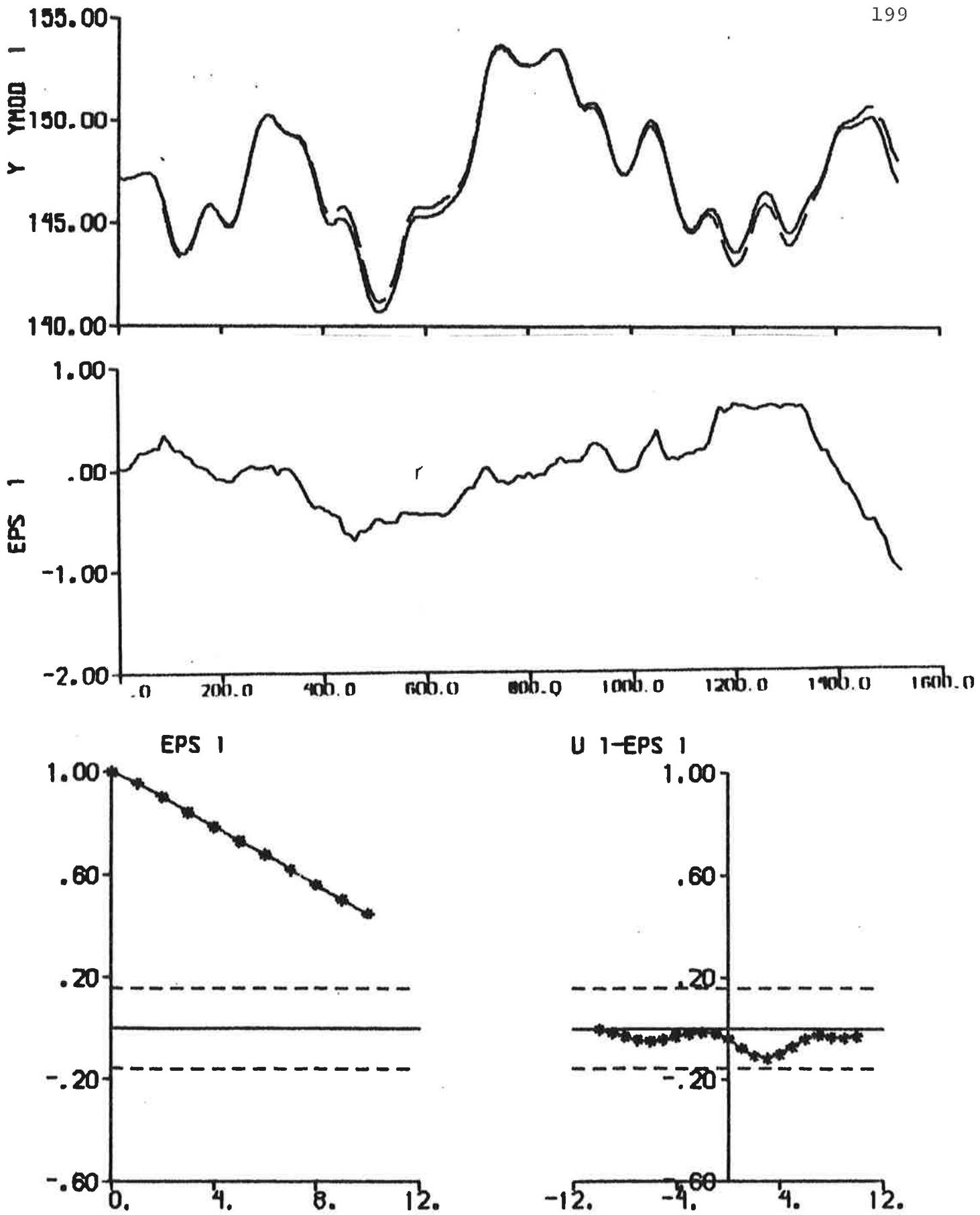
Fig. 6.47 - Result of output error identification to data from experiment E4. The transfer function (3.12) is used and the rudder angle is the input signal.
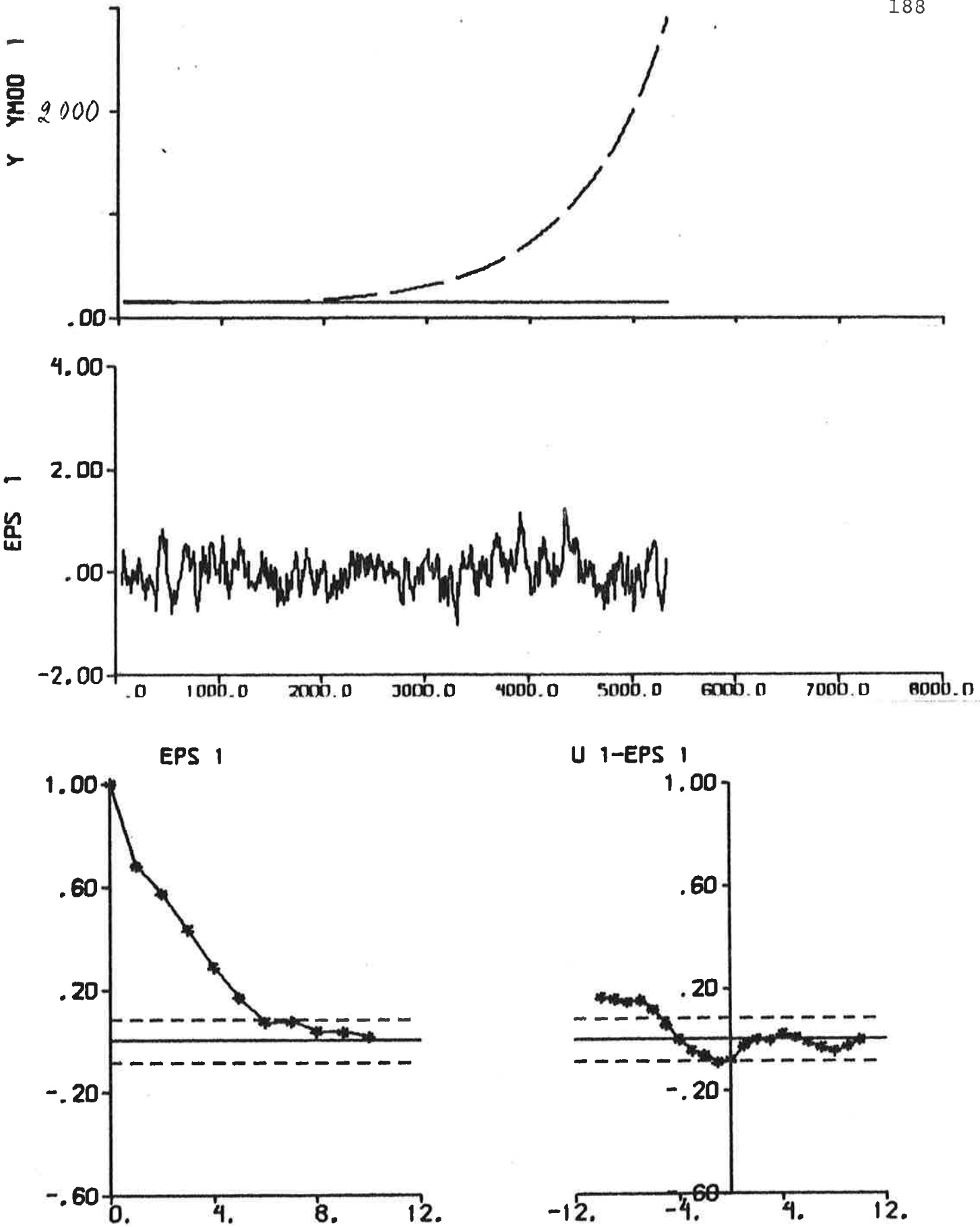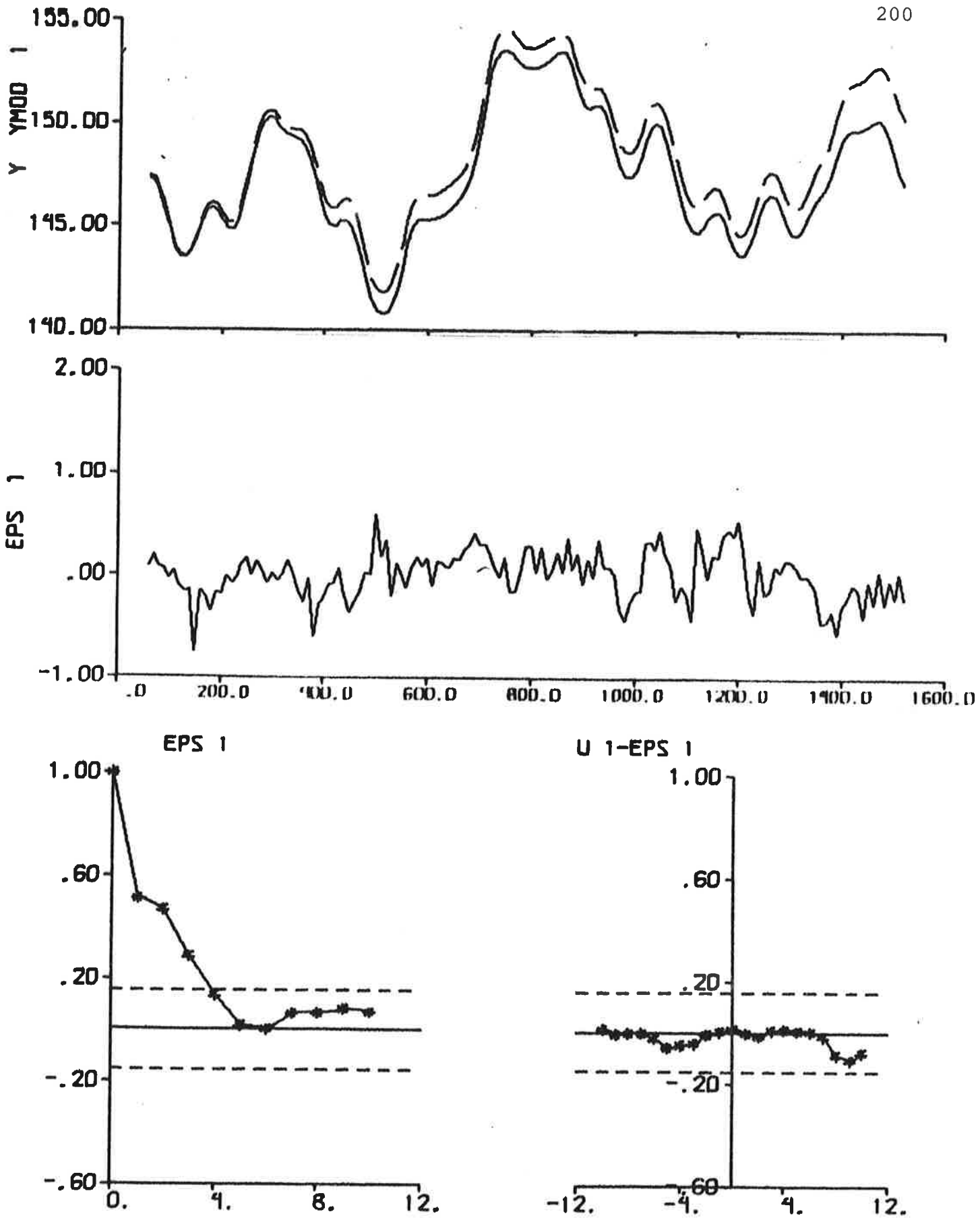
Fig. 6.48 - Result of prediction error identification (p = 6)
to data from experiment E4. The transfer function
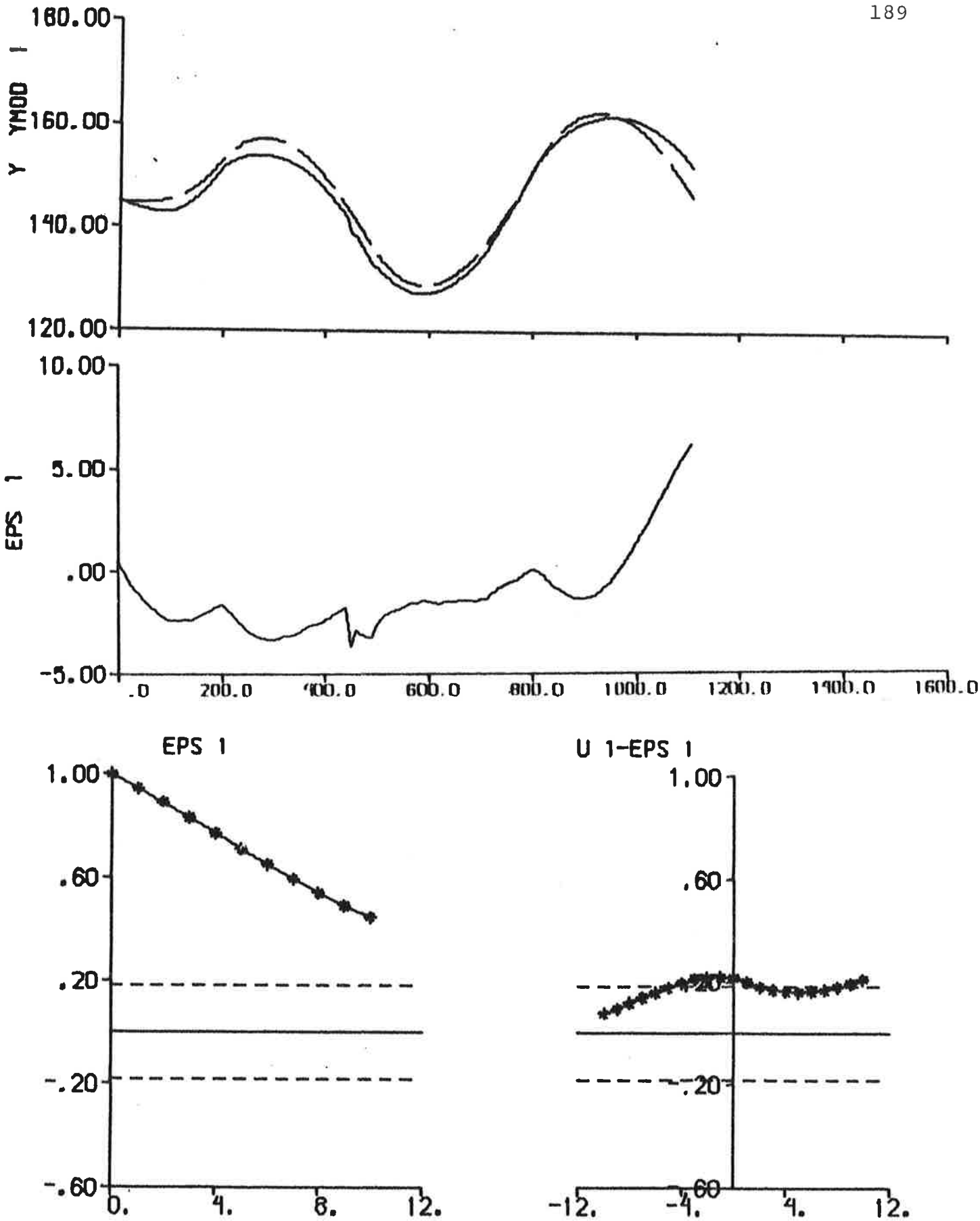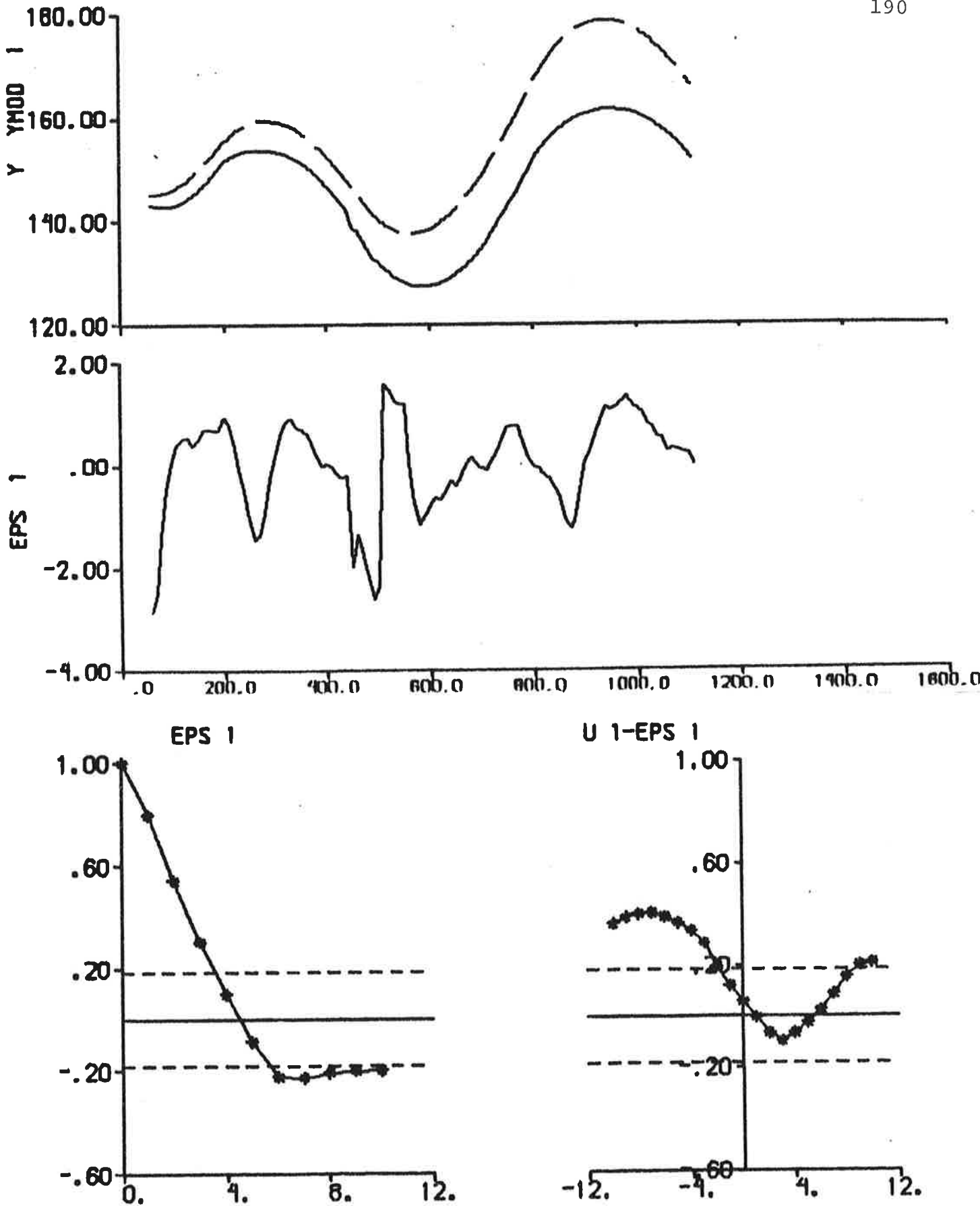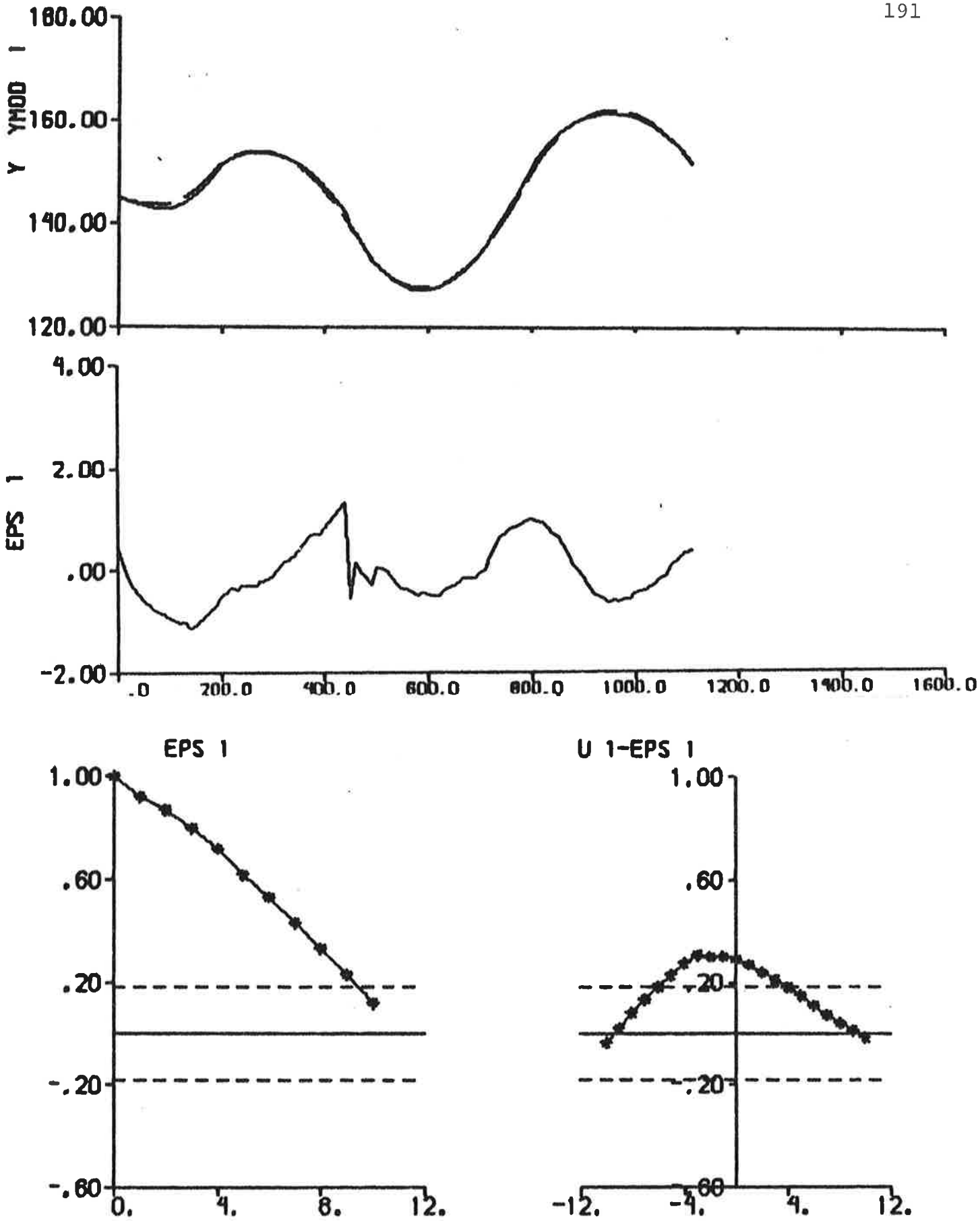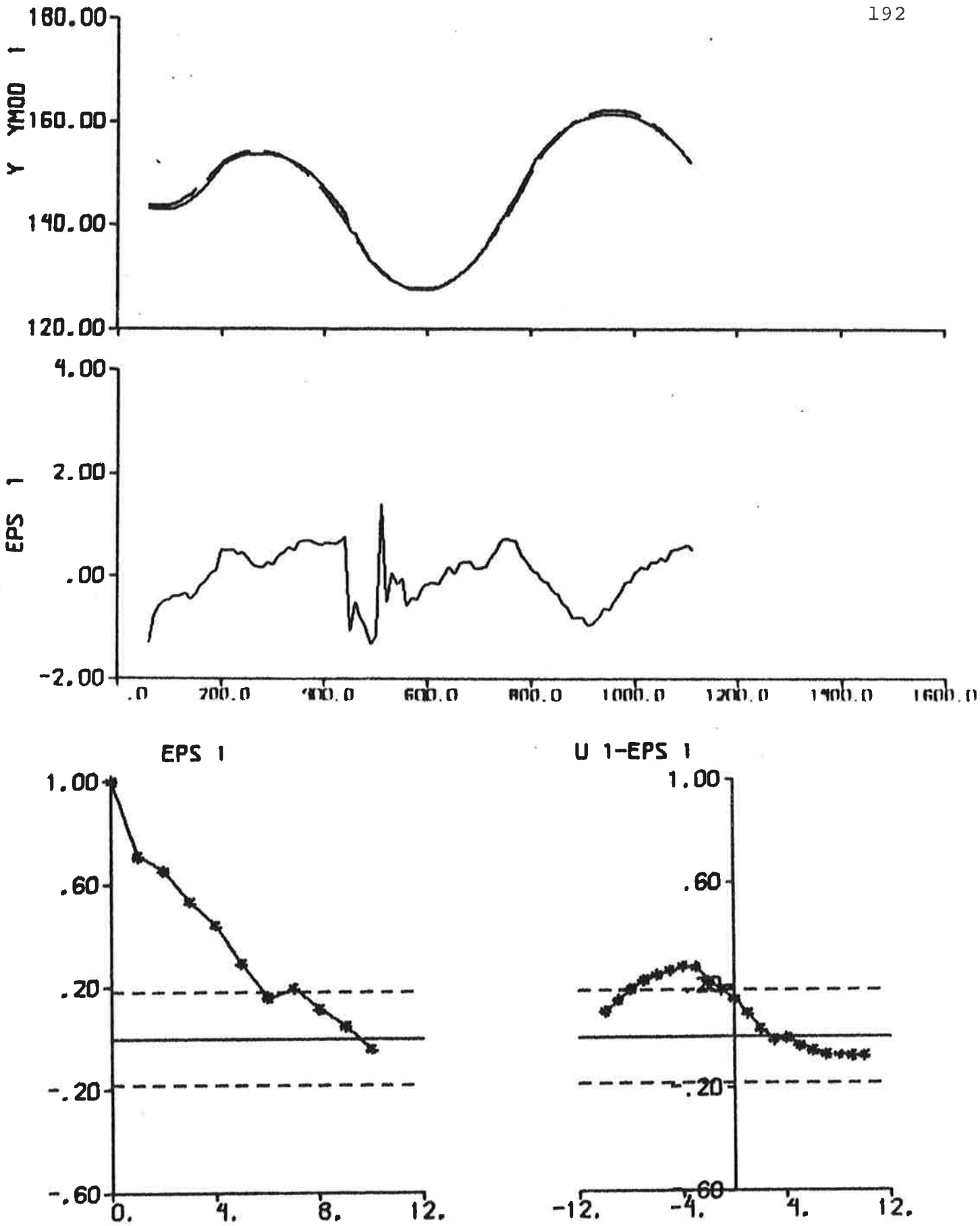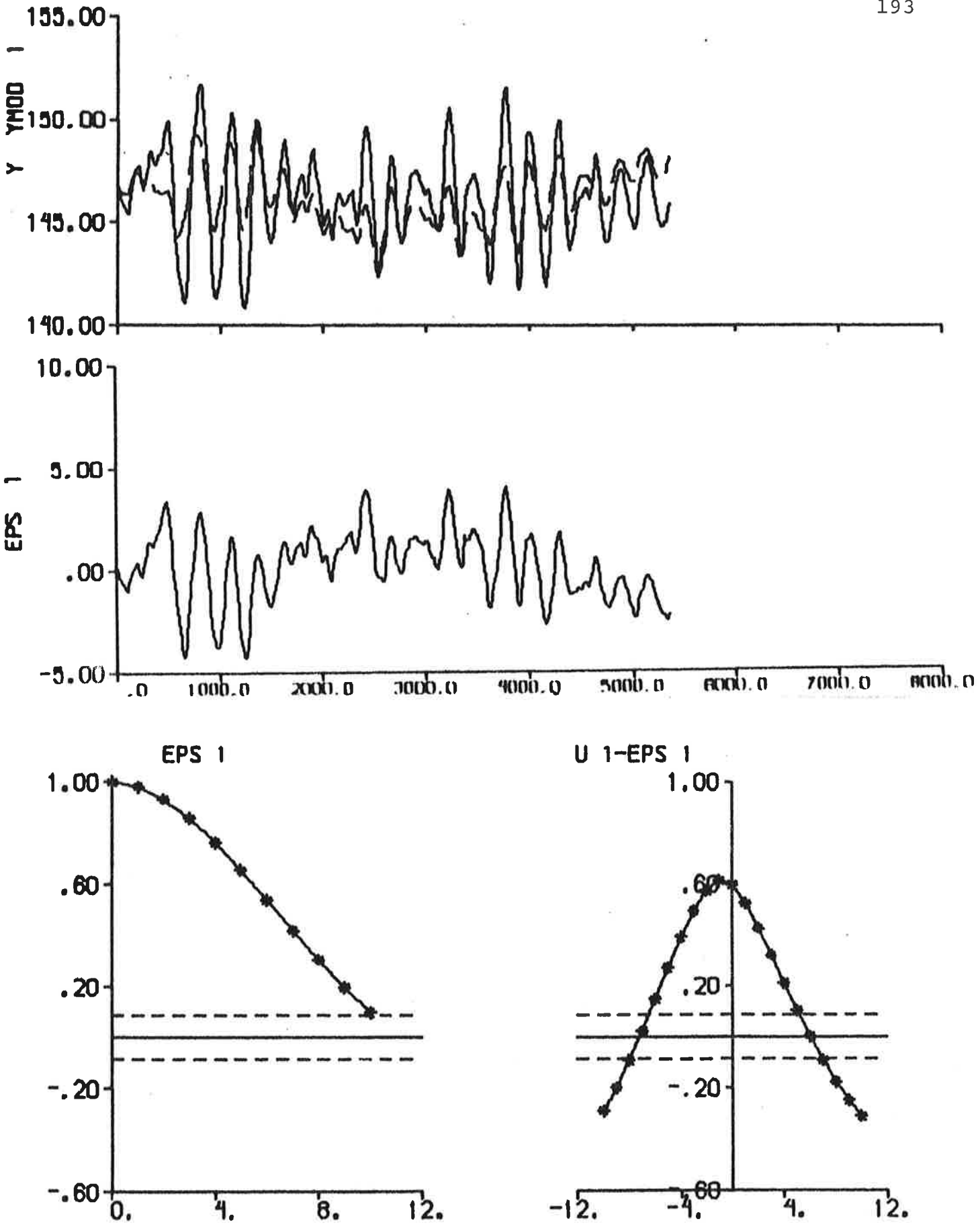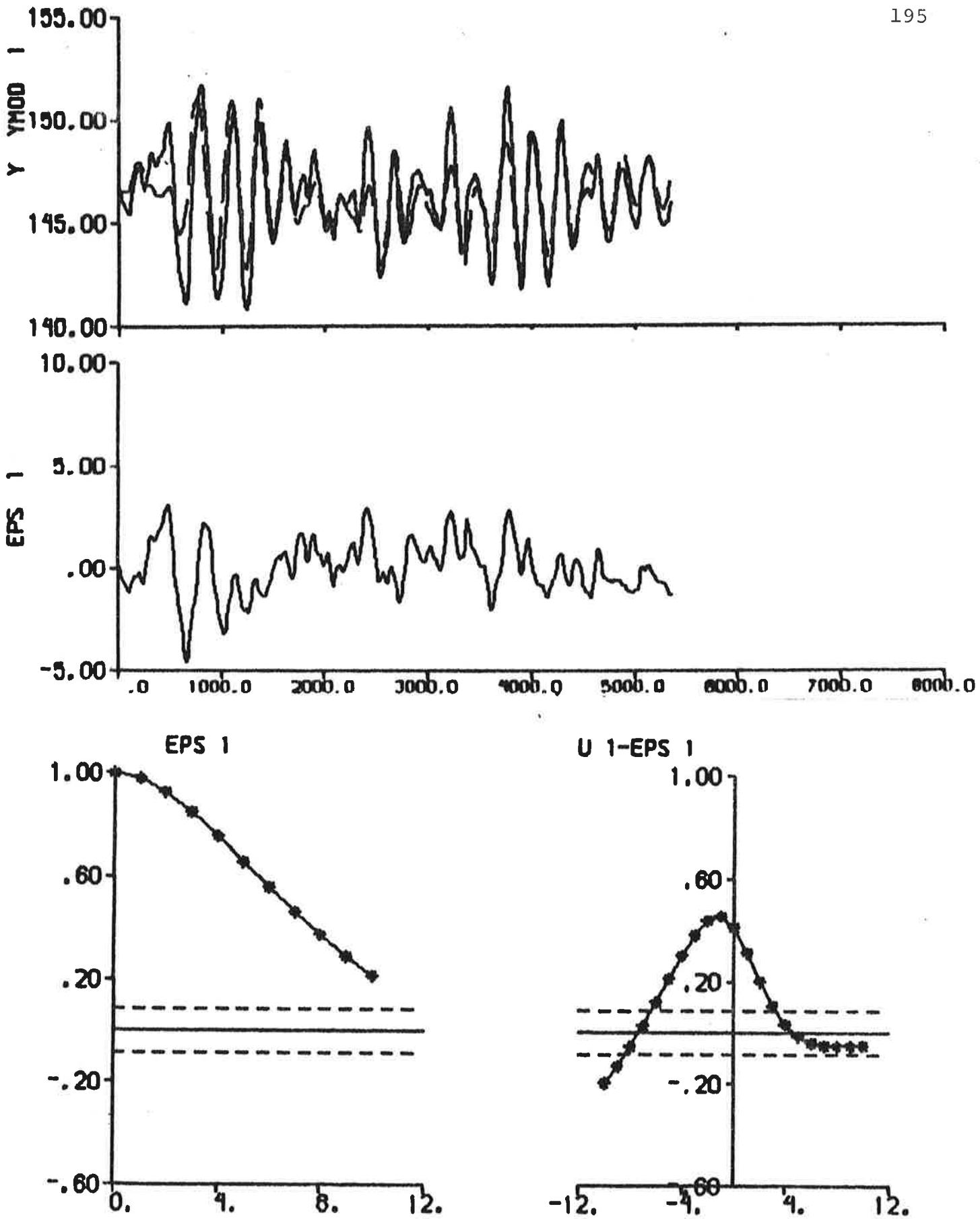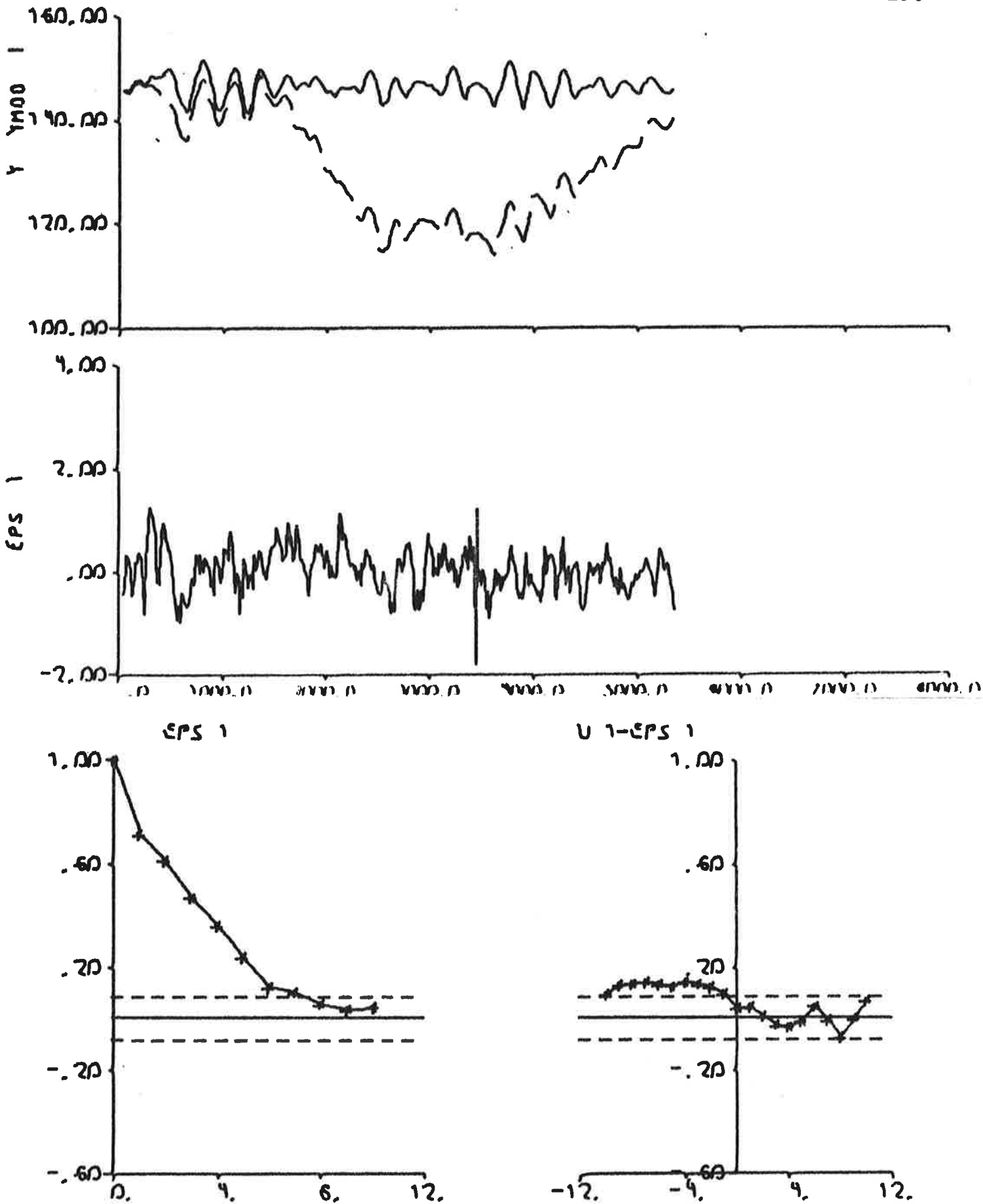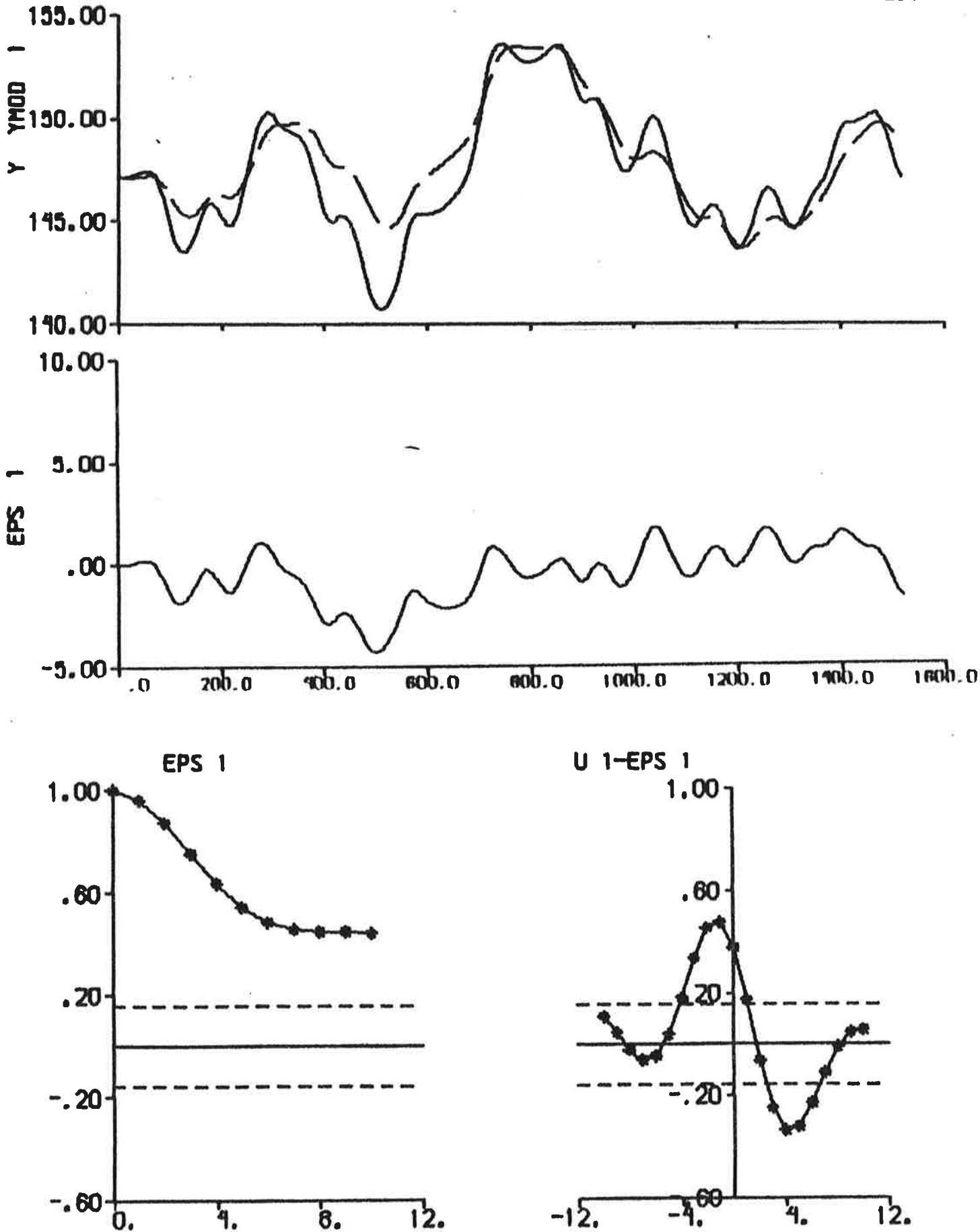(3.12) is used and the rudder angle is the input signal.

Nomoto's model is fitted to the data. The results are changed, but not improved, when the third-order transfer function (3.12) is fitted to the data using the output error method. The corresponding results obtained with the prediction error method (p = 6) are not changed very much when the rudder angle is used instead of the rudder command. It is thus concluded that no improvements are obtained by using the rudder angle as input signal instead of the rudder command.

Results of fitting the model (3.15) to data from experiments E1 and E3 by use of IDPAC are summarized in Table 6.4. The rudder command is chosen as input signal. The maximum likelihood method is used and parameters d_1 and d_2 for the initial state are also estimated. Mean values and linear trends are removed from both the rudder inputs and the heading measurements before the data are analysed. A pure integrator is almost obtained in all cases, since $1 + a_1 + a_2$ is approximately equal to zero. The parameters of Nomoto's model (3.17) are computed from the models in Table 6.4 by use of (3.20). The time delay T_D should be zero when $b_3 = 0$, if the model (3.13) is appropriate to the data. It can be concluded from Table 6.4 that T_D is different from zero, which means that the model (3.17) including a time delay should be used. The proper way of including a time delay is to also estimate b_3 (cf. (3.17) and (3.18)). See Table 6.4. It is also concluded that b_3 should be estimated according to Akaike's information criterion, since -1394 and -1095 should be compared with -1405 and -1154. Notice that the models obtained when b_3 is estimated do not differ much from the corresponding models obtained with LISPID (cf. Table 6.1). All models of Table 6.4 are non-minimum phase. This is a consequence of the fact that a model including a time delay describing the steering engine is sampled, and has nothing to do with the ship steering dynamics.

The autocorrelation functions of residuals and the cross correlation functions between rudder inputs and residuals are shown in Figs. 6.49 - 6.52. Figures 6.50 and 6.52 can be compared with the corresponding results from LISPID (Figs. 6.2 and 6.10).

It is concluded that the consistency between the results from
IDPAC and LISPID is very good.

Models of order 3 and 4 are also fitted to the data from experi-
ments El and E3 by use of IDPAC. The ML method is used and para-
meters for the initial state are also estimated. The results are
shown in Table 6.5 and in Figs. 6.53 - 6.56. A pure integrator
is almost obtained in all cases. Based on Akaike's information
criterion it is concluded that the 3rd-order models of Table 6.5
are better than the models of Table 6.4. It is also concluded
that the 4th-order models are to be preferred to the 3rd-order
models. Because of the long execution times the order was not
further increased. Notice, however, that the loss funtion V and
Akaike's information criterion AIC are changed very little
between the models of Table 6.4 where b_3 is estimated and the
models of Table 6.5. An investigation of the residuals confirms
the small differences.

The 3rd-order discrete time models of Table 6.5 have the zeros
-5.91, -0.72 (El) and -3.89, -0.49 (E3). The corresponding poles
are -0.41, 0.90, 1.03 (El) and -0.10, 0.80, 1.09 (E3). Both
models thus have a pole on the negative real axis. This problem
was discussed in Åström, Källström, Norrbin and Byström (1975)
and in Åström and Källström (1976). It was concluded that a
first-order model with a negative pole is typical for a case
where round-off noise occurs. However, this will probably not
explain the negative pole, since the autocorrelation functions
obtained with Nomoto's model (Figs. 6.50 and 6.52) indicate no
oscillatory behaviour.

The 4th-order discrete time models of Table 6.5 have the zeros
-6.32, -0.27 ±0.52 i (El) and -3.82, -0.54 ±0.55 i (E3). The poles
are -0.12 ± 0.57i, 0.91, 1.03 and -0.35 ± 0.44i, 0.81, 1.09.
Notice that the pair of complex poles are approximately cancelled
by the pair of complex zeros in both cases. The corresponding
continuous time models have the zeros -0.050 ± 0.21i , 0.29 (El)
and -0.018 ±0.22i, 0.29 (E3). The poles are -0.054± 0.18i, -0.0096,

0.0030 (E1) and -0.058 ± 0.22i, -0.022, 0.0088 (E3).

It is difficult to interpret the models obtained with IDPAC, when the order is increased. The advantages by using LISPID, where parameters of physical models are estimated, are obvious. Finally, it is important to remember that the results with LISPID indicated that a prediction interval of approximately 40 s was appropriate when a third-order transfer function was used. All identifications using IDPAC were performed with a prediction interval of 10 s.

7. CONCLUSIONS

Four experiments performed with the 356 000 tdw oil tanker Sea Stratus were analysed. The tanker was ballasted and the speed was approximately 12.6 knots during the experiments. A PRBS was approximately used as rudder perturbations during experiments E1 and E4, which were performed in open loop. Experiment E2 was a $5^{o}/5^{o}$ zig-zag test. Experiment E3 was carried out in closed loop, but extra rudder perturbations were added to secure the identifiability. Fore sway velocities, yaw rates and heading angles were measured and recorded with a precise, constant sampling interval of 10 s. By analysing the prediction errors obtained from system identification it was, however, possible to detect that one sampling event was missed during experiment E2 and that two incorrect sampling intervals were obtained during experiment E3.

The output error method, the maximum likelihood method and the prediction error method were applied to the data by use of the identification program LISPID. The identifications were based on 3 different models.

The first model is linear and contains hydrodynamic deriva- tives which are estimated. The outputs of the model are the sway velocity, the yaw rate and the heading angle. Strange parameter values were obtained when the output error method was applied to data from experiment E3. The estimated hydro- dynamic derivatives differed significantly from the values

Fig. 6.49 - Autocorrelation function of residuals and cross
correlation function between rudder input and
residuals, where the residuals are obtained from
ML identification using IDPAC to data from experi-
ment El ($b_3 = 0$).

Fig. 6.50 – Autocorrelation function of residuals and cross correlation function between rudder input and residuals, where the residuals are obtained from ML identification using IDPAC to data from experiment El (b_3 estimated).

	SSPA:s model	E 1		E 3	
		$b_3 = 0$	b_3 estim.	$b_3 = 0$	b_3 estim.
Figure		6.49	6.50	6.51	6.52
ν		8	9	8	9
V		$4.2 \cdot 10^{-3}$	$4.1 \cdot 10^{-3}$	$7.4 \cdot 10^{-3}$	$6.6 \cdot 10^{-3}$
AIC		-1394	-1405	-1095	-1154
a_1		-1.946 ± 0.006	-1.931 ± 0.008	-1.914 ± 0.007	-1.888 ± 0.007
a_2		0.943 ± 0.006	0.927 ± 0.008	0.902 ± 0.007	0.868 ± 0.007
b_1		-0.003 ± 0.001	-0.004 ± 0.001	-0.004 ± 0.001	-0.006 ± 0.001
b_2		-0.029 ± 0.001	-0.025 ± 0.001	-0.029 ± 0.001	-0.024 ± 0.001
b_3		—	-0.005 ± 0.001	—	-0.008 ± 0.001
c_1		-0.17 ± 0.04	-0.12 ± 0.05	-0.49 ± 0.05	-0.4 ± 0.05
c_2		-0.03 ± 0.05	0.02 ± 0.05	0.08 ± 0.05	0.13 ± 0.04
d_1		-1.47 ± 0.07	-1.47 ± 0.06	0.09 ± 0.12	0.09 ± 0.08
d_2		1.38 ± 0.07	1.35 ± 0.07	-0.28 ± 0.09	-0.29 ± 0.08
K'	1.59	-3.03	-2.52	-1.82	-1.56
K_1'	-0.28	-0.96	-1.03	-1.01	-1.19
T'	-5.77	3.16	2.44	1.80	1.31
T_D [s]	—	4.1	5.4	3.9	5.6

Table 6.4 – Parameter values from ML identifications using IDPAC.
Nomoto´s model (see (3.13) and (3.17)) is determined.
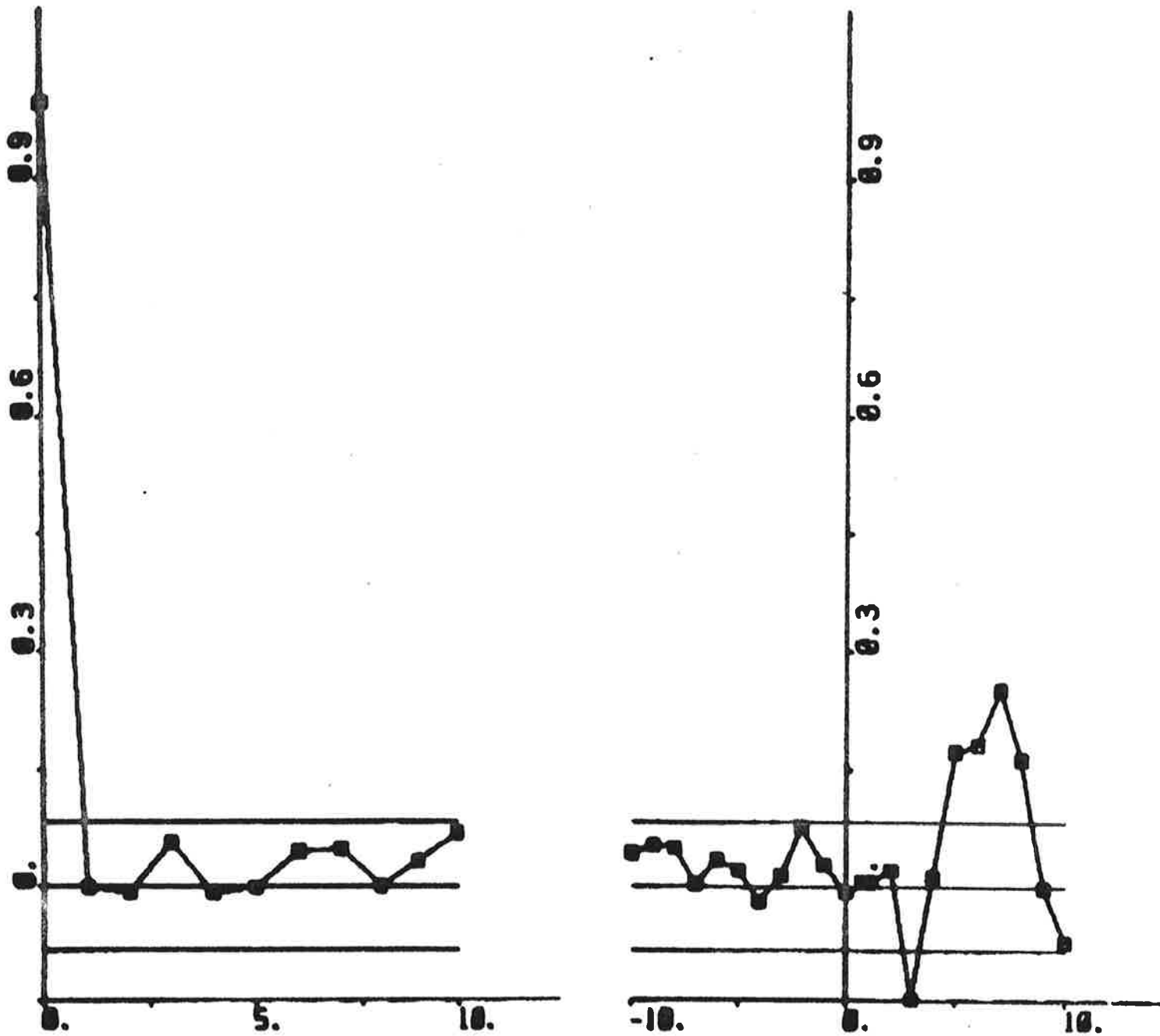Parameters d_1 and d_2 for the initial state are estimated.

Fig. 6.51 - Autocorrelation function of residuals and cross
correlation function between rudder input and
residuals, where the residuals are obtained from
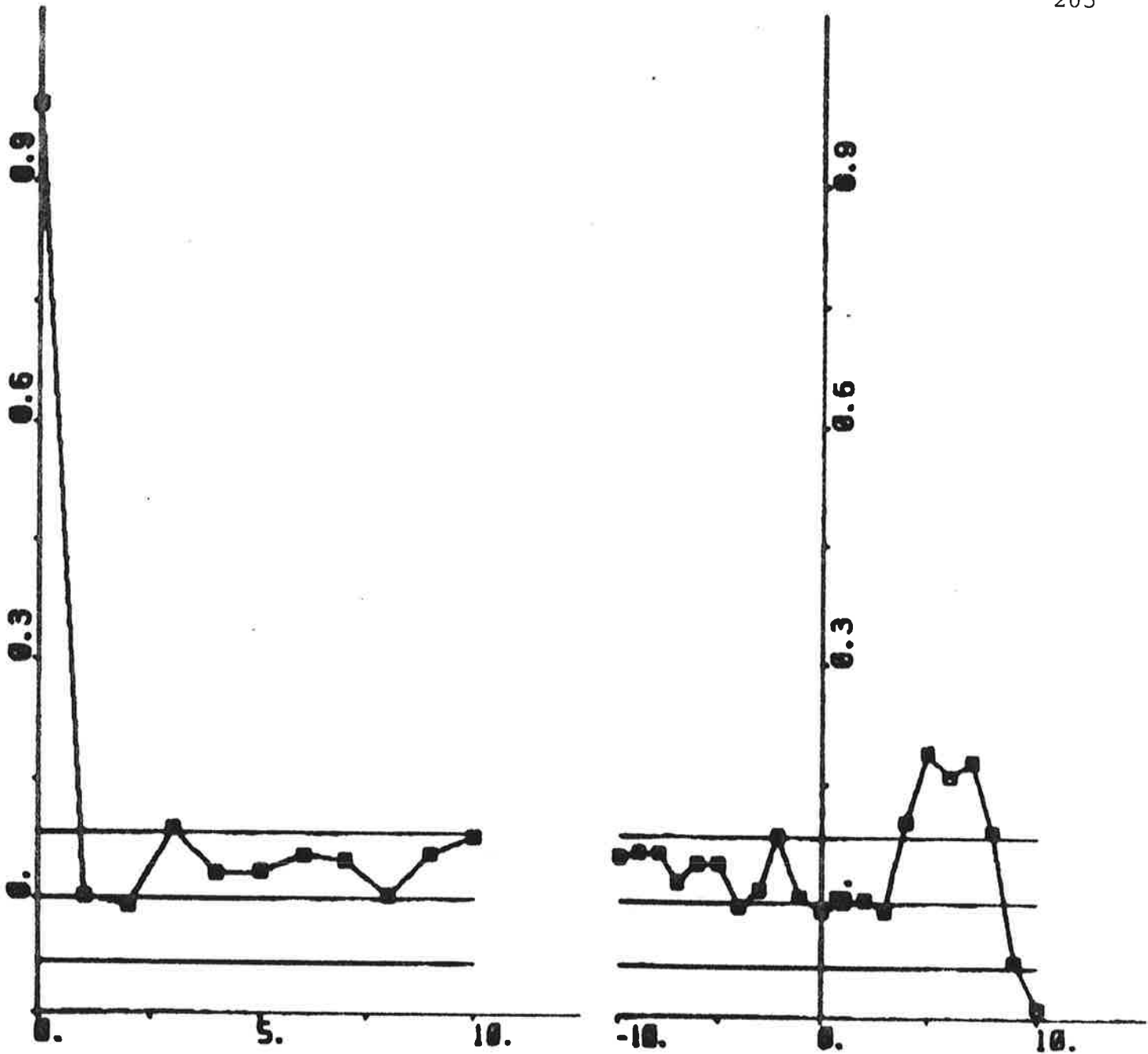ML identification using IDPAC to data from experiment
E3 (b_3 = 0).

Fig. 6.52 — Aurocorrelation function of residuals and cross correlation function between rudder input and residuals, where the residuals are obtained from ML identification using IDPAC to data from experiment E3 (b_3 estimated).

	E 1		E 3	
	3rd order	4th order	3rd order	4th order
Figure	6.53	6.54	6.55	6.56
ν	12	16	12	16
V	$4.0 \cdot 10^{-3}$	$3.9 \cdot 10^{-3}$	$6.5 \cdot 10^{-3}$	$6.4 \cdot 10^{-3}$
AIC	-1412	-1417	-1156	-1157
a_1	-1.523	-1.706	-1.791	-1.203
a_2	0.136	0.825	0.684	-0.124
a_3	0.383	-0.443	0.087	0.015
a_4	$-$	0.319	$-$	0.276
b_1	-0.004	-0.004	-0.006	-0.006
b_2	-0.026	-0.026	-0.025	-0.028
b_3	-0.017	-0.014	-0.011	-0.027
b_4	$-$	-0.008	$-$	-0.013
c_1	0.27	0.09	-0.32	0.26
c_2	-0.06	0.30	0.08	0.13
c_3	0.07	-0.004	0.03	-0.06
c_4	$-$	0.008	$-$	0.11
d_1	-1.49	-1.47	0.06	0.05
d_2	0.74	1.01	-0.25	-0.22
d_3	0.64	-0.11	-0.06	-0.22
d_4	$-$	0.56	$-$	-0.03

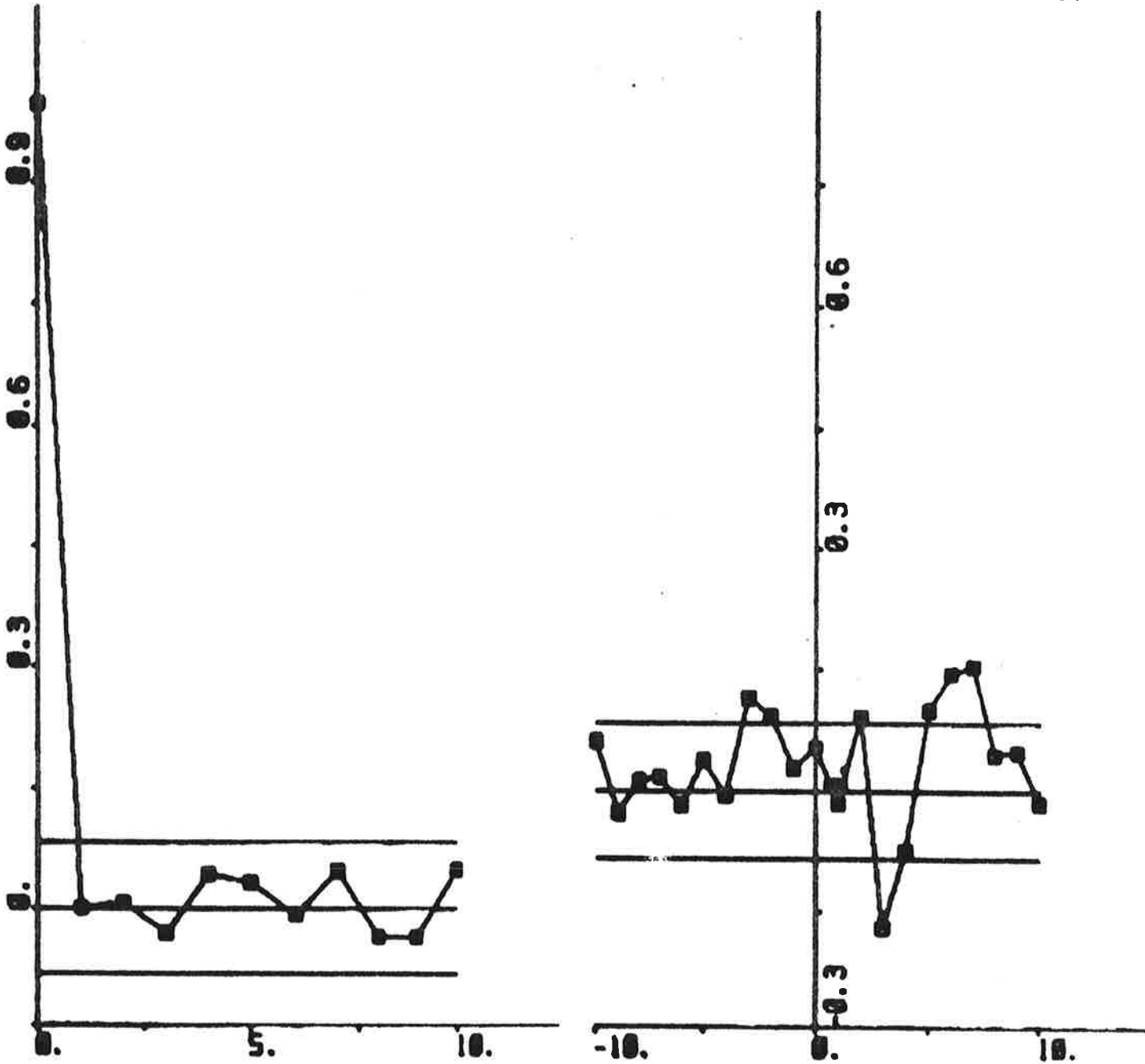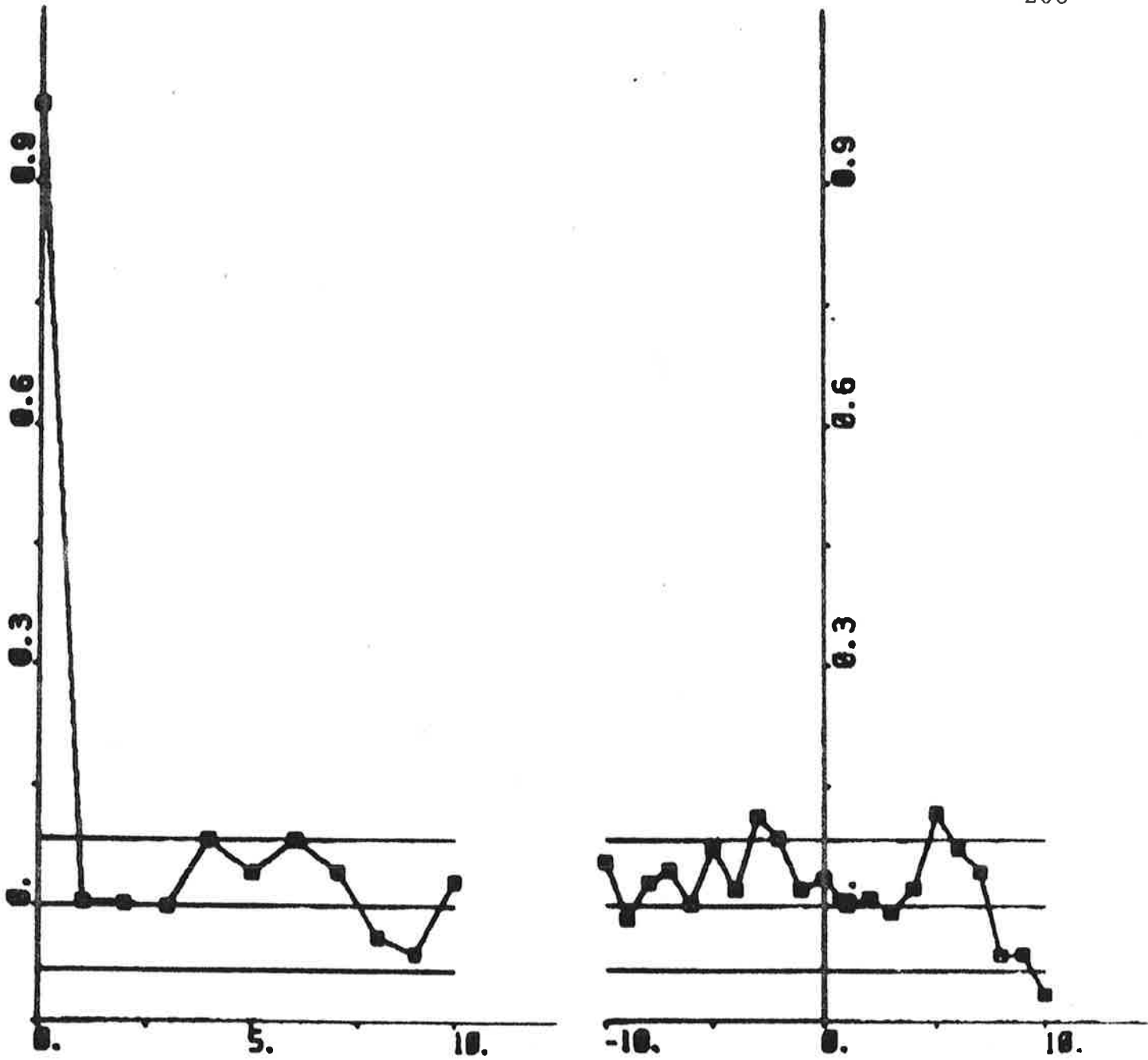Table 6.5 - Parameter values from ML identifications using IDPAC.

Fig. 6.53 — Autocorrelation function of residuals and cross
correlation function between rudder input and
residuals, where the residuals are obtained from
ML identification using IDPAC to data from experi-
ment E1 (3rd order model).

Fig. 6.54 — Aurocorrelation function of residuals and cross
correlation function between rudder input and
residuals, where the residuals are obtained from
ML identification using IDPAC to data from experi-
ment El (4th order model).

Fig. 6.55 — Autocorrelation function of residuals and cross
correlation function between rudder input and
residuals, where the residuals are obtained from
ML identification using IDPAC to data from experi-
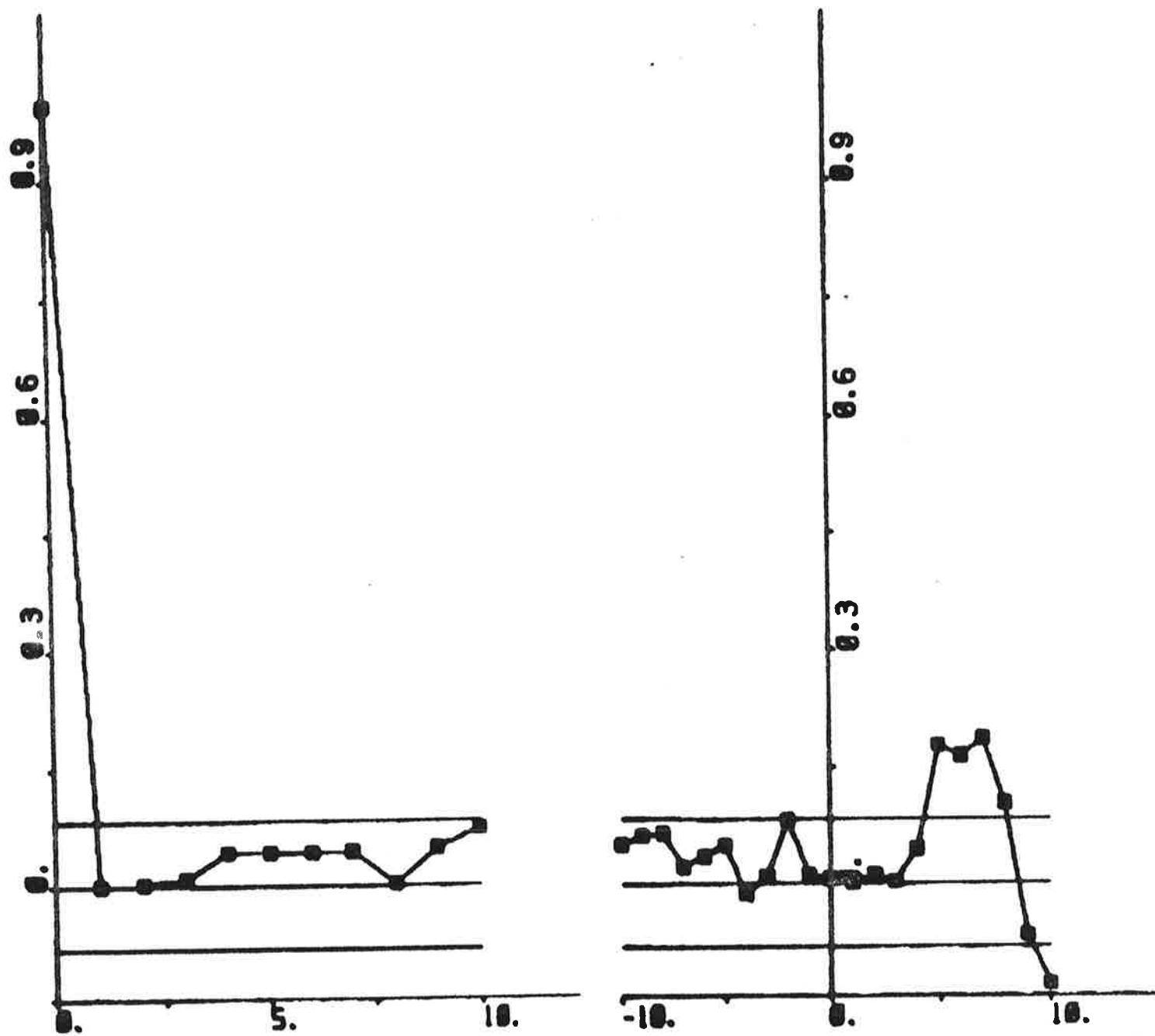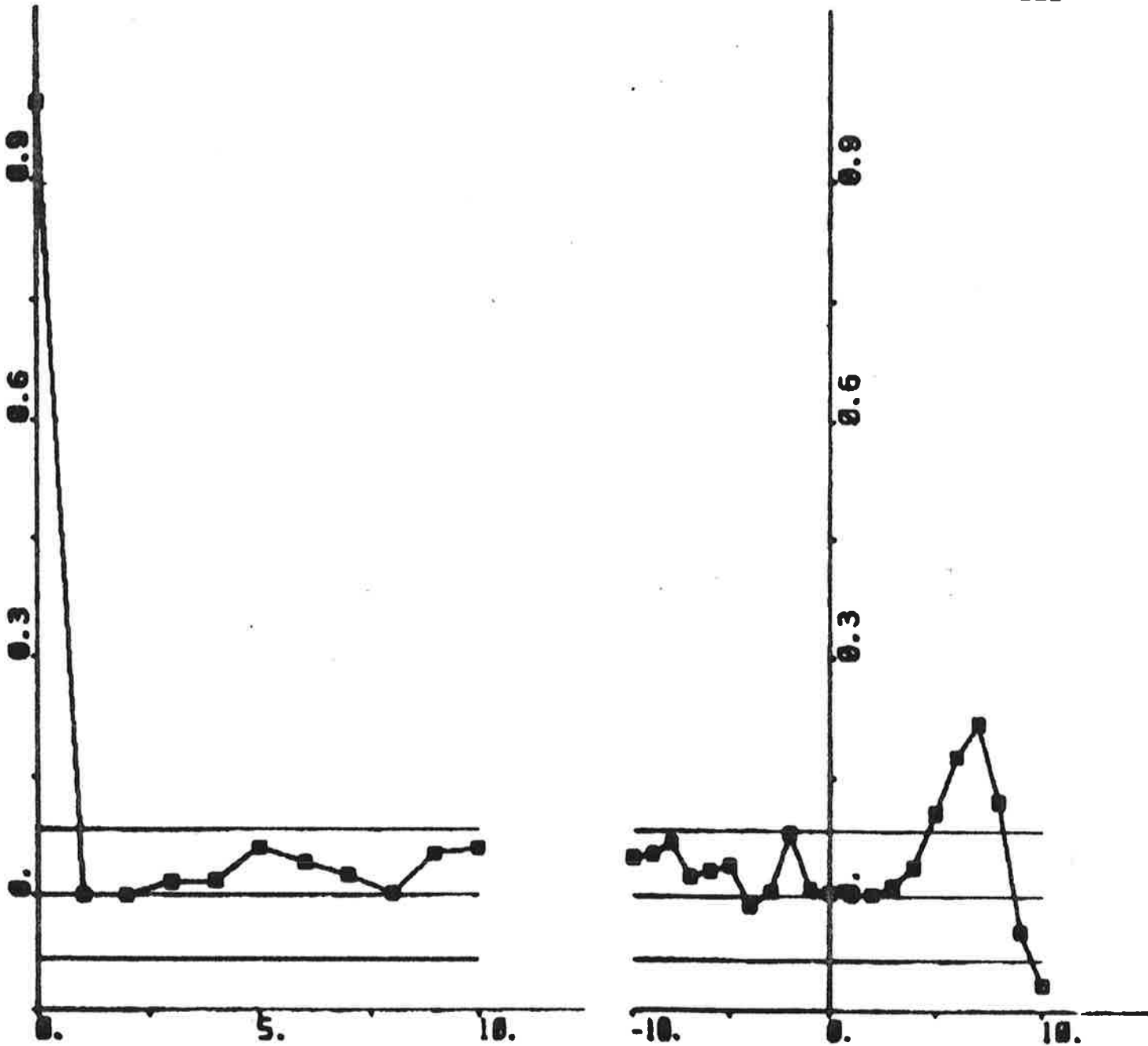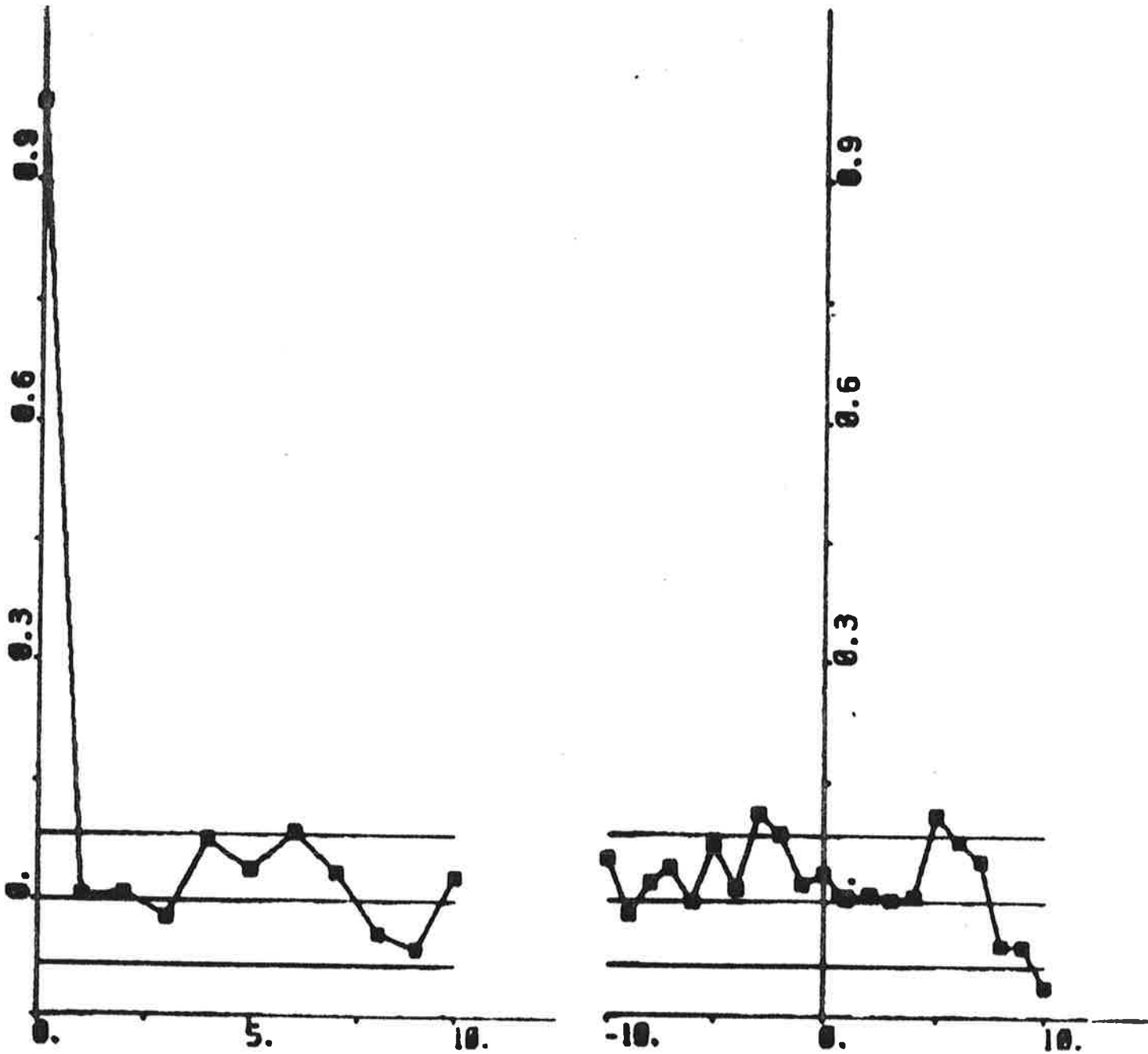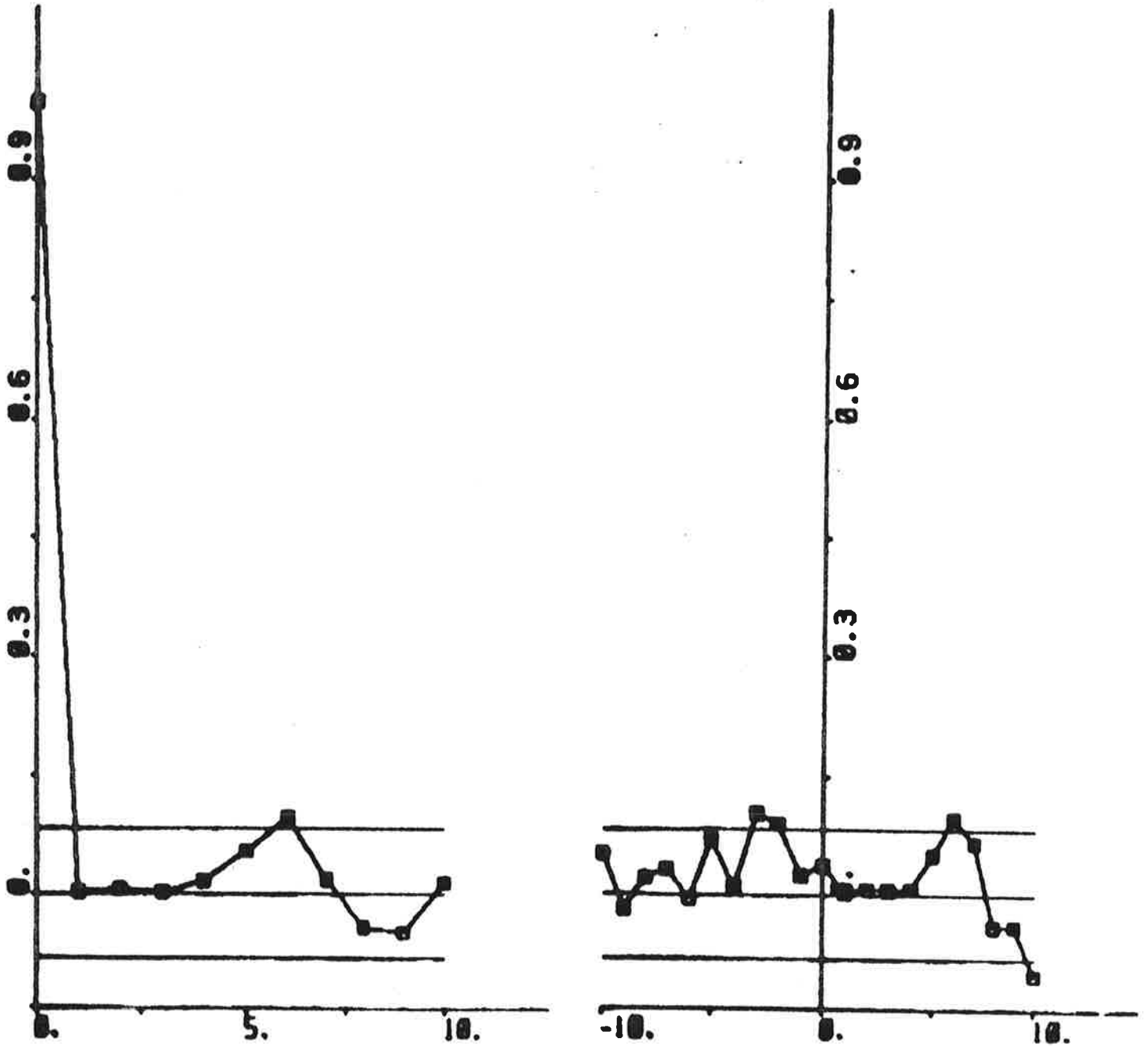ment E3 (3rd order model).

Fig. 6.56 - Autocorrelation function of residuals and cross correlation function between rudder input and residuals, where the residuals are obtained from ML identification using IDPAC to data from experiment E3 (4th order model).

calculated by SSPA. However, experiments E1, E2, and, above all, E4 gave significantly improved results. The estimates of the hydrodynamic derivatives obtained by applying the maximum likelihood method to data from all experiments were bad. However, Akaike's information criterion indicated distinctly that the process noise should be modelled. Significantly improved results were obtained when the prediction error method was applied to data from the 4 experiments. It was concluded that a prediction interval of about 60 s was appropriate. The estimated hydrodynamic derivatives obtained from experiments E1, E3 and E4 differed rather much from SSPA:s estimates. However, experiment E2 gave estimates close to SSPA:s values.

The second model used by LISPID is an extension of the first model, where the nonlinear cross-flow drag is included. The only unknown parameter of the added nonlinearity is the effective cross-flow drag coefficient. Approximately the same results were obtained by using the nonlinear model as were obtained by using the linear model when experiments E1 and E3 were analysed. The estimates of the hydrodynamic derivatives were not changed significantly. However, the effective cross-flow drag coefficient was badly estimated. Experiments E1 and E3 with the Sea Stratus were designed to determine the linear ship steering dynamics, so it is not surprising that no improvements are obtained by using the nonlinear model. Improved results were obtained when the nonlinear model was fitted to experiments E2 and E4 instead of the linear model using the output error method. The prediction error method with p = 6 applied to experiment E2 also gave a very good result. In these cases reasonable estimates of the effective cross-flow drag coefficient were obtained.

Identifications based on a third model were also performed by using LISPID. This linear model contains the parameters of the transfer function relating heading to rudder angle. The only output of this model is the heading angle. The gain and time constant of Nomoto's model were first determined. A rather bad consistency between the estimates from output error identifications to data from the 4 experiments was obtained. The consistency between parameter estimates obtained from maximum likelihood

identifications was improved. The results of prediction error
identifications were almost equivalent to the results from
maximum likelihood identifications. It was thus concluded that
a prediction interval of 10 s is sufficiently when the heading
angle only is used as output signal and Nomoto´s model is fitted
to the data. The gain and the 3 time constants of a third-order
transfer function were also determined. The output error method
applied to experiments E1 and E3 gave bad results, while the
results of experiment E2 and, above all, experiment E4, were
very good. Reasonable parameter estimates were obtained when
the ML method was applied to experiments E1 and E4, while
experiments E2 and E3 gave strange models. The results of pre-
diction error identifications with p = 4 were improved compared
to the ML results. Reasonable models were determined in all
cases. The results of prediction error identifications with
p = 6 were not changed much compared to the results with p = 4.
A prediction interval of approximately 40 s is thus reasonable
when a third-order transfer function is fitted to the data.
Usually a third-order transfer function was to be preferred
instead of Nomoto´s model, when the experiments were analysed
using LISPID.

The rudder input - heading output data from experiments E1
and E3 were also analysed by the identification program IDPAC.
The parameters of a linear difference equation model were esti-
mated by the maximum likelihood method. A model corresponding
to Nomoto´s model was first identified. The results obtained
were equivalent to the corresponding maximum likelihood results
from LISPID. A model corresponding to the thrid-order transfer
function was also identified by using IDPAC. A pole on the
negative real axis was then obtained. A model of order 4 was
also fitted to the data. Pairs of complex zeros and poles were
then obtained. They were, however, almost cancelling each other.
Akaike´s information criterion indicated that the 4th order
models were appropriate to the data. It is, however, difficult
to interpret the models of order 3 and 4 obtained with IDPAC.
The advantages by using LISPID, where parameters of physical
models are estimated, are obvious.

System identifications using the rudder angle as input signal instead of the rudder command were also performed. It was concluded that no improvements were obtained by using the rudder angle.

A wind of 9 - 14 m/s was blowing during the experiments. Investigations showed, however, that it was not necessary to estimate the wind parameters of the different models.

Experiment E3 was performed in closed loop. The identification results using this experiment seem usually to be not as good as the results of the other experiments. In Källström (1978b) it was, however, concluded that there was no difference between the results obtained from open loop and closed loop experiments.

8. ACKNOWLEDGEMENTS

9. REFERENCES

Akaike, H (1972): Use of an information theoretic quantity for statistical model identification. Proc. 5th Hawaii International Conference on System Sciences, pp. 249-250, Western Periodicals Co, North Hollywood, California, USA.

Åström, K J, and T Bohlin (1965): Numerical identification of linear dynamic systems from normal operating records. Proc. 2nd IFAC Symp on the Theory of Self-Adaptive Control Systems, Teddington, Great Britain.

Åström, K J (1970): Introduction to Stochastic Control Theory. Academic Press, New York.

Åström, K J, and C G Källström (1973): Application of system identification techniques to the determination of ship dynamics. Proc. 3rd IFAC Symp on Identification and System Parameter Estimation, pp. 415-424, the Hague/Delft, The Netherlands.

Åström, K J, N H Norrbin, C Källström, and L Byström (1974): The identification of linear ship steering dynamics using maximum likelihood parameter estimation. TFRT - 3089, Department of Automatic Control, Lund Institute of Technology, Lund Sweden. Also available as Report 1920-1, Swedish State Shipbuilding Experimental Tank, Gothenburg, Sweden.

Åström, K J, C G Källström, N H Norrbin, and L Byström (1975): The identification of linear ship steering dynamics using maximum likelihood parameter estimation. Publ. No 75, Swedish State Shipbuilding Experimental Tank, Gothenburg, Sweden.

Åström, K J, and C G Källström (1976): Identification of ship steering dynamics. Automatica, 12, 9.

Byström, L, and C G Källström (1978): System identification of linear and non-linear ship steering dynamics. Paper submitted to the 5th Ship Control Systems Symp., Annapolis, Maryland, USA.

Gustavsson, I, L Ljung and T Söderström (1977): Identification of processes in closed loop - identifiability and accuracy aspects. Automatica, 13, 59.

Källström, C (1976): The Sea Stratus experiments, April 1976. Department of Automatic Control, Lund Institute of Technology, Lund, Sweden. CODEN: LUTFD2/(TFRT - 7110)/1-587/ (1976).

Källström, C G, T Essebo, and K J Åström (1976): A computer program for maximum likelihood identification of linear, multivariable stochastic systems. Proc 4th IFAC Symp on Identification and System Parameter Estimation, Vol. 2, pp. 508-521, Tbilisi, USSR.

Källström, C G (1977a): Identification of the linear steering dynamics of the Sea Splendour. Department of Automatic Control, Lund Institute of Technology, Lund Sweden. CODEN: LUTFD2/(TFRT - 7129)/1-085/(1977).

Källström, C G (1977b): Determination of linear and nonlinear steering models for the USS Compass Island. Department of Automatic Control, Lund Institute of Technology, Lund Sweden. CODEN: LUTFD2/(TFRT-7130)/1-099/(1977).

Källström, C G (1977c): Identification of the steering dynamics of the Sea Scout. Department of Automatic Control, Lund Institute of Technology, Lund, Sweden. CODEN: LUTFD2/ (TFRT-7131)/1-137/(1977).

Källström, C G (1978a): LISPID - user's manual. Department of Automatic Control,Lund Institute of Technology, Lund, Sweden. CODEN: LUTFD2/(TFRT-7147)/1-147/(1978).

Källström, C G (1978b): Identification of the steering dynamics of the Sea Swift. Department of Automatic Control, Lund Institute of Technology, Lund, Sweden. CODEN: LUTFD2/(TFRT-7155)/1-175/(1978).

Norrbin, N H (1976): Om en kvasi-stationär integral för icke-linjär dämpning i fartygs girmanöver. PM B187, Swedish State Shipbuilding Experimental Tank, Gothenburg, Sweden (in Swedish).

Norrbin, N H, L Byström, K J Åström and C G Källström (1977): Further studies of parameter identification of linear and nonlinear ship steering dynamics. Report 1920-6, Swedish State Shipbuilding Experimental Tank, Gothenburg, Sweden.

Wieslander, J (1976): IDPAC, user's guide. TFRT-3099, Department of Automatic Control, Lund Institute of Technology, Lund, Sweden.